Development of an optimized perfused-continuous process of culture of human umbilical cord mesenchymal stem cells (hMSC) grown on innovative adhesion supports

Caroline Sion

École doctorale 608 : Sciences et Ingénierie des Molécules, des Produits, des Procédés et de l'Energie

THÈSE

Présentée et soutenue publiquement pour l'obtention du grade de

Docteur de l'Université de Lorraine

Spécialité "Procédés biotechnologiques"

par

Caroline SION

le 9 Octobre 2020

Development of an optimized perfused-continuous process of culture of human umbilical cord mesenchymal stem cells (hMSC) grown on innovative adhesion supports

Directeur de thèse : **Pr. Eric OLMOS**

Co-directrice de thèse : **Pr. Isabelle CHEVALOT**

Composition du jury

Pr. Hélène Rouard,	Professeure (Université Paris Créteil, EFS)	Rapportrice
Pr. Joaquim Cabral,	Professeur (Instituto Superior Técnico, Universidade de Lisboa)	Rapporteur
Pr. Dominique Toye,	Professeure (Université de Liège)	Examinatrice
Dr. Céline Martin,	Chercheuse (Thermo Fisher Scientific)	Examinatrice
Pr. Danièle Bensoussan,	Professeure des universités-praticien hospitalier (CHRU Nancy)	Examinatrice
Pr. Eric Olmos,	Professeur (Université de Lorraine)	Examinateur
Pr. Isabelle Chevalot,	Professeure (Université de Lorraine)	Examinatrice
Dr. Emmanuel Guedon,	Directeur de Recherche (CNRS)	Examinateur

Université de Lorraine

Laboratoire Réactions et Génie des Procédés (LRGP)

UMR CNRS 7274, Nancy, France

Acknowledgments

Les travaux présentés dans ce manuscrit ont été menés au sein de l'équipe BioProMo du laboratoire des réactions et génies des procédés (LRGP). Je souhaite donc remercier Dr. Laurent Falk, directeur du LRGP, de m'avoir accueillie dans le laboratoire, ainsi que Pr. Stéphane Delaunay pour son accueil au sein de l'équipe.

Je remercie également les membres du jury, Pr. Hélène Rouard et Pr. Joaquim Cabral d'avoir accepté de juger et évaluer ce travail en tant que membres rapporteurs. Je remercie Pr. Dominique Toye, Pr. Danièle Bensoussan et Dr. Céline Martin d'avoir accepté d'examiner ces travaux.

Je souhaite ensuite remercier tout particulièrement mes encadrants de thèse, pour leur confiance, leur aide et leur grande disponibilité pour moi. Un grand merci à Eric pour ton soutien, ta disponibilité ainsi que toutes les connaissances que tu as su me transmettre. Je me rappellerai pendant longtemps nos traversées de frontière pour les réunions Interreg, avec souvent, le coffre plein de bières au retour et les chansons des Kastelruther Spatzen en fond musical (mention spéciale pour Che bella la vita). Merci pour tous ces bons moments partagés pendant ces trois années de thèse, autour d'une correction de publication ou d'une bière. Je tiens également à remercier Isabelle pour son soutien et la confiance qu'elle m'a accordée. Nos voyages à Lisbonne ainsi qu'à Florence resteront parmis les bons moments partagés ensemble, ainsi que toutes nos discussions (scientifiques ou non). Je souhaite également remercier Emmanuel, qui a su m'encourager, me soutenir également pendant ces trois années de thèse. Le passage à Lisbonne et à Copenhague, malgré mon extinction de voix, seront toujours de bons souvenirs à se remémorer. Ainsi, je vous adresse ma très grande reconnaissance pour votre bienveillance, gentillesse et confiance à mon égard. Ces trois années de thèse sont le fruit de nombreuses réunions, discussions et aboutissements réalisés tous ensemble. Un grand merci également à Fabrice et Xavier pour leur soutien sans faille et leur aide au cours des trois ans.

Un grand merci à mes collègues de l'INTERREG, qui m'ont toujours fourni en échantillons (microporteurs, cellules et autre) et en idées d'expériences, j'ai beaucoup apprécié de travailler avec vous tous. Je souhaite tout particulièrement remercier Romain et David qui ont pu fournir des microporteurs et leur faire traverser les frontières. Merci à Dima, ma fournisseuse officielle de cellules. Merci à Gosia pour les expériences que l'on a réalisées en Allemagne, et surtout les bons moments partagés ensemble. Je tiens également à remercier l'Europe et la grande Région pour le transport de "marchandises" à travers les frontières dans ma petite voiture, et les fameux autocollants Interreg, merci à Arnaud d'avoir géré mes nombreuses commandes Interreg !

Je remercie tous mes collègues pour leur soutien dans la vie de tous les jours, car la vie de thèsard c'est un peu comme être dans des montagnes russes, il faut être bien accroché. Merci Aline, Léna, Mengyao, Chafik, Amani, Daniel, Xavier, Manu R, Latifa, Arnaud, Fabrice, Eric pour les joyeuses discussions du midi. Un remerciement encore plus particulier pour Céline, pour tous les moments partagés autour de nos petites cellules (oui, elles sont vraiment capricieuses !), ou autour d'une bière. On se souviendra aussi de ce premier bio lancé ensemble, drôle d'aventure ! Merci également pour toutes nos discussions et ton soutien. Merci à Julien, fournisseur officiel de bière et de patisseries !

Merci Fanny pour ta présence, ton sourire et ces moments passés ensemble sur le montage de bioréacteur, avec plus ou moins de succès. Merci à la team SVS, Sara, Mélo et Odile pour nos sorties, les bbq et autres visites. Sans oublier, mon Tic, Sophie, merci pour ton soutien, ton aide, et surtout pour nos séances de sport - potins - fous rires (traitement thérapeutique idéal), nos sorties, et toutes nos discussions. Je suis heureuse que l'on ait eu l'occasion de profiter de Florence ensemble, de supers souvenirs ! Heureusement que l'aventure a pu continuer après l'ENSAIA, et continuera encore !

Merci à la famille Olmos, Eric, Maud, Paco et Nina de m'avoir fait découvrir cette belle région Lorraine à travers des visites, des festivals, des barbecues et autres balades.

Merci à l'équipe du bureau, alias team trop mimi, Aurélia, Charlotte, Anne et Jonathan, pour tous les bons moments passés ensemble. Le combo bento/vidéo de hamster restera dans les mémoires. Merci pour votre soutien et votre présence, sans cela, la thèse n'aurait pas eu la même saveur. Merci Jo pour ton soutien, ton aide, nos chamailleries, nos discussions, et surtout nos innombrables formations de l'école doctorale faites ensemble. Tu noteras que je ne cite pas tes blagues...

Je tiens à remercier mes amis de toujours, pour les sorties, les week-ends ou même juste les coups de téléphone, mais qui font toujours du bien. Merci à Titou, Gabou, Marion, Tiphaine pour les week-ends à Tours, à Saint Quentin, à Naples, à Royan, et bien d'autres endroits encore à venir. Merci à Pauline, pour ta visite sur Nancy et d'être toujours là pour moi. Merci à Romain et Laura, pour les bons souvenirs ensemble, de l'ENSAIA jusqu' aux vacances en Espagne. Merci à VDK pour nos sorties entre Bordeaux et Nancy. Merci à Jeanne pour nos discussions téléphoniques ou nos retrouvailles à Arcachon. Merci à Laurie pour ton soutien. Merci à Camille, qui depuis le collège est là pour moi.

Merci à vous Papa et Maman, mes frères, Matthieu, Guillaume et Paul, Kinai mon petit chat, et toute ma famille pour votre soutien sans faille sans lequel cela n'aurait pas été possible à réaliser. Vous m'avez toujours soutenue et épaulée, je vous en remercie infiniment.

Enfin, je tiens à remercier la personne la plus importante, la plus méritante et sans qui je n'aurai pas pu aller aussi loin: Emile. Merci de m'avoir soutenue, réconfortée, et d'avoir toujours su m'écouter. Merci d'être à mes côtés, et je l'espère pour le plus longtemps possible encore.

Contents

List of Figures

List of Tables

Introduction

Biologic drugs are now ten years old, with the first discovery of monoclonal antibody production in 1970s, and with the first approbation for a human use in 1986 by the Food Drug Administration (FDA) (Othoclone OKT3). Monoclonal antibodies and vaccine production by biological platforms are now well documented and well known and industrial scale production is now well implemented. Advanced therapy medicinal products are becoming an increasingly important part of our healthcare systems for the last 5 years. They are classified in four main domains, (1) the gene therapy with for example the development of CAR-T cells, (2) the cellular therapy with the use of mesenchymal stem cells, (3) the cellular engineering and finally (4) the advanced therapy combination medicines. The introduction of these advanced therapy medicinal products requires scientific expertise, production facilities and dedicated research and development centers.

More specifically, mesenchymal stem cells extracted from the Wharton's jelly of human umbilical cords (hWJ-MSC) are of increasing interest for cell therapies due to their reduced immunogenicity, high expansion capabilities, fast growth kinetics and various growth factors production capabilities. Thanks to their specific properties, they offer promising results for diseases that lack of effective treatments, such as cardiac failures, neurodegenerative diseases, diabetes, septic shocks or CoronaVIrus Disease (CoVID-19), for example. However, despite their promising results, high quantities of cells (10^9 - 10^{12} cells per lot) are required to be effective, which clearly raises issues of cell production and thus bioprocess development and scale-up. In order to reach a high amount of cells for clinical application, it is important to develop scalable culture systems including bioprocess control and monitoring. In 2020, more than a thousand clinical trials were listed on the website http://clinicaltrial.gov.com, with over 47,000 of patients involved around the world. Olsen *et al.* established that the estimated yearly consumption of hMSC was 8×10^{12} in 2020, for academic and preclinical researches. In 2040, the MSCs consumption for only the cell therapy could reach 300×10^{12} cells if 10 products were approved by FDA. About million of T-flasks (175 cm^2) or stirred tank bioreactor of the order of magnitude of several m^3 would be required to produce this large amount of cells. Over the next few years, the high demand for cells will become a major bottleneck if no industrial production process is proposed for the efficient expansion of MSCs, while complying with the Good Manufacturing Practice (GMP). Moreover, in major crisis times, such as in 2020 with the COVID-19, it is an important issue to be able to obtain large quantities of cells in a short time with controlled costs for potential treatments of a large number of people.

A large variety of expansion processes technologies exist from 2D planar to 3D microcarrier

cultures. Historically, the first methods used for culture of adherent cells were the flasks, but major bottlenecks were revealed, such as the limited surfaces, high operating costs and risks of contamination. Then, in order to scale up cultures, stirred tank bioreactors appeared to be a good alternative. In the literature, a lot of studies were already published about the use of stirred tank bioreactor (STR) for the culture of mesenchymal stem cells, the majority of these STR were set-up in batch mode and were not well-optimized. Thanks to their versatility, different options of mode of operation could be implemented. Expansion in stirred tank bioreactors implies the use of microcarriers, spherical particles of 200 µm of diameter, as MSCs are adherent dependent-cells and consequently need to attach to surfaces to grow.

This thesis work is in the continuity of work carried-out in recent years at the Laboratory Réactions et Génie des Procécédés (LRGP) of Nancy (UMR 7274), under the direction of Pr. Eric Olmos, Dr. Emmanuel Guedon and Pr. Isabelle Chevalot. The first works in the field of MSCs were developed by Caroline Ferrari in 2008 in the laboratory. Validation of different expansion protocols were carried-out using porcine MSCs of bone marrow. In 2012, Céline Martin proposed a validated protocol for culture of human MSCs of bone marrow, in static and dynamic conditions. Finally, in 2015, Céline Loubière developed new strategies for the expansion of hWJ-MSCs. Knowledge has been acquired over the years on the culture of stem cells, and a real know-how belongs to the laboratory concerning this field of study. The aim of this thesis work is to continue the study of different methods of expansion of WJ-MSCs, notably to set-up a continuous perfused mode in a stirred tank bioreactor to improve process performance.

The work presented in this manuscript was carried-out in collaboration with different laboratories within the framework of an European INTERREG project called Improve-Stem. Five scientific tasks were defined as, (1) the surface modification of microcarriers, (2) the analysis of microcarriers reactivity with proteins and stem cells, (3) the bioreactor design, (4) the expansion of stem cells in bioreactor, (5) the MSCs harvesting and characterization after expansion. These different tasks are presented in the figure 1.

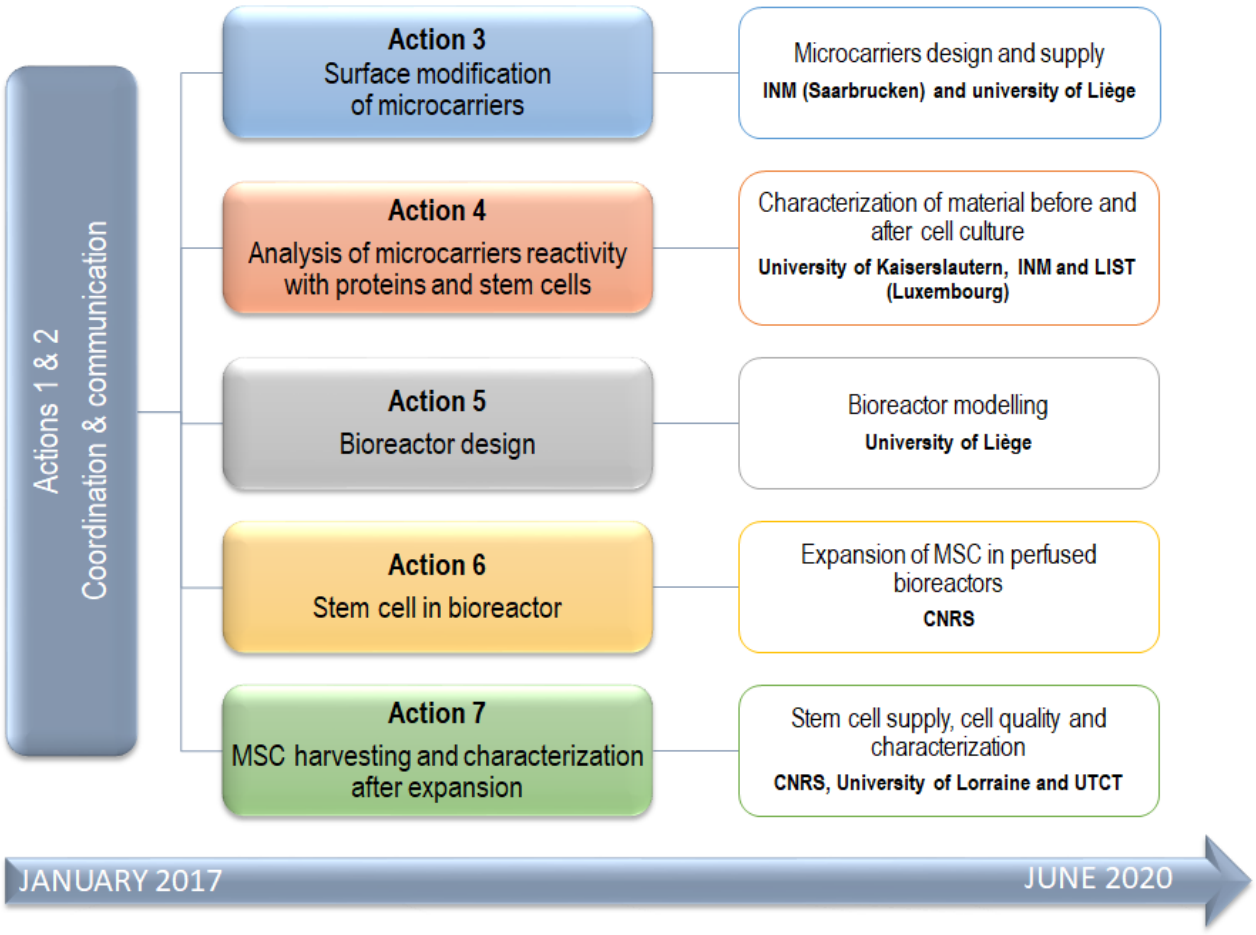

Figure 1 – Consortium organization and key actions in the frame of the INTERREG 'Improve-Stem' project.

In this context, the general objective of this thesis is to develop an optimized perfused-continuous process of culture of human umbilical cord mesenchymal stem cells (hMSC) grown on innovative adhesion supports.

The first part of the manuscript (State of the art) established all the current knowledge about the MSCs through the analysis of articles of the literature, with a specific attention paid to the methods of expansion and the control of their quality. Then, the different results obtained during the three years were organized as presented in the figure 2.

The first goal of this thesis work was to optimize and understand the interactions between cells and microcarriers. As WJ-MSCs are adherent-dependent cells, new insights about the cell adhesion on microcarriers would be useful to better understand cell expansion. WJ-MSCs culture on microcarriers are usually limited in time in batch-mode. Different causes are indeed involved in the stop of cell growth, such as a depletion in nutrients or a limitation of growth surfaces. In literature, various strategies of cell culture medium or sometimes of new microcarriers addition could be found to overcome this situation ; however, these strategies are generally set-up empirically. An adapted strategy of new microcarriers addition is developed in this chapter of the thesis to rationalize process operation.

The second task of this thesis is to transpose these developed methods of expansion in stirred

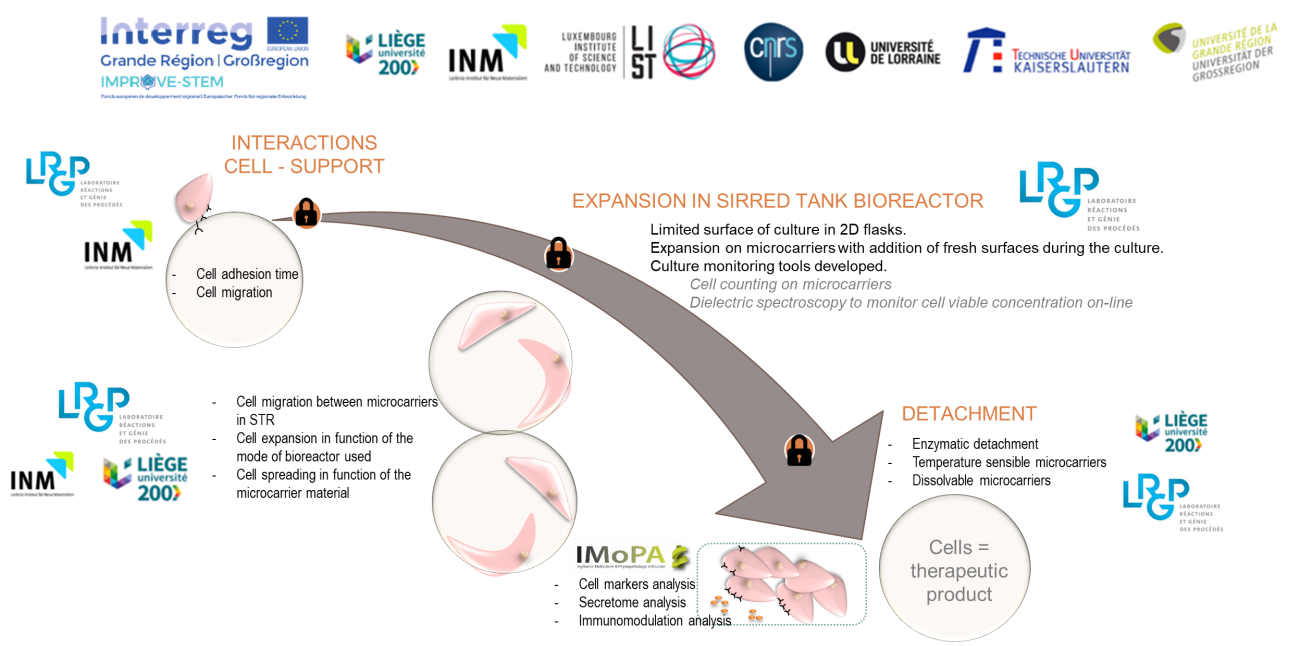

Figure 2 – Main problematics to solve for the study of MSCs expansion on microcarriers.

tank bioreactors. Bioreactors systems increased in interest thanks their ease to scale-up, the possible pH, temperature and dissolved gases monitoring and control and the limitation of nutrient concentration gradient via mechanical mixing. Optimization of the WJ-MSC expansion in stirred tank bioreactors by determining the most adaptive set of operating conditions and microcarrier chemistry is thus the aim of this chapter, by integrating the strategy of microcarriers addition developed in the previous chapter.

Finally, the last chapter of this thesis aims at developing an innovative mode of culture of WJ-MSC in stirred tank bioreactors. Development of bioprocesses capable of producing large numbers of hMSC in a robust and safe manner is critical for therapeutic applications. A new innovative perfusion system was implemented in the bioreactor, with addition of fresh microcarriers and a perfusion system for the cell culture medium in order to avoid depletion in nutrients and growth factors.

Chapter 1

State of the Art

Contents

1.1 Mesenchymal stem cells (MSCs) and their benefits in cell therapy

1.1.1 Variety of MSCs

Each multicellular organism is composed of a particular arrangement of specialized and non-specialized cells. These cells, depending on their localization and their integration into the tissue, have specific purposes, activated by the expression of specific and unique genes. These specialized cells come from non-specialized cells, called stem cells, because of their immature and undifferentiated profiles. Two main properties are used to describe stem cells, self-renewal and the ability to differentiate in more specialized cells. A first classification has been proposed, based on chronology. Thus, embryonic stem cells, fetal stem cells and adults stem cells could be distinguished. However, an other classification exists, and it is based on the potential of differentiation of stem cells. Originally, after the fertilization of the oocyte, the first cell divisions occurred. These cells are capable of differentiation into all cells of the organism (embryonic tissue and extra-embryonic), and are the only ones to ensure the complete development of the individual, and are described as totipotent stem cells. Pluripotent embryonic stem cells are derived from the 3-5 day embryo status, called a blastocyst. They participate in the formation of all cell types in the organism, with the exception of extraembryonic tissues, and they cannot lead to the construction of a complete person. Multipotent stem cells are cells whose spectrum of differentiation is limited to a number of cell types. Oligopotent cells can only generate few cell types from the same tissue. Finally, unipotent stem cells are able to differentiate into a single cell type with the ability to self-renew.

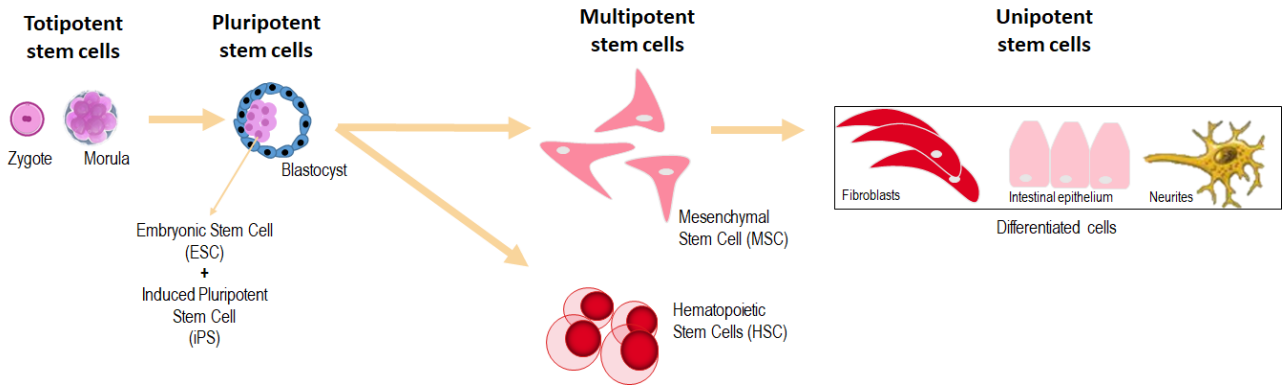

Figure 1.1 – Classification of stem cells. Figure inspired from Martin [1].

Pluripotent stem cells

Embryonic stem cells (ESCs) are pluripotent stem cells, derived from totipotent cells of the internal mass of the blastocytes [2, 3], as illustrated in the figure 1.1. These cells are described as cells with normal karyotypes and high expression of telomerase activity. As cited in the work of Thomson *et al.* [4], after undifferentiated proliferation *in vitro*, these cells maintained the developmental potential to form all the three embryonic layers, *i.e.*, endoderm (gut epithelium), mesoderm

(cartilage, bone, smooth muscle, and striated muscle), and ectoderm (neural epithelium, embryonic ganglia, and stratified squamous epithelium). However, concerns about the use of embryonic stem cells in clinical trials remain in mind, simultaneously regarding the possible mutation of cell lines in cancer lines, but above all ethical concerns. Indeed, the use of embryonic stem cells in clinical trial will require the destruction of embryos [5, 6]. In that regard, research on embryonic stem cells, in France, are only authorized with derogation. Nevertheless, they are authorized in United States, since 2009.

In 2006, Takahashi and Yamanaka discovered the possibility to convert somatic adult cells into cells presenting all the embryonic characteristics [16]. These cells called induced pluripotent stem cells (iPS), were obtained thanks to the transfer of viral vectors carrying genetic sequences of 4 defined factors, OCT4, SOX2, KLF4 and MYC. By cultivating in a favorable environment, these genetically modified cells will become pluripotent stem cells. Since now, the technology to produce iPS evolved in parallel with molecular biology, and would permit to avoid mutagenesis due to uncontrolled integration. The use of iPS is very promising in the creation of human disease *in vitro*, fabrication of organoid in 3D, and in regenerative therapy. However, the risks of a genetic instability, created by the artificial reprogramming of the cells still remain.

Adult stem cells

To avoid ethical concerns about the use of embryonic stem cells, scientists have focused their research on adult mesenchymal stem cells (MSCs) and their potential. Today, about 80 % of clinical trials use adult mesenchymal stem cells (Clinicaltrials.gov). Primary adult mesenchymal stem cells could be isolated and cultivated *in vitro*, they are considered as multipotent cells, and could come from different specific niches in the body, as represented in the figure 1.2. It is in 1978 that Schofield *et al.* [7] developed the concept of cellular niche. Primary adult stem cells could be localized in the bone marrow [8], in adipose tissue [8], in muscles [9] or in peripheral blood [10], and in a less amount, in dental pulp [11] and in thymus [12]. Other niches of mesenchymal stem cells could be used, without ethical concerns, and come from perinatal tissues. For instance, placenta [13], Wharton jelly [14] or umbilical blood could be used for mesenchymal stem cells extraction and expansion. This will be developed later in the study.

1.1.2 A brief history of MSCs

The concept of stem cells was born at the end of the XIXth century. It introduced the assumption of ability of self-renewal of certain tissues (as blood or skin, for example). It was in 1960, for the first time, that Friedenstein and co-workers [17] demonstrated that a minor sub-population of bone marrow (BM) cells had an osteogenic potential, revealed by heterotropic transplantation. These cells were distinguishable by their shape (fibroblast-like form) and in particular, rapid adherence to plastic. Bone marrow fibroblast cultures were able to spontaneously form bones in the adequate environment. Fibroblasts from bone marrow were inducible to osteogenesis in diffusion chamber. Moreover, scientists demonstrated ability of colony forming (Figure 1.3).

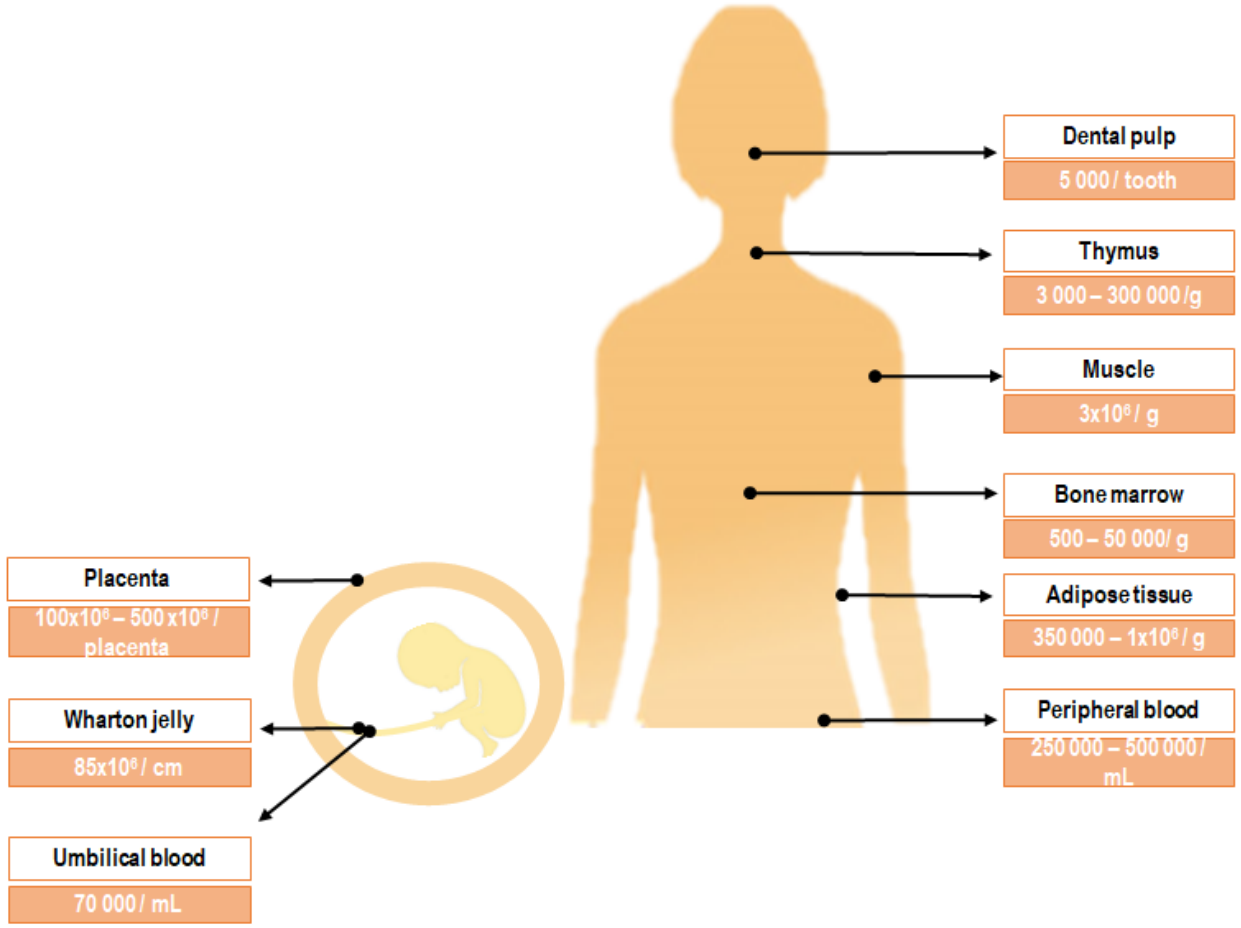

Figure 1.2 – Localization of sources of adult stem cells. Figure inspired from Loubière [15].

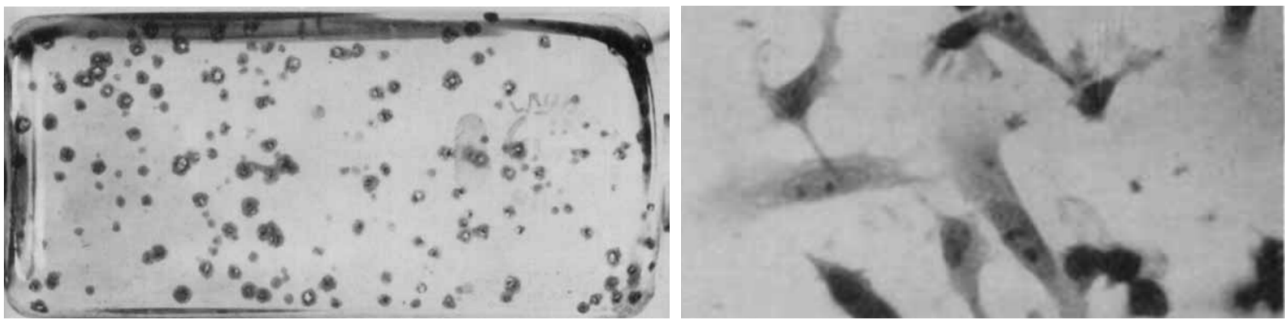

Figure 1.3 – First observation of mesenchymal stem cells. (A) Monolayer culture of bone marrow cells and colony forming demonstration after 12 days of culture and (B) fibroblast-like cells morphology of bone marrow cells of guinea pigs after 6 days of culture.

In 1990, Caplan gave the definition of mesenchymal stem cells, as an alternative to 'stromal' or 'osteogenic' stem cells [18]. The study of these mesenchymal stem cells provided basis of the first technologies of self-cell repair therapeutics. Indeed, first experiments of transplantation of bone marrow (BM) to heterotopic anatomical sites resulted in new generation of ectopic bone and marrow.

Then, Pittinger isolated for the first time a MSC population and observed their differentiation

in 1999 [19]. Leblanc *et al.*, demonstrated in 2003 that adult MSC seemed to be not immunogenic, reduced alloreactivity and the formation of cytotoxic lymphocytes *in vitro* [20]. The immature profile of MSC allowed their injection into patients without immunosuppressive therapies. However, it is only in 2006, that criteria defining the group of mesenchymal stem cells by the International Society for Cellular Therapy (ISCT) were published [21]. As the considerable therapeutic potential of human mesenchymal stem cells increased, minimal criteria to define these cells became necessary. First, MSC should be plastic-adherent in *in vitro* cultures. Secondly, MSC should respond positively to surface markers CD105, CD73, CD90, and should be negative to surface markers CD45, CD34, CD14, or CD11b, CD79a, CD19, as well as for HLA markers. Finally, MSC must be able to differentiate, *in vitro*, into osteocytes, chondrocytes and adipocytes. Those criteria are illustrated in figure 1.4. These different time-points are represented in the figure 1.5 A.

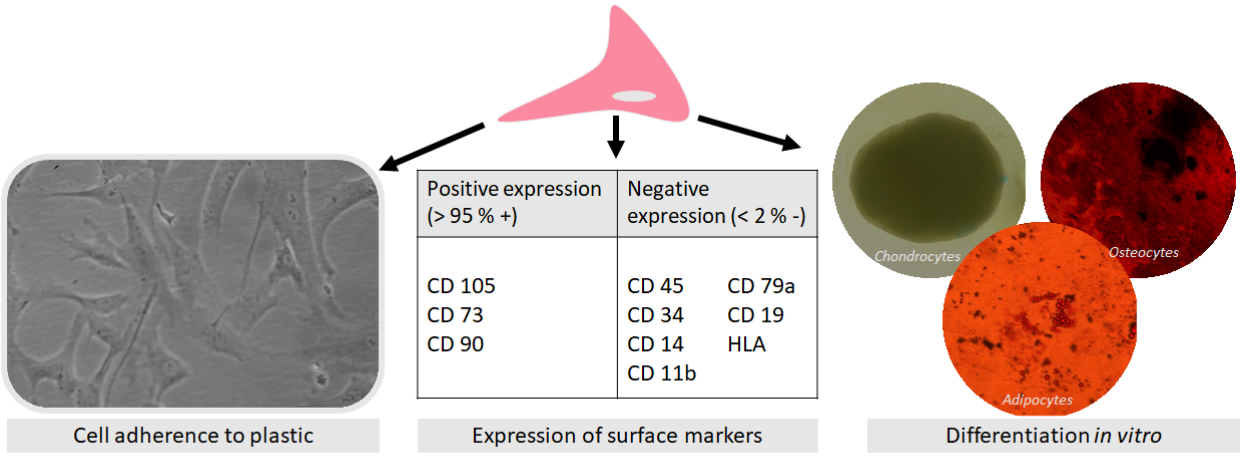

Figure 1.4 – Criteria of MSC definition adapted from Dominici [21].

Since then, an exponential increase of number of publications about the expansion of MSC, as it is shown in the figure 1.5 B, was noticed, demonstrating the potential in the therapeutic field of the MSC.

1.1.3 Therapeutic applications of cell therapies

As described before, MSCs are capable of differentiating into mesenchymal tissues, and contribute to the regeneration of these tissues such as bone, cartilage, muscle, cartilage, ligament, tendon, and adipose [22]. Highly interesting *in vitro* properties of MSCs, (i) self-renewable, (ii) clonogenicity, and (iii) differentiation, make these cells promising candidates for therapeutic treatments. Indeed, cell therapy is based on cell grafts in order to find back the organ or tissue function. Source of cells used in regenerative medicine is either autologous (from the patient himself) or allogenic (from a donor), with specific advantages and drawbacks, as shown in Figure 1.6.

In 2020, there was about 627 cases of MSC-based clinical completed, terminated or ongoing trials identified over the world (clinicaltrial.gov). These cases are mainly localized in United States,

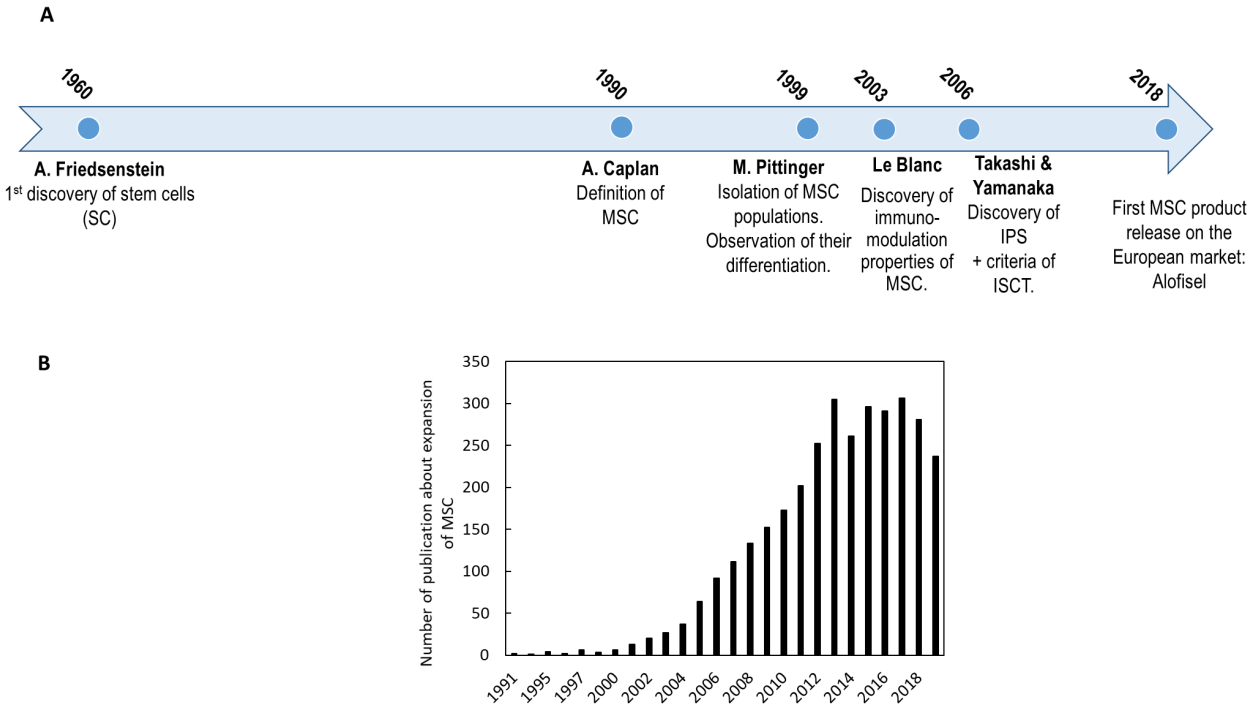

Figure 1.5 – Evolution of mesenchymal stem cells in the research area. (A) Time-line of the different discoveries about the MSC. (B) Exponential increase of number of publications about the expansion of MSC (Pubmed data base with the entry 'Expansion of mesenchymal stem/stromal cells', established in 2020).

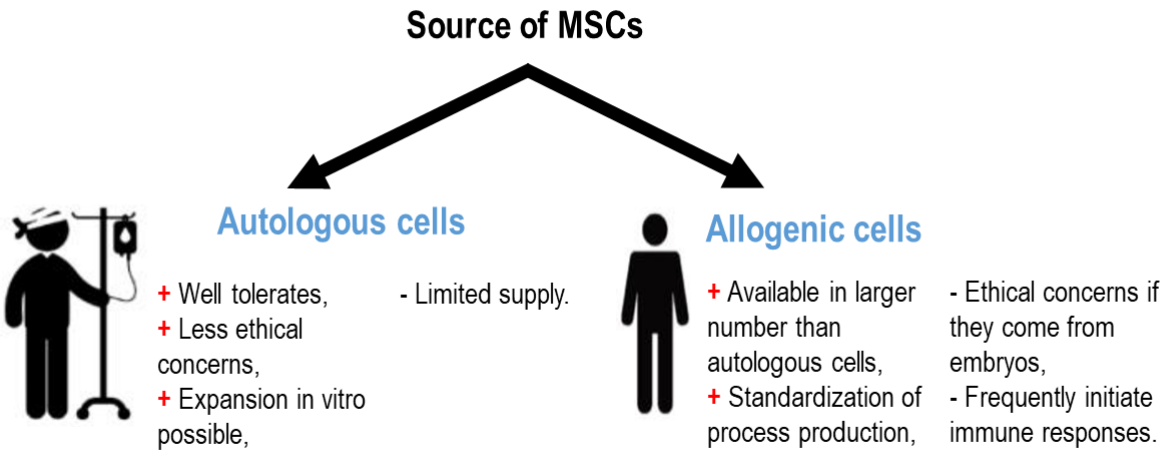

Figure 1.6 – Different sources of MSCs (LEEM).

Europe and East Asia (China). By looking more precisely at the different terminated trials using MSCs, presented in the table 1.1, a wide variety of diseases could be treated.

- **Cardiovasular applications**
  MSCs could have properties to heal cardiovascular diseases such as acute myocardial infarction or chronic heart failure thanks to the secretion of factors such as antifibrotic factors or proangiogenic cytokines. Several attempts have been made to induce MSCs to engraft in the myocardium, but it is controversial whether MSC undergo *in situ* differentiation. Since

the clinical tests demonstrated a better impact of the secreted factors of MSCs for healing, intravenous routes of administration were preferred and less invasive than intra-arterial or intra-myocardial administration [23].

- **Bone and cartilage applications**
  The major factor influencing the bone homeostasis is the balance between bone producing cells (osteoblast derived from MSCs) and bone resorbing cells (osteoclast derived from hematopoeitic stem cells). MSCs could directly impact the bone homeostasis by the production of factors stimulating the differentiation into osteoblasts. For example, bone marrow cells and expanded MSCs *in vitro* have been used in pre-clinical and in clinical trial to enhance bone engraftment. In animals, cells were introduced in hydroxyapatite tricalcium phosphate ceramics implants and re-introduced in femoral bone resection of the animals. Results showed a good enhancement of bone repair. Another good example of MSCs use in orthopaedic applications is for the treatment of osteogenesis imperfecta. This disease leads to fragile bones and skeletal deformities and is caused by defective type I collagen, a major structural protein in the bones. Horowitz *et al.* demonstrated that allogenic BM-MSCs transplantation could improve the growth velocity and mineralization of patients bones [24].

- **Central nervous system applications**
  An important number of studies showed that sites of strokes in adult rodent could be colonized by intravenously injected BM-MSC, able to migrate and differentiate into cells that express neuronal markers and thus, restored damaged neural cells [25, 26]. Importantly, reduction of functional deficits associated to strokes were found thanks to the safe transplantation of MSCs directly into adult rodent brains [26, 27]. It is well known that MSCs are able to secrete neurotrophic factors improving neuronal development, synaptogenesis and neurotransmission [28]. However, it is not totally clear how MSCs interact with the host tissues and the mechanisms or factors responsible for the improvement after stroke injuries are still unknown.

- **Hepatic and renal applications**
  MSC isolated from bone marrow, umbilical cord or adipose tissue could be differentiated into hepatic lineage after incubation with a specific growth factor as the hepatocyte growth factor (HGF) [23]. Adult rodent models have been implemented in order to mimic the progressive fibrosis and in order to evaluate the effect of injecting MSCs. Results seemed to be controversial, with sometimes attenuation of fibrosis and improvement of liver functions, and in some other studies, an impact of the MSCs was only noticed at the day of the injection, and 7 days after, no benefits of MSCs injection were noted [29]. Up to now, only limited data could be found about the impact of MSCs in treatment of kidney disorders. In some studies engrafted MSCs in damaged kidney restored renal structure and functionality by their differentiation ability [23]. Authors described a better effect of the local production of growth factors by MSCs either than their ability to differentiate for the renal applications.

- **Hematopoietic applications**

Stimulation of hematopoeitic cells growth is improved by MSCs in both *in vitro* and *in vivo* systems, thanks to the secretion of factors as interleukines, macrophage-colony forming stimulating, and other stem cells factors [23].

- **Crohn's disease**
  For patients with Crohn's disease, causing partially destruction of the intestinal mucosa, administration of MSCs appeared to be valuable. Usually, in phase II of clinical trials, when patients have failed classical treatments, an injection of MSCs seemed to decrease the Crohn's disease [23].

Table 1.1 – Clinical studies terminated or completed regarding the use of adult MSCs (www.clinicaltrials.gov, February 12^{th}, 2020)

Disease	**Enrollment number**	**Trial design**	**Effects**	**Clinical phase**	**Cell mass**	**Source**	**References**
Cardiovascular applications							
Ventricular dysfunction	9	MSC injection (low or high dose)	Reduction of infarct size and improved regional function. Importance of timing and localization injections.	Phase 1 Phase 2	2.0×10^7 cells and 4.0×10^7 cells	BM-MSC	[30]
Ischemic heart failure trial	37	Injection of autologous or allogenic hMSCs	Improvement of contractility of a chronic myocardial scar.	Phase 1 Phase 2	Autologous hMSC: 1.0×10^8 cells. Allogenic hMSC: 1.0×10^8 cells	BM-MSC	[31]
Non ischemic dilated cardiomyopathy	36	Injection of autologous or allogenic hMSCs	Clinically meaningful efficacy of allo-hMSC vs. auto-hMSC in NIDCM patients.	Phase 1 Phase 2	Autologous hMSC: 1.0×10^8 cells. Allogenic hMSC: 1.0×10^8 cells	BM-MSC	[32]
Arteriosclerosis	180	Transplantation of nanoparticules with a bio-engineered patch grown with allogenic stem progenitor cells.	Nanoburning + MSCs may improve the alteration of advanced plaque.	N/A	N/A	Aretery progenitor stem cells.	[33]

Disease	Enrollment number	Trial design	Effects	Clinical phase	Cell mass	Source	References
Bone and cartilage applications							
Osteoarthritis of knee	12	Injection of autologous hMSCs.	Valid alternative treatment for chronic knee osteoarthritis.	Phase 1 Phase 2	40×10^6	BM-MSCs	[34]
Neurological applications							
Incomplete spinal cord injury	10	Administration of adult autologous mesenchymal stroma cells.	BM-MSC intralesional transplantation can be useful to reverse sequels of traumatic injuries affecting the spinal cord.	Phase 1	Total of 120×10^6 cells.	BM-MSC	[35]
Spinal cord injury	12	Injection of autologous hMSCs.	Feasible, safe and may improve the quality of life for patients living with spinal cord injury.	Phase 1	100×10^6 then 30×10^6, three months later.	BM-MSC	[36]
Pancreatic, renal and hepatic applications							
Diabetes - diabetic peripheral neuropathy.	10	Transfusion of bone marrow mesenchymal stem cells.	Change of levels of fasting blood sugar after stem cells transfusion.	N/A	N/A	BM-MSC	NCT02387749
Diabetes - limb ischemia and foot ulcer.	40	Autologous transplantation of bone marrow mesenchymal stem cells.	Effective measure for recurrent bullosis diabeticorum. Study will require further investigation to be conclusive.	Phase 1	5.0×10^8 - 5.0×10^9 MSCs.	BM-MSC	[37]

Disease	Enrollment number	Trial design	Effects	Clinical phase	Cell mass	Source	References
Cirrhosis	6	Administration of adipose tissue derived stromal cells.	N/A	Phase 1	N/A	AD-MSC	[38]
Cirrhosis	266	Transplantation of umbilical cord mesenchymal stem cells.	Feasible and safe in the treatment of decompensated liver cirrhosis.	Phase 1 Phase 2	0.5×10^6 MSC/kg once per 4 week, for 8 weeks.	UC-MSC.	[39]
Chronic renal failure	6	Autologous bone marrow mesenchymal stem cells.	Safety and tolerability of intravenous transplantation of BM MSCs. Efficiency should be investigated with a larger population.	Phase 1	2×10^6 BM MSC/kg.	BM-MSC	[40]
Other applications							
Lupus nephritis	6	Injection of allogenic bone marrow mesenchymal stem cells.	Attenuation of lupus nephritis.	Phase 1	1.0×10^6 - 3.0×10^6 cells/kg.	BM-MSC	[41]
Skin disease - skin ulcers	20	Umbilical cord mesenchymal stem cells gel treatment.	N/A	Phase 1	N/A	UC-MSC	[42]

Disease	Enrollment number	Trial design	Effects	Clinical phase	Cell mass	Source	References
Idiopathic pulmonary fibrosis	8	Injection of placenta-derived MSCs.	N/A	N/A	1.0×10^6 - 2.0×10^6 MSC/kg.	Placenta derived MSCs	NCT01385644
Hematological disease.	6	Bone marrow mesenchymal stem cells transplantation.	Not sufficient for reliable engraftment in patients with advances hemoglobinopathy.	Phase 2	1.5×10^7 - 4.0×10^7 MSC/kg	BM-MSC	[43]
Acute Graft Versus Host Disease	1	BM MSCs infusions in addition to standard upfront therapy with corticosteroids.	N/A	Phase 1 Phase 2	10^6 MSC/kg 2 times up to 12 doses.	BM-MSC	NCT02379442
Crohn's disease	15	Implantation of autologous mesenchymal stem cells from adipose tissues.	Feasible and safe. Too low number of patients to demonstrate the treatment effectiveness, but encouraging for clinical phase 2.	Phase 1	3.0 - 30×10^6 cells.	AD-MSC	[44]
COVID-19	20	Infusion of BM-MSCs	Overall survival at 30 days post intervention. Clinical improvement.	Phase 2	2×10^6 MSC/kg 2 times	BM-MSC	NCT04444271

As presented in the table 1.1, a wide variety of diseases could be treated with MSC, especially with BM-MSCs. Nevertheless, they are limitations in the use of BM-MSCs for cell-based therapy. Indeed, procedure of collect of BM-MSC is invasive and painful. Limitations could also come from age of bone marrow stromal donors. Anyhow, the minimum dose required for those clinical trials was about 2.0×10^7 cells. A therapeutic dose should indeed contain between 2 and 3 millions of MSC$\cdot$ kg^{-1} [45], and repeated doses are often required. As it was shown on the figure 1.1, quantity and localization of MSCs are limited in the human body. While some companies as Osiris reported some failures in Phase 3 testing of their products, there are approved stem cell based products present in the global market, as presented in the table 1.2 [46].

Table 1.2 – List of commercialized treatments produced with MSCs

Name	**Disease**	**Source of cells**	**Country**	**Company**
Prochymal	GvHD	Allogenic BM-MSC	Canada	Osiris Therapeutic
Alofisel	Crohn's disease	Adipose stem cells	Europe	TiGenix and Takeda
Stempeucel	Crtical limb ischemia	Allogenic BM-MSC	India	Stempeutics
TemCell	GvHD	Autologous BM-MSC	Japan	JCR Pharmaceutical
HeartSheet	Heart failure	Allogenic skeletal myoblast	Japan	Teruno
Cupistem	Crohn's disease	Adipose stem cells	South Korea	Anterogen
Cartistem	Cartilage degeneration	UC-MSC	South Korea	Medipost
Pneumostem	Broncho-pulmonary dysplasia	UC-MSC	South Korea	Medipost
Neurostem	Alzheimer disease	UC-MSC	South Korea	Medipost
SMUP-IA-01	Treatment and prevention of osteoarthritis	UC-MSC	South Korea	Medipost
SMUP-IV-01	Treatment and prevention of diabetic neuphropathy	UC-MSC	South Korea	Medipost
HeartiCell gram-AMlis	Acute myocardial infarction	UC-MSC	South Korea	FCB-Pharmicell

Olsen *et al.* confronted the MSC global plan to the monoclonal antibody (mAb) production. Indeed, early discovery of mAb occurred in 1970, and the first approbation by FDA occurred in 1986 [47, 48]. Nowadays, in 2020, about 110 approved mAb drugs are available on the market in US and Europe [49]. hMSCs seemed to have the same trajectory to market development and infiltration [46]. In February 2020, about 1042 clinical trials using hMSCs were identified, with over 47,000

patients involved around the world. And by analyzing historical hMSC consumption, the high cell potentiality, and the developed applications based on the use of MSCs, it seems understandable that hMSC demand is today rising.

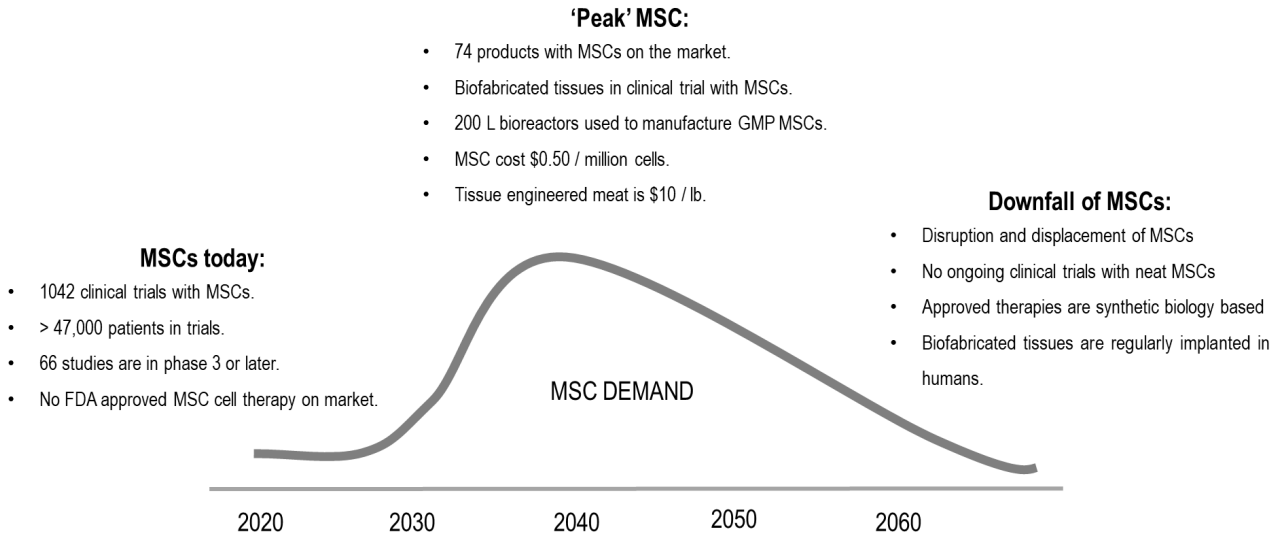

Figure 1.7 – Prediction of the rise and fall of MSCs [46].

Summary of the section

- High therapeutic potential of MSCs thanks to their specific properties;
- ISCT criteria to define MSCs;
- Abundance of niches in human body to find MSCs;
- Exponential peak of scientific publications and increase in number of clinical trials;
- Need of high quantity and quality cells in order to treat patients;
- 10 allogenic or autologous MSCs-based products obtained marketing authorization around the world.

1.2 Mesenchymal stem cells of the Wharton Jelly (WJ-MSCs)

1.2.1 Origin and characteristics of the Wharton jelly

The umbilical cord is embryologically derived on day 26, and develops from the allantois and yolk sac. It is the vital link between the developing fetus and the mother. At birth it weighs approximatively 40 g, and its lengh is about 30 - 65 cm. The mean diameter is 1.5 cm. An english physician and anatomist, Thomas Wharton (1614-1673), firstly discovered and described the umbilical cord stroma, as a gelatinous substance, called Wharton's jelly after his name [50]. The composition is rich in proteoglycans, hyaluronic acid, collagenous fibers and have a role of protection, notably of blood vessels. Indeed, thanks to the structure of highly hydrated matrix, the Wharton's jelly protects the two arteries and the vein from clumping and provides flexibility. The cell population present inside the Wharton's jelly is composed of fibroblasts, myofibroblasts, smooth muscle cells and mesenchymal stem cells. Those cells are a unique combination of prenatal and postnatal stem cells properties [50].

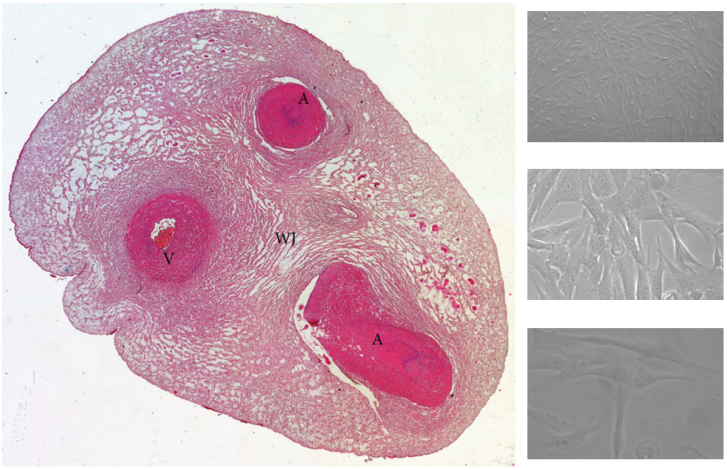

Figure 1.8 – Cross-section of the human umbilical cord. A: artery, V: vein, WJ: Wharton's jelly. Hematoxylin and eosin staining [50]. On the left side, microscopic observations of adhered mesenchymal stem cells of Wharton's jelly 3 days after the initial seeding. The cells have a fibroblast-like morphology.

A cross-section of the human umbilical cord is presented in the figure 1.8. The Wharton's jelly area is the connective tissue surrounding the umbilical vessels and includes the perivascular, intervascular and subamnion regions.

In 1974, after the extraction of progenitors and hematopoeitic stem cells in the umbilical cord blood, the remaining was considered as medical waste [14]. In 1991, when McElreavey *et al.* isolated fibroblast-like cells from Wharton's jelly, this point of view completely changed [51]. In 2004, Wang *et al.* [52], using flow cytometric analysis, found that WJ-MSCs express matrix receptors (CD44, CD105) and integrin markers (CD29, CD51), but no hematopoietic lineage markers (CD 34, CD45). Thus, by referring to the minimal criteria of ISCT, fibroblast-like cells could be considered as MSCs. Adherence to plastic and *in vitro* differentiation were also demonstrated. The origin of the MSC inside the Wharton's jelly is still discussed. The first established hypothesis was that fetal MSCs would migrated and colonized Wharton's jelly during the embryonic development. The

second hypothesis was based on that primitive MSC would be present in the matrix cord since the beginning of its formation [53].

Different techniques of cell isolation exist, the first one is based on enzymatic method and the second one is mechanical. After the delivery of the baby, the umbilical cord is collected and stored sterile. Ordinarily, the umbilical cord is processed in the 12-24 hours following birth [54].

1.2.1.1 Non-enzymatic technique of WJ-MSC extraction

Also called explant method, this method was firstly employed by McElreavey [51], in 1991. It is based on the inherent capacities of MSCs to migrate and adhere on plastic surfaces. After the withdrawal of blood vessels and epithelium, Wharton's jelly is cutted in pieces and placed in 6-well plates with cell culture medium. Spontaneously, WJ-MSCs migrated and colonized plastic surfaces of well-plates [55].

1.2.1.2 Enzymatic technique of WJ-MSC extraction

Pieces of Wharton's jelly were put into cocktails of enzymes as collagenase, hyaluronidase and trypsin [52]. The digestion occurred at 37°C during 30 minutes up to 16 hours. After the digestion, the suspension was filtered, washed then centrifuged. The remained cells are cultured. Recently, a new method associating enzymatic digestion and mechanical dissociation emerged. After an enzymatic digestion, the mix was homogenized mechanically. This method permitted to increase the cell extraction yield by a 160-fold factor [56]. After the cell extraction, cells could be either expanded in flask or cryopreserved in liquid nitrogen. In order to use cells in clinical trials, cell culture media have to be serum-free, and ideally, the isolation procedure has to involve minimal tissue handling and be less time consuming (about 3 or 4 hours to treat one cord).

1.2.2 Cells characteristics

Umbilical cord mesenchymal stem cells are particularly interesting because they are naturally more abundant than stem cells of the bone marrow. As it has been shown before they could be found in different specific areas. In addition, they exhibit promising proliferation performance [57]. Such characteristics reflect the relative primitive nature of these cells in comparison with their adult counterparts [58]. It has been shown an inverse relationship between adult age and MSC growth potential [59, 60], explaining the need to find alternative sources of MSCs. As demonstrated before, MSCs could be easily extracted from umbilical cord, without ethical concerns because extra-embryonic tissues are usually discarded after birth, while containing the needed characteristics of young cells.

1.2.2.1 Immunomodulatory properties of WJ-MSCs

Lu *et al.* demonstrated the ability of WJ-MSC to secrete cytokines, looking alike the ones secreted by BM-MSCs. Moreover, it seems that WJ-MSC were able to secrete factors as GM-CSF (Granulocyte Macrophage Colony Stimulating Forming) and G-CSFs (Granulocyte Colony Stimulating

Factor) which allow the multiplication of white blood cells [61]. This is noticeable from a therapeutic point of view, during a chemotherapy treatment, after a bone marrow transplant or during a treatment against Human Immunodeficiency Virus (HIV). The main area of use of WJ-MSCs would be allogenic transplantation, and one important requirement is low immunogenicity. In Prasanna & Jahnavi works, it was presented evidences that WJ-MSCs could be used in tissue repair and transplantation thanks to their unique inherent properties [62]. They express HLA-ABC (Human leukocyte antigen) at low levels, as a protection from Natural killer cell-mediated lysis [62]. WJ-MSCs do not express HLA-DR and co-stimulatory antigens (CD80 and CD86), implicated in activation of T and B cell responses [62, 63, 64]. Thus, WJ-MSCs would suppress the proliferation of simulated lymphocytes and have reduced immunogenicity.

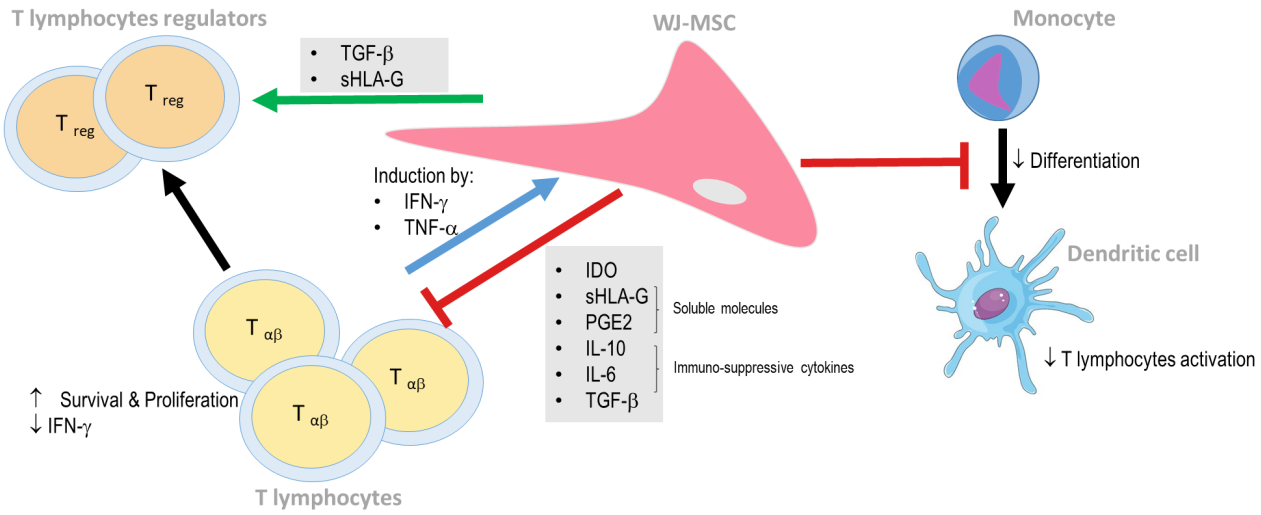

Figure 1.9 – Interaction process of WJ-MSCs with T lymphocytes. In allogenic situation, MSCs interact with immune system through several mechanisms leading to inhibition of proliferation of T lymphocytes, inhibition of differentiation of cells with antigens and appearance of T lymphocytes regulators. Figure adapted from Menard *et al.* [65].

The main immune response elements are T lymphocytes through their secretion of IFN-γ and TNF-α in allogenic situation [65]. MSCs are poor immunogen cells because of their low expression of HLA-DR or other co-stimulatory antigens molecules. Thus, they escape to the recognition by T lymphocytes. In parallel, MSC are able to modulate action of dendritic cells by altering their phenotypes, decreasing their cytokines secretion and blocking their differentiation process and their maturation.

1.2.2.2 Differentiation properties of WJ-MSCs

As required by ISCT, during *in vitro* cultures, and under specific culture conditions, WJ-MSCs are able to differentiate into chondrocytes, adipocytes, osteoblasts, but also into odonto-like cells, dermal fibroblasts, smooth muscle cells, skeletal muscle cells, cardiomyocytes, hepatocyte-like cells, insulin-producing cells, endothelial cells, neuroglia cells, and dopaminergic neurons [50]. Moreover, the authors of the study highlighted that the plasticity of UC-MSCs may depend on the conditions of the pregnancy. Thus, UC-MSCs from preclamptic patients, with a high blood pres-

sure associated with excessive proteins in urine, were more engaged in neuroglial differentiation [50]. Another example could be that UC-MSCs extracted from cords of preterm pregnancy lead to a decrease in osteogenic potential in comparison with cells from term pregnancy. At least, UC-MSCs obtained from gestational diabetes patients showed a decrease cell growth, a earlier cell senescence, lower adipogenic and osteogenic differentiation potential, and a low mitochondrial activity [50]. All these results could be interesting to take into account when choosing a source of cells for clinical use.

1.2.2.3 Secretory properties of WJ-MSCs

Mesenchymal stem cells are able to produce a wide variety of bioactive compounds. Quantitative studies of the proteome and the transcriptome showed that MSCs from different sources shared similarities, *e.g.* in their immune system process, response to stimuli. Although, MSCs are broadly used after differentiation and transplantation in the tissue to repair, these cells could be also used for their considerable potential of treatment thanks to their trophic secretions. Indeed, WJ-MSCs secrete a lot of different factors, involved in [66]:

- Angiogenesis (CXCL-1, CXCL, CXCL-5, CXCL-6 and CXCL-8) involved in the formation of new blood vessels;
- Vasculogenesis through the expression of genes for expression of CXCL-2, MDK, EGF, FGF-9;
- Outgrowth of neurites (NTF-3, MDK);
- Migration of neurons (HBEGF, MDK, EGF).

WJ-MSCs are also able to secrete cytokines and hematopoietic factors as G-CSF, GM-CSF, LIF, IL-1, IL-6, IL-8 and IL-11, which make them good candidates for hematopoietic stem cells expansion [50]. Two other studies demonstrated the ability of WJ-MSC to secrete specific factors as human insulin in response to physiological glucose levels, when they were differentiated into mature islet-like cell clusters [67, 68].

1.2.3 Therapeutic interests of WJ-MSC

Wharton jelly mesenchymal stem cells are used mainly in two distinct area: tissue engineering and cell therapy. Tissue engineering is a multidisciplinary area that combines techniques and principles of biology and engineering sciences. Thus, the goal of tissue engineering is to produce biological substitutes able to restore, fix or improve some organs or tissue. It is mainly used in bone regeneration, as cartilage for example [69, 70, 71, 72], but also, in skin regeneration, cornea layer regeneration, etc. The cell therapy is based on replacing deficient cells by healthy cells. The cell transplantation could be used in two ways: by regeneration of the pathological tissue thanks to the inner properties of differentiation and secretion of cytokines and growth factors, or by the induction of an inflammatory reaction thanks to immuno-modulations properties of MSCs. Therefore, in 2006, Weiss *et al.*, transplanted undifferentiated human UC-MSCs into brains of immunosuppressed hemiparkinsonian rats [73]. The injected cells improved the apomorphine-induced

rotations, a typical test settle for model of Parkinson's diseases. In the same time, in 2006, Conconi *et al.*, worked on the injection of undifferentiated WJ-MSCs into damaged skeletal muscles, and assisted to the muscle regenerative process thanks to the ability of WJ-MSC to spontaneously differentiate into myogenic lineage [74]. In 2007, Friedman *et al.* showed the applicability of the use of WJ-MSCs in human cell-based therapies, by using the cells as adjuvants for transplantation [75]. And in 2011, Peng *et al.* found WJ-MSC as a promising cell source for nerve tissue engineering by making the cells differentiated into Schwann-cell lineage [76].

Summary of the section

- Potentially unlimited source of WJ-MSCs. Non invasive and non painful for the donors. Absence of ethical concerns.
- WJ-MSCs show immuno-modulation properties, secretory properties and potential of differentiation that are promising for cell therapy and tissue engineering.

1.3 Towards scalable and manufacturing process for the production of human MSCs for cell therapy

1.3.1 The need in MSCs

Immunomodulatory hMSCs used in clinical treatments may involve autologous cells, isolated from the patient and used in personalized therapy, or allogenic cells, isolated from another individual and used in the patient after expansion. This second option offers the possibility to treat diseases affecting a large number of patients. Moreover as reported before, clinical trials have shown that a cell-dose required a minimum of 2.0 x 10^7 cells per dose, and often repeated doses are needed depending on the therapeutic indication.

As presented in the graph of the figure 1.10, the number of required cells only for clinical trials is huge, and consequently, it can be easily imaginable that for drugs and classic treatments a high demand of cells will occur. The main issue will be to produce a high amount of cells, cost-less and that they maintained their characteristics and properties in Good Manufacturing Process (GMP) conditions.

Moreover, MSCs naturally present in the human body represented only a few percentage of the total cell population, which will not permit to cover the needs for clinical therapies. Only a

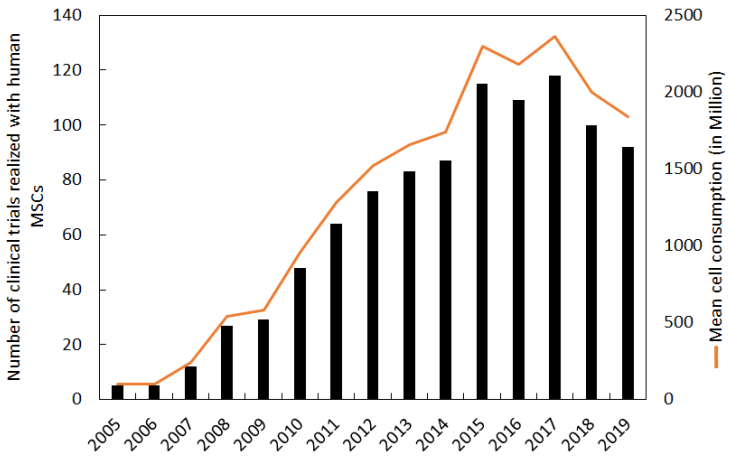

Figure 1.10 – Evolution of hMSC demand: number of clinical trials began with hMSCs and an estimated number of consumed cells during these clinical trials.

few drugs are already authorized on the cell therapy market, which highlights the importance of producing MSCs in large scale.

Human cells are classified as Advanced Therapy Medicinal Products (ATMP), and several rules and guidelines control the cell production. It is essential that extreme care is taken during the process production in order to produce the highest quality cells. Each step of the process requires to be controlled, regulated and checked regarding the GMP guidelines [77].

1.3.2 The market, current and potential

The therapeutic use of stem cells began with human hematopoietic stem cells (HSC), bone marrow and cord blood, in the treatment of aplasia, leukemia and hematological genetic diseases. Then, it developed with MSCs produced in small quantities by the marrow and other tissues as described above, and then used after isolation and culture. These new therapies are classified in Europe under the designation 'Medicinal Innovative Therapy ' or MTI whose regulatory requests are monitored by the European Medicines Agency and the national agencies of the member states. Value of market should reach 12 billion of $ in 2020, and 31 in 2026. Market growth has been of 11 % during the last five years. It represents only 1 % of the drug market today, but potential of cell engineering and cell therapy is important [78]. Thus, cell engineering of kidneys disease which aims at replacement of dialysis, the use of stem cells for dental bone regeneration or treatment of ischemic legs, frequently complication of diabetes with no solution nowadays, would permit, in case of validation of the clinical studies in progress, the emergence of very important new market segments. The market is driven mainly by the United States, with a value of $ 2.3 billion in 2016, facing Europe with 1.5 billion, where Germany dominates in front of its neighbors having an almost similar level of development: the United Kingdom, France in the 3^{rd} place, then Italy and Spain that are progressing rapidly. France has more than 90 academic teams mainly from 14 university hospitals and other public institutions: Inserm, CEA, CNRS, Institut Pasteur, Etablissement Francais du Sang. A dozen companies, mainly start-ups, work in the development of new products. However, none of the large national pharmaceutical companies have yet invested directly

in this market. The industrial production of MSCs is mainly based on the production of allogenic MSCs or iPS, and requires specific equipment of production (bioreactors), MSCs growth supports (microcarriers), separation process, and cell cryopreservation. Moreover these products are not only difficult to produce at large scales, but are also fragile and sensible to their environment. Furthermore, the regulatory framework for good practice manufacturing involves (i) standardizing the raw materials used which must also, be of reproducible quality over time and endorsed by the health authorities, (ii) allowing the implementation of batches large enough to meet all of the clinical features required by the regulator.

1.3.3 The cost of MSCs production

Based on the study of Mizukami *et al.* (2018) expansion and functionality maintenance of WJ-MSCs using different culture technologies were analyzed through a cost-prism. Indeed, cost of goods (COG) were determined for a multilayer vessel (MV), a stirred tank bioreactor (STR), for a pack-bed technology (PB) and an hollow fiber system (HF). The cost of production of MSCs is modeled for treatment of graft versus host disease [79].

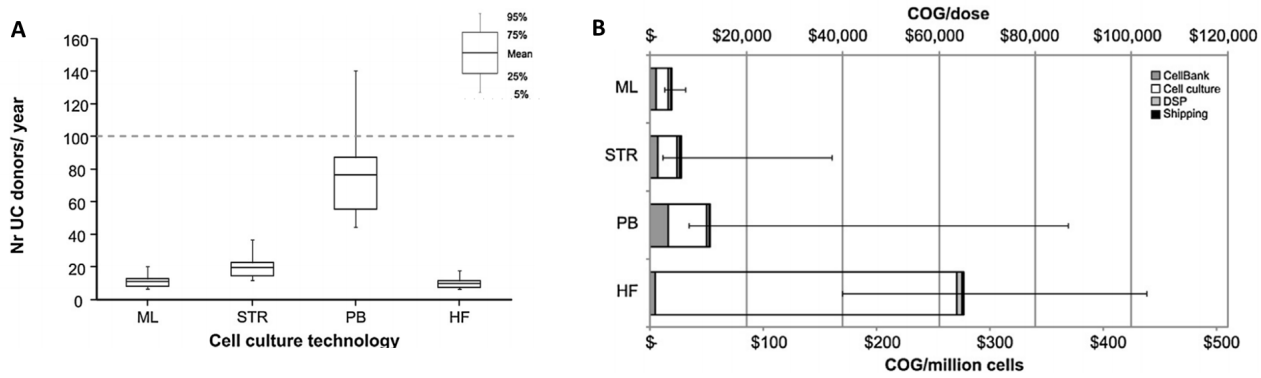

Figure 1.11 – Evaluation of the cost of MSCs production in bioreactors. (A) Distribution of number of donors required to manufacture 10,000 doses per year across multiple technologies. (B) Costs of goods (COG) breakdown per process stage with the error bars showing the min and max total COG/dose and COG/million cells across different technologies. The costs are expressed in US dollars ($) [79].

As shown in the figure 1.11, the most competitive technology to produce MSCs seemed to be multilayer vessels, with a COG/dose of 4.5 k$, followed by the stirred tank bioreactor with a COG/dose of 6.5 k$. In STR, a high yield of produced cells was obtained but the efficiency of harvesting needs improvements in order to be more competitive. In fact, if the harvest was optimized in STR, the COG/dose would decrease to 3.7 k$.

In order to produce MSCs for the clinical trials and large scale production, private companies based their research on the automated cell culture devices. Thus, systems like AutoCulture (Kawasaki) or the CompacT SelecT (Sartorius Stedim Biotech) implement robotics to automate some cell culture steps such as medium exchanges, centrifugation and passaging, performed during expansion in 2D-environment. However, several systems such as bioreactors are more effective for producing large scale of cells and do not employ standard cell culture flasks for the expansion.

For example the Xuri Cell expansion system (GE Healthcare) is an automated, controlled (temperature, pH and gases) expansion environment for the growth of cell therapies in volumes up to 25 L. Finally, the Quantum cell expansion system (Terumo BCT) cultivates MSCs adhered to a hollow fiber bioreactor, with a continuous medium perfusion (Figure 1.12 A, B & C). In the Russel *et al.* study, the cost of manufacturing doses of BM-MSCs produced in GMP conditions to treat 100 people was compared between a manual method of production and the use of the Quantum cell expansion system [80]. As presented in the figure 1.12 D, using an automated system permitted to divide by two the costs of consumables and reagents. Moreover, the time of production of 100 doses could be shortened of approximately 1 month, indeed 17 % of time could be saved using automated processes and that an average of clinical MSCs doses could be produced in 20 weeks. It is certain that these results depend on the growth kinetics of the cells and can be expected to change in function of the donor.

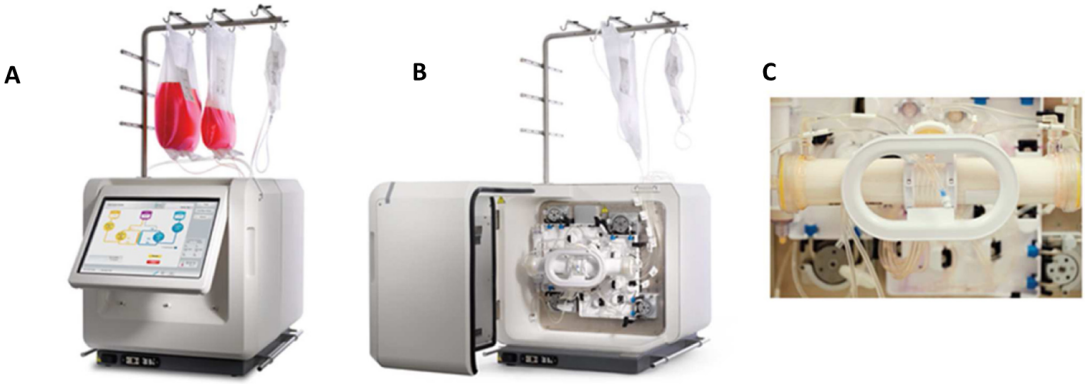

D

For trial of 100 patients	Quantum (Q)	Manual (M)	Difference (M – Q)
Cost to manufacture 100 doses	$107,743.38	$205,684.85	$97,941.47
Cost per dose of 100 × 10^6 cells	$1,077.43	$2,056.85	$979.41
Production time to manufacture 100 doses (weeks)	20.0	24.0	4.0
Hands-on time to manufacture 100 doses (hr)	35.0	361.6	326.6
Full-time equivalent	1	2	1

Figure 1.12 – Quantum cell expansion system and cost of MSC production. (A) Quantum cell expansion system showing touchscreen interface, partially filled medium and waste bags, and an empty harvest bag hanging from the integrated bag pole. (B) Quantum shown with door open and cell expansion set installed. Interior chamber serves as a 37°C incubator when door is closed. (C) Close-up view of hollow fiber bioreactor integrated within the cell expansion set where MSC expansion occurs. (D) Summary of the automated versus manual comparison to support clinical trial for 100 patients [80].

Summary of the section

- Production of allogenic hMSCs is challenging and there is a need of intensive research focusing on the production process.
- Until now, no large-scale protocols (> 50 L) were published.
- STR seemed to be the less cost-effective way to produce allogenic hMSCs for clinical therapies but still need improvements.

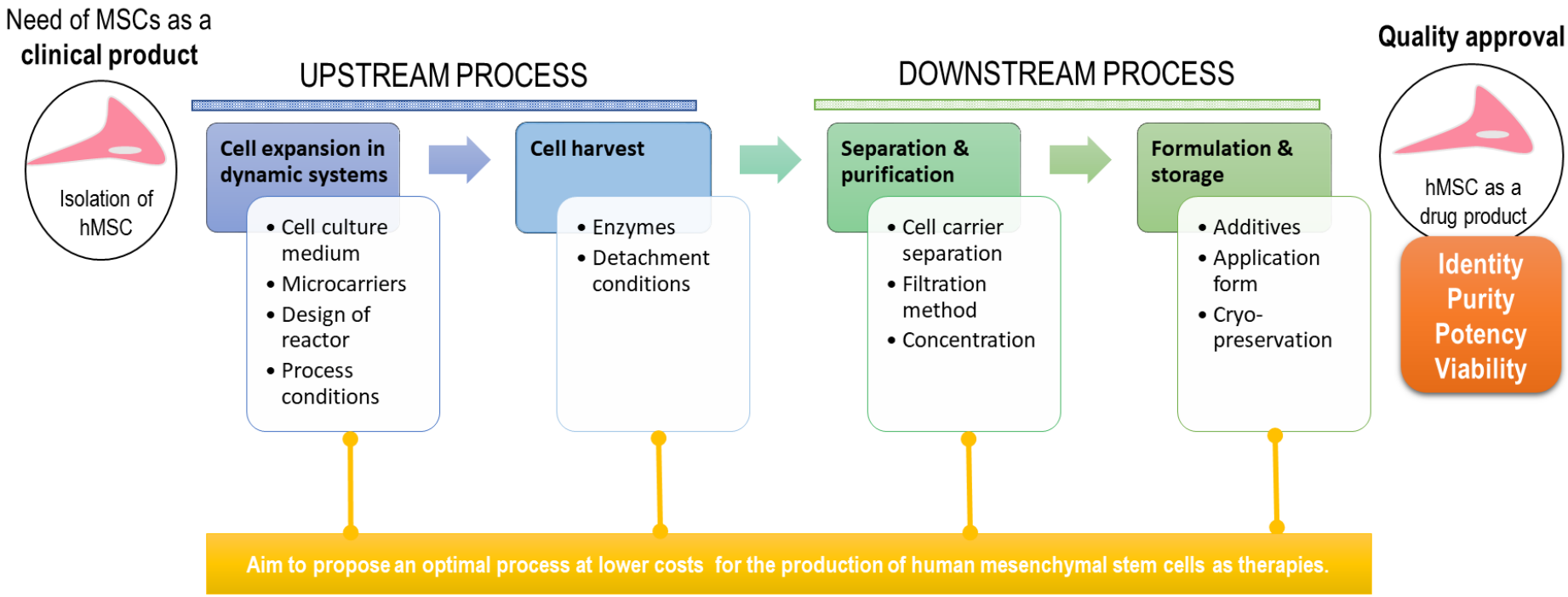

Figure 1.13 – General overview of a dynamic production process for hMSCs including various aspects that influence the final quality. Figure adapted from Elseberg *et al.* [77].

1.4 Description of MSCs production process

For cell therapies, number of cells purified from biopsies are generally not sufficient to display significant therapeutic efficacy, and *in vitro* expansion is generally needed.

1.4.1 Cell adherence

Cells are able to explore their environment through different mechanisms, notably through adhesion. Indeed, thanks to the extracellular matrix (ECM) cells can take into account physical and chemical properties of their environment, and the different signals transmitted will instruct the cells about the behavior to take (*i.e.* live, die or differentiate). ECM could be considering as the signaling centers, gathering and transmitted information to the cells through physically contact point called focal contacts, focal adhesion or focal complexes. Two levels of anchorage exist: (i) the cell to the ECM, and (ii) the ECM to the surface. In this section, macro-molecular mechanisms of cell adherence and migration would be developed, as well as the effects of the cell adherence on different types of materials and their characteristics from a molecular point of view.

1.4.1.1 Macro molecular mechanisms of cell adherence

In *in vitro* cultures, the cell life could be divided in to three main steps: (i) the adhesion to specific surface used for cell culture, (ii) the cell expansion and growth on its surface, and lastly (iii) the cell detachment. Cell adherence and migration are both mechanisms requiring energy because of the involvement of actin filaments, as a molecular motor. The phenomena of cell adherence and migration will be explained in details.

- **Cell adherence.**
  First, in suspension, adherent dependent cells have a specific rounded shape. By gravity, cells enter in contact with a surface, electrostatic and ionic forces permit a first contact between the ECM of the cell and the material. Usually, as it will be developed after, specific charged or hydrophobic surfaces are used in cell culture, in order to maximize the cell adherence. Integrins are the first compounds of the ECM to be involved during attachment. Transduction signals are sent to the cell, and the first morphological changes are noticed. The cell is spreading and flattening. Then focal adhesions are involved in stabilization of the cell adherence. The stabilization and the absence of movement on the surface require a continuously polymerization/ depolymerization of actin filament, an active process requiring energy to the cell. All these different steps are summarized in the figure 1.14.

- **Cell migration**.
  Cell movement is also an important process in a cell life. Cells are exploring their environment through the contact of their ECM and surfaces. Migration requires 4 steps. First, polymerization of actin filaments at the edge of the cells create a protusion and a cell extension, then new adhesion sites are created between the new cell extension and the surface, the cytoskeleton reorganization and the retrograde actin movement lead to contractile forces

pulling the cell body forward. Finally, a disassemble of focal adhesion and the contractile forces help to retract the cell extension.

Cell Adhesion Phases	Phase I	Phase II	Phase III
Schematic diagram of cell adhesion	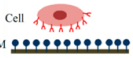	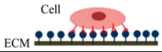	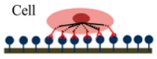
Schematic diagram of the transformation of cell shape	Initial attachment	Flattening	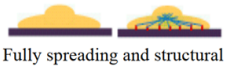 Fully spreading and structural organization
Cell adhesion intervension	Electrostatic interaction	Integrin bonding	Focal adhesion
Adhesion stages	Sedimentation	Cell attachment	Cell spreading and stable adhesion

Figure 1.14 – *In vitro* cell adhesion stages [81].

Modulation of cell activities and functions are possible as cells interact differently, in function of the material properties. In fact, cell adhesions are involved in transmembranal signaling processes that regulate cell behavior and fate.

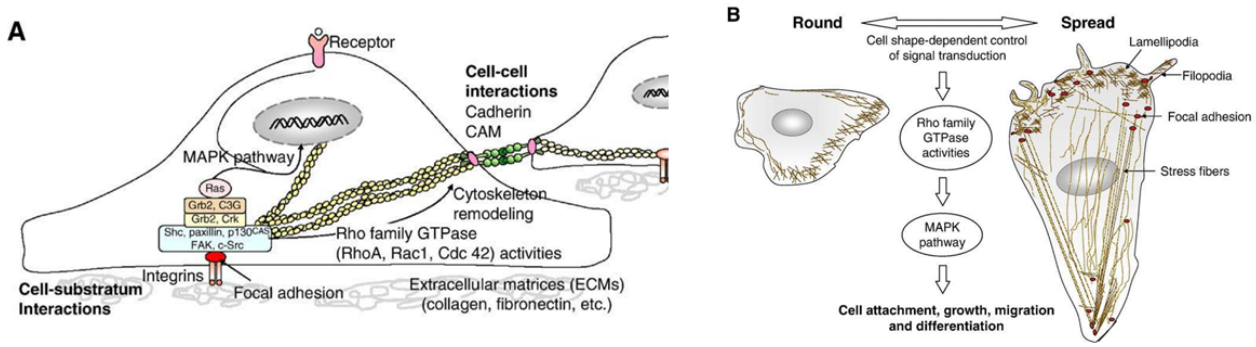

Figure 1.15 – Cell adherence and molecular mechanisms involved. (A) Schematic representations of focal adhesion and relevant elements. (B) Cell shape-dependant control of Rho family GTPases activites and MAPK pathway. Figure from Kim *et al.* [82].

1.4.1.2 Molecular complexity of focal complexes

Cell-matrix adhesions are crucial in biological processes as well as cell mobility, cell proliferation and cell differentiation. The adhesion to the matrix is made by the focal adhesion, a contact point between the cell plasma membrane and its ECM. At these sites, actin filaments are anchored to transmembrane receptors of integrins through a multimolecular complex made of plaque proteins. ECM are secreted by the cells and are made of complex chains of sugars (polysaccharides) and proteins (glycoproteins as fibronectin, laminin and thrombospondin), and include proteoglycans which confer to the ECM its hydrated structure. Inside this complex, some collagen and elastic fibers could be found. ECM are linked to the cells through integrins and focal adhesions. Integrins form strong ties between ECM and actin cytoskeleton of the cell. Focal adhesions are flat and elongated structures, associated with the actin filaments. It has been listed, at least, over 30 different molecules involved in the focal contacts [83]. In this great diversity of molecules, some are involved in physical linkage (of the membrane receptors to the cytoskeleton), while others are

involved as signal transduction molecules. The number of focal contacts, their size and distribution could widely vary between cells [84]. Focal adhesions and their interactions with cells could be observed in the figure 1.15 A.

1.4.1.3 Mechanisms related to cell-substrate interactions

According to the review of Kim *et al.*, changes in cell morphology activate signals transduction pathways involving FAK, Rho family GTPase and MAPK [82] (Figure 1.15 B). Rho family GTPases are involved in activation of the cytoskeleton, RhoA induced the formation of stress fibers and focal adhesion complexes. In addition, this cytoskeletal changes induced by Rho family GTPases are directly linked to the changes of cell morphology during migration or spreading. The different signaling proteins are activated during the initial phase of cell attachment, and during the last phase of cell spreading. In the case of MSCs, the cell fate could be affected by inner properties of the polymeric substrate on which cells adhered. Nanotopography or stiffness could influence cell expansion or differentiation, and biomaterial scientists will try to mimic physiologically relevant ECM stiffness, topography, and adhesion-ligand types [85]. Properties of stem cell/material interactions are not static during time. Degradation of by-products could influence stem cell function, as for example the endostatin a by-product of collagen degradation which acting on some growth factors production. Studies showed that ions (calcium, magnesium or fluoride) could influence the cell phenotype or differentiation [85]. Also, it has been shown that degradation of materials could impact cell metabolism. Nanostructural properties could also influence stem cells. It is not yet well clear how material stiffness can lead to large phenotypic changes, or how the rate of change in the stiffness of the material can influence cell behavior. Some transcription factors able to convert a stem cell to a mature cell have their expression sensible to material properties. Thus, cell contraction against a 40 kPa substrate in 2D or a shift of shape in a 3D matrix would induce transcription and expression of factors inducing osteogenic differentiation to the cells [85]. 'Hard material' would preferably lead to spreading, migration and sometimes to differentiation, whereas 'soft materials' have been shown to maintain self-renewal in embryonic stem cells and muscle satellite cells [86, 87].

Consequently, a particular attention should be paid to the surface material used for MSCs expansion in *in vitro* cultures.

1.4.2 Flask expansion: limitations of the 2D culture

The first developed technology to grow adherent-dependent cells was re-usable glass. Nowadays, treated plastic flat surfaces replaced the glass, and are single-use equipments. Plasma treatment permitted to obtain oxidized polystyrene, which favor cell adherence, and so, cell proliferation. Indeed, during the first phase of cell adherence, electrostatic and Van Der Waals forces are established by cells towards these charged surfaces. The amplification of cells is limited due to the mono-layer growth in flasks and that a too high MSCs concentration could lead to differentiation, or to apoptosis induced by contact inhibition. Moreover, they do not contain probes or sensors to control temperature, gas (*i.e.* oxygen, carbon dioxide) or pH. Among simplicity and low cost,

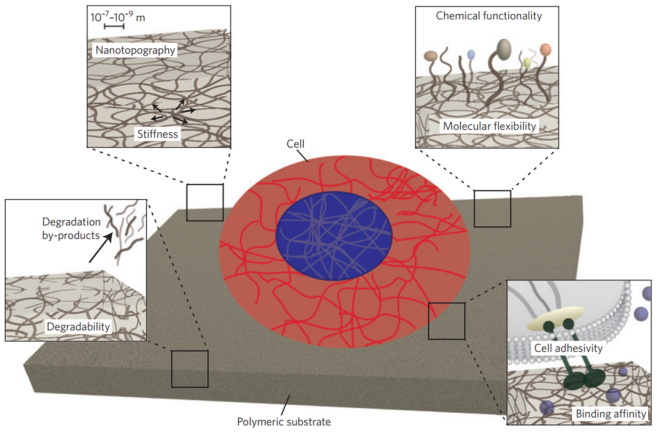

Figure 1.16 – Influence of material properties towards cells. Stem cell fate decisions can be affected by material properties (stiffness, nanotopography), by chemical functionality (colored beads), by degradability of co-products. Figure from Murphy *et al.* [85].

advantages of T-flasks are the microscopic observations of the adhered cells and the possibility to easily change the cell culture medium change. Nevertheless, the scalability is limited and needs a trypsination step that consists in cells detachment by enzymatic digestions. This process is time-consuming and increases contamination risks. The surface area for T-flasks ranges from few cm^2 to 300 cm^2. Based on this knowledge, companies developed multilayer systems. It consists in several stacks of culture plates, to provide surfaces in the order of 10 000 up to 100 000 cm^2. The developed protocols in single layer plates are the same in these systems, but they are more complicated to handle. Similarly to what occur in single layer plates, heterogeneity and gradients of nutrients, pH or gas in liquid phase may occur due to the lack of stirring of the system.

1.4.3 3D methods of expansion with the use of microcarriers.

Nowadays, 3D methods of expansion exist, namely, culture of cells on microcarriers, inside a scaffold, encapsulated and inside hydrogels. Only the culture with microcarriers will be developed in this section. In order to maximize the adherence surfaces available to the cells, culture processes of industrial and adherent continuous cell lines use for many years the technology of microcarriers in stirred tank bioreactors (STR) [88]. The microcarriers are particles with an average diameter between 100 and 300 µm, and that can be made of different materials. The agitation needs to be well-defined in order to efficiently homogenize the liquid-solid suspension and to permit a sufficient oxygen transfer while limiting hydrodynamic stresses.

1.4.3.1 Materials

A wide variety of materials have been used to produce microcarriers: plastics (polystyrene, polyethylene, polyester, polypropylene), glass, acrylamide, silica, cellulose, dextran, collagen, glycosaminoglycan, and designed to be either non-porous (*e.g.* plastic microcarriers), microporous (*e.g.* dextran based microcarriers) or macroporous (*e.g.* gelatin type microcarriers). One advantage of these macroporous microcarriers is to offer protection against shear stress to the cells in stirred tank bioreactors, but reduced nutrients and dissolved oxygen in the center of the macroporous micro-

carrier raised some concerns [89]. Apart from the core material that defines the matrix of each microcarrier, some functionalized surfaces can be added in order to improve either cell adhesion, growth or detachment.

1.4.3.2 Surface modifications

- **Chemical modifications**
  The most common modification of microcarriers is based on the addition of amino-groups (-NH_2) by chemical treatments, it is for example already the case for Cytodex-1 & 2, and Hillex-II [90]. The purpose of this modification is to improve cell adhesion. Carboxil groups (-COOH) are other common modifications to microcarriers to enhance cell adhesion, by increasing hydrophilicity of the surface. Different methods could be used, ultra-violet (UV) systems, and UV in combination with ozone plasma treatment. However, despite the chemical modifications, microcarriers lack of adhesive molecules (*i.e.* laminin and fibronectin), and supplementary coating could be considered. In addition, grafting of molecules such as (3-aminopropyl)trethoxy silane (APTES), enhanced the immobilization of either fibronectin or collagen type 1 on surfaces, and thus enhanced cell adhesion [91].

  Besides the chemical modifications to improve cell adhesion on the microcarriers as the NH_2 or COOH groups, it is also possible to graft sensible polymers to the cell environment. Thus, by modification of temperature or pH, the modification of the polymer layer will lead to the cell detachment. Moreover, some dissolvable microcarriers were also synthesized and under the action of enzymes lead to a total dissolution and release of the attached cells. This part is developed later in this chapter.

- **Microcarriers containing ECM-based materials**
  A specific pattern of amino-acids (arginin, glycine and aspartic acid) is usually present in ECM proteins such as collagen, laminin, fibronectin and vitronectin, and modification of microcarriers are based on this pattern, associated or not with chemical modifications. Thus, ECM from animals were the first compounds added to various commercial microcarriers (*e.g.* Cytodex-3, Collagen, FACT III), then commercial suppliers needed to respect GMP considerations and added xeno-free compounds or recombinant proteins. However, due to economic considerations, reduction of ECM compounds were more interesting for suppliers, and to keep the good cell adhesion factor, a combination of a cationic polymer (*i.e.* polylysine) and the specific amino-acid pattern was carried-out.

They could be positively charged or negatively charged, but also non-charged microcarriers are available. For hMSCs cultures it is possible to find in the literature properties of commercial available microcarriers, mammalian protein coated microcarriers, recombinant protein-coated microcarriers and xeno-free microcarriers, as presented in the table 1.3.

Table 1.3 – Properties of commercially available microcarriers

Microcarrier	Manufacturer	Diameter (in µm)	Matrix	Avg. density (g/mL)	Surface coating	Surface charge	Carrier porosity
MAMMALIAN PROTEIN-COATED MICROCARRIERS							
Collagen	Pall SoloHill	125-212	Polystyrene	1.02	Type 1 porcine collagen	None	Non-porous
Collagen coated MC	Corning	125-212	Polystyrene	1.02	Type 1 porcine collagen	None	Non-porous
Cultispher-G	Percell-Biolytica	130-180	Type 1 porcine gelatin	1.04	None	None	Macroporous
Cytodex-3	GE Healthcare	141-211	Dextran	1.04	Type 1 porcine collagen	None	Non-porous
Denatured-collagen coated dissolvable MC	Corning	200 - 300	Polygalacturonic acid (PGA) polymer chains cross linked via calcium ions	1.02	Denatured collagen	None	non-porous
FACT 3	Pall SoloHill	125-212	Polystyrene	1.02	Type 1 porcine collagen	+	Non-porous
SphereCol	Advanced BioMatrix	125-212	Polystyrene	1.02	Type 1 human collagen	None	Non-porous
RECOMBINANT PROTEIN-COATED MICROCARRIERS							
Pro-Nectin F	Pall SoloHill	125-212	Polystyrene	1.02	Recombinant fibronectin	None	Non-porous
XENO-FREE MICROCARRIERS							

Microcarrier	Manufacturer	Diameter (in µm)	Matrix	Avg. density (g/mL)	Surface coating	Surface charge	Carrier porosity
Cytodex-1	GE Healthcare	147-248	Dextran	1.03	DEAE	+	Non-porous
Cytopore-1 and 2	GE Healthcare	200-280	Cotton-cellulose	1.03	DEAE	+	Micro and Macro-porous
Enhanced attachment	Corning	125-212	Polystyrene	1.02	CellBind	None	Non-porous
Glass	Pall SoloHill	125-212	Polystyrene	1.02	High silica glass	None	Non-porous
Hillex CT	Pall SoloHill	90-212	Polystyrene	1.12	Cationic amine	+	Non-porous
Hillex II	Pall SoloHill	160-180	Polystyrene	1.12	Cationic amine	+	Non-porous
Plastic	Pall SoloHill	125-212	Polystyrene	1.02	None	None	Non-porous
PlasticPlus	Pall SoloHill	125-212	Polystyrene	1.02	None	+	Non-porous
Star-Plus	Pall SoloHill	125-212	Polystyrene	1.02	None	+	Non-porous
Synthemax II	Corning	125-212	Polystyrene	1.02	Proprietary peptide acrylate chemistry (Synthemax II)	None	Non-porous

Microcarrier	Manufacturer	Diameter (in µm)	Matrix	Avg. density (g/mL)	Surface coating	Surface charge	Carrier porosity
Synthemax II dissolvable MC	Corning	200 - 300	Polygalacturonic acid (PGA) polymer chains cross linked via calcium ions	1.02	Synthemax II	None	non-porous

1.4.3.3 Use of microcarrier in MSCs culture

No unified set of culture conditions of hMSCs (concentrations, protocols agitation) on microcarriers were described in the literature, but studies of microcarriers screening could be found. As for example, Schop *et al.* compared 9 different microcarriers in order to find the best candidate for the expansion of BM-MSCs [92]. This work was performed in serum supplemented medium, in spinner flasks with BM-MSCs. Nine microcarriers from different manufacturers were tested: Cytodex-1 and 3 (GE Healthcare), ProNectin F (SoloHill), Hillex II (SoloHill), Glass (SoloHill), Plastic (SoloHill), PlasticPlus (SoloHill), FACT III (SoloHill) and Collagen (SoloHill) (Figure 1.17). The Cytodex-1 showed the highest seeding efficiency compared to the other microcarriers. The highest number of hBM-MSCs was obtained by a combination of 50 % medium refreshment with addition of 30 % of microcarriers every 3 days. Duration of cultures was about 9 days after seeding.

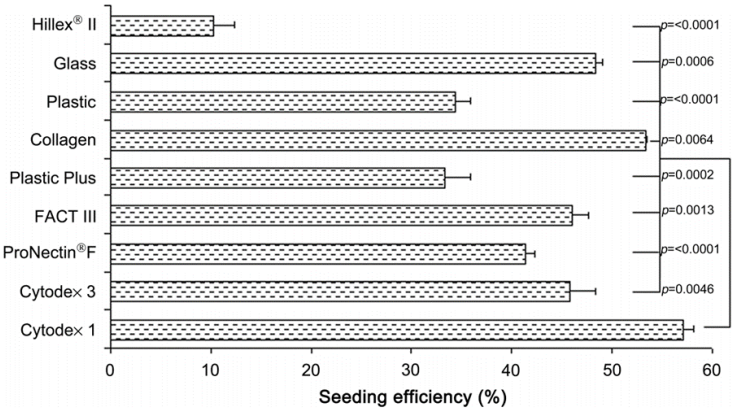

Figure 1.17 – hBM-MSCs seeding efficiencies obtained for various microcarriers. Each microcarrier type was seeded with 5 000 cells/cm^2. After 18 h, the seeding efficiency per microcarrier was analyzed in triplicate using Alamar blue assay [92].

In 2011, Dos Santos and colleagues proposed a GMP approach for the culture of MSCs using xeno-free microcarriers (Plastic P102L). After 14 days of culture in spinner vessels, BM-MSCs reached a maximal cell density of 2.0 $\times$ 10^5 cells $\cdot$ mL^{-1} (18 fold increase), whereas AD-MSCs reached a maximal cell density of 1.4 $\times$ 10^5 cells $\cdot$ mL^{-1} (14 fold increase) [93]. In 2016, Rafiq *et al.* evaluated 13 different microcarriers for the expansion of BM-MSCs in static and dynamic modes (Figure 1.18). Authors showed that Collagen and Plastic P102 L were optimal for MSCs growth [94] (Figure 1.18).

In 2019, Loubière *et al.* proposed to determine a standardized method of WJ-MSC cultivation in xeno-free system of culture by comparing and analyzing the impact of agitation mode (static, orbital and mechanical) on the expansion of WJ-MSCs [95]. Referring to this study (Figure 1.19), it seems that Cytodex-1 offered promises concerning cell attachment and expansion performances, but, Star Plus and Plastic Plus seemed to present a better compromise for orbital and mechanical agitation modes, respectively.

In literature, a various number of articles indeed exists describing protocols of hMSCs expansion with microcarriers, in dynamic modes. The cultures on microcarriers are thus intended to be mainly used in bioreactors with different modes of culture.

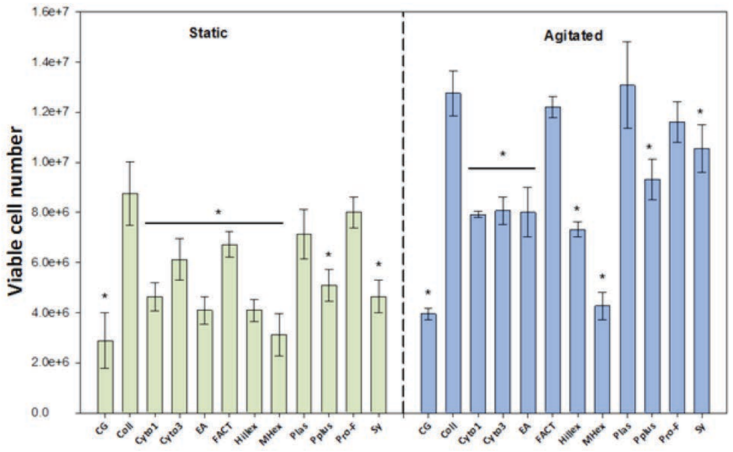

Figure 1.18 – Comparison of static and agitated conditions for hBM-MSCs microcarrier culture [94].

Microcarrier	Cytodex-1	Star-plus	Plastic	Plastic-plus	Hillex II
Static mode					
Cell attachment on microcarriers	++	++	–	++	++
Cell distribution and microcarrier occupancy	–	++	–	–	++
Cell expansion	++	++	–	+	++
Ease of detachment	–	++	–	++	++
Orbital agitation					
Cell attachment on microcarriers	++	+	N/A	+	–
Cell distribution and microcarrier occupancy	++	++	N/A	++	–
Cell expansion	+	++	N/A	+	–
Ease of detachment	–	++	N/A	++	+
Mechanical agitation					
Cell attachment on microcarriers	++	++	N/A	++	–
Cell distribution and microcarrier occupancy	++	++	N/A	++	–
Cell expansion	++	+	N/A	++	–
Ease of detachment	–	++	N/A	++	+

Note: –: Lowest performances observed in the study; +: Intermediate performances; ++: Best performances observed in the study; N/A: Not applicable.

Figure 1.19 – Microcarrier performances depending on the agitation mode [95].

Among other essential parameters to be considered when developing process of microcarrier-based cultures of MSC, the ability to detach from microcarrier during culture and upon division, and to attach to another, phenomena called bead-to-bead transfer [96], should be considered as well.

1.4.4 Bioreactor technologies

Nowadays, a high number of dynamic bioreactors have been used to expand MSCs. They can be divided according to the mode of mechanical agitation, mechanically driven bioreactors, pneumatically and hydraulically driven systems (Figure 1.20). Mechanically driven bioreactors include stirred tank bioreactors, wave-mixed systems and rotating bioreactors. This last one is mainly used for tissue engineering and not for cell expansion. Pneumatically driven systems such as 3 L Air-Wheel from PBS Biotech are scarce in the literature. Finally, hydraulically driven systems include hollow fiber bioreactors and fixed-bed bioreactors. Among all these various types of bioreactors, it could be possible to differentiate them between reusable and single-use bioreactors.

All the different technologies described are represented in the figure 1.20.

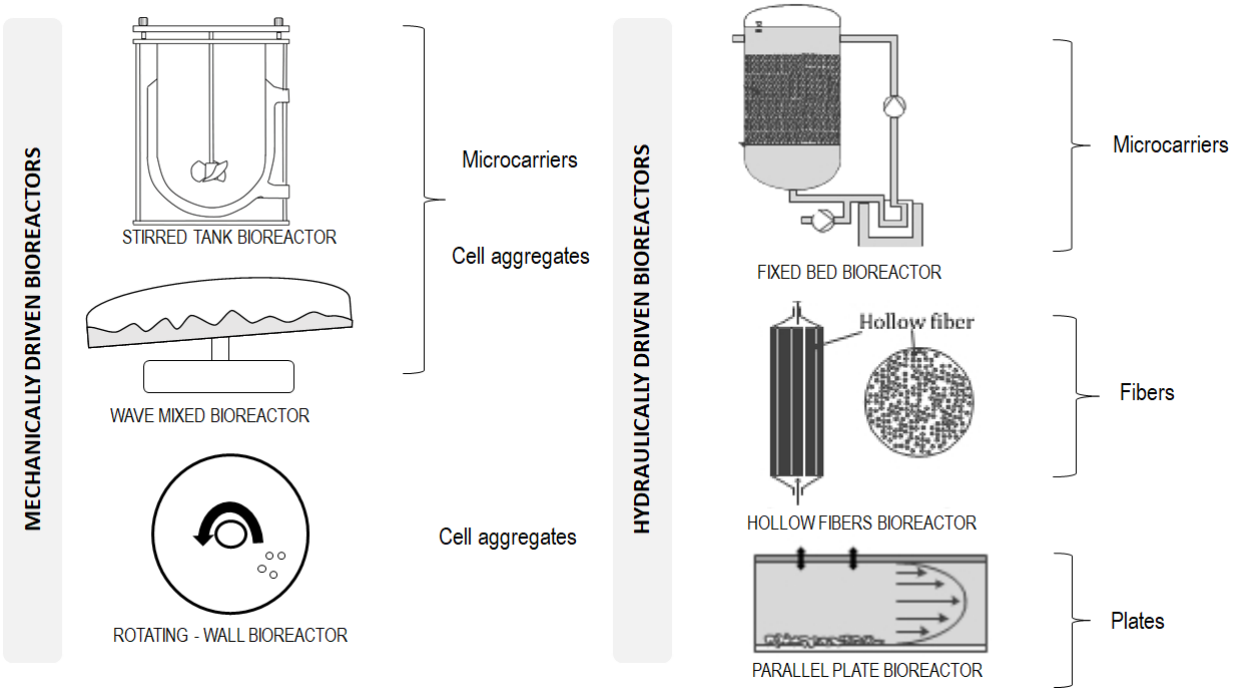

Figure 1.20 – Suitable bioreactors for MSC expansion. Figured from Jossen *et al.* [97].

1.4.4.1 Mechanically driven bioreactors

As described before, hMSCs are adherent - dependent cells and need surfaces for adherence and expansion. In mechanically driven bioreactors, microcarriers or perfused plates provided surfaces for the MSCs growth. Mechanically driven bioreactors include stirred systems, wave mixed system and more recently rotating bed bioreactors. Moreover, except the spinner flasks, mechanically driven bioreactors are instrumented with sensors that enable monitoring and control different parameters such as temperature, pH value, DO and carbon dioxide concentrations, gas and liquid flow rates, impeller or rocking speed. As presented in the table 1.4, a lot of studies using spinner vessels, small-scale bioreactors with a stirrer or a magnetic bar impeller, could be found. They are generally used for research, operating with magnetic impeller at slow speed (100 rpm max). Limitations of the use of spinner flask for producing MSCs to large scale are the limited volume (250 mL of working volume) and the absence of monitoring in basic configurations. Moreover, they are usually placed in incubators for temperature and humidity control, requiring space in incubators. Moreover, as it is presented in the table 1.4, there does not seem to be a well-established protocol for the culture of WJ-MSCs in spinner, and very different results are obtained in terms of expansion factors.

Table 1.4 – Cell culture conditions for MSCs growth in spinner flasks.

Adherence surface	**Working volume**	**MSC origin**	**Duration (in days)**	**Medium supplementation**	**Agitation (rpm)**	**Expansion factor**	**References**
Non porous plastic	80 mL	AD-MSC	9	StemPro MSC SFM	40	14	DosSantos *et al.* [93]
Cultispher S	N/A	BM-MSC	10	FBS		8.4	Eibes *et al.* [98]
Cytodex-3	50 mL	BM-MSC	10	FBS	50	4	Caruso *et al.* [99]
pNIPAM MC	50 mL	BM-MSC	5	FBS	40	2.5	Yang *et al.* [100]
Cytodex-3	50 mL	BM-MSC	5	FBS	40	2.5	Yang *et al.* [100]
Cytodex-1	100 mL	BM-MSC	9	FBS	30	4	Schop *et al.* [92]
pNIPAM MC	100 mL	BM-MSC	7	FBS	85	4.7	Yuan *et al.* [101]
Cytodex-3	100 mL	BM-MSC	7	FBS	85	4.9	Yuan *et al.* [101]
Synthemax II	35 mL	BM-MSC	40	Mesencult - XF medium	30	6	Hervy *et al.* [102]
Enhanced Attachment	80 mL	BM-MSC	8	StemPro MSC SFM	40	7	Carmelo *et al.* [103]
Plastic	80 mL	BM-MSC	8	StemPro MSC SFM	40	7	Carmelo *et al.* [103]
Synthemax II	80 mL	BM-MSC	8	StemPro MSC SFM	40	7	Carmelo *et al.* [103]
Plastic P-102 L	100 mL	BM-MSC	6	HPL	30	4	Heathman *et al.* [104]
Plastic P-102 L	100 mL	BM-MSC	9	Prime XV SFM	30	5	Rafiq *et al.* [105]

Adherence surface	**Working volume**	**MSC origin**	**Duration (in days)**	**Medium supplementation**	**Agitation (rpm)**	**Expansion factor**	**References**
Synthemax II	120 mL	BM-MSC	7	Mesencult - XF medium	45	10.4	Cunha *et al.* [106]
Non porous plastic	80 mL	BM-MSC	9	StemPro MSC SFM	40	18	DosSantos *et al.* [93]
Cytodex-1	100 mL	goat BM-MSC	16	FBS	30	6	Schop *et al.* [92]
Cytodex-1	40 mL	porcine BM-MSC	28	FBS	20	4	Frauenschuch *et al.* [107]
Cultispher S	1 L	E-MSC	4	FBS	70	18	Sart *et al.* [108]
Cytodex-3	100 mL	F-MSC	8	FBS	30	9	Chen *et al.* [109]
Enhanced Attachment	100 mL	hMSC-TERT	6	FBS	100	4	Leber *et al.* [110]
Glass coated MC	100 mL	hMSC-TERT	6	FBS	100	4	Leber *et al.* [110]
Pronectin	100 mL	hMSC-TERT	6	FBS	100	3	Leber *et al.* [110]
Synthemax	100 mL	hMSC-TERT	6	FBS	100	3	Leber *et al.* [110]
Biosilon/ P102 L / Rapidcell	250 mL	hMSC-TERT	9	FBS	30	11	Weber *et al.* [111]
Peptide-conjugated pLL treated MC	250 mL	pl-MSC	6	mTeSR2	60	18	Fan *et al.* [112]
Cytodex-3	100 mL	P-MSC	10	FBS	50	10	Hewitt *et al.* [113]
Plastic Plus	100 mL	UC-MSC	8	HPL	40	15	Petry *et al.* [45]

Adherence surface	**Working volume**	**MSC origin**	**Duration (in days)**	**Medium supplementation**	**Agitation (rpm)**	**Expansion factor**	**References**
Plastic	80 mL	UC-MSC	6	UltraGro	40	13	deSourre *et al.* [114]
Cytodex-1	100 mL	UC-MSC	7	SFM medium	38	5	Tan *et al.* [115]
Plastic P-102 L	100 mL	UC-MSC	8	human serum	30	20.8	Tozetti *et al.* [116]

Stirred tank bioreactor is also an other technology for culture volume superior to 1 L, as cylindrical bioreactors with various sizes, and use a top or bottom mounted rotating mixing system with generally either a marine, elephant ear or Rushton impellers in function of the mixing parameters chosen. Thanks to the on-line monitoring, temperature can be precisely controlled at 37°C, pH between 7.2 and 7.4, and generally, in MSCs cultures hypoxia conditions are preferred and the value of DO is set at 20 % of air saturation (4 % of pure O_2). As it could be observed in the table 1.5, higher expansion factors than in spinner flasks could be found. On the contrary to spinner flasks, stirred tank bioreactors can also be designed in function of the agitation mode. In adherent-dependent cell cultures a compromise has to be found between sufficient mixing to suspend the microcarriers and low hydrodynamic stresses, to avoid cell damages. Thus, researchers in the laboratory were able to propose different choices of mobile and rate of agitation in order to preserve the fragile balance between: the just suspension of particles and lowering hydrodynamic stresses encountered by the cells [117, 118, 119].

Table 1.5 – Cell culture conditions for MSC growth in bioreactors.

Adherence surface	**Reactor (W.V.)**	**MSC origin**	**Duration (in days)**	**Medium supplementation**	**Agitation (rpm)**	**Mode of culture**	**Expansion factor**	**References**
Plastic MC	STR (3.75 L)	AD-MSC	20	FBS	35	Batch	7	Siddiquee *et al.* [120]
Collagen coated MC	STR (3.75 L)	AD-MSC	20	FBS	35	Batch	14	Siddiquee *et al.* [120]
Non porous plastic MC	STR (0.8 L)	AD-MSC	7	StemPro MSC SFM	60	Fed-batch	9	DosSantos *et al.* [121]
ProNectin-F coated MC	STR (35 L)	AD-MSC	8	FBS	14	Batch	35	Schirmaier *et al.* [122]
Plastic P-102 L	STR (2.5 L)	BM-MSC	12	FBS	75	Batch	6	Rafiq *et al.* [123]
Plastic P-102 L	STR (0.1 L)	BM-MSC	6	Prime XV SFM	115	Batch	4	Heathman *et al.* [124]
Non porous plastic MC	STR (0.8 L)	BM-MSC	7	StemPro MSC SFM	60	Fed-batch	22	DosSantos *et al.* [121]
Synthemax II	STR (2 L)	BM-MSC	7	Mesencult - XF medium	100	Perfusion	13.6	Cunha *et al.* [106]
Plastic P-102 L	Ambr systems	BM-MSC	9	Prime XV SFM	400	Batch	10	Rafiq *et al.* [105]
Synthemax II	PBS-VW (2.2 L)	BM-MSC	14	Mesencult - XF medium	45	Batch	12	Sousa *et al.* [125]
Cytodex-3	STR (0.8 L)	F-MSC	8	FBS	80	Fed-batch	8	Chen *et al.* [109]

Adherence surface	Reactor (W.V.)	MSC origin	Duration (in days)	Medium supplementation	Agitation (rpm)	Mode of culture	Expansion factor	References
Collagen coated MC	STR (50 L)	hMSC	11	HPL	64	Fed-batch	43	Lawson *et al.* [126]
Vitronectin coated MC	PBS-VW (0.08 or 0.3 L)	iPS	9	mTeSR1 medium	10	Batch	3.5	Rodrigues *et al.* [127]
Cultispher S	Wave bioreactor (0.5 L)	P-MSC	7	FBS		Batch	15	Timmins *et al.* [128]
Polycarbonate plates	Rotating bed bioreactor (0.34 L)	UC-MSC	9	FBS	2	Perfusion	39	Reichardt *et al.* [129]
Cytodex-1	STR (1.5 L)	UC-MSC	6	FBS	80	Batch	7	Hupfeld *et al.* [130]
Cultispher S	Wave bioreactor (0.6 L)	UC-MSC	10	FBS	24	Batch	11.6-25.6	Da Silva *et al.* [131]
Cultispher S	STR (0.8 L)	UC-MSC	6	StemPro MSC SFM	50	Batch	6	Mizukami *et al.* [132]
Plastic P-102 L	STR (0.8 L)	UC-MSC	7	human serum	30	Batch	8.9	Tozetti *et al.* [116]
Poly-ε-caprolactone (PCL)	STR (0.3 L)	WJ-MSC	7	FBS	80	Fed-batch	8.7	Lam *et al.* [133]
Cytodex-3	STR (0.3 L)	WJ-MSC	7	FBS	80	Fed-batch	8.1	Lam *et al.* [133]

1.4.4.2 Hydraulically driven bioreactors

Hydraulically driven bioreactors include parallel plate bioreactors, hollow fiber bioreactors and fixed bed bioreactors, for which the power input is generated by pumps. The cells are grown either on perfused plastic surfaces, hollow fibers or packed particles. The different technologies of bioreactor are presented in the table 1.6.

- **Hollow fibers bioreactors**
  Hollow fibers bioreactors are described as high density continuous perfusion culture systems. Indeed, hollow fibers are small tubes settled in a cartridge shell, the cell culture medium is pumped inside whereas cells are growing in the space outside or surrounding the fibers. Advantage of hollow fibers is to provide a large surface in a small volume. However, an important difficulty lies in ineffective cell detachment.

- **Fixed-bed bioreactors**
  In fixed-bed bioreactors, the cells are immobilized or encapsulated in a matrix made of particles packed in a cylindrical column. It could be macro-porous beads, porous ceramic beads, porous glass beads, glass fibers, polyester discs, alginate beads and hydrogels. The cell culture medium is supplied to cells through the bed-packing.

Table 1.6 – Cell culture conditions of MSC in hydraulically driven bioreactors.

Adherence surface	**Reactor**	**MSC origin**	**Duration (in days)**	**Medium supplementation**	**Expansion factor**	**References**
N/A	Hollow fiber bioreactor	BM-MSC	20	HPL	20	Hanley *et al.* [134]
FibraCell disks	Fixed bed bioreactor	UC-MSC	7	FBS	7	Mizukami *et al.* [135]

1.4.4.3 Mode of culture

- **Batch cultures (discontinuous mode)**
  A batch culture is characterized by the absence of further addition of substrates (glucose, glutamine or other supplemented factors) during the cell expansion. Thus, before the inoculation an appropriate amount of substrates, present in the cell culture medium, is available in the system of culture. MSC culture were mainly performed in batch mode, in bioreactors whose volume ranged from one to ten liters. Thus no culture medium nor microcarrier addition were considered. As Hupfeld *et al.* [130] and Mizukami *et al.* [132] showed in their work, the cultures of WJ-MSCs lasted only few days because of a rapid nutrient depletion and a lack of available surface of growth. The limited productivity of a batch culture can be surpassed by using a fed-batch mode of culture.

- **Fed-batch cultures (semi continuous mode)**
  This bioreactor operation mode consists in the increase in the working volume during the process, as soon as the substrates are consumed by cells. For MSC cultures in bioreactors, the fed-batch mode was usually used in order to enhance cell adhesion in small volume of cell culture medium, and then, the increase of the cell culture medium volume allows to feed the culture with nutrients and to dilute the concentration of toxic metabolites produced by cells.

- **Perfusion mode (continuous mode)**
  Perfused bioreactors require specific technologies to be performed. In MSCs cultures, cells are usually kept inside the bioreactor, and the used medium is removed. One of the major advantage of perfused bioreactors is the control of feed and withdrawal rates of cell culture medium of up to several volumes of reactor per day, while, in continuous modes, these rates are dependent on cell growth kinetics [138]. In 2010, Serra *et al.* described the use of a perfused stirred tank bioreactor for the expansion of undifferentiated human embryonic stem cells (hESC) [136]. Experiments were performed with a probe, adapted to the bioreactor cap, using an automated gravimetric control [136]. The perfusion system allowed a renewal of nutrients and growth factors, and removal of "waste" by-products of metabolism. Mizukami *et al.* [135] used fixed bed systems for the expansion of MSCs. However, as in batch or most fed-batch systems, the available growth area was still a limitation. Dos Santos *et al.* [121], tested a perfusion mode in STR with BM-MSC. A perfusion rate of 0.25 day^{-1} was applied, and the working volume of the bioreactor was maintained to 400 mL. A cell device retention was used in order to keep cells and microcarriers inside the stirred tank and consisted in a modified alternating tangential flow (ATF) system (Repligen Corporation, Masachusetts, USA). By this system, authors obtained an expansion factor of 18.5. Finally, in 2015, Cunha *et al.* [137], tested an TFF (Tangential Flow Filtration) system, in order to maintain cells and microcarriers in the STR. This TFF permitted to obtained higher expanded cells ratio, and for longer time. In all these reported studies, the focus was mainly put on the limitation of substrates but not on the limitation of growth surfaces.

- **Cell retention technologies**

  Mechanically driven bioreactors, and more specifically, stirred tank bioreactors could be divided in function of the medium feeding and withdrawal strategy (Figure 1.21). When continuous perfusion mode is considered, appropriate retention systems have to be designed. A perfusion rate, or dilution rate D, is an important parameter for the cultures operating in a continuous perfused mode.

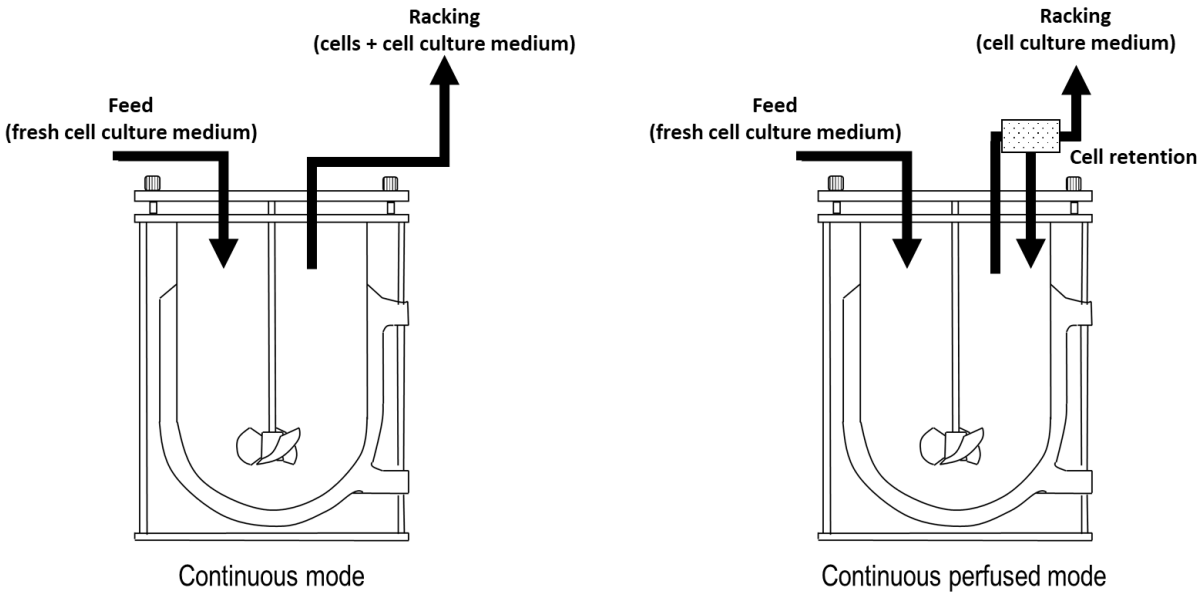

Figure 1.21 – Schematic representation of the different culture modes in continuous feeding strategies.

Different technologies of cell retention exist and were described from literature (Figure 1.22).
The membrane filtration systems (Figure 1.22 A) have a pore size ranging of 0.1 to 10 µm and are made of cellulose ester, nylon, poly (ethylensulfone), polypropylene, or poly (vinyldifluoride) (PVDF). The degree of cell retention is high but clogging of the membrane may cause problems due to cell debris [139].
The tangential flow filtration (TFF) (Figure 1.22 B) is a system using hollow fiber filters, a peristaltic pump is used to recirculate the cell culture supernatant over the permeable membrane surface. This process reduces the risk of filter fouling. In TFF, liquid and compounds with molecular weights less than the membrane cut-off can pass through the membrane (permeate), whereas larger molecules are retained (retentate).
The alternating tangential flow (ATF) (Figure 1.22 C) is a system using the TFF technique but the cell suspension is alternately pumped into the hollow fiber filter and back to the bioreactor by a diaphragm pump. This system is well adapted to suspension cells as well as to anchorage-dependent cells grown on microcarriers.
The vortex-flow filter (Figure 1.22 C) uses the same principle that the membrane filtration but with a different design. It is made of three different cylinders. The outer cylinder is housing the two others, the intermediate cylinder is supporting the membrane, and the inner cylinder is rotating.
The spin filter (Figure 1.22 D) is a system allowing to retain particles in the stirred tank biore-

actor by a rotating mesh with a pore size larger than the cell size. It is usually fixed on the stirrer axis.

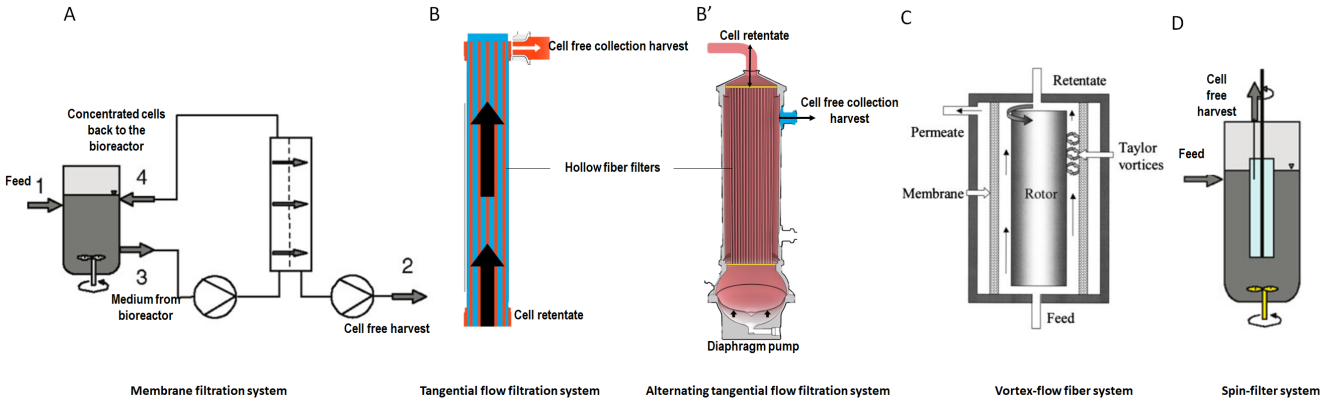

Figure 1.22 – Schematic representation of the different systems of cell retention devices for continuous perfused bioreactors. (A) Membrane filtration system. (B) & (B') Tangential and alternating tangential flow filtration systems. (C) Vortex-flow filter system. (D) Spin filter system. Reproduced from Catapano *et al.* [140].

Other systems as gravity settlers are also used as cell retention devices, and are the simplest devices using difference density to retain cells [141]. As the cells and microcarriers are slightly denser than the cell culture medium, the decantation would permit to retain cells inside the bioreactor while the medium is withdrawn.

Summary of the section

- A large number of technologies exists for the hMSCs expansion from 2D to 3D systems.
- Historically used for adherent cells expansion, the 2D cultures exhibit limitations due to limited surfaces, the absence of sensors to monitor cultures and higher risks of contamination with multiple handling.
- The use of stirred tank bioreactors and microcarriers is a good strategy for scaling-up cultures of hMSCs.
- Different modes of cultures were studied, with the focus to avoid substrate limitations but without taking into account the available surface limitation that is also a crucial parameter for cell growth on microcarriers.

1.5 Impact of the culture process on MSCs quality

1.5.1 Critical quality attributes of WJ-MSCs

As described before, hMSCs are the product of interest, and in the healthcare sector, strict rules of production are implemented for the production of cell-based therapeutic products. A fully defined biological product and, in particular, cell-based products, is really hard to develop, due to variabilities, such as donor variability for example. One major constraint when developing a cell manufacturing process is thus to guarantee that the critical quality attributes (CQA) of the final product, such as identity, potency and safety, are maintained.

hMSCs identity

A validation of the identity of the product is essential after the process of production in order to confirm that the produced cells will have the desired therapeutic effect. Indeed, sudden modifications in the cell process of production, such as a scaling-up, a different batch of microcarriers or even a modification of detachment enzymes, may modify the cell phenotype [142]. Different methods were developed in order to identify MSCs populations (Figure 1.23).

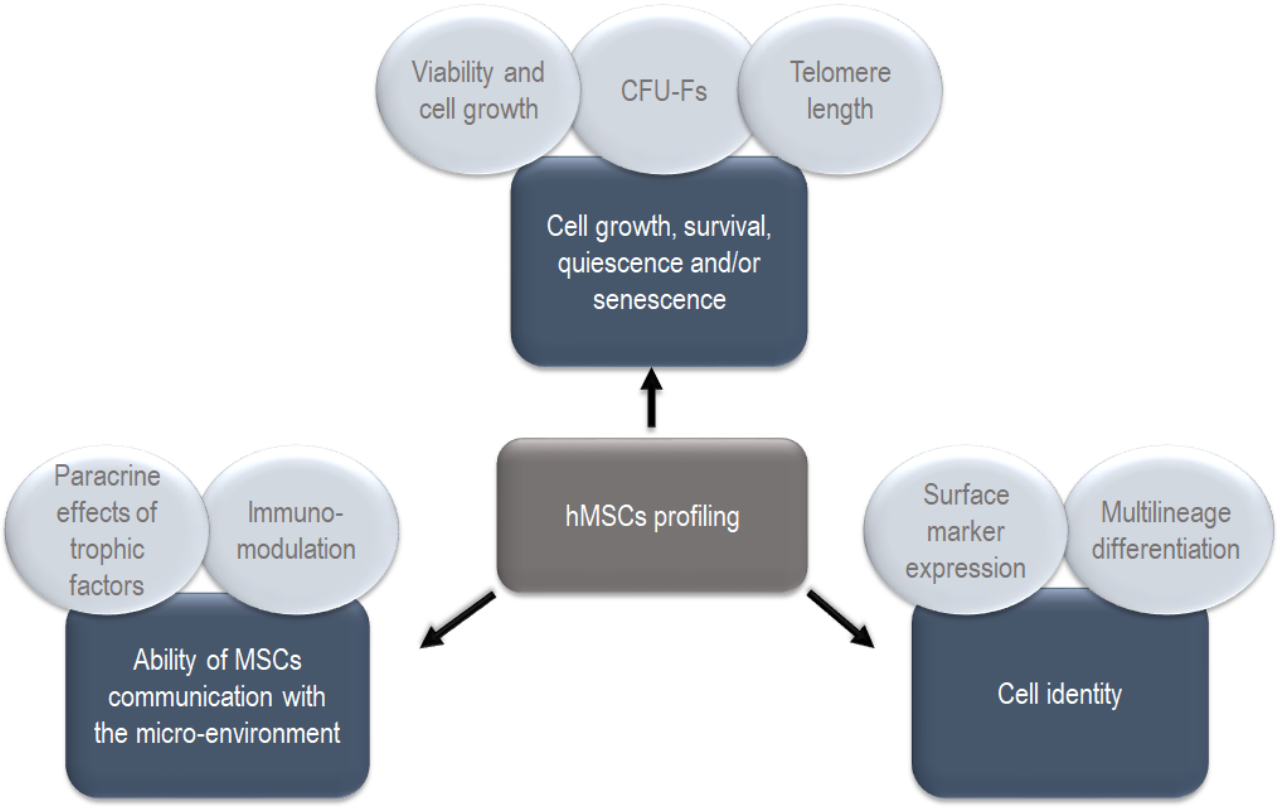

Figure 1.23 – Profiling of MSCs population. Key parameters for the characterization of adult stem cells from different sources. Reproduction from Samsonraj *et al.* [143].

- **Colony forming unit (CFU-F).**

This technique is routenely used and accepted as a standard for MSCs identification and characterization. It consists in a seeding of 100 to 500 cells per 10-cm dish and, after 14 days, a counting

of formed colonies is realized with a crystal violet staining [144].

- **Surface expression markers**.

To obtain homogeneous populations of MSCs, the principal method developed and used is to target specific cell surface markers. Thus, it is well established that MSCs should express CD105, CD73 and CD90, but not CD54, CD34, CD14, CD19 and HLA-DR (ISCT criteria) [21]. Authors have to based their research on multiple surface antigens markers among those recommended by the ISCT in order to know if the cell population quality derived during the expansion phase.

Potency of hMSCs

The potency tests allowed to confirm that the product has the biological functions relevant for the treatment of the clinical indication. Alteration of the hMSCs can occur during the upstream and the downstream processes ; it is therefore important to validate potency of the cells trough different tests.

- **Differentiation**.

The capacity of MSCs to differentiate is the major criterion defining cells as MSCs. This cell differentiation could be initiated thanks to specific cell culture medium and with some specific cell contacts. Thus, during about 20 days, specific culture medium supplementation are carried-out and allowed MSCs to express an adipocyte, chondrocyte or osteocyte phenotypes. Then, the confirmation of the phenotypes is realized by histochemical staining. It is a long process which is only qualitative. Other tests are available, based on a short term induction (7 days), and variation of mRNA or protein expression can be detected quantitatively. On-line monitoring is also available to monitor cell differentiation, as with the Raman spectroscopy. The increase of relative intensity of protein/lipids bands and the decrease of nucleic acids can be detected as changes in Raman spectra. Therefore, micro-Raman spectroscopy is sufficient to discriminate differentiated cells from the others [145].

- **Secretome**.

As undifferentiated cells, MSCs could produce immunomodulatory, anti-inflammatory, anti apoptotic, anti-oxydant, anti-microbial or angiogenic factors. This induce the secretion of cytokines, growth factors, enzymes, prostaglandine and exosome [146]. These secretions can be detected by proteomic physiochemical techniques as ELISA mass spectroscopy [147]. Based on the immunomodulation properties of MSCs, *in vitro* tests to characterize the hMSCs secretome exist, as for example the mixed-lymphocyte reaction (MLR) in transwell systems [148, 149].

Purity and safety

Purity tests allowed to confirm the absence of some contaminant components, such as residual process reagents or cell debris. And the safety tests allowed to confirm the absence of microbial contaminants and the sterility of the product.

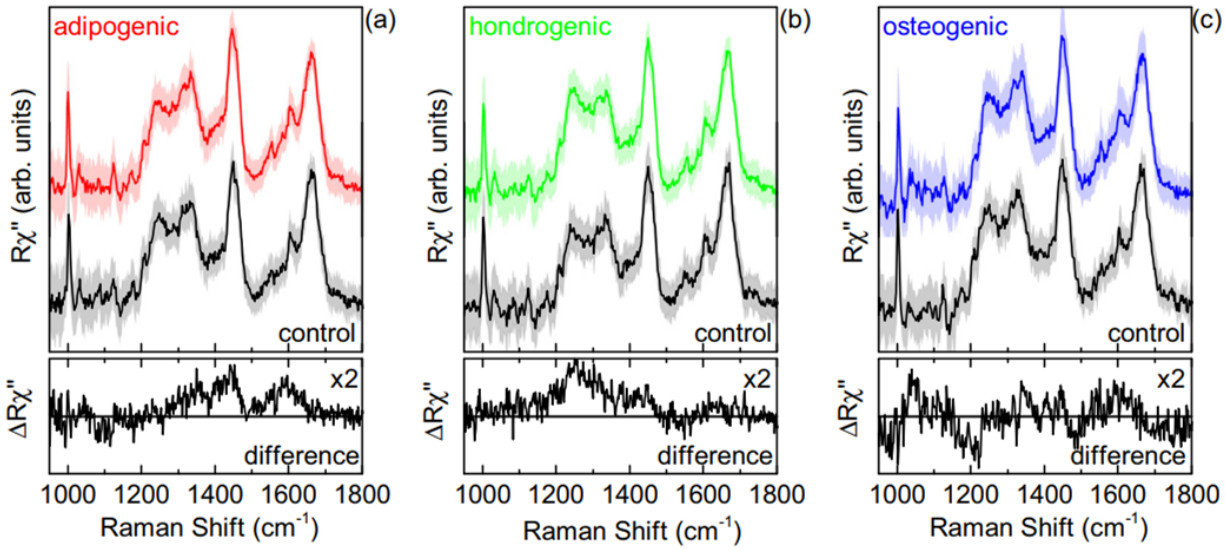

Figure 1.24 – Averaged Raman spectra of hMSCs (control samples), differentiated hMSCs (adipogenic, chondrogenic and osteogenic lineages) and spectrum difference between these two groups of cells. Lazarevic *et al.* [145].

- **Purity.**

Cell therapy products have to be free from unintended substances, such as endotoxin, residual proteins, or other unwanted biological agents [142]. The cells are suspended in a suitable buffer for human administration. Residual protein can be detected thanks to standard Enzyme-Linked Immuno Assay (ELISA) based tests. A good strategy to better characterize the purity of the product is to use multi-targeted flow cytometry or gene arrays [142].

- **Safety.**

In order to limit the potential cell contaminations (bacteria, mycoplasma, yeasts, viruses) the process of production needs to tend to a completely closed-system of production, but this may raises technical issues. However, methods of genome screenings are available in order to detect if the cell therapy products are free from viruses, bacteria or mycoplasma.

hMSCs aging

Contrary to the cell-lines producing recombinant proteins, which are well known, the balance between stemness, senescence and malignancy for hMSCs is delicate; these cells are fragile and can be thus altered their phenotype during the manufacturing process [146].

- **Stemness**.

One of the characteristic of stemness is based on clonogenicity, that is the historical method used for BM-MSC isolation. The method of evaluation of clonogenictiy is simple and based on a clonal seeding density and its comparison to the number of colonies obtained 14 days after [146]. Moreover, expression of pluripotent markers also can be an indication of stemness as the self-renewal and the multipotency.

- **Senescence**.

Expression of pluripotent markers is a symbol of stemness, but their expression decreases over time (due to cell passaging for example). Equally, late passage MSCs demonstrated to have less ability of colony forming compared to earlier passage MSCs [150]. This negative evolution, called 'senescence' could be characterized by morphological changes (enlarged or flattened cells), by the increase of senescence-associated β galactosidase and senescence-associated lysosomal α-L-fucosidase, by alteration of surface markers, or by a growth arrest in G1 phase of the cell cycle [151]. Concerning morphological changes, senescent MSCs become flat, with a constrained nuclei, a granular cytoplasm due to accumulation of cell debris. Moreover, an excess of actin fibers and a decreased of adherence to plastic surfaces can be also observed [151].

- **Malignancy**.

The cancerous transformation of human MSC is a rare event. Indeed, it has been shown in the study of Prockop *et al.* (2010), that the probability of MSCs becoming tumorigenic is extremely low (frequency less than 10^{-9} per cycle of cell division) [152]. Identified parameters that can promote tumorigenicity are, for example long-term cell expansion, cell culture conditions, the donor, etc. Usually, abnormalities only lead to senescence but it is difficult to exclude the risks of cell transformation due to DNA damages, the central process in tumor formation [153]. In order to exclude these possible abnormal cells, G-band karyotyping and fluorescence *in situ* hybridization (FISH) is possible [77].

1.5.2 Impact of environmental factors on MSCs expansion

1.5.2.1 Cell culture medium

Maintenance and expansion of MSCs require a special cell culture medium, composed of a basal medium (*e.g.* Dulbecco's modified Eagle's medium (DMEM), Iscove's modifed Dulbecco's medium (IMDM), Minimum essential medium eagle alpha (α - MEM)) with salts, glucose, glutamine, amino-acids and supplemented by serum. Serum is widely used because it contains proteins, adhesion factor, vitamins, growth factors, hormones, fatty acids and lipids promoting cell adhesion and cell growth. Until a few years ago, cell culture media were mainly composed of basal media and supplemented with 10 % of fetal bovine serum (FBS). However, there are several risks to use serum in *in vitro* cultures of hMSCs if they are devoted to clinic therapies, through the wide batch-to-batch variability, the risk of contamination with prions and viruses. Indeed, for these reasons, European Medicine Agency advises against the use of serum and other alternatives need to be found ([89], European Medicines Agency: EMA/CHMP/BWP/457920/2012, May 2013).

In order to fit to these requirements, new cell culture media were developed. They could be classified as follow [77]:

- **Serum-free medium**
  It contains supplementary hormones, growth factors, proteins and polyamines derived from bovine, human, yeast or plant sources.

- **Protein-free medium**
  It contains peptide fragments from hydrolysis of animal or plant source proteins.

- **Recombinant xeno-free medium**
  This medium contains recombinant proteins and hormones, but are completely free from animal or human sources.

- **Chemically defined medium**
  It is a protein free basal medium containing synthetic peptides or hormones, and some recombinant or synthetic proteins. They only contain chemically defined elements and in a controlled quantity. They are usually more expensive.

With the aim of producing clinical-grade WJ-MSCs, humanized and serum/xeno-free medium formulations were tested and evaluated for cell expansion.

• Humanized medium formulations:
It has been demonstrated that human platelet lysate (HPL) obtained from platelet concentrates can replace fetal bovine serum (FBS) as xeno-free clinical grade supplement of growth media to expand MSCs. Firstly, allogenic human serum were used for the isolation and expansion of MSCs. Various results were reported in literature with for certain, MSCs growth arrest, whereas, in other cases, MSCs exhibited a more proliferative profile, with no significant morphology differences, viability and differentiation abilities. Using allogenic human serum implies donor-specific variability and, to reduce this disadvantage, a pool of human sera from significant amount of donors is required. Thus, MSCs isolated and expanded in medium containing HPL showed higher proliferate profile when compared to the ones cultivated in media containing FBS [154, 155, 156]. While HPL is described as safer than FBS, there are still some limitations regarding its use, such as risks of human disease transmission, the necessity to use anticoagulant such as heparin to prevent gelatinization, being ill-defined and the possible immune-response [155]. In order to overcome these limitations, companies started to develop new serum/xeno-free medium formulations.

• Serum/ xeno-free media formulations:
A serum-free medium is composed of growth factors, proteins and hormones directly derived and purified from human serum. In the other hand, xeno-free media, could be completely free from animal and human components. Different cell culture media are available for MSC isolation and expansion. Thus, StemPro MSC SFM XenoFree culture medium from Life Technologies has been used for isolation and expansion of MSCs from different sources (adipose, bone marrow or umbilical cord derived mesenchymal stem cells) [103, 93, 121, 157]. As presented in the figure 1.25, WJ-MSCs have a higher proliferation rate when cultured in StemPro MSC SFM XenoFree medium than in medium supplemented with FBS. MesenCult-XF from STEMCELL-Technologies is also a chemically undefined serum/xeno free medium formulation, used for expansion of bone-marrow MSCs [106, 125], umbilical cord derived MSCs [158]. Chemically defined medium such as MSC GM-CD (Lonza) and MSC Nutristem XF (Biological Industries) have been described for expansion of MSC [115, 159], but remained scarce.

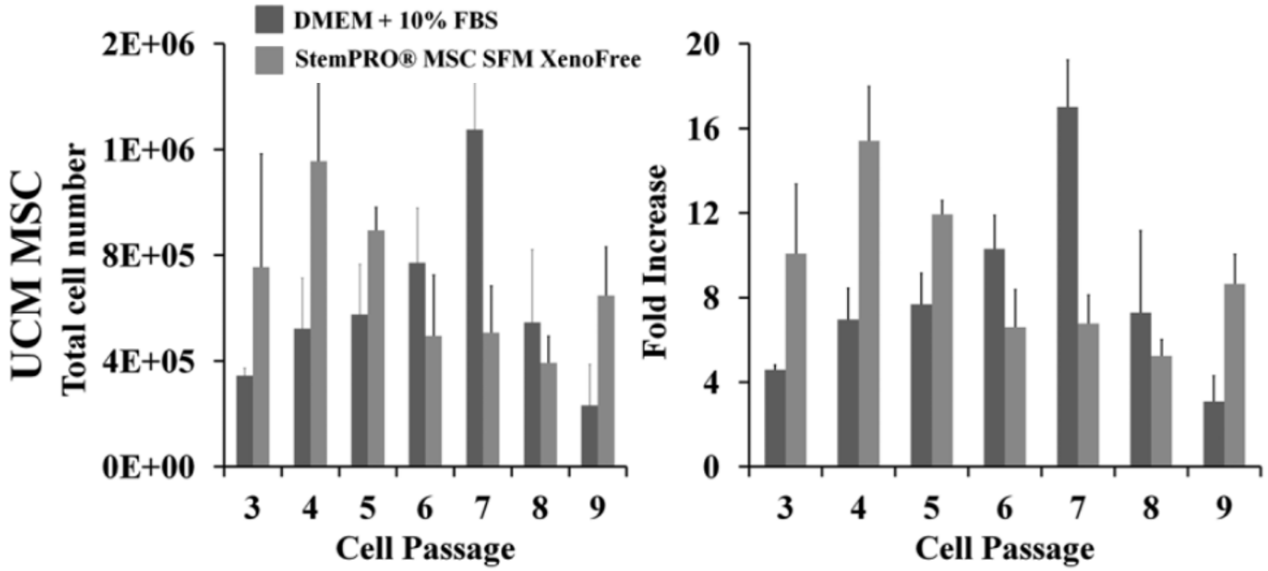

Figure 1.25 – Proliferative capacity of WJ-MSCs cultured using different media. Black bars represent the condition of DMEM + 10 % FBS. Grey bars represent the condition of StemPro MSC SFM XenoFree. With these conditions of culture, 70-80 % confluence was reached in 4-5 days of culture. (Simoes *et al.* [157]).

1.5.2.2 Cell culture parameters

In addition to biochemical parameters such as nutrient, metabolite and growth factors concentrations and physico-chemical parameters (*e.g.* oxygen concentration, pH and osmolarity) are also key parameters for MSC expansion.

- **Biochemical parameters**

Glucose is a determinant factor in animal cell culture, one of the main energy sources for the cells. High glucose levels (4.5 g L^{-1}) can induce early MSCs senescence and morphological changes (Figure 1.26 A) [160], and low-level of glucose (1 g L^{-1}) induce MSCs phenotypes towards a chondrogenic type (Figure 1.26 B) [161]. Apart as a protein constituent, the glutamine is also an amino acid used to produce energy through metabolic and non metabolic mechanisms. After its transfer inside the cell, it could be either exported in exchange of other amino acids, either consumed through different metabolic pathways to produce energy. In MSCs expansion, as demonstrated in the study of Schop and colleagues [92], it seems that glutamine is not critical as source of energy but its presence is needed.

Glucose oxidation, through the glycolytic pathway, induces the production of a high level of lactate, meaning an oxydative phosphorylation with limited activity. This biochemical parameter is a crucial factor that needs to be precisely monitored in MSCs cultures. Indeed, lactate inhibitory levels (35 mM) were described by authors [92], causing arrest of growth due to too high acidification of the medium. Similarly to lactate, ammonium ions produced by the metabolic degradation of glutamine, exhibit also potent inhibitory properties at concentrations as high as 2-3 mM [92].

Growth factors are found in HPL or FBS, or added individually in the cell culture medium, they act as chemical messengers. Growth factors are proteins or peptides able to interact with membrane receptors and by this way induce proliferation, survival mechanisms or differentiation. In-

side the niche, the auto-secretion of growth factors maintains the multipotence of MSCs, notably with leukemia inhibitory factor (LIF) and the fibroblastic growth factor 2 (FGF2). Some of these factors, including also epidermal growth factor (EGF) and platelet-derived growth factor (PDGF) among others, could be added in the cell culture medium.

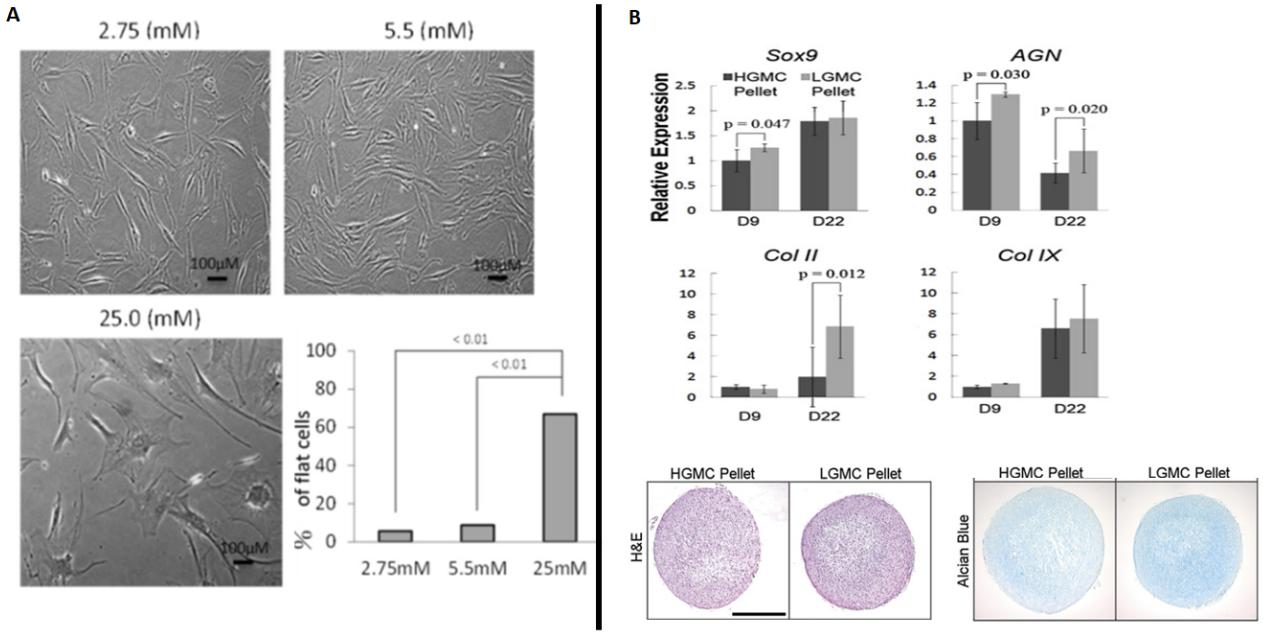

Figure 1.26 – Influence of glucose concentration on MSCs. (A) High glucose alters BM-MSC morphology. Cells became flat and rounded in presence of 25 mM glucose (Chang *et al.* [160]). (B) Low level of glucose induced the transcription of cartilage-related markers (Sox9 and aggrecan), as revealed by Alcian blue staining, showing a higher intense blue color (Tsai *et al.* [161]).

- **Physiochemical parameters**

The physicochemical environment contributes to regulate viability, growth, and differentiation of cells thanks to information relays sent by intracellular proteins or membrane receptors. In *in vivo* environment, MSCs from Wharton jelly encounter poor levels of oxygen, at a temperature of 37°C and with a pH value regulated around 7.4 in the blood. Cultivating MSCs in normoxic conditions (atmospheric oxygen levels, *i.e.* 21 %) could lead to early senescence, lower growth rates and DNA damages [162, 163, 164, 165]. In other studies, it has been demonstrated that culturing WJ-MSC and AD-MSC at low oxygen tensions mimicking the *in vivo* environment (5 % and 1 % respectively) improved proliferation and clonogenecity of the cells while maintaining the specific characteristics of the stem cells [166, 167]. Dos Santos *et al.* [168] also observed a modification of the BM-MSCs metabolism depending on the oxygen concentration, describing as a higher glucose and glutamine consumption while lactate and ammonium were less produced in hypoxic conditions than in normoxic conditions, as it is shown in Figure 1.27. This higher glucose consumption could be explained by the requirement of carbon for the faster cell proliferation induced by the low oxygen tension.

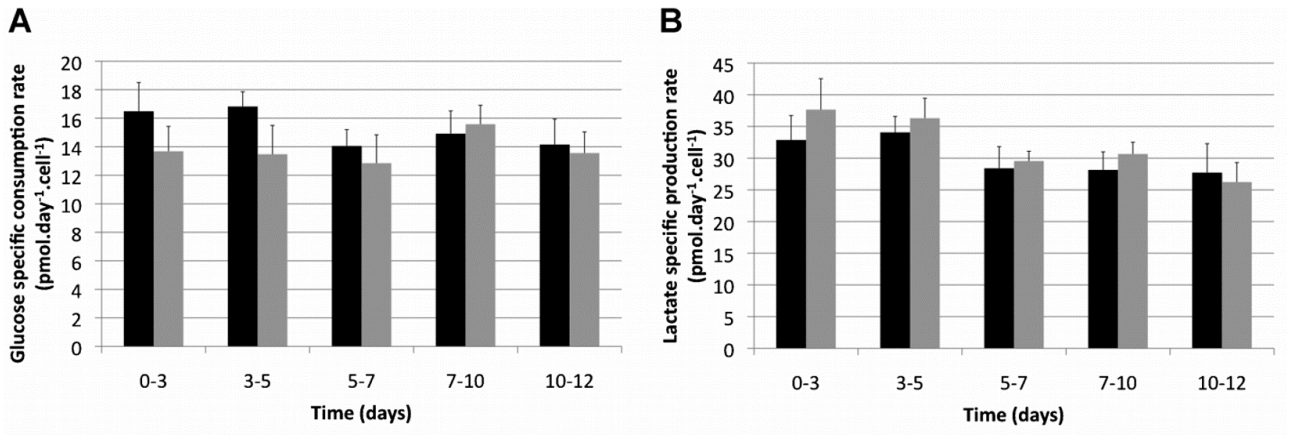

Figure 1.27 – Specific growth rates of glucose consumption and lactate production. Black bars represent the condition at a pO_2 of 2 % in the gas phase and grey bars represent the condition at a pO_2 of 20 % in the gas phase (Dos Santos *et al.* [168]).

1.5.2.3 Shear stress and agitation

In order to reach culture conditions favorable to MSC expansion, agitation is generally set to a minimal agitation rate, given by the symbol N_{js} (s^{-1}), able of retaining microcarriers in suspension, while avoiding the microcarriers settling in the reactor bottom more than 5 seconds [169]. In these conditions, agitation allows to keep minimal suspension of microcarriers and generate sufficient mass transfer of nutrients and oxygen. Sufficient agitation for a just-suspended state of microcarriers needs to be set-up to avoid cell aggregation in the bottom of the vessels. However, the associated hydrodynamic shear stresses generated by the impeller increases with the increase in the agitation rate and, then could cause damages to the cells. Establishing the balance between the necessity to maintain an homogeneous suspension of microcarriers to ensure uniform growth environment, to lower the impact on cells of hydrodynamical shear forces resulting of the agitation, and to maintain a sufficient bulk liquid mixing for appropriate aeration, remains a challenge that must be addressed (Figure 1.28).

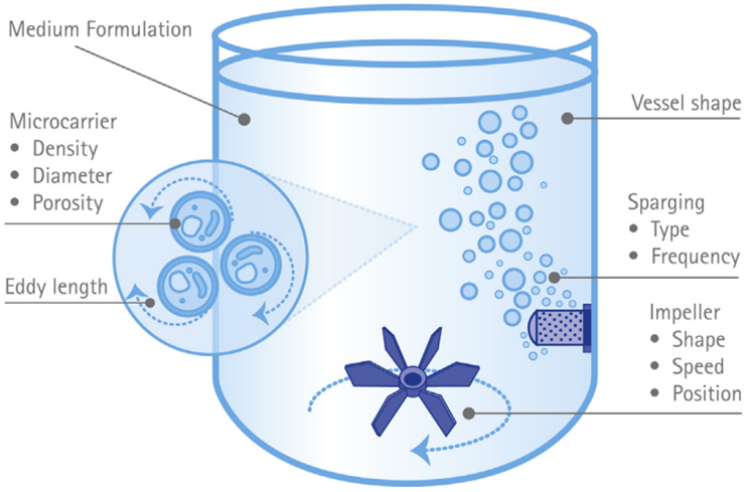

Figure 1.28 – Factors influencing hydrodynamic forces exerted on cells in a stirred tank reactor (Schnittzler *et al.* [170]).

Shear in a fluid system has two components:

• Shear stress (τ), a force per unit area acting on and parallel to the surfaces;

• Shear rate ($\dot{\gamma}$), a velocity gradient (velocity / length).

Thus, these two components could be related through the formula, as:

$$\tau = \eta \cdot \dot{\gamma} \tag{1.1}$$

where η is the viscosity of the fluid.

In model systems (laminar flow between two parallel plates) the shear rate (γ) and the related shear stress (τ) could be calculated with simple mathematical equations [171], while in stirred tank bioreactors, in a more complex and turbulent environment, it is difficult to relate and quantify cell damages to shear stress or shear rate. In this case, the occurrence of shear damage is generally taken into account by the determination of the Kolmogorov scale, as:

$$l_k = \left(\frac{\mu^3}{\rho^3 \epsilon}\right)^{1/4} \tag{1.2}$$

with ϵ ($m^2\ s^{-3}$) the turbulent dissipation rate.

• Shear stress applied on anchorage-dependent cells,

Usually shear stresses on anchorage-dependent cells adhered to solid surfaces are studied in flow chambers. Cells are adhered to the bottom plate of the flow chamber and, when they reached confluence, a fluid with a known velocity is applied on the cells for a determined duration, and cell parameters are analyzed such as cell morphology, number of viable cells, and concentrations of molecules released when cells are damaged (lactate dehydrogenase for instance).

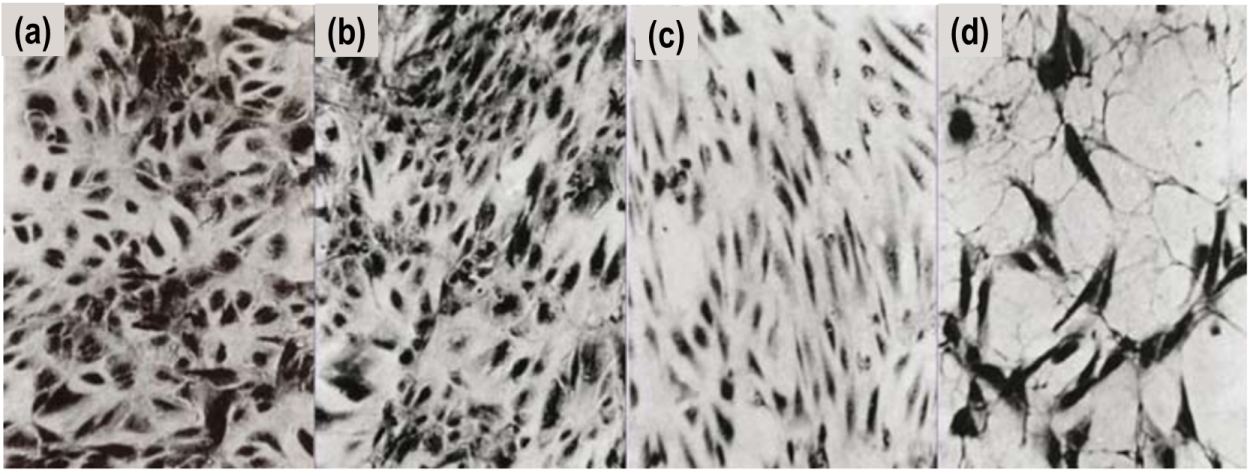

Figure 1.29 – Effects of shear stress on adherent growing primary epithelial cells in a flow chamber after (a) 1 week without shear stress (b) 4h with shear stress (1.3 N m^{-2}) (c) 24h with shear stress (1.3 N m^{-2}) (d) 24h with shear stress (5.4 N m^{-2}) (Stathopoulos *et al.* [172]).

• Shear stress on stem cell grown in bioreactors for cell expansion,

Cells cultivated on microcarriers are submitted to more severe hydrodynamics forces than suspended cells. In these turbulent environment, the scale of fluid eddies approaches dimensions

of microcarriers. In these conditions, energy of eddies can be dissipated on the surface of microcarriers, causing high local velocity gradients between the solid (*i.e.* microcarriers) and the liquid. In a turbulent flow created by stirring, different sizes of fluid eddies could be found and impact differently cells [173, 174]. The impact of the fluid eddies on the cells on microcarriers depends on the ratio between smallest eddy size (l_k) and microcarrier diameter (Figure 1.30).

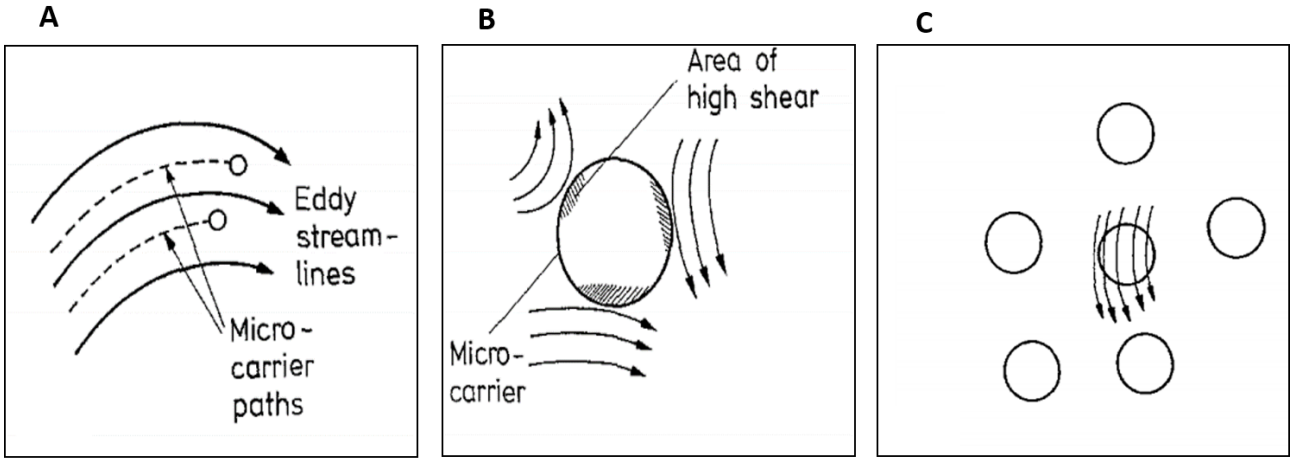

Figure 1.30 – Effects of shear forces on microcarriers in a turbulent flow. Microcarrier-eddies interactions: (A) eddies much larger than microcarriers, (B) multiple eddies with the same size of the microcarrier, (C) eddy size with the same size as inter-microcarrier spacing. (Cherry and Papoustakis [173]).

When the size of the eddies is much larger than the size of microcarriers (Figure 1.30 A), it is established that the beads will follow the streamlines and will not interact. In the case B ($l_k < d_c$), the beads interact with local streamlines and local shear stresses are applied on the microcarrier surface. Finally, in case C (similar microcarrier size and eddy length), beads are following streamlines but the probability of collision between microcarriers is higher. In order to quantify this severity of impact and collisions, the notion of turbulent collision severity (TCS) was introduced in Cherry and Papoustakis work [174]. The specific growth rate significantly decreases with the increase of TCS (Figure 1.31 A, B), and the high velocity of stirring increases the percentage of empty microcarriers (Figure 1.31 C).

The description of fluid flows in stirred tank bioreactors can be done by using computational fluid dynamic (CFD) simulations. Thus, parameters as fluid velocity, oxygen tension, stress which are difficult to determine with experiments can be calculated from CFD simulations and correlated to cellular parameters. These studies applied to WJ-MSC cultures were the subject of the PhD thesis work of Céline Loubière in LRGP laboratory [15].

• Effects of shear stress on stem cell fate

Some other studies reported an impact of hydrodynamical stress on MSCs and their differentiation. Indeed, phenotype of MSCs cultured in 2D systems could be osteogenically primed by mechanical stresses [175, 176, 177]. Maul *et al.* [178] described a possible induction of differentiation towards vascular and endothelial cells related to mechanical stimuli and shear stresses.

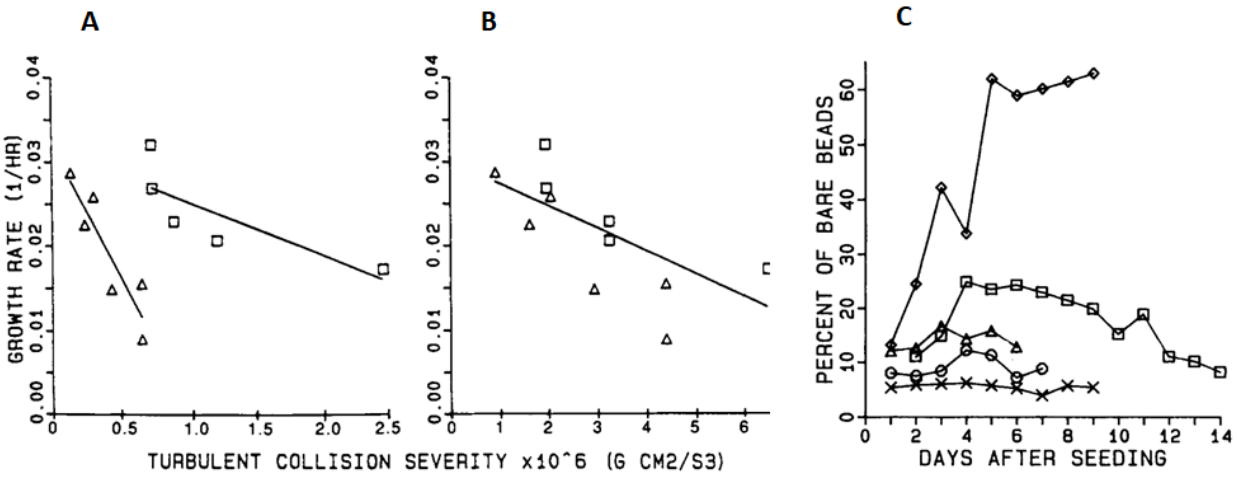

Figure 1.31 – Effects of turbulent collision severity on BEK cell growth rates (A) and (B) in function of the impeller diameter (□) 6cm impeller (△) 4cm impellers. (C) Impact of the impeller speed on the empty microcarriers concentration (×) 45 rpm, (□) 60 rpm, (○) 80 rpm, (△) 100 rpm, (◇) 136 rpm (Cherry and Papoustakis [174]).

1.5.3 Integration of Process Analytical Technology (PAT) in MSCs cultures and applications

Expansion in stirred tank bioreactors of MSCs seems appropriate for clinical scales and objectives. One major advantage of using STR is indeed the possible on-line monitoring of critical parameters such as temperature, pH and oxygen. Monitoring and control of these biochemical parameters allow to ensure quality of cells. In more advanced processes, data from cells could be analyzed and used to choose appropriate operational conditions, but off-line measurements are still needed to be correlated with these on-line measurements. Thus, the concept of process analytical technology (PAT) proposed by the FDA in 2004 and endorsed by other major pharmaceutical regulatory agencies such as EMEA (European Medicines Agency) of the European union or MHLW (Ministry of Health, Labor & Welfare) of Japan has contributed and strengthened the pharmaceutical good manufacturing practices (GMP). The objectives of the PAT approach are numerous: (1) to reduce the costs by reducing production cycling time and preventing rejection of batches, (2) to improve the biological yields through a better knowledge of the process indor to guarantee quality of products, (3) to provide optimal exploitation of the cell factory, enabling real time release, and (4) to give a routinely audit of the process. Among all the different process analytical chemistry tools, on-line analytical sensors based on Near Infrared, Raman or dielectric spectroscopies are the most implemented in bioprocesses. The dielectric spectroscopy, used in this PhD work, will be more precisely described in the following section.

1.5.3.1 On-line monitoring of cellular concentration by permittivity measurement

The commonly used methods to determine cell concentrations of adherent-dependent cells are based on cell and nuclei counting, which are laborious and time consuming due to the large number of samples. The application of dielectric spectroscopy could be a promising tool for monitor-

ing cell density on microcarriers, in stirred tank bioreactors.

• Principle of dielectric spectroscopy

A medium is described as isolated (or di-electric) if it does not contain free moving charges, in opposition to a charge conductor (electrons, ions) able to freely move. In animal cells, positive and negative charges could not freely move. Under an electromagnetic field, charges are moving inside the biovolume, delimited by the intact cytoplasmic membrane. Thus, cells act as capacitors that can be polarized under application of an electric field, and the measurement of this polarization is related to the permittivity. If the cytoplasmic membrane is not intact, cells can not be polarized under the electric field, and no permittivity can be detected ; thus, microcarriers, cell debris and gas bubbles also can not be detected (Figure 1.32).

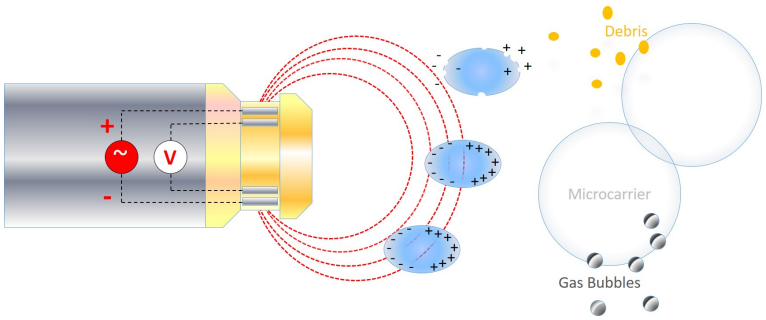

Figure 1.32 – Principle of dielectric spectroscopy applied to cell culture on microcarriers.

A finer control of cell cultures can be achieved thanks to additional data monitored by the dielectric probe, such as the critical frequency. This parameter gives information about the physiological state of the cells (*i.e.* changes in cell size and morphology, cell size distribution, membrane capacitance, intracellular conductivity).

• Application of dielectric spectroscopy to the monitoring of cell culture

First studies using dielectric spectroscopy in mammalian cell cultures began in XXIst century [179, 180, 181, 182], mostly used for Chinese hamster ovarian cells (CHO) culture monitoring. In 2012, Petiot *et al.*, in Vero cell cultures, observed that the relationship between cell concentration and permittivity is depending on the composition of the cell culture medium, this result could be explained by changes in cell morphology or size, impacting the permittivity signal [183]. In 2011, Justice *et al.* described, for the first time, the use of the dielectric spectroscopy to monitor MSCs adhered on microcarriers [184]. As presented in the figure 1.33, a linear correlation between online permittivity and concentration of adhered cells could allow to monitor the cell adhesion, the start of the exponential growth phase and the ideal timing for cell harvesting to guaranty high quality products.

• Other on-line monitoring technologies

Fourier transform infrared (FTIR) and Raman spectroscopies allow to detect vibrational modes of bio-molecules and the recognition of fingerprints of molecules. By associating these techniques to multivariate analysis, such as the partial least square (PLS) regression, prediction of consumption or production of metabolites during cell cultures is possible. The interest of FTIR spectroscopy is the possibility to use it in mid-infrared (MIR) and in near-infrared regions of the electromagnetic

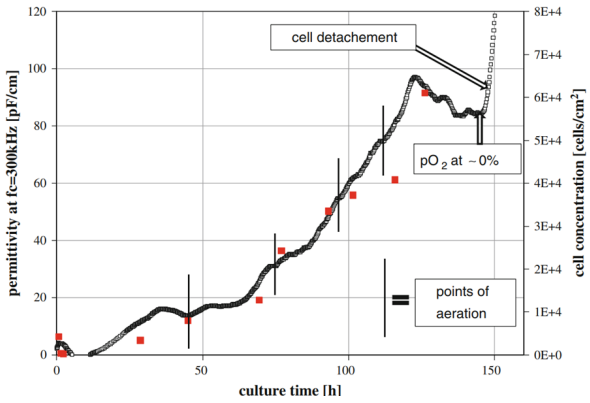

Figure 1.33 – Cell concentration and permittivity as function of the culture time. Red square: offline data from fluorescent assay; black: online permittivity data. Graph from the study of Justice *et al.* [184].

spectrum. These both methods have already been used to predict metabolite concentrations in Chinese Hamster Ovarian (CHO) cell lines, in human embryonic kidney (HEK) cell lines and in Vero cell lines [185]. The technique of MIR spectroscopy was also used for monitored the glucose and lactate concentrations in human MSCs culture in spinner vessels. Associated with the PLS regression, good prediction of metabolite concentrations were determined (Figure 1.34).

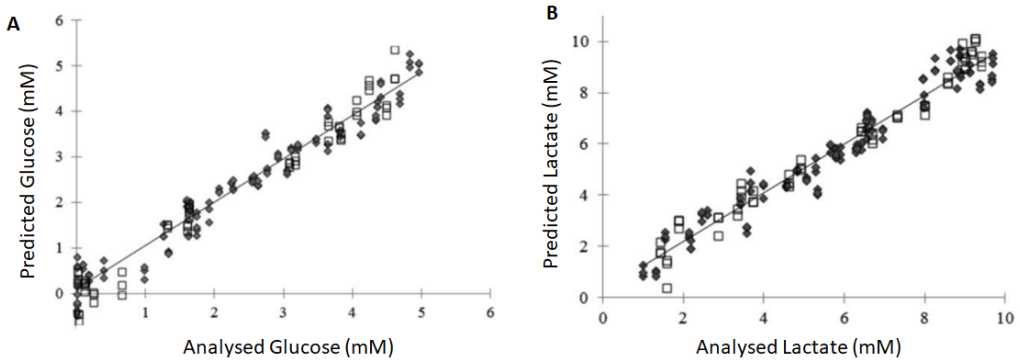

Figure 1.34 – Glucose and lactate concentrations predicted by global PLS regression models, based on MIR spectra. A. Predicted glucose concentration. B. Predicted lactate concentration. ♦ represent calibration samples and □ represent validation samples. Graph from the study of Rosa *et al.* [185].

Raman spectroscopy provides information about vibrational, rotational, and other low frequency transitions in molecules which the polarization changed by the light excitation. Therefore, Raman spectroscopy permit to analysze qualitatively and quantitatively the structure of a sample [186]. The first results obtained in mammalian cell lines with Raman spectroscopy dated from 2011 and were reported by Abu-Absi *et al.* [187]. Then, in 2012, Whelan *et al.* used this technique at the laboratory scale (3-15 L) [186]. Finally, the spectroscopy Raman was also used in qualitative way, to characterize a cell culture medium [188] or to characterize the cell itself [189]. Thus, it was possible to distinguish different stages of apoptosis of CHO cells via Raman spectroscopy (Figure 1.35) [189].

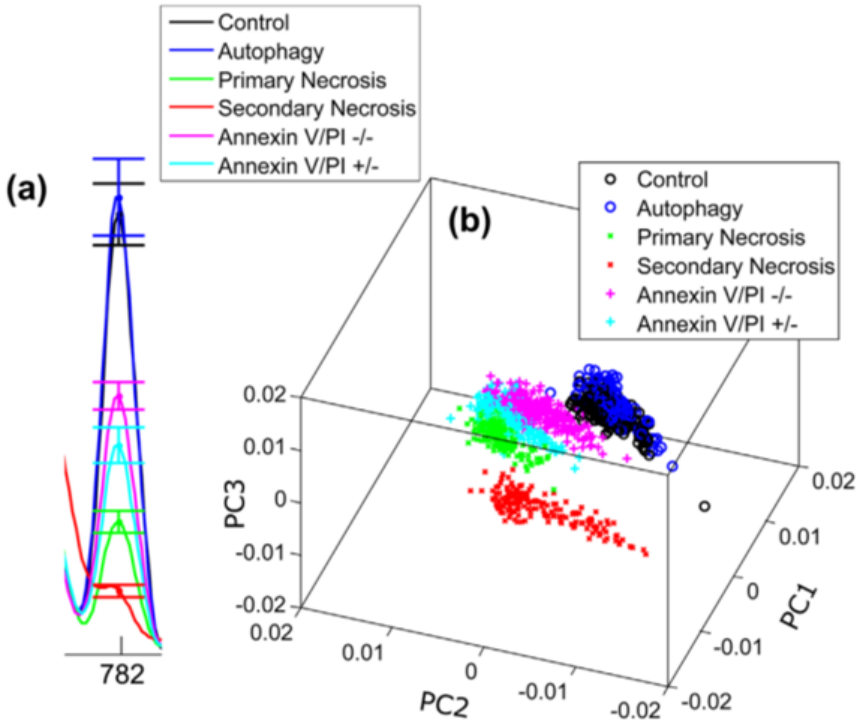

Figure 1.35 – Comparison of different CHO population distinguished by Raman spectra. (a) Comaprison of the nucleic acid peak at 782 cm^{-1}. (b) PCA reveals a separation between all the assessed populations, however control and autophagic cell data overlap. Graph from the study of Rangan *et al.* [189].

1.5.4 Cell detachment

Cell purification processes include first, the cell harvesting from microcarriers, the separation of the cells from the microcarriers and finally, the cell washing and storage. Different protocols have been described in the literature for cell detachment (Table 1.7).

- **Enzymatic detachment**

A large majority of protocols reported the use of proteases, such as trypsin, in combination with a cationic chelating agent like EDTA. Tryspin is a serine protease cliving the peptide bond between lysine or arginin and no-specific amino-acids. Thus, the enzyme acts on cell cytoskeleton and membrane surface compounds and provokes the typical rounded shape of the cell. Concerning the cell detachment of cultures on microcarriers different protocols were proposed by authors. First, the one described by Nienow *et al.*, using a mix of trypsin and EDTA, directly applied in the spinner vessel for 7 min at 37°C. Agitation rate was set up at 150 rpm, corresponding to a 5 × N_{js} value [190]. Thanks to this method, authors obtained a high efficiency of detachment (> 95 %) and a good cell viability. The second protocol of detachment is adapted from the first protocol established by Nienow *et al.* [190]. Authors could adapt the ratio of enzymes/ EDTA or used a recombinant trypsin (*i.e.* the TrypLE) [45]. They could also modulate the duration of enzyme action, the agitation rate among multiple parameters. Lastly, Varani *et al.* tested the same protocol of trypsination on different microcarriers (*i.e.* plastic, dextran, and glass types) with Vero cells and found that a longer period of trypsination with further vortexing was required to detach cells from dextran type microcarriers [191].

Table 1.7 – List of human MSCs detachment protocols in the literature.

MSC origin	**Reactor**	**Enzyme**	**Agitation**	**Time (min)**	**Temperature**	**Efficiency**	**Viability**	**References**
BM-MSC	SV	Trypsin EDTA	150 rpm	7	37°C	>95 %	No effect on hMSC quality	Nienow *et al.* [190]
AD-MSC	STR	TrypLE Express	60 rpm	10	37°C	>90 %	>95 %	Schirmaier *et al.* [122]
f-MSC	STR	0.25 % Trypsin EDTA	90 oscillations/ min	5	37°C	85 %	>95 %	Goh *et al.* [192]
f-MSC	STR	TrypLE	90 oscillations/ min	5	37°C	60 %	>95 %	Goh *et al.* [192]
UC-MSC	SV	Trypsin	No	10	37°C	90 %	>90 %	Petry *et al.* [45]
BM-MSC	SV	Tryple Express	Occasional flicking	15	37°C	88 %	95 %	Caruso et al. [99]
TERT-MSC	SV	Trypsin	N/A	10	37°C	< 20 %	55 - 65 %	Weber *et al.* [111]
TERT-MSC	SV	Accutase	N/A	10	37°C	< 20 %	55 - 65 %	Weber *et al.* [111]
TERT-MSC	SV	Trypsin + Accutase (1:1)	N/A	10	37°C	< 20 %	55 - 65 %	Weber *et al.* [111]

- **Non enzymatic detachment**

Considering the risks of damages applied to cells by the action of enzymes, other strategies of cell detachment were proposed, with for example the development of microcarriers with cleavable surfaces or microcarriers degradable with certain enzymes and reagents. Thus, authors reported the use of modified microcarriers with a thermo-sensible layer as coating. The pNIPAAM is a repeated chain of hydrophilic amide and hydrophobic isopropyl groups which allow the layer to undergo conformational changes with the decrease of temperature in an aqueous environment. When the temperature is above 32°C, the pNIPAAM layer takes a globule form, suitable for cell adhesion, and when the temperature is below 32°C, the layer takes a swelled shape which cause cell detachment (Figure 1.36) [193]. With all these different techniques of cell detachment, a step of filtration is needed, in order to exclude microcarriers and debris which can alter the quality of the product. As most of microcarriers are larger than cells, the size exclusion could be used as a method. Cell strainer or vacuum filters could also be used. Recently, with the objective to avoid filtration steps, dissolvable microcarriers were developed by Corning. Made of polygalacturonic acid (PGA) and calcium, the action of a pectinase combined with EDTA and a proteolytic enzyme such as trypsin allow the detachment of cells by digesting the microcarrier.

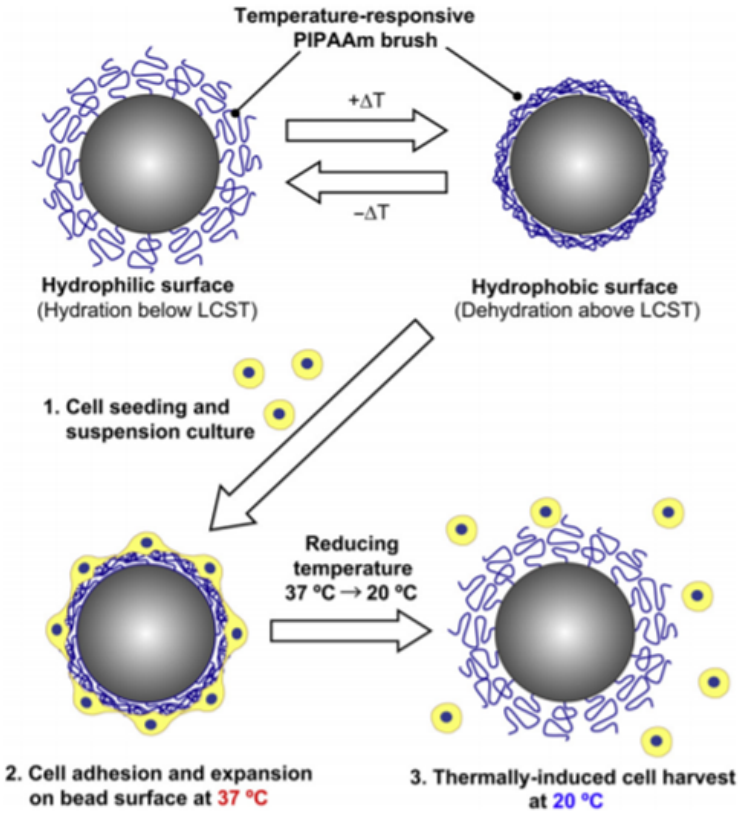

Figure 1.36 – Schematic representation of pNIPAAM-grafted microcarriers exhibiting a temperature-dependent conformational changes for cell expansion and harvesting [194].

After the filtration steps and the exclusion of wastes, the cell solution required to be concentrate in order to be injected or infused to patients. Different techniques were reported in the literature, for small volumes (up to 10 L) a centrifugation step can be performed, for larger volumes,

tangential flow filtration should be preferred [137]. Finally, to remove all traces of enzymes and serum a washing step of the concentrated cells is required. Diafiltration or expanded bed chromatography were explored and proposed by Cunha *et al.* [195]. Then, concentrated and washed cells could be cryoconserved and stored until their use.

Summary of the section

- Production of allogenic human MSCs with both high quantity and quality is challenging.
- Critical quality attributes of human MSCs are necessary to define and validate in order to standardize the quality controls during batch production.
- Environmental factors such as cell culture medium, surface of growth, cell culture parameters (pH, temperature, O_2), shear stress and agitation may have a high impact on cell quality.
- On-line monitoring is emerging in order to control quality of human MSCs during expansion process.

1.6 Thesis aims and objectives

The development of cultures of human MSCs fulfills the promises for cell-based therapeutics as tissue engineering and cellular therapies, but many milestones must be achieved before to be able to produce characterized and functionalized human MSCs for large-scale therapies at minimal cost. To enable the use of human MSCs in cell therapies, it is necessary to have large quantities of cells which have preserved their functions and quality, as the differentiation ability, the stem phenotype, the immuno-modulation and, more generally, secretome properties.

In order to achieve these objectives, a better understanding of the expansion process of human MSCs in bioreactor is crucial, and the impact of modes of culture and mechanical (agitation, shear stress) parameters on the cellular response has to be investigated.

The main objective of this work, that is integrated into a collaborative European INTERREG project 'IMPROVE - STEM', is to develop a validated and innovative continuous culture process of human mesenchymal stem cells extracted from the Wharton's jelly (hWJ-MSC). As presented in the figure 1.37, the different scientific partners are from Belgium, France, Germany and Luxembourg. The different area of excellence of each teams were used in order to develop an optimized mode of production of WJ-MSCs on innovative adhesion supports. After conducting a literature review, presented in Chapter 1, three issues were identified and divided the work into three study tasks.

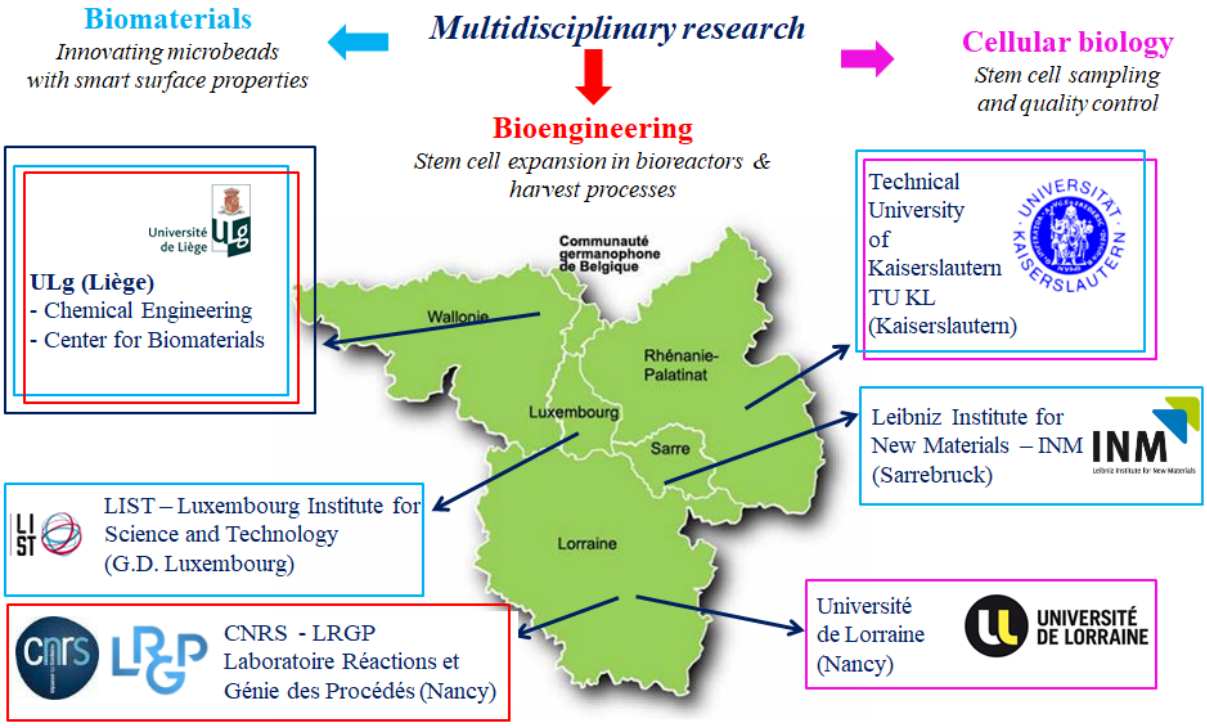

Figure 1.37 – Structure of the IMPROVE-STEM Interreg Project.

- **Chapter 2:** As WJ-MSCs are adherent-dependent cells, new insights about the cell adhesion on microcarriers would be useful for a better understanding of cell expansion. To help understanding the mechanisms underlying the cell adhesion phase and thus improve it, the use of dielectric spectroscopic measurements to detect adhesion is evaluated in this chapter. Moreover, thanks to time lapse microscopy technology, kinetics of cell migrations could also be evaluated. WJ-MSCs culture on microcarriers are usually limited in time. Different causes are involved to explain the limit of cell expansion such as, a depletion in nutrients or a limitation of growth surfaces. In literature, various strategies based on the modification of cell culture medium or sometimes on the addition of new microcarriers addition could be find to overcome this situation. However, these strategies are generally empirical. An adapted strategy of new microcarriers addition is proposed in this chapter. **Validation and improvement of bead-to-bead transfer of hMSC in order to increase cell expansion duration is thus the main objective of this chapter.**

- **Chapter 3:** Planar multilayer flasks are currently most often applied for the commercial manufacture of WJ-MSC, however these systems present numerous drawbacks. Bioreactors systems raised interest thanks to their ease to scale-up, the possible pH, temperature and dissolved gases monitoring and the possibility to control their stirring in order to avoid nutrient gradient concentrations. **Optimization of the WJ-MSC expansion in stirred tank bioreactors by determining the most adaptive set of operating conditions and microcarrier chemistry is the aim of this chapter, by integrating the strategy of microcarriers addition developed in the previous chapter.**

- **Chapter 4:** Development of bioprocesses capable of producing large numbers of hMSC in a robust and safe manner is critical for therapeutic applications. The phase of the separation of the cells from their supports, at the end of the process, is very dependent on the triptych medium/ cell/support surface chemistry. Scalable expansion of hWJ-MSC on Cytodex-1 or other types of microcarriers usually found in cell culture, involved specific cell detachment using trypsin. Trypsin or other cell detachment enzymes could have harmful effects on cells and their viability. Besides, a filtration step is required because carriers remained in the cell culture medium. **In this chapter, the efficiency of novel xeno-free dissolvable microcarriers for the culture and detachment of hWJ-MSC is demonstrated. Moreover, a new innovative perfusion system is implemented in the bioreactor, with addition of fresh microcarriers and a perfusion system for the cell culture medium in order to avoid depletion in nutrients or growth factors.** Dielectric spectroscopy also permitted to monitor cell growth on-line.

Development of an optimized continuous-perfused process of culture of human umbilical cord mesenchymal stem cells grown on innovative adhesion supports
Chapter 2
Optimization and understanding of the interactions between cells and microcarriers.
Chapter 3
Characterization of innovative microcarriers for the expansion of mesenchymal stem cells.
Chapter 4
An innovative perfused mode of culture of WJ-MSCs with empty microcarrier removal and on-line monitoring of cell concentration.
To propose an innovative robust and 'low-cost' culture process to produce fully characterized WJ-MSC

Bibliography

[1] C. Martin. *Etude des procédés d'amplification de cellules souches mésenchymateuses humaines*. PhD thesis, Universite de Lorraine, 2016.

[2] M. J. Evans and M. H. Kaufman. Establishment in culture of pluripotential cells from mouse embryos. *Nature*, 292(5819):154–156, 1981.

[3] G. R. Martin. Isolation of a pluripotent cell line from early mouse embryos cultured in medium conditioned by teratocarcinoma stem cells. *Proceedings of the National Academy of Sciences*, 78(12):7634–7638, 1981.

[4] J. A. Thomson, J. Itskovitz-Eldor, S. S. Shapiro, M. A. Waknitz, J. J. Swiergiel, V. S. Marshall, and J. M. Jones. Embryonic stem cell lines derived from human blastocysts. *Science*, 282(5391):1145–1147, 1998.

[5] G. Q. Daley. The promise and perils of stem cell therapeutics. *Cell Stem Cell*, 10(6):740–749, 2012.

[6] H.-T. Lin, M. Otsu, and H. Nakauchi. Stem cell therapy: an exercise in patience and prudence. *Philosophical Transactions of the Royal Society B: Biological Sciences*, 368(1609):20110334, 2013.

[7] R. Schofield. The relationship between the spleen colony-forming cell and the haemopoietic stem cell. *Blood Cells*, 4(1-2):7–25, 1978.

[8] D. A. De Ugarte, K. Morizono, A. Elbarbary, Z. Alfonso, P. A. Zuk, M. Zhu, J. L. Dragoo, P. Ashjian, B. Thomas, P. Benhaim, et al. Comparison of multi-lineage cells from human adipose tissue and bone marrow. *Cells Tissues Organs*, 174(3):101–109, 2003.

[9] W. Jackson, A. Aragon, F. Djouad, Y. Song, S. Koehler, L. Nesti, and R. Tuan. Mesenchymal progenitor cells derived from traumatized human muscle. *Journal of Tissue Engineering and Regenerative Medicine*, 3(2):129–138, 2009.

[10] P.-P. Chong, L. Selvaratnam, A. A. Abbas, and T. Kamarul. Human peripheral blood derived mesenchymal stem cells demonstrate similar characteristics and chondrogenic differentiation potential to bone marrow derived mesenchymal stem cells. *Journal of Orthopaedic Research*, 30(4):634–642, 2012.

[11] N. F. Lizier, A. Kerkis, C. M. Gomes, J. Hebling, C. F. Oliveira, A. I. Caplan, and I. Kerkis. Scaling-up of dental pulp stem cells isolated from multiple niches. *PLoS One*, 7(6), 2012.

[12] M. Mouiseddine, N. Mathieu, J. Stefani, C. Demarquay, and J.-M. Bertho. Characterization and histological localization of multipotent mesenchymal stromal cells in the human post-natal thymus. *Stem Cells and Development*, 17(6):1165–1174, 2008.

[13] G. Brooke, T. Rossetti, R. Pelekanos, N. Ilic, P. Murray, S. Hancock, V. Antonenas, G. Huang, D. Gottlieb, K. Bradstock, et al. Manufacturing of human placenta-derived mesenchymal stem cells for clinical trials. *British Journal of Haematology*, 144(4):571–579, 2009.

[14] S. Knudtzon. In vitro growth of granulocytic colonies from circulating cells in human cord blood. *Blood*, 43(3):357–361, 1974.

[15] C. Loubière. *Characterization and impact of the hydrodynamics on the performance of umbilical-cord derived stem cells culture in stirred tank bioreactors*. PhD thesis, Université de Lorraine, 2018.

[16] K. Takahashi and S. Yamanaka. Induction of pluripotent stem cells from mouse embryonic and adult fibroblast cultures by defined factors. *Cell*, 126(4):663–676, 2006.

[17] A. Friedenstein, R. Chailakhjan, and K. Lalykina. The development of fibroblast colonies in monolayer cultures of guinea-pig bone marrow and spleen cells. *Cell Proliferation*, 3(4):393–403, 1970.

[18] A. Caplan. Mesenchymal stem cells. *Journal of Orthopaedic Research*, 9(5):641–650, 1991.

[19] M. F. Pittenger, A. M. Mackay, S. C. Beck, R. K. Jaiswal, R. Douglas, J. D. Mosca, M. A. Moorman, D. W. Simonetti, S. Craig, and D. R. Marshak. Multilineage potential of adult human mesenchymal stem cells. *Science*, 284(5411):143–147, 1999.

[20] K. Le Blanc. Immunomodulatory effects of fetal and adult mesenchymal stem cells. *Cytotherapy*, 5(6):485–489, 2003.

[21] M. Dominici, K. Le Blanc, I. Mueller, I. Slaper-Cortenbach, F. Marini, D. Krause, R. Deans, A. Keating, D. Prockop, and E. Horwitz. Minimal criteria for defining multipotent mesenchymal stromal cells. the international society for cellular therapy position statement. *Cytotherapy*, 8(4):315–317, 2006.

[22] G. Chamberlain, J. Fox, B. Ashton, and J. Middleton. Concise review: mesenchymal stem cells: their phenotype, differentiation capacity, immunological features, and potential for homing. *Stem Cells*, 25(11):2739–2749, 2007.

[23] G. Brooke, M. Cook, C. Blair, R. Han, C. Heazlewood, B. Jones, M. Kambouris, K. Kollar, S. McTaggart, R. Pelekanos, et al. Therapeutic applications of mesenchymal stromal cells. In *Seminars in Cell & Developmental Biology*, volume 18, pages 846–858. Elsevier, 2007.

[24] E. M. Horwitz, D. J. Prockop, P. L. Gordon, W. W. Koo, L. A. Fitzpatrick, M. D. Neel, M. E. McCarville, P. J. Orchard, R. E. Pyeritz, and M. K. Brenner. Clinical responses to bone marrow transplantation in children with severe osteogenesis imperfecta. *Blood, The Journal of the American Society of Hematology*, 97(5):1227–1231, 2001.

[25] M. Chopp, X. H. Zhang, Y. Li, L. Wang, J. Chen, D. Lu, M. Lu, and M. Rosenblum. Spinal cord injury in rat: treatment with bone marrow stromal cell transplantation. *Neuroreport*, 11(13):3001–3005, 2000.

[26] J. Chen, Y. Li, L. Wang, Z. Zhang, D. Lu, M. Lu, and M. Chopp. Therapeutic benefit of intravenous administration of bone marrow stromal cells after cerebral ischemia in rats. *Stroke*, 32(4):1005–1011, 2001.

[27] Y. Li, J. Chen, C. L. Zhang, L. Wang, D. Lu, M. Katakowski, Q. Gao, L. H. Shen, J. Zhang, M. Lu, et al. Gliosis and brain remodeling after treatment of stroke in rats with marrow stromal cells. *Glia*, 49(3):407–417, 2005.

[28] Y.-C. Chang, W.-C. Shyu, S.-Z. Lin, and H. Li. Regenerative therapy for stroke. *Cell Transplantation*, 16(2):171–181, 2007.

[29] B. Fang, M. Shi, L. Liao, S. Yang, Y. Liu, and R. C. Zhao. Systemic infusion of flk1+ mesenchymal stem cells ameliorate carbon tetrachloride-induced liver fibrosis in mice. *Transplantation*, 78(1):83–88, 2004.

[30] V. Karantalis, D. L. DiFede, G. Gerstenblith, S. Pham, J. Symes, J. P. Zambrano, J. Fishman, P. Pattany, I. McNiece, J. Conte, et al. Autologous mesenchymal stem cells produce concordant improvements in regional function, tissue perfusion, and fibrotic burden when administered to patients undergoing coronary artery bypass grafting: the prospective randomized study of mesenchymal stem cell therapy in patients undergoing cardiac surgery (prometheus) trial. *Circulation Research*, 114(8):1302–1310, 2014.

[31] A. R. Williams, B. Trachtenberg, D. L. Velazquez, I. McNiece, P. Altman, D. Rouy, A. M. Mendizabal, P. M. Pattany, G. A. Lopera, J. Fishman, et al. Intramyocardial stem cell injection in patients with ischemic cardiomyopathy: functional recovery and reverse remodeling. *Circulation Research*, 108(7):792–796, 2011.

[32] J. M. Hare, D. L. DiFede, A. C. Rieger, V. Florea, A. M. Landin, J. El-Khorazaty, A. Khan, M. Mushtaq, M. H. Lowery, J. J. Byrnes, et al. Randomized comparison of allogeneic versus autologous mesenchymal stem cells for nonischemic dilated cardiomyopathy: Poseidon-dcm trial. *Journal of the American College of Cardiology*, 69(5):526–537, 2017.

[33] A. N. Kharlamov and J. L. Gabinsky. Plasmonic photothermic and stem cell therapy of atherosclerotic plaque as a novel nanotool for angioplasty and artery remodeling. *Rejuvenation Research*, 15(2):222–230, 2012.

[34] L. Orozco, A. Munar, R. Soler, M. Alberca, F. Soler, M. Huguet, J. Sentís, A. Sánchez, and J. García-Sancho. Treatment of knee osteoarthritis with autologous mesenchymal stem cells: a pilot study. *Transplantation*, 95(12):1535–1541, 2013.

[35] J. Vaquero and M. Zurita. Functional recovery after severe cns trauma: current perspectives for cell therapy with bone marrow stromal cells. *Progress in Neurobiology*, 93(3):341–349, 2011.

[36] L. Geffner, P. Santacruz, M. Izurieta, L. Flor, B. Maldonado, A. Auad, X. Montenegro, R. Gonzalez, and F. Silva. Administration of autologous bone marrow stem cells into spinal cord injury patients via multiple routes is safe and improves their quality of life: comprehensive case studies. *Cell Transplantation*, 17(12):1277–1293, 2008.

[37] Y. Chen, Y. Ma, N. Li, H. Wang, B. Chen, Z. Liang, R. Ren, D. Lu, J. Boey, D. G. Armstrong, et al. Efficacy and long-term longitudinal follow-up of bone marrow mesenchymal cell transplantation therapy in a diabetic patient with recurrent lower limb bullosis diabeticorum. *Stem Cell Research & Therapy*, 9(1):99, 2018.

[38] S. Kaneko. Liver regeneration therapy using autologous adipose tissue derived stromal cells, http://clinicaltrials.gov/ct2/show/NCT00913289, 2011.

[39] Z. Zhang, H. Lin, M. Shi, R. Xu, J. Fu, J. Lv, L. Chen, S. Lv, Y. Li, S. Yu, et al. Human umbilical cord mesenchymal stem cells improve liver function and ascites in decompensated liver cirrhosis patients. *Journal of Gastroenterology and Hepatology*, 27:112–120, 2012.

[40] A. Makhlough, S. Shekarchian, R. Moghadasali, B. Einollahi, S. E. Hosseini, N. Jaroughi, T. Bolurieh, H. Baharvand, and N. Aghdami. Safety and tolerability of autologous bone marrow mesenchymal stromal cells in adpkd patients. *Stem Cell Research & Therapy*, 8(1):116, 2017.

[41] E. Jang, M. Jeong, S. Kim, K. Jang, B.-K. Kang, D. Y. Lee, S.-C. Bae, K. S. Kim, and J. Youn. Infusion of human bone marrow-derived mesenchymal stem cells alleviates autoimmune nephritis in a lupus model by suppressing follicular helper t-cell development. *Cell Transplantation*, 25(1):1–15, 2016.

[42] K. Kim, G. Blasco-Morente, N. Cuende, and S. Arias-Santiago. Mesenchymal stromal cells: properties and role in management of cutaneous diseases. *Journal of the European Academy of Dermatology and Venereology*, 31(3):414–423, 2017.

[43] S. Kharbanda, A. R. Smith, S. K. Hutchinson, D. H. McKenna, J. B. Ball, L. S. Lamb Jr, R. Agarwal, K. I. Weinberg, and J. E. Wagner Jr. Unrelated donor allogeneic hematopoietic stem cell transplantation for patients with hemoglobinopathies using a reduced-intensity conditioning regimen and third-party mesenchymal stromal cells. *Biology of Blood and Marrow Transplantation*, 20(4):581–586, 2014.

[44] D. García-Olmo, M. García-Arranz, D. Herreros, I. Pascual, C. Peiro, and J. A. Rodríguez-Montes. A phase i clinical trial of the treatment of crohn's fistula by adipose mesenchymal stem cell transplantation. *Diseases of the Colon & Rectum*, 48(7):1416–1423, 2005.

[45] F. Petry, J. R. Smith, J. Leber, D. Salzig, P. Czermak, and M. L. Weiss. Manufacturing of human umbilical cord mesenchymal stromal cells on microcarriers in a dynamic system for clinical use. *Stem Cells International*, 2016, 2016.

[46] T. R. Olsen, K. S. Ng, L. T. Lock, T. Ahsan, and J. A. Rowley. Peak msc—are we there yet? *Frontiers in medicine*, 5:178, 2018.

[47] A. Beck and J. M. Reichert. Approval of the first biosimilar antibodies in europe: a major landmark for the biopharmaceutical industry. In *MAbs*, volume 5, pages 621–623. Taylor & Francis, 2013.

[48] D. M. Ecker, S. D. Jones, and H. L. Levine. The therapeutic monoclonal antibody market. In *MAbs*, volume 7, pages 9–14. Taylor & Francis, 2015.

[49] H. Kaplon and J. M. Reichert. Antibodies to watch in 2019. In *MAbs*, volume 11, pages 219–238. Taylor & Francis, 2019.

[50] I. Arutyunyan, A. Elchaninov, A. Makarov, and T. Fatkhudinov. Umbilical cord as prospective source for mesenchymal stem cell-based therapy. *Stem Cells International*, 2016, 2016.

[51] K. D. McElreavey, A. I. Irvine, K. T. Ennis, and W. I. McLean. Isolation, culture and characterisation of fibroblast-like cells derived from the Wharton's jelly portion of human umbilical cord, BiochemSoc Trans; 19:29S, 1991.

[52] H.-S. Wang, S.-C. Hung, S.-T. Peng, C.-C. Huang, H.-M. Wei, Y.-J. Guo, Y.-S. Fu, M.-C. Lai, and C.-C. Chen. Mesenchymal stem cells in the wharton's jelly of the human umbilical cord. *Stem Cells*, 22(7):1330–1337, 2004.

[53] D.-W. Kim, M. Staples, K. Shinozuka, P. Pantcheva, S.-D. Kang, and C. V. Borlongan. Wharton's jelly-derived mesenchymal stem cells: phenotypic characterization and optimizing their therapeutic potential for clinical applications. *International Journal of Molecular Sciences*, 14(6):11692–11712, 2013.

[54] K. Seshareddy, D. Troyer, and M. L. Weiss. Method to isolate mesenchymal-like cells from wharton's jelly of umbilical cord. *Methods in Cell Biology*, 86:101–119, 2008.

[55] K. E. Mitchell, M. L. Weiss, B. M. Mitchell, P. Martin, D. Davis, L. Morales, B. Helwig, M. Beerenstrauch, K. Abou-Easa, T. Hildreth, et al. Matrix cells from wharton's jelly form neurons and glia. *Stem Cells*, 21(1):50–60, 2003.

[56] C. K. Tong, S. Vellasamy, B. C. Tan, M. Abdullah, S. Vidyadaran, H. F. Seow, and R. Ramasamy. Generation of mesenchymal stem cell from human umbilical cord tissue using a

combination enzymatic and mechanical disassociation method. *Cell Biology International*, 35(3):221–226, 2011.

[57] D. L. Troyer and M. L. Weiss. Concise review: Wharton's jelly-derived cells are a primitive stromal cell population. *Stem Cells*, 26(3):591–599, 2008.

[58] R. J. Emnett, A. Kaul, A. Babic, V. Geiler, D. Regan, G. Gross, and S. Akel. Evaluation of tissue homogenization to support the generation of gmp-compliant mesenchymal stromal cells from the umbilical cord. *Stem Cells International*, 2016, 2016.

[59] K. Stenderup, J. Justesen, C. Clausen, and M. Kassem. Aging is associated with decreased maximal life span and accelerated senescence of bone marrow stromal cells. *Bone*, 33(6):919–926, 2003.

[60] S. M. Mueller and J. Glowacki. Age-related decline in the osteogenic potential of human bone marrow cells cultured in three-dimensional collagen sponges. *Journal of Cellular Biochemistry*, 82(4):583–590, 2001.

[61] L.-L. Lu, Y.-j. Liu, S.-G. Yang, Q.-J. Zhao, X. Wang, W. Gong, Z.-B. Han, Z.-S. Xu, Y.-X. Lu, D. Liu, et al. Isolation and characterization of human umbilical cord mesenchymal stem cells with hematopoiesis-supportive function and other potentials. *Haematologica*, 91(8):1017–1026, 2006.

[62] S. Jyothi Prasanna and V. Sowmya Jahnavi. Wharton's jelly mesenchymal stem cells as off-the-shelf cellular therapeutics: a closer look into their regenerative and immunomodulatory properties. *The Open Tissue Engineering and Regenerative Medicine Journal*, 4(1), 2011.

[63] S. Prasanna, D. Gopalakrishnan, S. Shankar, and A. Vasandan. Pro-inflammatory cytokines, IFNc and TNFa, Influence Immune Properties of Human Bone Marrow and Wharton's Jelly Mesenchymal Stem Cells Differentially *PLos One*, 5(2), 2010.

[64] M. L. Weiss, C. Anderson, S. Medicetty, K. B. Seshareddy, R. J. Weiss, I. VanderWerff, D. Troyer, and K. R. McIntosh. Immune properties of human umbilical cord Wharton's jelly-derived cells. *Stem Cells*, 26(11):2865–2874, 2008.

[65] C. Ménard and K. Tarte. Immunosuppression et cellules souches mésenchymateuses-mieux comprendre une propriété thérapeutique majeure. *Médecine/Sciences*, 27(3):269–274, 2011.

[66] J.-Y. Hsieh, H.-W. Wang, S.-J. Chang, K.-H. Liao, I.-H. Lee, W.-S. Lin, C.-H. Wu, W.-Y. Lin, and S.-M. Cheng. Mesenchymal stem cells from human umbilical cord express preferentially secreted factors related to neuroprotection, neurogenesis, and angiogenesis. *PloS One*, 8(8), 2013.

[67] K. C. Chao, K. F. Chao, Y. S. Fu, and S. H. Liu. Islet-like clusters derived from mesenchymal stem cells in wharton's jelly of the human umbilical cord for transplantation to control type 1 diabetes. *PloS One*, 3(1), 2008.

[68] H.-S. Wang, J.-F. Shyu, W.-S. Shen, H.-C. Hsu, T.-C. Chi, C.-P. Chen, S.-W. Huang, Y.-M. Shyr, K.-T. Tang, and T.-H. Chen. Transplantation of insulin-producing cells derived from umbilical cord stromal mesenchymal stem cells to treat nod mice. *Cell Transplantation*, 20(3):455–466, 2011.

[69] L. Wang, K. Seshareddy, M. L. Weiss, and M. S. Detamore. Effect of initial seeding density on human umbilical cord mesenchymal stromal cells for fibrocartilage tissue engineering. *Tissue Engineering Part A*, 15(5):1009–1017, 2009.

[70] L. Wang, L. Zhao, and M. S. Detamore. Human umbilical cord mesenchymal stromal cells in a sandwich approach for osteochondral tissue engineering. *Journal of Tissue Engineering and Regenerative Medicine*, 5(9):712–721, 2011.

[71] R. S. Nirmal and P. D. Nair. Significance of soluble growth factors in the chondrogenic response of human umbilical cord matrix stem cells in a porous three dimensional scaffold. *Eur Cell Mater*, 26(11):234–51, 2013.

[72] X. Chen, F. Zhang, X. He, Y. Xu, Z. Yang, L. Chen, S. Zhou, Y. Yang, Z. Zhou, W. Sheng, et al. Chondrogenic differentiation of umbilical cord-derived mesenchymal stem cells in type i collagen-hydrogel for cartilage engineering. *Injury*, 44(4):540–549, 2013.

[73] M. L. Weiss, S. Medicetty, A. R. Bledsoe, R. S. Rachakatla, M. Choi, S. Merchav, Y. Luo, M. S. Rao, G. Velagaleti, and D. Troyer. Human umbilical cord matrix stem cells: preliminary characterization and effect of transplantation in a rodent model of parkinson's disease. *Stem Cells*, 24(3):781–792, 2006.

[74] M. T. Conconi, P. Burra, R. Di Liddo, C. Calore, M. Turetta, S. Bellini, P. Bo, G. G. Nussdorfer, and P. P. Parnigotto. Cd105 (+) cells from wharton's jelly show in vitro and in vivo myogenic differentiative potential. *International Journal of Molecular Medicine*, 18(6):1089–1096, 2006.

[75] R. Friedman, M. Betancur, L. Boissel, H. Tuncer, C. Cetrulo, and H. Klingemann. Umbilical cord mesenchymal stem cells: adjuvants for human cell transplantation. *Biology of Blood and Marrow Transplantation*, 13(12):1477–1486, 2007.

[76] J. Peng, Y. Wang, L. Zhang, B. Zhao, Z. Zhao, J. Chen, Q. Guo, S. Liu, X. Sui, W. Xu, et al. Human umbilical cord wharton's jelly-derived mesenchymal stem cells differentiate into a schwann-cell phenotype and promote neurite outgrowth in vitro. *Brain Research Bulletin*, 84(3):235–243, 2011.

[77] C. Elseberg, J. Leber, T. Weidner, and P. Czermak. The challenge of human mesenchymal stromal cell expansion: current and prospective answers. *New Insights into Cell Culture Technology*, page 99, 2017.

[78] GlobalData. Stem cell technologies and applications market report 2016-2026. 2015.

[79] A. Mizukami, T. D. P. Chilima, M. D. Orellana, M. A. Neto, D. T. Covas, S. S. Farid, and K. Swiech. Technologies for large-scale umbilical cord-derived msc expansion: Experimental performance and cost of goods analysis. *Biochemical Engineering Journal*, 135:36–48, 2018.

[80] A. L. Russell, R. C. Lefavor, and A. C. Zubair. Characterization and cost–benefit analysis of automated bioreactor-expanded mesenchymal stem cells for clinical applications. *Transfusion*, 58(10):2374–2382, 2018.

[81] A. A. Khalili and M. R. Ahmad. A review of cell adhesion studies for biomedical and biological applications. *International Journal of Molecular Sciences*, 16(8):18149–18184, 2015.

[82] M.-H. Kim, M. Kino-Oka, and M. Taya. Designing culture surfaces based on cell anchoring mechanisms to regulate cell morphologies and functions. *Biotechnology Advances*, 28(1):7–16, 2010.

[83] B. Geiger and A. Bershadsky. Assembly and mechanosensory function of focal contacts. *Current Opinion in Cell Biology*, 13(5):584–592, 2001.

[84] E. Zamir, B.-Z. Katz, S.-i. Aota, K. M. Yamada, B. Geiger, and Z. Kam. Molecular diversity of cell-matrix adhesions. *Journal of Cell Science*, 112(11):1655–1669, 1999.

[85] W. L. Murphy, T. C. McDevitt, and A. J. Engler. Materials as stem cell regulators. *Nature Materials*, 13(6):547–557, 2014.

[86] P. M. Gilbert, K. L. Havenstrite, K. E. Magnusson, A. Sacco, N. A. Leonardi, P. Kraft, N. K. Nguyen, S. Thrun, M. P. Lutolf, and H. M. Blau. Substrate elasticity regulates skeletal muscle stem cell self-renewal in culture. *Science*, 329(5995):1078–1081, 2010.

[87] F. Chowdhury, Y. Li, Y.-C. Poh, T. Yokohama-Tamaki, N. Wang, and T. S. Tanaka. Soft substrates promote homogeneous self-renewal of embryonic stem cells via downregulating cell-matrix tractions. *PloS One*, 5(12), 2010.

[88] A. Van Wezel. Growth of cell-strains and primary cells on micro-carriers in homogeneous culture. *Nature*, 216(5110):64–65, 1967.

[89] M. António, A. Fernandes-Platzgummer, C. L. da Silva, and J. M. Cabral. Scalable microcarrier-based manufacturing of mesenchymal stem/stromal cells. *Journal of Biotechnology*, 236:88–109, 2016.

[90] S. Derakhti, S. H. Safiabadi-Tali, G. Amoabediny, and M. Sheikhpour. Attachment and detachment strategies in microcarrier-based cell culture technology: A comprehensive review. *Materials Science and Engineering: C*, page 109782, 2019.

[91] S. Kuddannaya, Y. J. Chuah, M. H. A. Lee, N. V. Menon, Y. Kang, and Y. Zhang. Surface chemical modification of poly (dimethylsiloxane) for the enhanced adhesion and proliferation of mesenchymal stem cells. *ACS applied materials & interfaces*, 5(19):9777–9784, 2013.

[92] D. Schop, R. van Dijkhuizen-Radersma, E. Borgart, F. Janssen, H. Rozemuller, H.-J. Prins, and J. D. de Bruijn. Expansion of human mesenchymal stromal cells on microcarriers: growth and metabolism. *Journal of Tissue Engineering and Regenerative Medicine*, 4(2):131–140, 2010.

[93] F. d. Santos, P. Z. Andrade, M. M. Abecasis, J. M. Gimble, L. G. Chase, A. M. Campbell, S. Boucher, M. C. Vemuri, C. L. d. Silva, and J. M. Cabral. Toward a clinical-grade expansion of mesenchymal stem cells from human sources: a microcarrier-based culture system under xeno-free conditions. *Tissue Engineering Part C: Methods*, 17(12):1201–1210, 2011.

[94] Q. A. Rafiq, K. Coopman, A. W. Nienow, and C. J. Hewitt. Systematic microcarrier screening and agitated culture conditions improves human mesenchymal stem cell yield in bioreactors. *Biotechnology Journal*, 11(4):473–486, 2016.

[95] C. Loubière, C. Sion, N. De Isla, L. Reppel, E. Guedon, I. Chevalot, and E. Olmos. Impact of the type of microcarrier and agitation modes on the expansion performances of mesenchymal stem cells derived from umbilical cord. *Biotechnology Progress*, page e2887, 2019.

[96] D. Schop, F. Janssen, E. Borgart, J. D. de Bruijn, and R. van Dijkhuizen-Radersma. Expansion of mesenchymal stem cells using a microcarrier-based cultivation system: growth and metabolism. *Journal of Tissue Engineering and Regenerative Medicine*, 2(2-3):126–135, 2008.

[97] V. Jossen, R. Pörtner, S. C. Kaiser, M. Kraume, D. Eibl, and R. Eibl. Mass production of mesenchymal stem cells—impact of bioreactor design and flow conditions on proliferation and differentiation. In *Cells and Biomaterials in Regenerative Medicine*, volume 2014. InTech, 2014.

[98] G. Eibes, F. dos Santos, P. Z. Andrade, J. S. Boura, M. M. Abecasis, C. L. da Silva, and J. M. Cabral. Maximizing the ex vivo expansion of human mesenchymal stem cells using a microcarrier-based stirred culture system. *Journal of Biotechnology*, 146(4):194–197, 2010.

[99] S. R. Caruso, M. D. Orellana, A. Mizukami, T. R. Fernandes, A. M. Fontes, C. A. Suazo, V. C. Oliveira, D. T. Covas, and K. Swiech. Growth and functional harvesting of human mesenchymal stromal cells cultured on a microcarrier-based system. *Biotechnology Progress*, 30(4):889–895, 2014.

[100] H. S. Yang, O. Jeon, S. H. Bhang, S.-H. Lee, and B.-S. Kim. Suspension culture of mammalian cells using thermosensitive microcarrier that allows cell detachment without proteolytic enzyme treatment. *Cell Transplantation*, 19(9):1123–1132, 2010.

[101] X. Yuan, A.-C. Tsai, I. Farrance, J. A. Rowley, and T. Ma. Aggregation of culture expanded human mesenchymal stem cells in microcarrier-based bioreactor. *Biochemical Engineering Journal*, 131:39–46, 2018.

[102] M. Hervy, J. L. Weber, M. Pecheul, P. Dolley-Sonneville, D. Henry, Y. Zhou, and Z. Melkoumian. Long term expansion of bone marrow-derived hmscs on novel synthetic microcarriers in xeno-free, defined conditions. *PLoS One*, 9(3), 2014.

[103] J. G. Carmelo, A. Fernandes-Platzgummer, M. M. Diogo, C. L. da Silva, and J. M. Cabral. A xeno-free microcarrier-based stirred culture system for the scalable expansion of human mesenchymal stem/stromal cells isolated from bone marrow and adipose tissue. *Biotechnology Journal*, 10(8):1235–1247, 2015.

[104] T. R. Heathman, A. Stolzing, C. Fabian, Q. A. Rafiq, K. Coopman, A. W. Nienow, B. Kara, and C. J. Hewitt. Scalability and process transfer of mesenchymal stromal cell production from monolayer to microcarrier culture using human platelet lysate. *Cytotherapy*, 18(4):523–535, 2016.

[105] Q. A. Rafiq, M. P. Hanga, T. R. Heathman, K. Coopman, A. W. Nienow, D. J. Williams, and C. J. Hewitt. Process development of human multipotent stromal cell microcarrier culture using an automated high-throughput microbioreactor. *Biotechnology and Bioengineering*, 114(10):2253–2266, 2017.

[106] B. Cunha, T. Aguiar, S. B. Carvalho, M. M. Silva, R. A. Gomes, M. J. Carrondo, P. Gomes-Alves, C. Peixoto, M. Serra, and P. M. Alves. Bioprocess integration for human mesenchymal stem cells: from up to downstream processing scale-up to cell proteome characterization. *Journal of Biotechnology*, 248:87–98, 2017.

[107] S. Frauenschuh, E. Reichmann, Y. Ibold, P. M. Goetz, M. Sittinger, and J. Ringe. A microcarrier-based cultivation system for expansion of primary mesenchymal stem cells. *Biotechnology Progress*, 23(1):187–193, 2007.

[108] S. Sart, Y.-J. Schneider, and S. N. Agathos. Ear mesenchymal stem cells: an efficient adult multipotent cell population fit for rapid and scalable expansion. *Journal of Biotechnology*, 139(4):291–299, 2009.

[109] A. K.-L. Chen, Y. K. Chew, H. Y. Tan, S. Reuveny, and S. K. W. Oh. Increasing efficiency of human mesenchymal stromal cell culture by optimization of microcarrier concentration and design of medium feed. *Cytotherapy*, 17(2):163–173, 2015.

[110] J. Leber, J. Barekzai, M. Blumenstock, B. Pospisil, D. Salzig, and P. Czermak. Microcarrier choice and bead-to-bead transfer for human mesenchymal stem cells in serum-containing and chemically defined media. *Process Biochemistry*, 59:255–265, 2017.

[111] C. Weber, S. Pohl, R. Pörtner, C. Wallrapp, M. Kassem, P. Geigle, and P. Czermak. Expansion and harvesting of hmsc-tert. *The Open Biomedical Engineering Journal*, 1:38, 2007.

[112] Y. Fan, M. Hsiung, C. Cheng, and E. S. Tzanakakis. Facile engineering of xeno-free microcarriers for the scalable cultivation of human pluripotent stem cells in stirred suspension. *Tissue Engineering Part A*, 20(3-4):588–599, 2014.

[113] C. J. Hewitt, K. Lee, A. W. Nienow, R. J. Thomas, M. Smith, and C. R. Thomas. Expansion of human mesenchymal stem cells on microcarriers. *Biotechnology Letters*, 33(11):2325, 2011.

[114] A. M. de Soure, A. Fernandes-Platzgummer, F. Moreira, C. Lilaia, S.-H. Liu, C.-P. Ku, Y.-F. Huang, W. Milligan, J. M. Cabral, and C. L. da Silva. Integrated culture platform based on a human platelet lysate supplement for the isolation and scalable manufacturing of umbilical cord matrix-derived mesenchymal stem/stromal cells. *Journal of Tissue Engineering and Regenerative Medicine*, 11(5):1630–1640, 2017.

[115] K. Y. Tan, K. L. Teo, J. F. Lim, A. K. Chen, S. Reuveny, and S. K. Oh. Serum-free media formulations are cell line–specific and require optimization for microcarrier culture. *Cytotherapy*, 17(8):1152–1165, 2015.

[116] P. A. Tozetti, S. R. Caruso, A. Mizukami, T. R. Fernandes, F. B. da Silva, F. Traina, D. T. Covas, M. D. Orellana, and K. Swiech. Expansion strategies for human mesenchymal stromal cells culture under xeno-free conditions. *Biotechnology Progress*, 33(5):1358–1367, 2017.

[117] M.-L. Collignon, A. Delafosse, M. Crine, and D. Toye. Axial impeller selection for anchorage dependent animal cell culture in stirred bioreactors: methodology based on the impeller comparison at just-suspended speed of rotation. *Chemical Engineering Science*, 65(22):5929–5941, 2010.

[118] A. Delafosse, C. Loubière, S. Calvo, D. Toye, and E. Olmos. Solid-liquid suspension of microcarriers in stirred tank bioreactor–experimental and numerical analysis. *Chemical Engineering Science*, 180:52–63, 2018.

[119] C. Loubière, A. Delafosse, E. Guedon, D. Toye, I. Chevalot, and É. Olmos. Optimization of the impeller design for mesenchymal stem cell culture on microcarriers in bioreactors. *Chemical Engineering & Technology*, 42(8):1702–1708, 2019.

[120] K. Siddiquee and M. Sha. Billion-cell hypoxic expansion of human mesenchymal stem cells in bioblu® 5c single-use vessels. *BioProcessing*, 14(2):1538–8786, 2015.

[121] F. dos Santos, A. Campbell, A. Fernandes-Platzgummer, P. Z. Andrade, J. M. Gimble, Y. Wen, S. Boucher, M. C. Vemuri, C. L. da Silva, and J. M. Cabral. A xenogeneic-free bioreactor system for the clinical-scale expansion of human mesenchymal stem/stromal cells. *Biotechnology and Bioengineering*, 111(6):1116–1127, 2014.

[122] C. Schirmaier, V. Jossen, S. C. Kaiser, F. Jüngerkes, S. Brill, A. Safavi-Nab, A. Siehoff, C. van den Bos, D. Eibl, and R. Eibl. Scale-up of adipose tissue-derived mesenchymal stem cell production in stirred single-use bioreactors under low-serum conditions. *Engineering in Life Sciences*, 14(3):292–303, 2014.

[123] Q. A. Rafiq, K. M. Brosnan, K. Coopman, A. W. Nienow, and C. J. Hewitt. Culture of human mesenchymal stem cells on microcarriers in a 5 l stirred-tank bioreactor. *Biotechnology Letters*, 35(8):1233–1245, 2013.

[124] T. R. Heathman, A. W. Nienow, Q. A. Rafiq, K. Coopman, B. Kara, and C. J. Hewitt. Agitation and aeration of stirred-bioreactors for the microcarrier culture of human mesenchymal stem cells and potential implications for large-scale bioprocess development. *Biochemical Engineering Journal*, 136:9–17, 2018.

[125] M. F. Sousa, M. M. Silva, D. Giroux, Y. Hashimura, R. Wesselschmidt, B. Lee, A. Roldão, M. J. Carrondo, P. M. Alves, and M. Serra. Production of oncolytic adenovirus and human mesenchymal stem cells in a single-use, vertical-wheel bioreactor system: impact of bioreactor design on performance of microcarrier-based cell culture processes. *Biotechnology Progress*, 31(6):1600–1612, 2015.

[126] T. Lawson, D. E. Kehoe, A. C. Schnitzler, P. J. Rapiejko, K. A. Der, K. Philbrick, S. Punreddy, S. Rigby, R. Smith, Q. Feng, et al. Process development for expansion of human mesenchymal stromal cells in a 50 l single-use stirred tank bioreactor. *Biochemical Engineering Journal*, 120:49–62, 2017.

[127] C. A. Rodrigues, T. P. Silva, D. E. Nogueira, T. G. Fernandes, Y. Hashimura, R. Wesselschmidt, M. M. Diogo, B. Lee, and J. M. Cabral. Scalable culture of human induced pluripotent cells on microcarriers under xeno-free conditions using single-use vertical-wheel™ bioreactors. *Journal of Chemical Technology & Biotechnology*, 93(12):3597–3606, 2018.

[128] N. Timmins, M. Kiel, M. Günther, C. Heazlewood, M. Doran, G. Brooke, and K. Atkinson. Closed system isolation and scalable expansion of human placental mesenchymal stem cells. *Biotechnology and Bioengineering*, 109(7):1817–1826, 2012.

[129] A. Reichardt, B. Polchow, M. Shakibaei, W. Henrich, R. Hetzer, and C. Lueders. Large scale expansion of human umbilical cord cells in a rotating bed system bioreactor for cardiovascular tissue engineering applications. *The Open Biomedical Engineering Journal*, 7:50, 2013.

[130] J. Hupfeld, I. H. Gorr, C. Schwald, N. Beaucamp, K. Wiechmann, K. Kuentzer, R. Huss, B. Rieger, M. Neubauer, and H. Wegmeyer. Modulation of mesenchymal stromal cell characteristics by microcarrier culture in bioreactors. *Biotechnology and Bioengineering*, 111(11):2290–2302, 2014.

[131] J. d. S. da Silva, A. Mizukami, L. V. G. Gil, J. V. de Campos, O. B. Assis, D. T. Covas, K. Swiech, and C. A. T. Suazo. Improving wave-induced motion bioreactor performance for human mesenchymal stromal cell expansion. *Process Biochemistry*, 84:143–152, 2019.

[132] A. Mizukami, A. Fernandes-Platzgummer, J. G. Carmelo, K. Swiech, D. T. Covas, J. M. Cabral, and C. L. da Silva. Stirred tank bioreactor culture combined with serum-/xenogeneic-free culture medium enables an efficient expansion of umbilical cord-derived mesenchymal stem/stromal cells. *Biotechnology Journal*, 11(8):1048–1059, 2016.

[133] A. T.-L. Lam, J. Li, J. P.-W. Toh, E. J.-H. Sim, A. K.-L. Chen, J. K.-Y. Chan, M. Choolani, S. Reuveny, W. R. Birch, and S. K.-W. Oh. Biodegradable poly-ε-caprolactone microcarriers for efficient production of human mesenchymal stromal cells and secreted cytokines in batch and fed-batch bioreactors. *Cytotherapy*, 19(3):419–432, 2017.

[134] P. J. Hanley, Z. Mei, A. G. Durett, M. da Graca Cabreira-Harrison, M. Klis, W. Li, Y. Zhao, B. Yang, K. Parsha, O. Mir, et al. Efficient manufacturing of therapeutic mesenchymal stromal cells with the use of the quantum cell expansion system. *Cytotherapy*, 16(8):1048–1058, 2014.

[135] A. Mizukami, M. D. Orellana, S. R. Caruso, K. de Lima Prata, D. T. Covas, and K. Swiech. Efficient expansion of mesenchymal stromal cells in a disposable fixed bed culture system. *Biotechnology Progress*, 29(2):568–572, 2013.

[136] M. Serra, C. Brito, M. F. Sousa, J. Jensen, R. Tostões, J. Clemente, R. Strehl, J. Hyllner, M. J. Carrondo, and P. M. Alves. Improving expansion of pluripotent human embryonic stem cells in perfused bioreactors through oxygen control. *Journal of Biotechnology*, 148(4):208–215, 2010.

[137] B. Cunha, T. Aguiar, M. M. Silva, R. J. Silva, M. F. Sousa, E. Pineda, C. Peixoto, M. J. Carrondo, M. Serra, and P. M. Alves. Exploring continuous and integrated strategies for the up- and downstream processing of human mesenchymal stem cells. *Journal of Biotechnology*, 213:97–108, 2015.

[138] A. Wagner, A. Marc, J. Engasser, S. Villermaux, and A. Einsele. Continuous production of prourokinase in feed harvest and perfusion cultures. *Biotechnology and Bioengineering*, 36(6):623–629, 1990.

[139] G. Belfort. Fluid mechanics in membrane filtration: recent developments. *Journal of Membrane Science*, 40(2):123–147, 1989.

[140] G. Catapano, P. Czermak, R. Eibl, D. Eibl, and R. Pörtner. Bioreactor design and scale-up. In *Cell and Tissue Reaction Engineering*, pages 173–259. Springer, 2009.

[141] D. Voisard, F. Meuwly, P.-A. Ruffieux, G. Baer, and A. Kadouri. Potential of cell retention techniques for large-scale high-density perfusion culture of suspended mammalian cells. *Biotechnology and Bioengineering*, 82(7):751–765, 2003.

[142] J. Carmen, S. R. Burger, M. McCaman, and J. A. Rowley. Developing assays to address identity, potency, purity and safety: cell characterization in cell therapy process development. *Regenerative Medicine*, 7(1):85–100, 2012.

[143] R. M. Samsonraj, M. Raghunath, V. Nurcombe, J. H. Hui, A. J. van Wijnen, and S. M. Cool. Concise review: multifaceted characterization of human mesenchymal stem cells for use in regenerative medicine. *Stem Cells Translational Medicine*, 6(12):2173–2185, 2017.

[144] R. Pochampally. Colony forming unit assays for mscs. In *Mesenchymal Stem Cells*, pages 83–91. Springer, 2008.

[145] J. Lazarević, T. Kukolj, D. Bugarski, N. Lazarević, B. Bugarski, and Z. Popović. Probing primary mesenchymal stem cells differentiation status by micro-raman spectroscopy. *Spectrochimica Acta Part A: Molecular and Biomolecular Spectroscopy*, 213:384–390, 2019.

[146] C. Martin, E. Olmos, M.-L. Collignon, N. De Isla, F. Blanchard, I. Chevalot, A. Marc, and E. Guedon. Revisiting msc expansion from critical quality attributes to critical culture process parameters. *Process Biochemistry*, 59:231–243, 2017.

[147] H. K. Skalnikova. Proteomic techniques for characterisation of mesenchymal stem cell secretome. *Biochimie*, 95(12):2196–2211, 2013.

[148] S.-H. Yang, M.-J. Park, I.-H. Yoon, S.-Y. Kim, S.-H. Hong, J.-Y. Shin, H.-Y. Nam, Y.-H. Kim, B. Kim, and C.-G. Park. Soluble mediators from mesenchymal stem cells suppress t cell proliferation by inducing il-10. *Experimental & Molecular Medicine*, 41(5):315–324, 2009.

[149] P. C. Demircan, A. E. Sariboyaci, Z. S. Unal, G. Gacar, C. Subasi, and E. Karaoz. Immunoregulatory effects of human dental pulp-derived stem cells on t cells: comparison of transwell co-culture and mixed lymphocyte reaction systems. *Cytotherapy*, 13(10):1205–1220, 2011.

[150] C. M. DiGirolamo, D. Stokes, D. Colter, D. G. Phinney, R. Class, and D. J. Prockop. Propagation and senescence of human marrow stromal cells in culture: a simple colony-forming assay identifies samples with the greatest potential to propagate and differentiate. *British Journal of Haematology*, 107(2):275–281, 1999.

[151] Y. Li, Q. Wu, Y. Wang, L. Li, H. Bu, and J. Bao. Senescence of mesenchymal stem cells. *International Journal of Molecular Medicine*, 39(4):775–782, 2017.

[152] D. J. Prockop, M. Brenner, W. E. Fibbe, E. Horwitz, K. Le Blanc, D. G. Phinney, P. J. Simmons, L. Sensebe, and A. Keating. Defining the risks of mesenchymal stromal cell therapy. *Cytotherapy*, 12(5):576–578, 2010.

[153] L. Barkholt, E. Flory, V. Jekerle, S. Lucas-Samuel, P. Ahnert, L. Bisset, D. Büscher, W. Fibbe, A. Foussat, M. Kwa, et al. Risk of tumorigenicity in mesenchymal stromal cell–based therapies—bridging scientific observations and regulatory viewpoints. *Cytotherapy*, 15(7):753–759, 2013.

[154] P. Horn, G. Bokermann, D. Cholewa, S. Bork, T. Walenda, C. Koch, W. Drescher, G. Hutschenreuther, M. Zenke, A. D. Ho, et al. Impact of individual platelet lysates on isolation and growth of human mesenchymal stromal cells. *Cytotherapy*, 12(7):888–898, 2010.

[155] H. Hemeda, B. Giebel, and W. Wagner. Evaluation of human platelet lysate versus fetal bovine serum for culture of mesenchymal stromal cells. *Cytotherapy*, 16(2):170–180, 2014.

[156] M.-S. Chen, T.-J. Wang, H.-C. Lin, and B. Thierry. Four types of human platelet lysate, including one virally inactivated by solvent-detergent, can be used to propagate wharton jelly mesenchymal stromal cells. *New Biotechnology*, 49:151–160, 2019.

[157] I. N. Simões, J. S. Boura, F. dos Santos, P. Z. Andrade, C. M. Cardoso, J. M. Gimble, C. L. da Silva, and J. M. Cabral. Human mesenchymal stem cells from the umbilical cord matrix: Successful isolation and ex vivo expansion using serum-/xeno-free culture media. *Biotechnology Journal*, 8(4):448–458, 2013.

[158] G. Chen, A. Yue, Z. Ruan, Y. Yin, R. Wang, Y. Ren, and L. Zhu. Human umbilical cord-derived mesenchymal stem cells do not undergo malignant transformation during long-term culturing in serum-free medium. *PloS One*, 9(6), 2014.

[159] Y. Wang, H. Wu, Z. Yang, Y. Chi, L. Meng, A. Mao, S. Yan, S. Hu, J. Zhang, Y. Zhang, et al. Human mesenchymal stem cells possess different biological characteristics but do not change their therapeutic potential when cultured in serum free medium. *Stem Cell Research & Therapy*, 5(6):132, 2014.

[160] T.-C. Chang, M.-F. Hsu, and K. K. Wu. High glucose induces bone marrow-derived mesenchymal stem cell senescence by upregulating autophagy. *PloS One*, 10(5), 2015.

[161] T.-L. Tsai, P. Manner, and W.-J. Li. Regulation of mesenchymal stem cell chondrogenesis by glucose through protein kinase c/transforming growth factor signaling. *Osteoarthritis and Cartilage*, 21(2):368–376, 2013.

[162] R. Bétous, M.-L. Renoud, C. Hoede, I. Gonzalez, N. Jones, M. Longy, L. Sensebé, C. Cazaux, and J.-S. Hoffmann. Human adipose-derived stem cells expanded under ambient oxygen concentration accumulate oxidative dna lesions and experience procarcinogenic dna replication stress. *Stem Cells Translational Medicine*, 6(1):68–76, 2017.

[163] N. Haque, M. T. Rahman, A. Kasim, N. Hayaty, and A. M. Alabsi. Hypoxic culture conditions as a solution for mesenchymal stem cell based regenerative therapy. *The Scientific World Journal*, 2013, 2013.

[164] C. Fehrer, R. Brunauer, G. Laschober, H. Unterluggauer, S. Reitinger, F. Kloss, C. Gülly, R. Gaßner, and G. Lepperdinger. Reduced oxygen tension attenuates differentiation capacity of human mesenchymal stem cells and prolongs their lifespan. *Aging Cell*, 6(6):745–757, 2007.

[165] J. Estrada, C. Albo, A. Benguria, A. Dopazo, P. Lopez-Romero, L. Carrera-Quintanar, E. Roche, E. Clemente, J. Enriquez, A. Bernad, et al. Culture of human mesenchymal stem cells at low oxygen tension improves growth and genetic stability by activating glycolysis. *Cell Death & Differentiation*, 19(5):743–755, 2012.

[166] K. Drela, A. Sarnowska, P. Siedlecka, I. Szablowska-Gadomska, M. Wielgos, M. Jurga, B. Lukomska, and K. Domanska-Janik. Low oxygen atmosphere facilitates proliferation and maintains undifferentiated state of umbilical cord mesenchymal stem cells in an hypoxia inducible factor-dependent manner. *Cytotherapy*, 16(7):881–892, 2014.

[167] C. Fotia, A. Massa, F. Boriani, N. Baldini, and D. Granchi. Hypoxia enhances proliferation and stemness of human adipose-derived mesenchymal stem cells. *Cytotechnology*, 67(6):1073–1084, 2015.

[168] F. Dos Santos, P. Z. Andrade, J. S. Boura, M. M. Abecasis, C. L. Da Silva, and J. M. Cabral. Ex vivo expansion of human mesenchymal stem cells: a more effective cell proliferation kinetics and metabolism under hypoxia. *Journal of Cellular Physiology*, 223(1):27–35, 2010.

[169] A. W. Nienow. Aeration in biotechnology. *Kirk-Othmer Encyclopedia of Chemical Technology*, pages 1–23, 2000.

[170] A. C. Schnitzler, A. Verma, D. E. Kehoe, D. Jing, J. R. Murrell, K. A. Der, M. Aysola, P. J. Rapiejko, S. Punreddy, and M. S. Rook. Bioprocessing of human mesenchymal stem/stromal cells for therapeutic use: current technologies and challenges. *Biochemical Engineering Journal*, 108:3–13, 2016.

[171] P. Czermak, R. Pörtner, and A. Brix. Special engineering aspects. In *Cell and Tissue Reaction Engineering*, pages 83–172. Springer, 2009.

[172] N. Stathopoulos and J. Hellums. Shear stress effects on human embryonic kidney cells in vitro. *Biotechnology and Bioengineering*, 27(7):1021–1026, 1985.

[173] R. Cherry and E. Papoutsakis. Hydrodynamic effects on cells in agitated tissue culture reactors. *Bioprocess Engineering*, 1(1):29–41, 1986.

[174] R. S. Cherry and E. T. Papoutsakis. Physical mechanisms of cell damage in microcarrier cell culture bioreactors. *Biotechnology and Bioengineering*, 32(8):1001–1014, 1988.

[175] Y. J. Li, N. N. Batra, L. You, S. C. Meier, I. A. Coe, C. E. Yellowley, and C. R. Jacobs. Oscillatory fluid flow affects human marrow stromal cell proliferation and differentiation. *J Orthop Res*, 22(6):1283–1289, 2004.

[176] M. R. Kreke, W. R. Huckle, and A. S. Goldstein. Fluid flow stimulates expression of osteopontin and bone sialoprotein by bone marrow stromal cells in a temporally dependent manner. *Bone*, 36(6):1047–1055, 2005.

[177] S. Scaglione, D. Wendt, S. Miggino, A. Papadimitropoulos, M. Fato, R. Quarto, and I. Martin. Effects of fluid flow and calcium phosphate coating on human bone marrow stromal cells cultured in a defined 2d model system. *J Biomed Mater Res A*, 86(2):411–419, 2008.

[178] T. M. Maul, D. W. Chew, A. Nieponice, and D. A. Vorp. Mechanical stimuli differentially control stem cell behavior: morphology, proliferation, and differentiation. *Biolech Model Mechanobiol*, 10(6):939–953, 2011.

[179] C. Cannizzaro, R. Gügerli, I. Marison, and U. von Stockar. On-line biomass monitoring of cho perfusion culture with scanning dielectric spectroscopy. *Biotechnology and Bioengineering*, 84(5):597–610, 2003.

[180] H. E. Cole, A. Demont, and I. W. Marison. The application of dielectric spectroscopy and biocalorimetry for the monitoring of biomass in immobilized mammalian cell cultures. *Processes*, 3(2):384–405, 2015.

[181] B. J. Downey, L. J. Graham, J. F. Breit, and N. K. Glutting. A novel approach for using dielectric spectroscopy to predict viable cell volume (vcv) in early process development. *Biotechnology Progress*, 30(2):479–487, 2014.

[182] H. W. Lee, J. Carvell, K. Brorson, and S. Yoon. Dielectric spectroscopy-based estimation of vcd in cho cell culture. *Journal of Chemical Technology & Biotechnology*, 90(2):273–282, 2015.

[183] E. Petiot, A. El-Wajgali, G. Esteban, C. Gény, H. Pinton, and A. Marc. Real-time monitoring of adherent vero cell density and apoptosis in bioreactor processes. *Cytotechnology*, 64(4):429–441, 2012.

[184] C. Justice, J. Leber, D. Freimark, P. P. Grace, M. Kraume, and P. Czermak. Online-and offline-monitoring of stem cell expansion on microcarrier. *Cytotechnology*, 63(4):325–335, 2011.

[185] F. Rosa, K. C. Sales, J. G. Carmelo, A. Fernandes-Platzgummer, C. L. da Silva, M. B. Lopes, and C. R. Calado. Monitoring the ex-vivo expansion of human mesenchymal stem/stromal cells in xeno-free microcarrier-based reactor systems by mir spectroscopy. *Biotechnology Progress*, 32(2):447–455, 2016.

[186] J. Whelan, S. Craven, and B. Glennon. In situ raman spectroscopy for simultaneous monitoring of multiple process parameters in mammalian cell culture bioreactors. *Biotechnology Progress*, 28(5):1355–1362, 2012.

[187] N. R. Abu-Absi, B. M. Kenty, M. E. Cuellar, M. C. Borys, S. Sakhamuri, D. J. Strachan, M. C. Hausladen, and Z. J. Li. Real time monitoring of multiple parameters in mammalian cell culture bioreactors using an in-line raman spectroscopy probe. *Biotechnology and Bioengineering*, 108(5):1215–1221, 2011.

[188] A. Calvet and A. G. Ryder. Monitoring cell culture media degradation using surface enhanced raman scattering (sers) spectroscopy. *Analytica Chimica Acta*, 840:58–67, 2014.

[189] S. Rangan, S. Kamal, S. O. Konorov, H. G. Schulze, M. W. Blades, R. F. Turner, and J. M. Piret. Types of cell death and apoptotic stages in chinese hamster ovary cells distinguished by raman spectroscopy. *Biotechnology and Bioengineering*, 115(2):401–412, 2018.

[190] A. W. Nienow, Q. A. Rafiq, K. Coopman, and C. J. Hewitt. A potentially scalable method for the harvesting of hmscs from microcarriers. *Biochemical Engineering Journal*, 85:79–88, 2014.

[191] J. Varani, F. Piel, S. Josephs, T. F. Beals, and W. J. Hillegas. Attachment and growth of anchorage-dependent cells on a novel, charged-surface microcarrier under serum-free conditions. In *Cell Culture Engineering VI*, pages 101–109. Springer, 1998.

[192] T. K.-P. Goh, Z.-Y. Zhang, A. K.-L. Chen, S. Reuveny, M. Choolani, J. K. Y. Chan, and S. K.-W. Oh. Microcarrier culture for efficient expansion and osteogenic differentiation of human fetal mesenchymal stem cells. *BioResearch Open Access*, 2(2):84–97, 2013.

[193] A. Higuchi, Q.-D. Ling, S. S. Kumar, Y. Chang, T.-C. Kao, M. A. Munusamy, A. A. Alarfaj, S.-T. Hsu, and A. Umezawa. External stimulus-responsive biomaterials designed for the culture and differentiation of es, ips, and adult stem cells. *Progress in Polymer Science*, 39(9):1585–1613, 2014.

[194] A. Tamura, J. Kobayashi, M. Yamato, and T. Okano. Temperature-responsive poly (n-isopropylacrylamide)-grafted microcarriers for large-scale non-invasive harvest of anchorage-dependent cells. *Biomaterials*, 33(15):3803–3812, 2012.

[195] B. Cunha, R. J. Silva, T. Aguiar, M. Serra, J. Daicic, J.-L. Maloisel, J. Clachan, A. Åkerblom, M. J. Carrondo, C. Peixoto, et al. Improving washing strategies of human mesenchymal stem cells using negative mode expanded bed chromatography. *Journal of Chromatography A*, 1429:292–303, 2016.

Chapter 2

Optimization and understanding of the interactions between cells and microcarriers

Contents

Introduction

As highlighted in the previous chapter, WJ-MSCs are valuable sources of mesenchymal stem cells as they are naturally more abundant than stem cells from bone marrow and they exhibit high proliferation performances [1]. Moreover, they could be easily extracted without ethical concerns. However, to use WJ-MSCs in therapeutic treatments, large number of cells are required. As described before, doses of billion or trillion cells are generally required to treat patients. In order to produce large quantities of WJ-MSCs, in GMP conditions, researchers mainly focused part of their work on microcarriers, one of the most adapted system for large scale culture of adherent-dependent cells.

The goal of this chapter was to apply and develop the expansion methods acquired in recent years. Interactions between cells and microcarriers are highly important to understand in order to propose adapted systems for large scale production of WJ-MSCs. These interactions depend not only on the nature of the microcarrier but also on the cells. The first interaction between cells and their microcarriers is the step of cell adherence, implying proteins and complex molecules of the extra-cellular matrix. Once the cells adhered on microcarriers, an expansion phase is expected, leading to a total covering of the surfaces. In this case, interactions will be studied at a microcarrier scale. In order to highlight these different interactions between cells and microcarriers, this chapter is divided in three sections as presented in the figure 2.1 to provide some element of answers to these major issues.

The definition of rationalized cycles of adherence/ expansion/ medium renewal still remains empirical. Through different information taken in literature, protocols of adherence were determined, but the lack of tools permitting to monitor the CSM adherence was noticed except Justice *et al.* The monitoring of cell adhesion makes sense in view of the importance of this first stage of culture, which is then decisive for efficient cell expansion. In this chapter, the use of a dielectric spectroscopy will be presented as a tool for the detection of the adhesion duration. Usually used for the monitoring of cell growth, as presented in the state of the art, this probe can also be used as a cell adhesion detection tool as presented in the section 2.1.

As the others MSCs (bone marrow, adipose tissue) WJ-MSCs have self-renewal capabilities . They are able to proliferate to 100 % of confluence (maximum), then, once the totality of the surface recovered by cells a phenomenon, called contact inhibition, occur and the cells stop their growth. Moreover, the specificity of WJ-MSCs is to form cell aggregates beyond the confluence and to detach from the surface of microcarriers, as demonstrated in the work of Caroline Ferrari [31]. This phenomenon implies, either passages when cells are cultivated in flasks leading to a premature aging, either addition of fresh surfaces available for growth in 3D cultures. Thus, one major bottleneck in MSCs area is the expansion limited in time, due to this lack of surfaces of growth ; and the section 2.2 will propose alternatives to limit this surface limitation issue. Addition of fresh surfaces in the form of added microcarriers is realized and monitored by microscopy. Time-lapse microscopy realized at the INM laboratory (Leibniz Institute for New Materials, Saarbrücken/Germany), will permit to better visualize the cell migration between two microcarriers and, even, to calculate the kinetics of migration and displacements of cells.

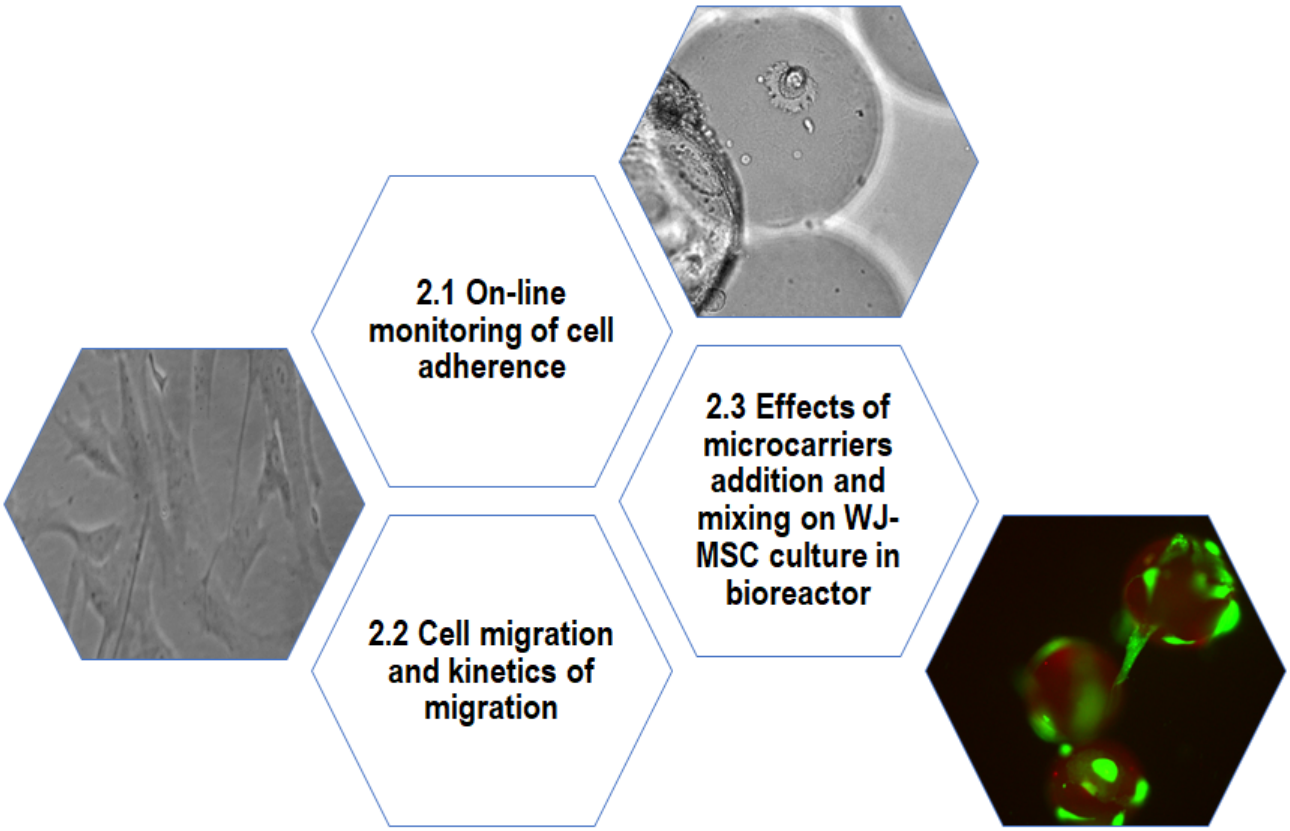

Figure 2.1 – Presentation of the different sections of chapter 2, dedicated to the study of the interactions between cells and microcarriers.

Finally, interactions between cells and microcarriers can also have an important impact on their quality. In order to answer this bottleneck, the section 2.3 will propose a new method of culture to extend MSCs cultures over time consisting in controlled additions of fresh microcarriers, at specific times of culture, and with specific quantities. However, the addition of new microcarriers requests to determine appropriate conditions of agitation to maintain cell viability and to not impact cell quality.

2.1 On-line monitoring of cell adherence

Dielectric spectroscopy is a tool already used by biotechnological industries, (yeast, CHO, ...), to monitor cell growth on-line. Cells with intact membrane plasma become polarized under alternative electric field, and behave as tiny capacitors (Figure 2.2). The permittivity measurement is proportional to the total biovolume of the culture. However, the polarization of the cells depends on the frequency, this is called the β dispersion, and is primarily caused by the build up of charge on cell membrane [2]. Over the last decades, biomass monitoring via permittivity measurements of suspension cultures has considerably been developed. Furthermore, this tool was also used also in adhered cells on microcarriers but mainly on continuous cell lines [3]. Only one study reported use of spectroscopy dielectric for MSC culture monitoring [4]. Most of the studies on permittivity reported a linear correlation between permittivity and cell growth, but it seems that

other properties of cultures could be also described thanks to the dielectric spectroscopy. Thus, in yeast cultures, Maskow *et al.* observed changes in critical frequency (fc) values that occurred during in specific times of cultures, and correlated with physiological changes during the culture [5]. The detection of the cell adhesion has also been described in literature. As Justice *et al.* described an important decrease of the critical frequency in the first hours of culture, and then when cells were in exponential growth phase, the critical frequency tends to constant values varying between 300 and 400 MHz. This detection of morphology change was also demonstrated with depletion of oxygen, leading to cell detachment, and modification of the critical frequency [4]. In the study of Petiot *et al.*, a monitoring of the apoptotic cell population was possible thanks to the detection of the critical frequency changes. Indeed apoptotic cells could still be detected by the electric field as they are split into small apoptotic bodies but with intact membranes [3]. Thus, with the formation of these apoptotic bodies an important reduction of the radius occurred [6], and this radius reduction was possible to detect with the modification of the critical frequency. The derivative critical frequency tended to 0 when the apoptotic cell population increased.

Material and Methods

WJ-MSC culture

WJ-MSCs were thawed and seeded at a concentration of 3000 cells cm^{-2} in 7 T-175 cm^2 and cultivated for a week before their use in dynamic conditions. The cell culture medium was alpha-minimum essential medium (α MEM medium) (Lonza BE12-169F), supplemented with 5 % of Human Platelet Lysate (HPL) (Macopharma BC0190020), 4 mM glutamine (Sigma G7513), 1 % antibiotics (Antibiotic antimycotic solution, Sigma A5955), and 2 iU/mL heparin (Sigma H3149).

Microcarrier preparation

Commercial Cytodex-1 microcarriers (GE-Healthcare) were preliminary hydrated at 20 g L^{-1} in phosphate buffer saline (dPBS Sigma D8537), autoclaved and subsequently washed with cell culture medium. A cut Erlenmeyer's flask (Fisher PBV125) was loaded with 0.9 g of Cytodex-1, and 35 million of WJ-MSCs to obtain a ratio cell/microcarrier of 10. The culture was performed in a drying oven controlled at 37°C in 100 mL of cell culture medium. Agitation was carried-out every 45 minutes.

On-line permittivity measurement

Multi-frequency permittivity was measured by using the Incyte Biomass system (Hamilton) (Figure 2.2). Measurements were made over a frequency of 0.3 - 10 MHz during the whole culture time, and frequency scans were collected every minute.

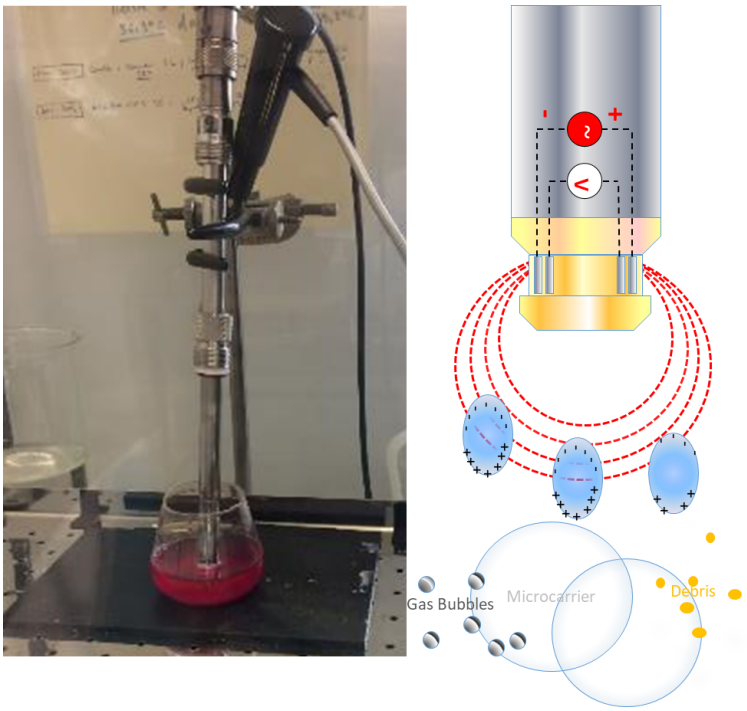

Figure 2.2 – Experimental setup for monitoring WJ-MSC adhesion on Cytodex-1.

Cole-Cole model

The permittivity, Δ ϵ, is related to the magnitude of cell polarization, and more specifically to the membrane polarization. If cells are polarized by increasing frequencies from 0.01 to 10 MHz, a drop of permittivity is observed (Figure 2.3). This drop is called the β dispersion, and described through empirical model established for spherical cells. According to the work of Schawn (1957), two parameters, specific for each cell population, the characteristic frequency (f_c) and the empirical factor α could characterize the β dispersion.

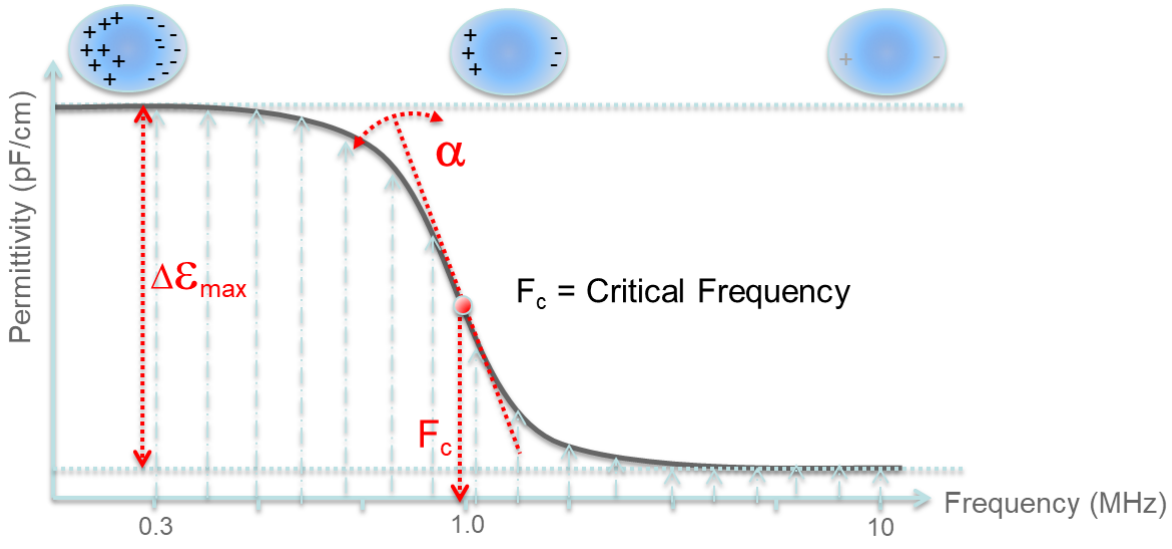

Figure 2.3 – Schematic representation of the β-dispersion of permittivity (Ansorge *et al.*, 2007).

Δ ϵ, f_c and α are values reported by the biomass spectrometer software for each scan frequency.

During the permittivity measurements, the static suspension conductivity, σ was measured and related to the static medium conductivity σ_a using the Bruggeman equation (Eq. (2.1))

$$\sigma_a = \sigma/(1-p_p)^{1.5} \tag{2.1}$$

with p_p the predicted biovolume from the previous calculation.

The predicted average cell radius r_p was calculated using Eq. (2.2),

$$r_p = \frac{1}{2\pi f_c c_m (\frac{1}{\sigma_i} + \frac{1}{2\sigma_a})} \tag{2.2}$$

c_m and σ_i were assumed to be constant during the culture with defined values of 1.1 µF cm^{-2} and 4.0 mS cm^{-1}. The predictive biovolume was calculated using Eq. (2.3),

$$p_p = \frac{4\Delta\epsilon}{9 r_p c_m} \tag{2.3}$$

2.1.1 Use of dielectric spectroscopy to detect cell adhesion on microcarriers

First, thanks to time-lapse microscopy (see 2.2), images of cell adherence have been taken and time of adherence could be determined (Figure 2.4). It appeared on this sample of images that the adherence of cells seemed well established after 4 hours.

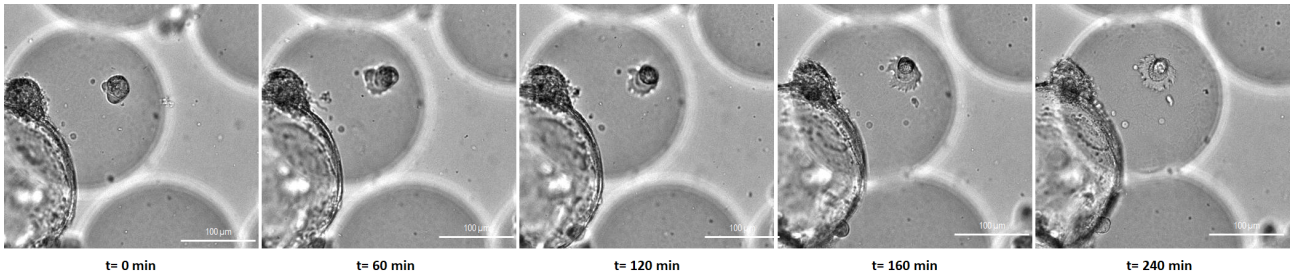

Figure 2.4 – Evolution of the cell morphology during the adhesion process on microcarriers.

In order to better understand the cell adhesion on microcarriers, the dielectric spectrometer was immersed inside an Erlenmeyer's flask (Figure 2.2) and the dielectric spectroscopy monitoring was performed in the culture for few hours the culture. Three different cultures were realized with intermittent stirring every 45 minutes.

First, the critical frequency measurement allowed to calculate the predictive cell diameter and informed about the theoretical shape of the cells (Figure 2.5 A, A' and A"). Results show that the predictive cell diameter is divided by two after two hours of culture (Figure 2.5 B, B' and B"). This change is most likely linked to a modification in the shape of the cells. Indeed, while in suspension, the MSCs have a spherical morphology, they spread out and adhere as soon as a compatible surface is encountered. Photos were taken to verify that these two main morphologies (circular and spread out) could be observed on a microcarrier after six hours of culture (Figure 2.6).

In conclusion, it seems possible to detect a change in shape of the cells during their adhesion to the microcarrier using dielectric spectroscopy. On the other hand, what has been observed in

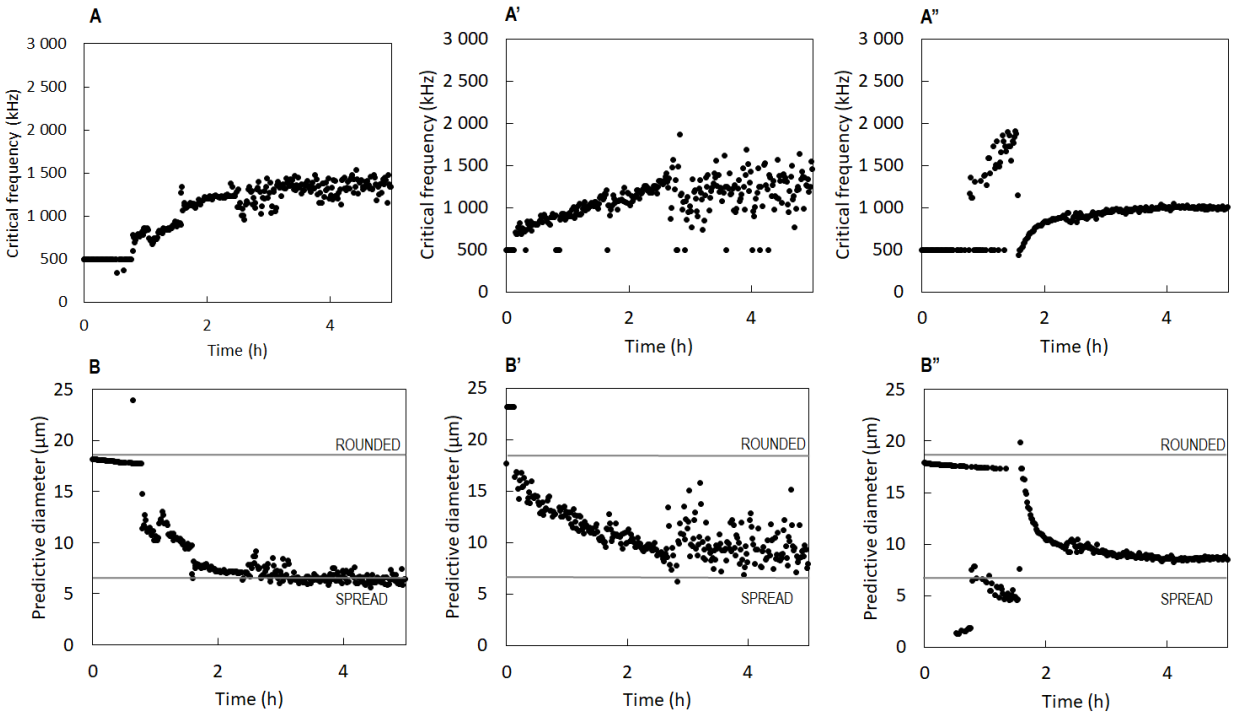

Figure 2.5 – Cell adhesion monitored on-line. (A, A', A") Time course of the critical frequency. (B, B', B") Time course of the predictive cell diameter. Data from three different experiences.

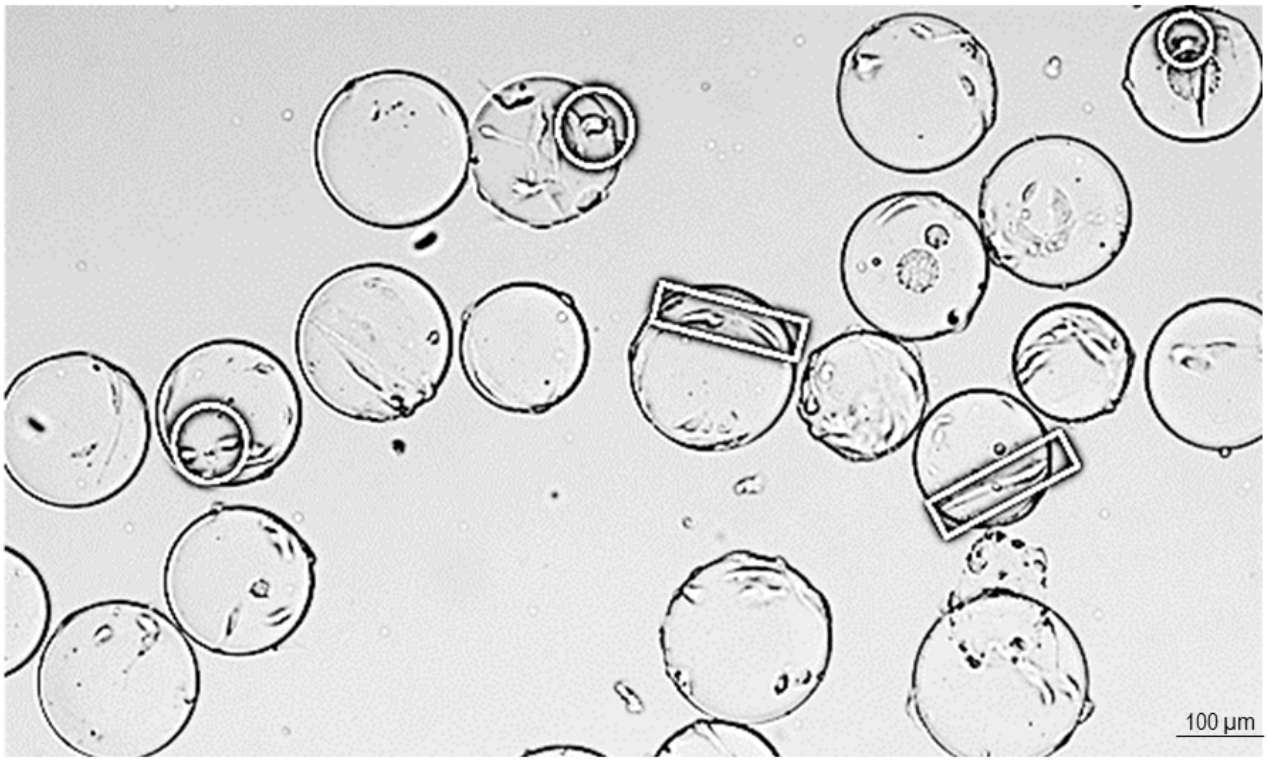

Figure 2.6 – Cell adhesion on microcarriers. Microscopic observation of two cell populations: circles show rounded cells while square show spread cells, after at least two hours of culture.

time-lapse between the second and fourth hour seems more difficult to detect with dielectric spectroscopy. This method will then be implemented on a bioreactor, and will allow online monitoring of cultures over time (biomass and viability).

2.2 Kinetics of cell migration

It has been previously detailed that large-scale suspension cultivation of WJ-MSCs requires the use of microcarriers. These micrometric spheres offer the optimal ratio surface on volume, and a wide diversity of material and coating suitable for cell culture exist. However, during long cell expansion limited surfaces for cell adherence is the main bottleneck in cultures using microcarriers, before nutrient depletion. Thus, a research study was carried-out to develop a strategy including the possible addition of new microcarriers to maintain cultures over time. Thanks to the partnership with the INM laboratory (Saarbrücken/Germany), the study of the migration kinetics of WJ-MSC was possible. Indeed, their skills in imagery, notably in microscopy, allowed to study interactions between cells and materials.

Materials and methods

Time-lapse microscopy

Epi-fluorescence images were acquired by an inverted microscope (Ti-Eclipse; Nikon). The light source used was an Intensilight Epi-Fluorescence illuminator (Nikon). The microscope was equiped with a temperature controlled (37°C) environmental chamber (Okolab) that provided 5 % CO_2 and 100 % humidity for the live-cell imaging. In 6-well plate ultra low attachment (Corning CLS3471), 0.5 mL of Cytodex-1 (20 g L^{-1}) were loaded in the well. Then, one million of cells were loaded in each well and placed inside the temperature controlled environmental chamber and image acquisitions were started for 4 h to detect cell adhesion. Then, after 4 hours, fresh Cytodex-1 (0.3 mL) were added, and camera was started for 24 h, with an image acquisition period of 20 min.

2.2.1 Evaluation of cell migration kinetics by time-lapse imagery

The videos carried-out during the microscopic experiments permitted to determine the time needed for the cell migration (Figures 2.7 and 2.8), and after the cell tracking of more than 30 sequences, it seemed that about 3 hours would be necessary to get a complete cell migration. By analyzing the results of the cell tracking, an average time of complete migration was determined at 168 minutes, but a majority of cell migration occurred between 60-140 minutes. A lot of duration variability can be detected, depending on the cells, the distance between microcarriers, presence or not of aggregates. Moreover this system was realized without agitation, and does not exactly mimic what could happen in stirred cultures, but it can give a good overview about how much time is needed for cell migration from a microcarrier to another one.

From a qualitative point of view, it seemed that MSCs were able to migrate from their initial carriers to the new ones only if these new carriers were in a close contact, or in an aggregate. Secondly, it seemed that overcrowded carriers had cells moving towards empty closed microcarriers. On the contrary, if the microcarriers contained less than 5 cells, it is unlikely to observe a cell migration. Moreover, calculation of the average rate of migration was compared to the literature [7]. WJ-MSCs capability of migration is exploited in clinical therapies. Indeed thanks to their hom-

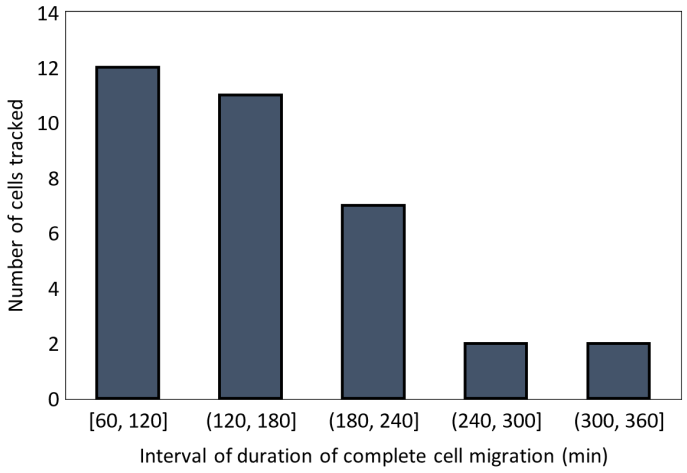

Figure 2.7 – Cell tracking and evaluation of the time needed for cells for a complete migration.

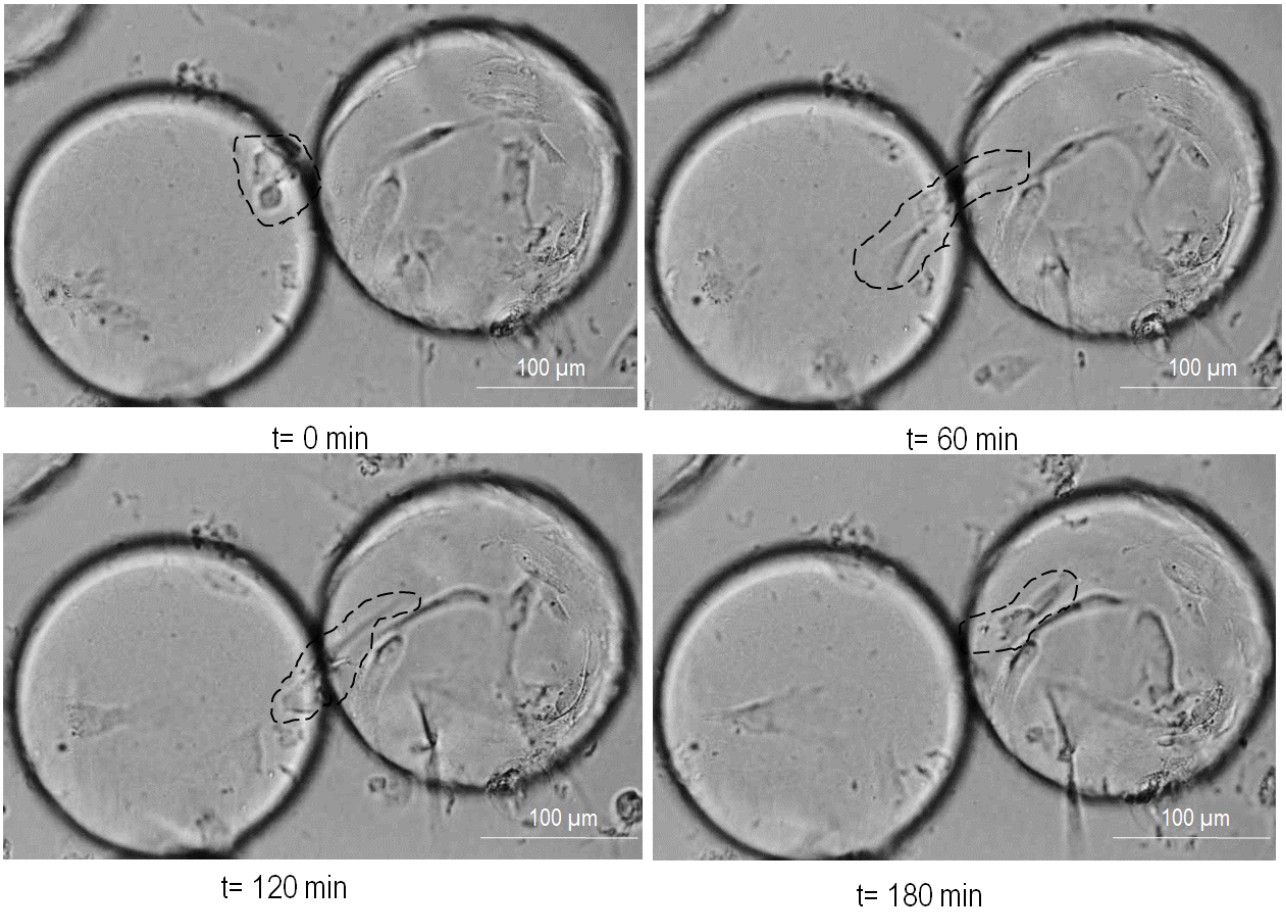

Figure 2.8 – Examples of cell migration from a movie taken by time-lapse. The hatched lines surround a cell migrating toward a microcarrier in 3 hours.

ing properties, WJ-MSCs are able to migrate towards the area of injury. Migration is a regulated process which involves changes in cytoskeleton conformations as described in the section **1.4.1**. Arora *et al.*, highlighted the importance of the role of the nonmuscle myosin II in migration and adherence of WJ-MSCs. They also did some time-lapse experiments, in 2D, and calculated an average of rate of migration of 10 cells and from two different donors, as presented in the figure 2.9. Also presented in this figure, the average rate of cell displacements on microcarriers. 10 cells were

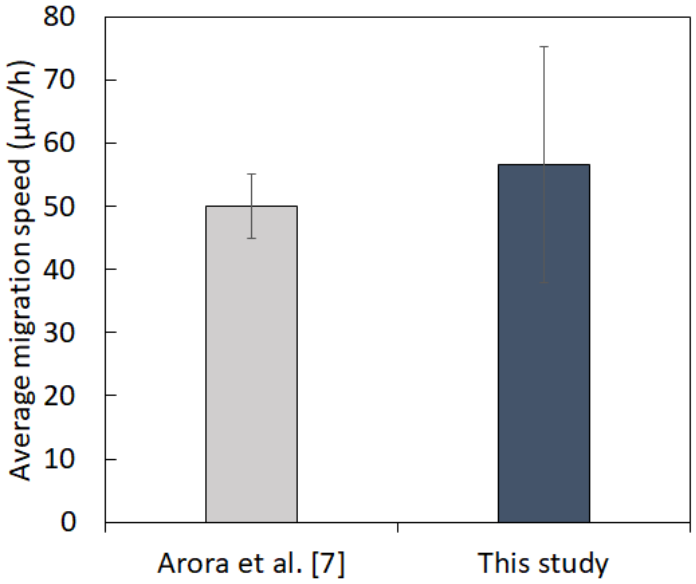

Figure 2.9 – Evaluation of the average velocity of cell migration on microcarriers.

tracked, and measurement of their rate was realized with ImageJ program. Migration rate of control WJ-MSCs in tissue culture dish was calculated to be around 50 µm/h [7]. Authors noticed an alteration of the migration properties of WJ-MSCs if cell-cell contact was lost. In this study, an average of migration rate was calculated to be around 60 µm/h (calculated for 10 tracked cells), this value is very similar to the one found in the literature but was subjected to a more pronounced uncertainty. On the contrary of Arora *et al.*, work, movements of cells were indeed measured on 3D microcarriers making trickier the measurement of cell displacement. However, further studies would be necessary to better characterize the migration on 3D surface as for example, study of ECM proteins expression and adhesion protein expression.

In conclusion, migration of cells towards new added microcarriers seemed possible and was calculated to last about 3 hours to be complete (Figure 2.7). It would be interesting to conduct further studies on the conditions of migration, in dynamic modes or with different materials.

2.3 Effects of microcarrier addition and mixing on WJ-MSC culture in bioreactor

This section was the subject of a manuscript published in Biochemical Engineering Journal. Volume 157, (2020).

Effects of microcarrier addition and mixing on WJ-MSC culture in bioreactor

C. Sion, C. Loubière, M.K. Wlodarczyk-Biegun, N. Davoudi, C. Müller, E. Guedon, I. Chevalot, E. Olmos

Abstract

Mesenchymal stem cells isolated from the Wharton's jelly of human umbilical cords (WJ-MSC) are of increasing interest for cell therapies, but scalable cell production in stirred tank bioreactors (STR) still requires further investigations in order to be more efficient and with decreased costs. To handle the problem of cell confluence on microcarriers leading to cell aggregation, a new strategy of microcarriers addition was proposed. The 'bead-to-bead transfer' ability of WJ-MSC was indeed used to maintain constant the number of cells per microcarriers. However, the resulting increase of bead shocks frequency could also negatively impact cell quantity and quality. Until now, no quantitative study describing the impact of bead interactions on WJ-MSC death was reported. In this study the influence of microcarriers addition as well as mixing characteristics on cell viability were determined. Obtained results showed that, when particle mixing is below the just-suspended state condition (N_{js}), local increase of particle volume fraction promotes a significant cell death in an agitation mode of orbital stirring. However, an increase in agitation rate at N_{js} is clearly beneficial to cell viability and growth. These effects were magnified during microcarrier addition due to the increase of mean volume fraction of particles. The present study also demonstrates the critical influence of N_{js} and particle distributions within the bioreactor on WJ-MSC culture performances.

Intronduction

Mesenchymal stem cells (MSC) are self-renewable cells which show high therapeutic potential in clinical trials. They are very attractive for use in regenerative medicine thanks to their low immunogenicity profile, immature characteristics and capabilities of immunomodulation and cytokines secretion. In May 2019, 955 cases of MSC-based clinical trials, completed or ongoing, have been identified (www.clinicaltrials.gov). Additionally, MSC could be a reliable solution for cell based therapy dealing with degenerative diseases. One of MSCs specificity is that, depending on their origin, they may show different characteristics of expansion, immunogenic profile, etc. Among the various MSCs origins such as bone marrow, adipocyte tissue, placental tissue, umbilical blood, MSCs from umbilical cords (UC-MSC) are especially interesting due to their immature

profile [8], and as such, could be used in allogenic grafts or treatments. Promising therapeutic solutions were proposed in various cardiac diseases thanks to their properties of growth factors secretion. Moreover, MSCs extracted from Wharton's jelly cells (WJ-MSC) represent a unique, easily accessible and non-controversial source of stem cells [9]. However, in order to complete a cell-based therapy, a high number of cells is required. A typical therapeutic dose contains between 2 and 3 millions of MSC kg^{-1} of body weight [10] and usually repeated doses are required [11, 12, 13]. To reach these cell quantities at reasonable production costs, the development of an efficient expansion process is crucial. In the past decades, cultivation of MSC has generally been performed in plastic culture flasks but these systems present significant drawbacks such as: a limited culturing surface area (1), a limited control over culture parameters such as pH or dissolved O_2 (2), and an extensive handling and labor efforts required during the culture process (3) [14]. To overcome these issues, cell culture methods in stirred tank bioreactors have been proposed. Among different solutions, the use of microcarriers as adherence supports has been established as the most reliable method from a scale-up point of view [15]. However, the choice of optimal microcarriers significantly depends on the source of the MSC [16, 17, 18, 19, 20]. Recent improvements of materials permitted to better adapt the microcarriers to the cell culture needs, by enhancing the cell adhesion or improving the efficiency of cell detachment [21].

The use of microcarriers in stirred tank bioreactors requires agitation to ensure particle suspension and to limit the formation of microcarriers clusters or nutrient concentration gradients. However, an excessive agitation may lead to damage of animal cells on microcarriers. Three main mechanisms causing cell damages are theoretically considered: (i) collisions between cells attached to the microcarriers and parts of the reactor (wall, impeller, etc), (ii) collisions with other microcarriers, and (iii) interactions with turbulent fluid eddies [22, 23]. Croughan *et al.,* [24] assigned the cell propensity to be damaged by agitation to the lack of protective cell wall, and the relative large size of cells. However, these studies were carried out with continuous cell lines and none was specifically performed with MSC cultivated on microcarriers. Moreover, other studies reported an impact of hydromechanical stress on MSC and their differentiation. Li *et al.,* [25], Kreke *et al.,* [26] and Scaglione *et al.,* [27] demonstrated that phenotype of MSC cultured in 2D systems could be osteogenically primed by mechanical stresses. Maul *et al.,* [28] suggested that mechanical stimuli could induce phenotype modifications of MSC towards vascular and endothelial cells. One compromise commonly accepted today to limit the negative effects of agitation is to maintain the agitation at the just-suspended state (N_{js}), that is described as the minimum agitation speed required to suspend solid particles in a liquid [20].

Currently, there is limited number of studies on WJ-MSC cultivated in stirred tank bioreactors. Setting up of bioreactors from 0.8 L up to 1.5 L of working volume for WJ-MSC culture [29, 30], during 6 or 13 days, using two different types of microcarriers (dextran and gelatin) was reported. In these two studies, one of the limitation put into evidence was the available surface for cells growth. In fact, after few days of culture, cell growth stopped due to a lack of available surface area. Once confluence was reached on the carriers, cells and microcarriers aggregated, limiting the culture performance. These phenomena were already observed by Ferrari *et al.,* [31] who showed

that porcine MSC tended to aggregate after 7 days of culture. The authors also showed that the addition of microcarriers could delay cell confluence and lengthen cell expansion. By this implicit demonstration, authors formulated the hypothesis of 'bead-to-bead transfer' phenomenon for porcine bone marrow MSCs. Rafiq *et al.,* [32] demonstrated this particular property of bead-to-bead transfer with human bone marrow mesenchymal stem cells (BM-MSC), using different types of microcarriers in the same culture. More recently, Lawson *et al.,* [33], developed a 50 L single use bioreactor with BM-MSC. The scale-up of the production volume was achieved by progressively adding fresh microcarriers and culture medium and by implicitly using bead-to-bead transfer mechanisms. To the best of our knowledge, in the case of human WJ-MSC cultures, cell migration from one bead to another was neither explicitly demonstrated nor used to enhance culture performance. Furthermore, for none of the MSC types, until now, the rational optimization protocol of microcarriers addition (time of addition, quantity added) has never been proposed in literature so far; till now the use of bead-to-bead transfer remains mostly empirical.

Therefore the aim of the present work is, first of all, to propose an original strategy for the control of fresh microcarriers addition (time, quantity) using off-line determination of cell distribution on microcarriers; secondly, to define optimal culture conditions based on the strategy of microcarriers addition. Among the various culture parameters that possibly impact bead-to-bead transfer efficiency, agitation conditions (orbital in shaken flasks / mechanical in spinner flasks) were studied in details. WJ-MSC cells were cultivated on Cytodex-1 microcarriers in 250 mL spinner flasks and 25 mL Erlenmeyer flasks agitated. Direct cell counting was achieved by fluorescent staining (DAPI and Live/Dead) associated with an automated Matlab post-treatment script. By this way, cell distribution on microcarriers and the total cell number were determined. The proposed method allows for a quantitative characterization of cell migration and its impact on the cell culture duration and expansion factor.

Material and Methods

Cell extraction and primary cell culture of WJ-MSC

Umbilical cord stem cells were extracted from fresh umbilical cords of just born babies (Centre Hospitalier Universitaire Nancy, France). Umbilical cords were treated during the 24 h following the birth. The method of extraction was non-enzymatic using cells spontaneous migration on 175 cm^2 plastic culture flasks [34]. The cell culture medium was alpha-minimum essential medium (α MEM medium) (Lonza BE12-169F), supplemented with 5 % of Human Platelet Lysate (HPL) (Macopharma BC0190020), 4 mM glutamine (Sigma G7513), 1 % antibiotics (Antibiotic antimycotic solution, Sigma A5955), and 2 iU/mL heparin (Sigma H3149). The medium was changed twice a week. After ten days, the remaining adherent cells were trypsinized and seeded in new 175 cm^2 T-flasks at a density of 3000 cells cm^{-2}. After one supplementary passage, WJ-MSC were pooled and cryopreserved at a concentration of 2×10^6 cells mL^{-1}, in fetal bovine serum and 10 % of dimethyl sulfoxyde (DMSO) for cell banking and kept in liquid nitrogen. Thereafter, cells were thawed and seeded at a concentration of 3000 cells cm^{-2} in T-175 cm^2 and cultivated for a week before their

use in dynamic conditions.

WJ-MSC expansion on microcarriers

Commercial Cytodex-1 microcarriers (GE Healthcare) were preliminary hydrated at 20 g L^{-1} in phosphate buffer saline (dPBS Sigma D8537), autoclaved, and subsequently rinsed with cell culture medium. The medium was adapted to avoid the appearance of a matrix gathering carriers and cells. Based on the protocol of Laner *et al.,* [35], a mechanical defibrination of the medium was implemented. This modified medium was used during all the experiments. All cultures were performed in an incubator (Sanyo) at 37°C and 5 % of CO_2. Erlenmeyer's flasks of 125 mL (Fisher PBV125) were seeded with 2 g L^{-1} of Cytodex-1 and 0.8 × 10^5 cells mL^{-1} in 25 mL of adapted medium. The initial targeted ratio of cells per microcarrier was six to eight cells per carrier, corresponding to 7500 cells cm^{-2} approximately. After one hour in the incubator without agitation, Erlenmeyer's flasks were agitated at N ≃ 70 rpm, and spinner flasks were agitated at the just-suspended state agitation rate N_{js}, N_{js} ≃ 40 rpm. From the fourth day of culture, 50 % of the medium was changed simultaneously with fresh microcarriers addition. This protocol is further developed in the 'Results' section.

WJ-MSC metabolite analysis

Analysis of glucose, lactate and lactate dehydrogenase (LDH) concentrations in the medium were performed using the Gallery multiparametric analyzer (Thermo Fisher Scientific). Release of LDH in the cell culture medium is usually linked to cell damages (e.g. disrupted membranes). As a control sample, a known amount of cells was subjected to three cycles of freezing at -80°C and thawing at 37°C, which ensured lysis of all cells, before LDH measurement.

WJ-MSC growth analysis

A fluorescent staining of the cells was performed for cell counting. Every two days, 100 µL of homogeneous sample was withdrawn from the Erlenmeyer's or spinner flasks. The supernatant was discarded and 0.5 mL solution of DAPI (1 µg/mL) (Sigma 10236276001) prepared in methanol was added to the cells on microcarriers. After fifteen minutes of incubation protected from the light, samples were washed with PBS and observed by epi-fluorescence microscopy. Six different areas were randomly chosen per sample and for each area two pictures were taken: one with the bright field and the other with the fluorescent field.

The viability was determined using a Live/Dead staining (Calcein AM/ Ethidium Homodimer, Life Sciences, ThermoFisher). The supernatant was discarded and the samples were incubated with 3 µM of calcein AM and 3 µM of ethidium homodimer-1 for thirty minutes in the dark at 37 °C and 5 % CO_2. Samples were then visualized with a Leica LEITZ DMR epi-fluorescence microscope. The automatic counting method described by Loubière *et al.,* [20] was used to determine cell distribution on microcarriers, the average number of cells per microcarrier and the total cell number.

Microcarriers addition during cell culture

In order to demonstrate the ability of WJ-MSC to migrate, distinguishable microcarriers were prepared as follows. Commercial Cytodex-1 carriers (GE Healthcare) were labeled by incubation with rhodamine-fibronectin (17 µg/mL) in cell culture medium during one hour at 37°C and 5 % CO_2. Afterwards, cells were detached from plastic flasks and inoculated with the labeled microcarriers as described in the previous section. After 24 h of cell culture under agitation, new unlabeled commercial Cytodex-1 carriers were added. The agitation was stopped for one hour, in order to enhance cell migration, then cells were suspended by an agitation at N_{js} with the two types of microcarriers (labeled and unlabeled).

Hydrodynamics characterization

Bioreactor hydrodynamics can be macroscopically characterized using common parameters such as Reynolds number, Kolmogorov scale or power dissipation per unit of volume.
As described in the publication of Olmos *et al.* [36], a scaling law of critical agitation rate for the complete suspension of Cytodex-1 microcarriers (s^{-1}) in Erlenmeyer's flask was established in Eq. (2.4).

$$N_{js} \propto d_0^{-0.25} \cdot d^{-0.18} \tag{2.4}$$

The fluid used in the present study was cell culture medium at a temperature 37°C with similar density and viscosity to water (μ_L=0.7 mPa s, ρ_L=993 kg m^{-3}). Calculation of a Reynolds number was possible thanks to the equation Eq. (4.9)

$$Re = N \cdot d^2 / \nu_L \tag{2.5}$$

where N is the agitator rate (s^{-1}), d the impeller (in spinner flasks) or flask (in Erlenmeyer flask) diameter (m) and ν_L is the kinematic viscosity of the medium (m^2 s^{-1}).

Analysis of the impact of stresses generated by agitation on animal cell culture with microcarriers is based on Kolmogorov's theory and determination of the microscale of turbulence would be calculated with Eq. (2.6)

$$\lambda_K = (\nu^3 / \varepsilon_T)^{1/4} \tag{2.6}$$

where ε_T is the local specific energy dissipation rate (W kg^{-1}). In spinner flask, it could be calculated as follow (Eq. (2.7)):

$$\varepsilon_T = N_p \cdot N^3 \cdot d^5 / V_L \tag{2.7}$$

where V_L is the liquid volume (m^3), N_p the impeller power number (dimensionless). Following recommendation of Hewitt *et al.,* [37], power number was supposed constant to $N_p \approx 1$. In shaking flask, the definition of the Newton number N_e was preferred to determine ε_T [38]:

$$\varepsilon_T = N_e \cdot N^3 \cdot d^4 \cdot V_L^{-2/3} \tag{2.8}$$

with

$$N_e = 70 \cdot Re^{-1} + 25 \cdot Re^{-0.6} + 1.5 \cdot Re^{-0.2} \tag{2.9}$$

WJ-MSC characterization

At the end of the culture, cells were detached and expanded in flasks to characterize their differentiation capabilities. Cells were seeded in 24-well plates and specific differentiation media (StemPro Differentiation kit, Gibco, LifeTechnologies) were added following manufacturer's instructions. The medium was changed every three days during 40 day culture. At the end of the differentiation period, cells were rinsed three times with PBS, fixed with 4 % (v/v) PFA at room temperature. Adipocytes were stained with 1 % (w/v) Oil Red O. Osteoblasts were incubated with Alizarin Red S. Finally, chondrocytes were stained with Alcian Blue. After staining, differentiated cells were rinsed with distilled water and observed by light microscopy.

WJ-MSC immunostaining

During the culture, 200 µL of samples were taken and fixed with 4 % (v/v) paraformaldehyde (PFA) at room temperature. After three washings with PBS, the samples were permeabilized using 500 µL of 0.5 % Triton x-100 buffer for 10 minutes. Then the buffer was removed, and 500 µL of blocking solution (0.1 % Triton x-100, 5 % BSA in PBS) was added for 20 minutes, followed by addition of staining solution. The 200 µL actin-vinculin staining was prepared by mixing 1:200 phalloidin Alexa 488 and 1:1000 anti-vinculin (Merck) in blocking buffer. Samples were incubated for 1 hour at room temperature, and after dPBS washing, the secondary antibody (goat anti-mouse Alexa 647) was added for one hour. After several washing steps, DAPI (1:1000) was added for 5 minutes. Finally, the last washing was done, and samples were visualized or stored at 4°C until use.

Analysis of the composition of microcarriers by X-Ray photoelectron spectrometry

Different samples of microcarriers were analyzed by X-Ray photoelectron spectrometry (XPS). Detached microcarriers which were in contact with cells for more than ten days of culture, microcarriers in the dry state (as control), microcarriers without cells in cell culture medium (as control). Samples were irradiated with a beam of X-Ray, the measurement of the kinetics energy of escaping electrons permitted to determine a composition of elemental structure.

2.3.1 Cell growth kinetics of WJ-MSC on microcarriers

WJ-MSC culture on microcarriers was investigated in shaken Erlenmeyer's flasks as a reference culture. No fresh microcarriers were added during these cultures.

Microcarriers colonization by WJ-MSC

As shown in figure 2.10 A, the percentage of colonized microcarriers was nearly 90% during the whole culture (as measured at day 1, day 3 and day 13), indicating that the seeding strategy was efficient. The mean cell number per microcarrier increased over time until a maximum value of approximately 8 cells per microcarrier. Whereas almost all microcarriers were colonized by at least one cell, the cell distribution on these microcarriers was heterogeneous, while at the beginning of the culture less variation in the cell number per particle was observed. The number of cells per microcarrier varied from 1 to 11 cells per microcarrier after 13 days of cultures (Figure 2.10 B). When a critical cell confluence (above 10 cells per microcarriers) was achieved on the microcarriers, aggregates made of cells and microcarriers formed, as shown in figure 2.10 C. These phenomena were previously qualitatively described by Ferrari *et al.,* [31] who showed during porcine bone-marrow MSC cultures that cell aggregation and detachment from microcarriers occurred when confluence was achieved on the microcarrier. Furthermore, kinetic analysis of glucose and glutamine concentrations in cell culture medium (data not shown) revealed that, although these compounds were still in excess in the culture medium, their consumption stopped after cell confluence on microcarrier was reached. It was observed that, from day 7, aggregates appeared in cell culture medium and in the same time, the concentration of empty microcarriers increased. Moreover, as observed in figure 2.10 C, from day 8, a slowdown in growth was noticed. It seemed that a critical number of cells per microcarrier lead to cell aggregation or confluence. Cell confluence was shown to be one of the main mechanisms that can inhibit expansion [39]. Aggregates formation was described as to be detrimental for WJ-MSC cultures [40]. Moreover, one of the major difficulty of aggregated culture is to control the size of the spheroids formed by aggregates [41]. Interestingly, Bartosh *et al.,* [42] and Sart *et al.,* [43] described MSC 3D aggregates as beneficial systems regarding trophic functions. Nonetheless, it is accepted that aggregated MSC cultures present limitations regarding cell expansion [40].

Composition of microcarriers

By microscopic observation, an heterogeneous cell population could be noticed on some microcarriers. Interestingly, DAPI stained cell nuclei were observed on some microcarriers with no visible cell cytoskeleton (Figure 2.11), indicating that some microcarriers were initially occupied by cells, before cell death.

One of possible implications of these findings might be that the microcarriers on which MSC attached and spread, may not be used again for cell expansion due to the surface chemistry evolution. One way to explain the occurrence of the heterogeneous cell distribution was to analyze the microcarrier composition by XPS measurements, after 14 days of MSC culture (Table 2.1). Changes in the composition of the previously occupied microcarriers were identified. An enrichment in carbon as well as depletions in oxygen, chloride and sodium, in comparison with fresh microcarriers were observed. As shown in figure 2.10 B, after 13 or 14 days of cell culture, microcarriers were occupied by 1, 5 or even 11 cells. This heterogeneity of cell distribution on the microcarriers might explain a modification of the microcarriers elemental composition.

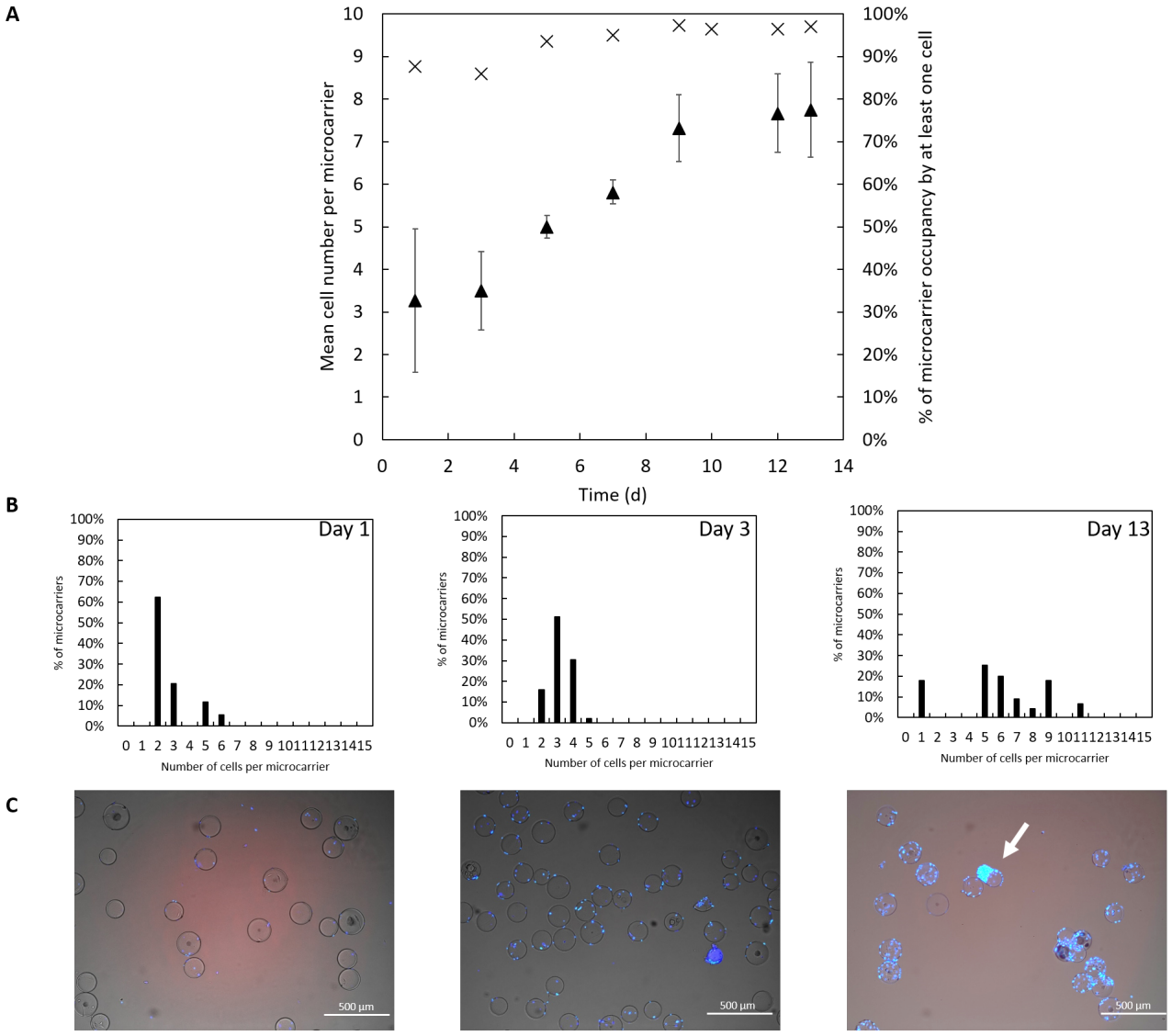

Figure 2.10 – Cell distribution on microcarriers and analysis of cell growth in batch culture in Erlenmeyer's flask without microcarrier addition. (A) Microcarrier colonization and cell distribution on microcarriers, (▲) represents the mean cell number per microcarrier obtained with the Matlab algorithm and (×) represents the percentage of microcarrier colonized by at least one cell. Standard deviation were calculated with three Erlenmeyer's flasks (n = 3). (B) Cell distribution on microcarriers at days 1, 3 and 13 of the culture. (C) DAPI cell nuclei staining at days 1, 3 and 13 of culture. White arrow emphasizes the heterogeneity of cell distribution on carriers.

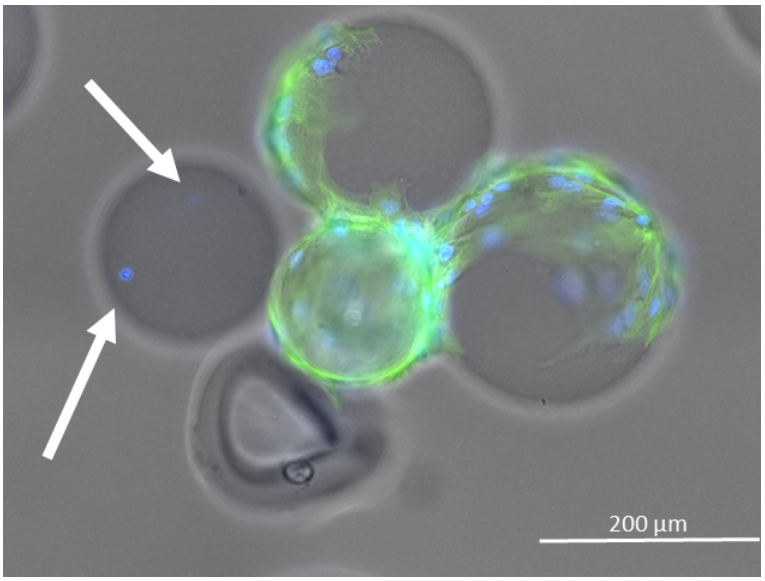

Figure 2.11 – Immunostaining of WJ-MSC on microcarriers. DAPI (blue) stained nuclei, actin stained cytoskeleton (green). Arrows indicate the presence of nuclei without cell bodies.

Table 2.1 – Atomic composition of microcarriers

Composition in atomic element (%)	**Carbon**	**Oxygen**	**Chloride**	**Sodium**
Before cell culture	27.6	16.5	21.9	31.9
After cell culture	41.2	13.8	18.1	25.9
Variation	+36 %	-16 %	-17 %	-19 %

The increase in relative percentage of carbon could be an indication of cell debris on the microcarriers, either due to cell death or to cell migration.

To verify this, already used microcarriers were trypsinized in order to remove most of cellular bodies and used again for cell expansion. The cell growth performances were compared, with cell culture performed in the same conditions but with fresh microcarriers. The Live/Dead stainings carried-out after 3 days of culture indicated that MSCs did not spread on the reused microcarriers and cell growth was dramatically reduced in comparison with cultures performed on fresh microcarriers (Figure 2.12). These results showed that Cytodex-1 microcarriers could not be colonized once again after cells left them and, consequently, microcarriers should also not be recycled after cell detachment.

The analysis of the batch culture results thus clearly confirmed that the limiting factor in WJ-MSC expansion was the growth surface availability. A strategy of fresh microcarriers addition during the WJ-MSC culture would be an interesting way to limit cell aggregation and cell heterogeneity distribution. Moreover, it was suggested that a critical number of cells per microcarrier had to be reached to allow the formation of cell aggregation. Thus, a pertinent strategy of microcarrier addition should be based on the monitoring of cell number per microcarrier.

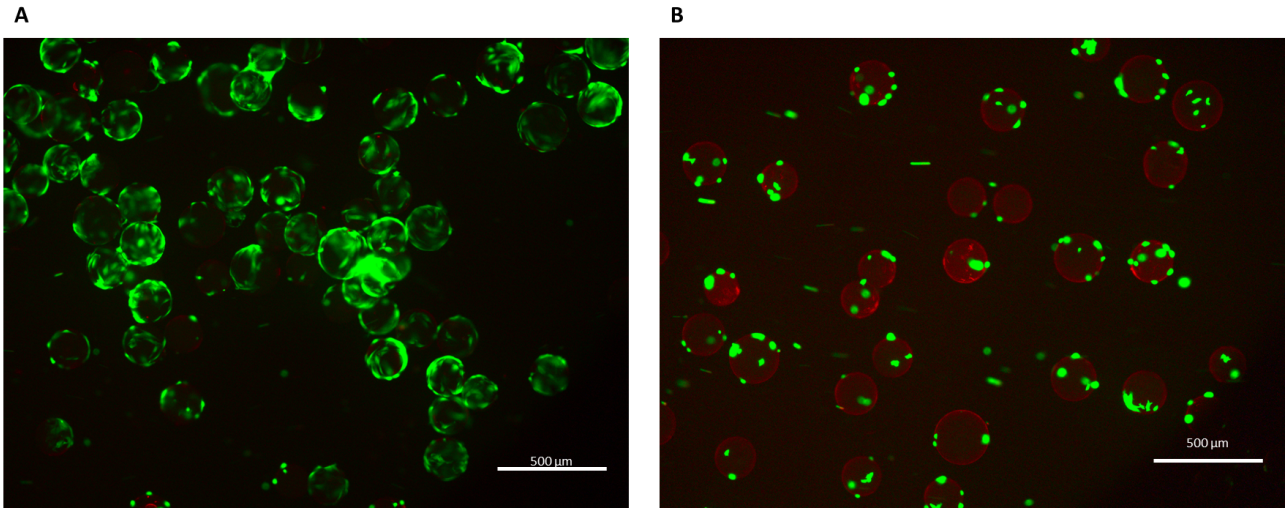

Figure 2.12 – Cell behavior as a function of the age of the microcarrier. (A) Live/Dead staining of cells grown on fresh Cytodex-1 at day 3. (B)Live/Dead staining of cells grown on 'used' Cytodex-1 at day 3.

2.3.2 Strategy of fresh microcarrier addition

Considering the expected capability of cell to move from one bead to another and considering that used microcarriers could not be reused for cell expansion anymore, the addition of fresh microcarriers during the culture was studied with the aim of delaying cell confluence and thus cell aggregation. Firstly, the cell migration was investigated using two distinguishable Cytodex-1 particle types, one with a fluorescent tag and the other without. Once migration has been demonstrated, the optimized moment of carriers addition and the suitable stirring system were determined in Erlenmeyer's flasks.

Cell migration ability

Cells were initially seeded on the labeled microcarriers (red on the picture of figure 2.13) and, after few hours, unlabeled ones were added. As indicated by the arrows in figure 2.13, cells initially attached to the stained microcarriers appeared to move towards the unlabeled one. The use of distinguishable carriers (stained with fluorescent rhodamine) permitted to highlight the WJ-MSC migration towards freshly added unlabeled microcarriers.

A particularity of WJ-MSC is that these are support-dependent cells, and the adhesion sites are one of the main part allowing cells to attach to their support. The adhesion sites are flat, elongated structures of about ten micrometers square and are mainly positioned at the extremities of the cells. Vinculin is a membrane-cytoskeletal protein in focal adhesion plaques that is involved in linkage of integrin adhesion molecules to the actin cytoskeleton. Thus, it is a molecule involved in cell-cell or cell-matrix junctions. As it is shown on the figure 2.14 A and B, adhesion sites were clearly visible, and it could be observed based on the presence of vinculin on the edges of cytoskeleton.

Cell migration may take place after cell division. During mitosis, focal adhesions and all the proteins involved in adhesion of cells on substrate are modified. Important changes occurred in the interactions between cell membrane proteins and the extracellular matrix (ECM). In prophase,

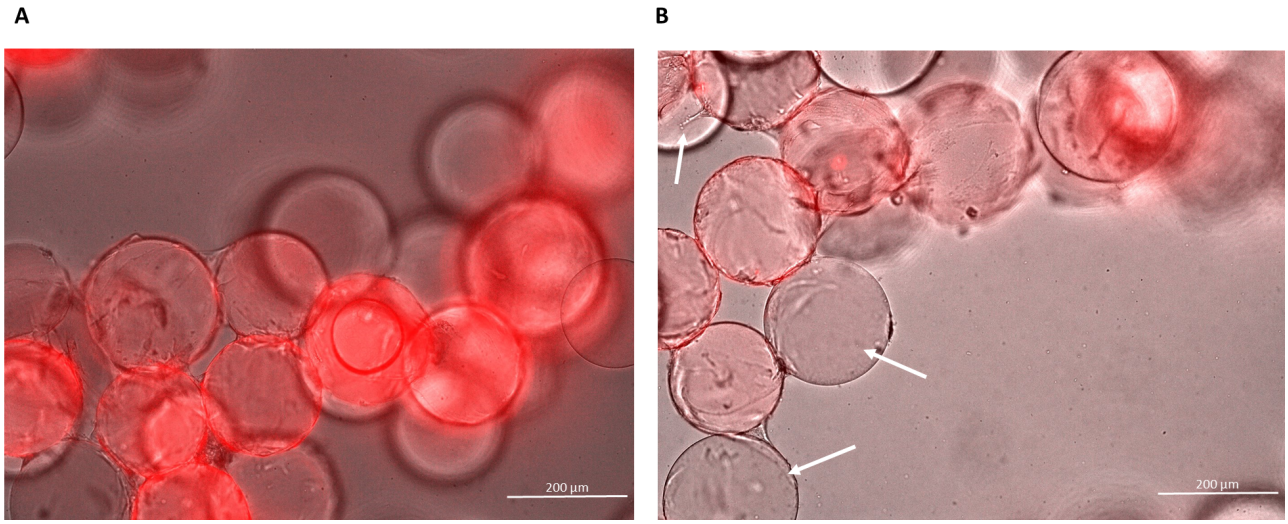

Figure 2.13 – Cell migration ability showed by using stained microcarriers. (A) Initial microcarriers labeled with fluorescent rhodamine with MSCs (appeared red on the picture). (B) Addition of unlabeled Cytodex-1 (appeared gray on the picture and indicated by the white arrows) which were colonized by MSCs after few hours of co-culture.

cells round up and lose attachment with the substrate [44]. Cells in division on carriers could thus undergo important changes in their morphology, and can migrate to other carriers upon contact between carriers.

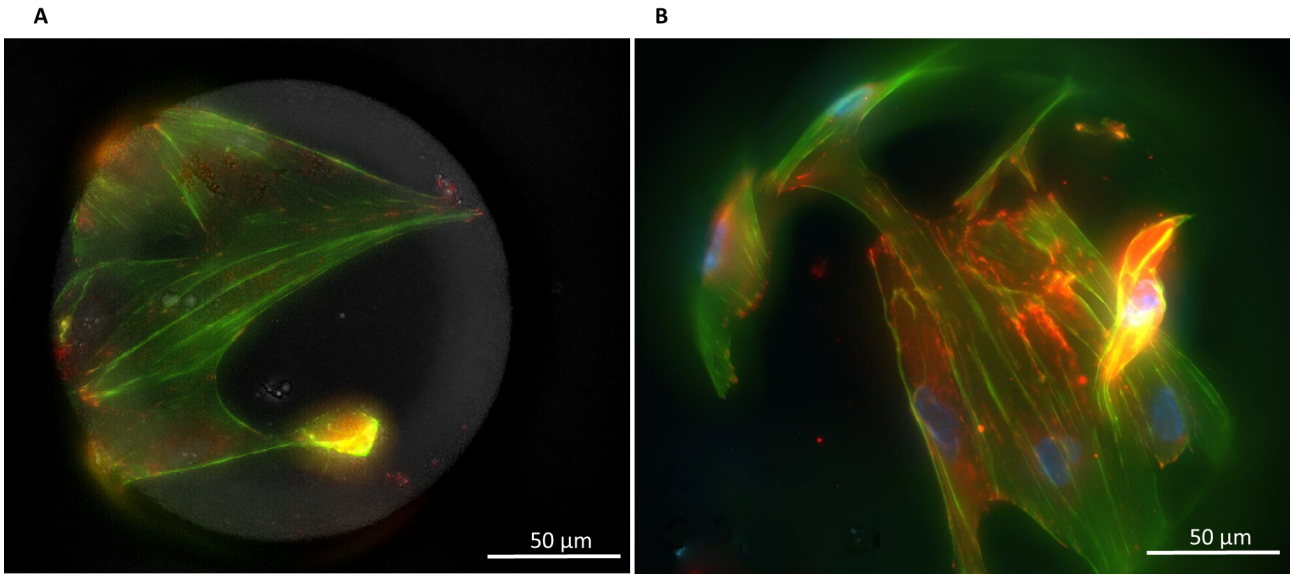

Figure 2.14 – Immunostaining of WJ-MSC on carriers showing focal adhesions (A and B). Actin (green), DAPI (blue) and vinculin (red).

These results showed that WJ-MSC were able to migrate towards fresh microcarriers. To determine the influence of the addition of new available growth surfaces on the cell distribution, analyzes of the mean cell number per carrier after addition of fresh particles were performed.

2.3.2.1 Influence of the addition of fresh microcarriers to control the mean number of cells per microcarriers

It was previously shown that the cell number per microcarrier is a crucial parameter that impacts cell growth. If confluence is achieved, cell growth is stopped; but if the cell number per microcarrier was too low, latency could occur in the culture. This phenomenon was already observed in previous experiments (data not shown). In this work, the cell counting method described by Loubiere *et al.,* [20] was used to determine the variation of the mean cell number per microcarrier and the cell number distribution on the carriers during the culture. Using this approach, the amount of carriers added and the time of addition were adjusted to reach an approximate number of 6 cells per microcarrier. This number was chosen on the basis of the results of the growth kinetics obtained without microcarrier addition, in batch mode. Moreover, Hewitt *et al.,* [37] described that an optimal ratio of cells per microcarrier was five. They analyzed that an increase in cell concentration on the microcarriers could have deleterious effects on growth as previously observed for human fibroblast cultures [45].

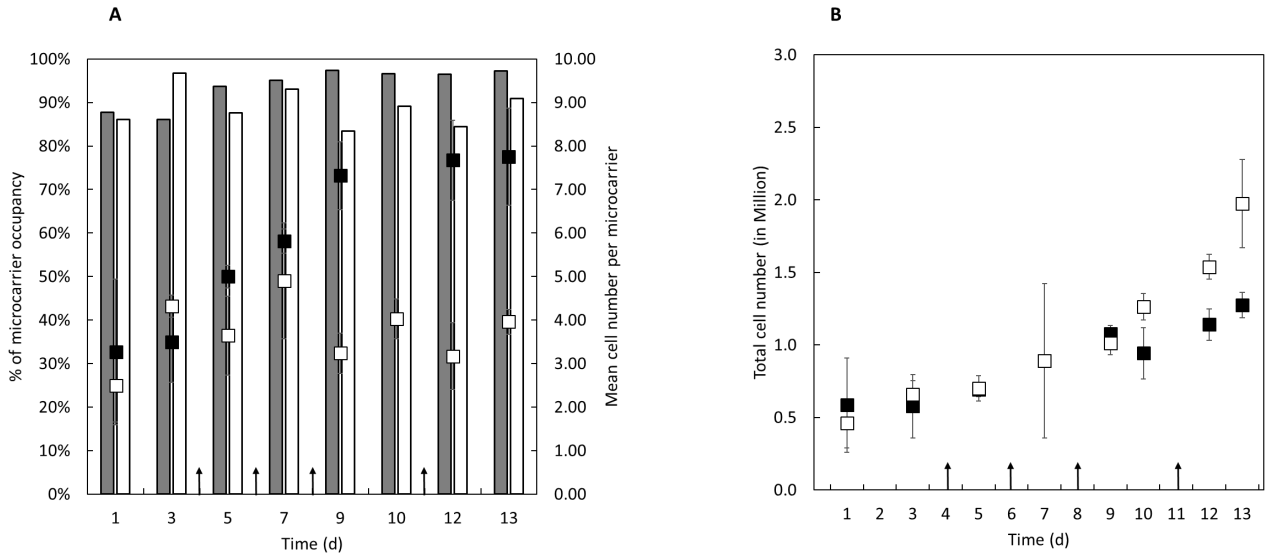

Figure 2.15 – Cell growth kinetics with or without addition of fresh microcarriers in Erlenmeyer's flasks. (A) Analysis of the percentage of microcarrier occupancy by at least one cell. Grey bars represent a batch culture (without addition of Cytodex-1) and white bars represent the condition of Cytodex-1 feed. Carriers addition is indicated by (↑). Analysis of the mean cell number per microcarrier: (■) represents mean number of cells in batch culture, (□) represents the mean cell number in the feed condition. (B) WJ-MSC growth kinetics. (■) represents the batch culture (without addition of Cytodex-1) and (□) represents the condition of Cytodex-1 feed. Carriers addition is indicated by (↑).

As it could be observed in the figure 2.15A, after each addition of microcarriers, indicated by (↑), the mean cell number was effectively maintained around 4 to 5 cells. Although the targeted number was not obtained, the mean number of cells was nevertheless controlled. The percentage of microcarriers colonized was between 80 and 90 %, indicating that added microcarriers were effectively colonized by the cells. On the contrary, in the batch cell culture, the mean cell number per microcarrier increased to a critical value below 8. For this critical cell number, the formation of aggregates was confirmed, leading to a significant heterogeneity of cell distribution on carriers.

The comparison of total cell number at the end of the culture, between batch and cultures with microcarriers addition, showed that the feed of Cytodex-1 improved the expansion by a factor of 1.5 (Figure 2.15 B). Ferrari *et al.*,[31] reported a 1.3 higher expansion factor when microcarriers are added at day 10 of the culture. These results confirmed that the addition of fresh microcarriers was also beneficial for WJ-MSC expansion and that cells/particles aggregation limited the cell growth.

To sum up, after each addition of fresh microcarriers, cells were able to colonize the new added surfaces, and in this way it was possible to control the mean cell number per microcarrier. With bead-to-bead transfer, cells were maintained at a constant number on the carriers, and the cell expansion was promoted.

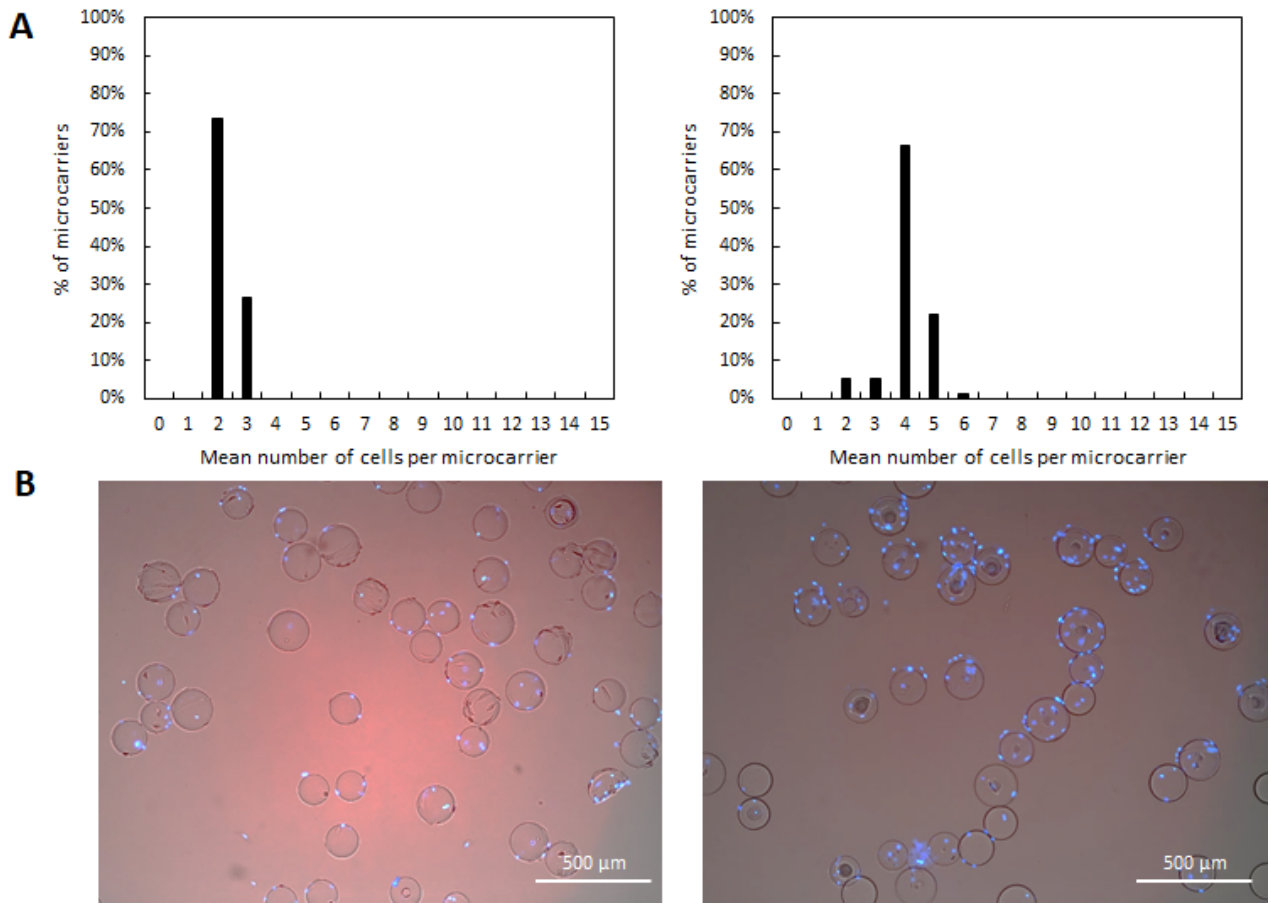

Figure 2.16 – Cell distribution on microcarriers in Erlenmeyer's flasks. (A) Cell distribution after fresh Cytodex-1 carriers were added (day 1 & 13). (B) DAPI staining after addition of fresh Cytodex-1 carriers.

Comparison of microcarriers colonization without (Figure 2.10A) and with addition of fresh microcarriers (Figure 2.16 A) indicated that a better cell distribution could be obtained after addition of microcarriers. In this case, colonization was over 80 % and a mean cell number per microcarrier around 5 was maintained, and having a positive impact on the cell growth (Figure 2.16B), avoiding the formation of cell aggregates.

In addition, metabolite kinetics (Figure 2.17 A) showed that cells cultivated with addition of fresh carriers consumed twice more glucose at the end of the culture (between day 10 and 12) than in the batch condition. Figure 2.17 B, representing lactate yield, showed a value of 0.6 in

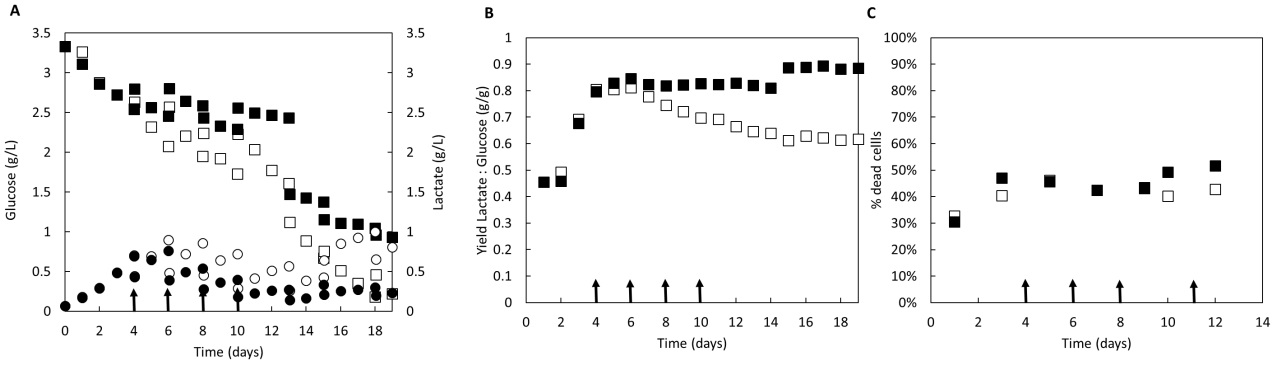

Figure 2.17 – Kinetics in WJ-MSC cell culture in Erlenmeyer's flasks. (A) Glucose consumption and lactate production: Cytodex-1 feed (□) or batch culture (■). (B) Yield of lactate on glucose: Cytodex-1 feed (□) or batch culture (■). (C) Kinetics of dead cells: Cytodex-1 feed (□) or batch culture (■). Time of carriers addition was indicated by (↑).

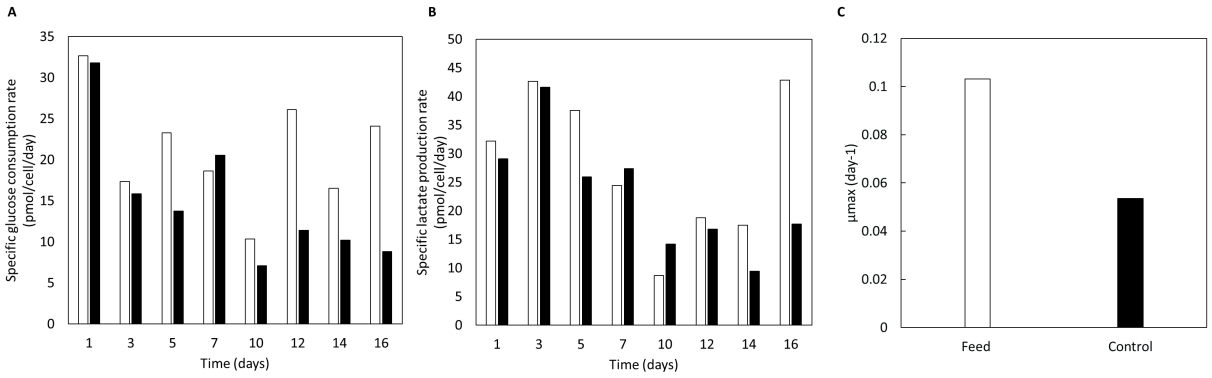

Figure 2.18 – Comparison of specific kinetics in WJ-MSC cell culture. (A) Specific glucose consumption rate: Cytodex-1 feed (white bars) or batch culture (black bars). (B) Specific lactate production rate: Cytodex-1 feed (white bars) or batch culture (black bars). (C) Specific growth factor: Cytodex-1 feed (white bars) or batch culture (black bars).

the condition of Cytodex-1 feed, against 0.8 in the batch culture. This decrease of lactate on glucose yield indicated that energy metabolism of WJ-MSC is preferentially promoted from oxidative phosphorylation instead of from the glycolytic path. The last one, called Warburg effect is typical of some cancerous cell lines and did not occur when fresh carriers are added during the culture [46]. The enhanced glucose consumption and the efficiency of energy production could also explain the improvement of cell growth in cultures carried out with Cytodex-1 feed. As it could be observed in figure 2.18, the specific glucose consumption was twice higher for cells grown with addition of microcarriers than without (figure 2.18 C). The consumed glucose was then certainly mainly used for cell growth. However, in both cultures (batch culture and Cytodex-1-fed) carried-out in Erlenmeyer's flasks, an unexpected LDH release showed that almost 50 % of the total cell population were dead cells. The addition of fresh microcarriers seemed to be effective to increase the total cell number, but a particular attention should be paid to the agitation mode of the culture. Complementary discussion regarding the viability quantification for both cultures will be proposed in the next part of this study.

Stemness after cell migration

The WJ-MSC multipotency was determined after 18 days of culture. Cells successfully differentiated into adipocytes, chondrocytes and osteocytes. Figure 2.19 indicates that cells maintained their stemness properties during the expansion phase whatever the imposed culture condition. It is also important to note that these differentiation tests provided only qualitative results and that a finer analysis using cytometry would be necessary to quantitatively evaluate the cell multipotency.

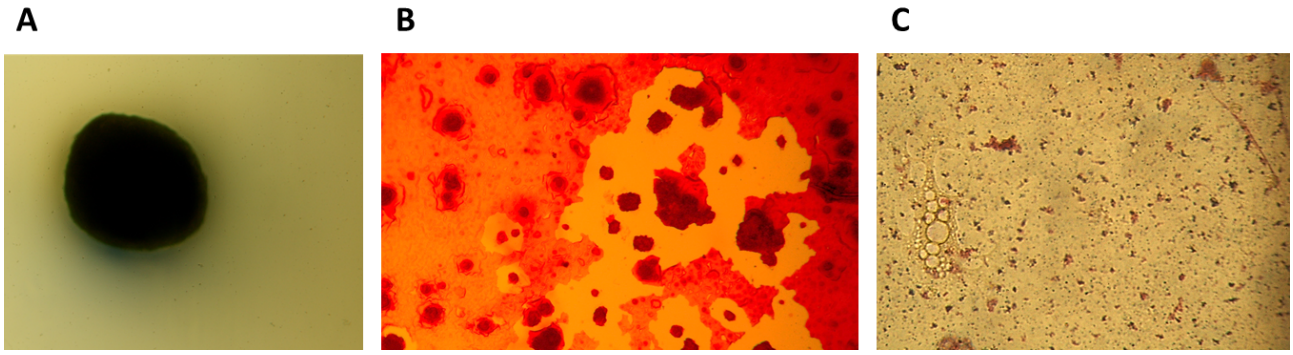

Figure 2.19 – MSC multipotency determined after addition of fresh carriers in Erlenmeyer's flasks (Day 18). Cells were differentiated along the chondrogenic (x10 magnification) (A), osteogenic (x10 magnification) (B), and adipogenic (x50 magnification) (C) pathways.

2.3.3 Impact of the agitation mode on the cell growth during addition of fresh microcarriers

Agitation mode

Despite the fact that hydromechanical stresses are generally considered as a main cause of cell damages in cultures with microcarriers, the local microcarrier concentration may also significantly impact the cell death by bead-to-bead transfer interactions, specifically through particle friction or collisions, as mentioned by Cherry *et al.,* [47]. Thus, it could be expected that a compromise should be found between a high concentration of microcarriers that provides a high adherence surface and a lower one to limit collisions and friction. Additionally, the homogeneity of the particle suspension in the system should be optimized to limit the local particle accumulation within the system.

In order to determine how the particles dispersion within the bioreactor may impact cell culture, the cultures carried out in the orbital shaking flasks were compared with cultures in a spinner flask, mixed by a pendular mechanical agitation, in a batch culture or in a Cytodex-1 fed culture.

As shown in Figure 2.20, cell death was more pronounced in Erlenmeyer's flasks than in spinner flasks. Around 40 % of the total cell number were dead at day 10 in cultures with microcarriers addition while only 10 % of the total cell number were dead in spinner vessels, after addition of microcarriers. This was confirmed by the higher cell mortality observed with Live/Dead assay in a batch culture and in culture with Cytodex-1 addition (Figure 2.20).

One way to explain the increase of dead cells when Cytodex-1 are added in cultures is the rise

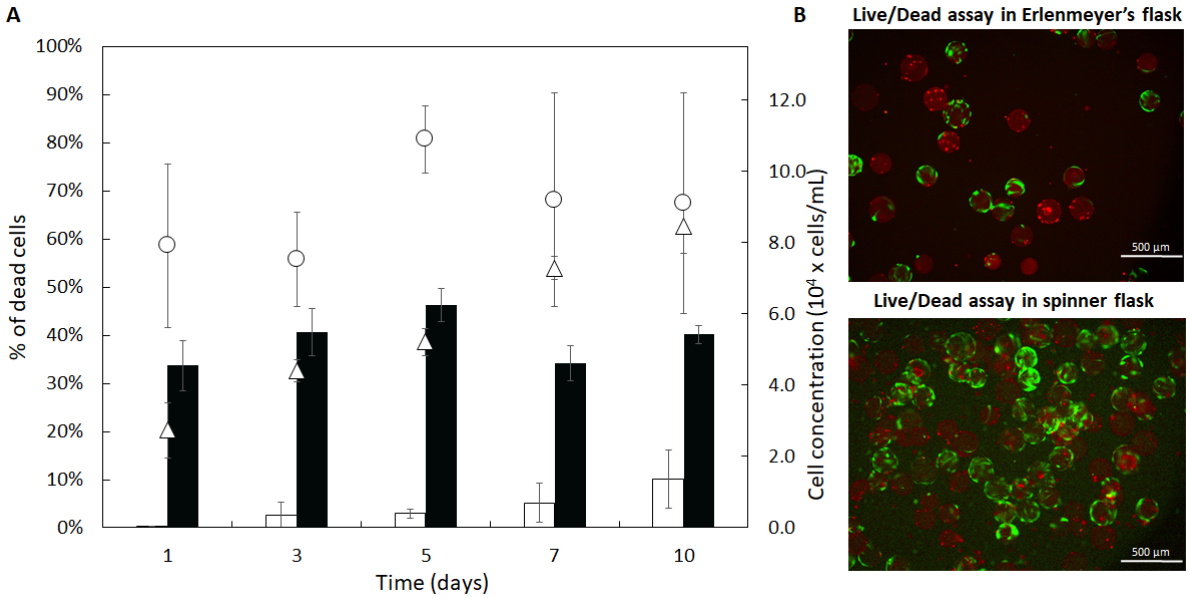

Figure 2.20 – Comparison of percentage of dead cells in Erlenmeyer's flasks (orbital agitation) and in Spinner vessel (mechanical agitation). (A) Total cell concentration in the spinner flask (n=2) (∘) and total cell concentration in Erlenmeyer's flask (n=3) (△). Black histogram represents percentage of dead cells in the Erlenmeyer's flask and white histogram represents percentage of dead cells in the spinner flask. (B) Exemplary pictures of Live/dead staining of cells grown on Cytodex-1 at Day 7, in either Erlenmeyer's flask or in spinner flask.

of microcarrier concentration in the orbital shaking flask system. Too high concentration of microcarriers could promote shocks between particles and cells, leading to cell death. Nienow *et al.*, [48] showed that with an increase in particle concentration in the culture medium, an increase of collision number proportional to the square concentration of particles was observed. A theoretical just-suspended state (N_{js}) was calculated using the model of Olmos *et al.*,[36]. In Erlenmeyer's flask, a 310 rpm agitation is required, in order to obtain a complete suspension of the microcarriers in the culture medium. For technical reasons, this agitation condition is not suitable for cell culture, especially for MSC on microcarriers. For agitation rates lower than N_{js}, a heterogeneous distribution of microcarriers is obtained [36]. This can lead to an increase collisions, particularly at the center of the Erlenmeyer's flask, where particles concentrate. In this condition of culture, in order to obtain a complete and homogenous suspension, a too high agitation rate would be required (310 rpm). A decrease in the agitation rate led to heterogeneous systems, enhancing cell death. In the next step, a system with mechanical stirring was investigated. While orbital shaking led to the local increase of the mean volume fraction of particles and promoted collisions, the more homogeneous dispersion observed in spinner flasks did not promote cell death by lysis. By controlling the agitation mode, it was possible as expected, to decrease the occurrence of the cell death (Figure 2.20), with only 10 % of dead cells at day 10 of cell culture.

Discussion

As previously mentioned, cell death could also be related to the hydromechanical stress. To better understand the influence of the agitation condition on MSC cell culture on microcarriers,

Table 2.2 – Comparison of hydrodynamic parameters of cell culture agitation conditions.

Condition	**Reynolds number**	**Agitation rate (rps)**	**Power number (N_p or N_e)**	**Specific energy dissipation rate (ε_T) ($W\,kg^{-1}$)**	**Estimate microscale of turbulence (λ_K) (µm)**	**(λ_K/d_p)**
Erlenmeyer's flask N < N_{js} (This work)	7260	1.2	0.38	0.014	71	0.4
Erlenmeyer's flask N = N_{js} (This work)	32097	5.1	0.24	0.73	26	0.14
Spinner flask N = N_{js} (This work)	1524	0.67	1	1.5×10^{-4}	218	1.2
Spinner flask N = N_{js} (Hewitt et al. 2011)	1700	0.5	1	8.8×10^{-4}	183	1.03

Reynolds number, specific energy dissipation rate (ε_T) and estimated microscale of turbulence (λ_K) were calculated and compared to those obtained in the work of Hewitt *et al.*,[37]. It is important to note that the occurrence of turbulent regime in shaking flasks and thus of the use of the dissipation scale λ_K is still debated. For instance, Peter *et al.,* [49] proposed a value of $Re \approx 60,000$ for turbulent regime transition. Thus, the conditions reported here for experimental Erlenmeyer flasks should rather be related to a transitional regime. Results are presented in the table 2.2. Based on the obtained ratio λ_K/d_p, it appeared that few damages were expected to the cells on microcarriers in the spinner vessels. Croughan *et al.,* [24] suggested for culture of FS-4 fibroblasts that λ_K/d_p over 2 or 3 was a good criterion for a condition of agitation without cell damages. In this study, this factor was 1.2 in spinner vessels, which is higher than the one determined by Hewitt *et al.*,[37] in their culture systems. In Erlenmeyer's flasks the obtained ratio λ_K/d_p was below 1 (if turbulent regime is assumed) and a higher cellular death was noticed. Apart from direct hydromechanical stress acting on microcarriers, additional cell death could be explained by the agitation rate used, which was lower than N_{js}. In this condition of agitation microcarriers were indeed packed at the flask center and were probably submitted to more intense friction and abrasions, deleterious for cells.

To conclude, mechanical agitation (spinner flasks in this study) seemed more suitable for MSC cell culture than orbital agitation (Erlenmeyer's flasks). A better distribution of the particles was observed in this system of culture, leading to a decrease of cell death by lysis. An innovative way to monitor WJ-MSC cell cultures in bioreactor could be the use of fed-batch mode. Until now, mainly bioreactors in batch mode have been carried out for Wharton's jelly MSC [19, 29, 30]. However, when using fed-batch mode, careful attention must be paid to mixing of microcarriers and cell distribution.

The present study revealed, in a first point, the benefit of using fed-batch modes during culture of WJ-MSC on the microcarriers. The carriers addition required to be carefully controlled with a targeted number of 5 cells per microcarrier limiting cell aggregation phenomena. Stemness was not influenced by the addition of microcarriers. Secondly, the ability of WJ-MSC to migrate was demonstrated by using distinguishable microcarriers. Thirdly, a strategy was successfully implemented to maintain a mean cell number per microcarrier under the critical value provoking cell aggregation. With the addition of fresh carriers, the total number of cells was increased and the percentage of microcarrier occupancy maintained over 80 %. Finally, this study showed the importance of just-suspended state and particle distribution in the bioreactor on the WJ-MSC performances, notably concerning the bead-to-bead transfer phenomenon. In order to maintain the cell growth after six days of cell culture, it seemed necessary to add fresh surfaces to avoid cell confluence on carriers. This study demonstrated that if the composition and the concentration in microcarriers changed, impact could be noticed on cell death, through cell lysis more precisely. However, if the concentration in particles increased and the agitation was not well adapted, cell damages clearly occurred. Collisions and friction between particles are the most probable cause of the early cell death but it remained difficult to quantify their respective effects. Therefore, controlled agitation mode is crucial to limit particles collisions and, consequently, cell death. Finally, this study permitted to establish the basis of a fed-batch process for mesenchymal stem cells in bioreactor.

Acknowledgments

The authors would like to thank the Interreg project for its financial support. They also acknowledge Fabrice Blanchard (LRGP, Nancy) and Jenny Brinkmann (INM, Saarbrücken) for their technical contribution to this work.

Conclusions of the chapter 2

In this chapter, cell adhesion and migration were intensively studied to control the addition of microcarriers and thus to improve MSC culture strategies. The main results obtained are summarized in Figure 2.21.

Dielectric spectroscopy is a powerful tool and well described in literature to monitor concentration of viable cells. Thanks to the interpretation of some specific data recorded by the spectrometer, particularly the critical frequency, data concerning the physiologic state of the cells, their biovolume and radius could be obtained. The adhesion steps could be indeed detected and analyzed. Thus, about 2 hours were necessary for the first steps of adhesion to establish (probably due to electrostatic and Van der Waals interactions). However, further studies will be required with different materials for example to tweak these preliminary results. Thereafter, the dielectric probe could be implemented inside bioreactors to monitor cell growth and cell physiology states and modification (see Chapter 3).

To overcome cell confluence and the limitation of available surfaces during cultures, one strategy consists in feeding the culture with fresh microcarriers. However, a more detailed knowledge of this cell migration is required to optimize the culture conditions. Migrations of cells were, for the first time, visualized by time-lapse microscopy in this study. An average duration for complete migration has been calculated and about 3 hours were necessary for a complete cell migration, with an average velocity of displacement of 60 $\mu m\ h^{-1}$. This migration process seemed to depend on different factors, such as the presence of cells on the targeted microcarrier or cell-cell contact, for example. Further studies will be necessary to better investigate this phenomenon, because these experiments were carried out in static modes, which is not representative of dynamics cultures in stirred tank bioreactors, but at least of the rest conditions imposed after microcarriers addition.

During small scale cultures, the addition of precise amounts of microcarriers at specific time of cultures improved cell growth with a 1.3 cell expansion factor in Erlenmeyer's flasks. However, different results were obtained between Erlenmeyer's flasks and vessel spinners in terms of cell viability, related to the stirring system. In orbital system a higher death rate was observed when concentration of microcarriers was increased. With mechanically stirring, a better distribution of microcarriers is expected. Thus, thanks to these results, a particular attention should be paid to the necessity of increasing reasonably microcarriers concentration, and to prefer a mechanical stirring and microcarrier homogenization. Finally, the controlled addition of fresh microcarriers is one of the strategies of improvement of MSC expansion in microcarrier culture. Knowing the average time of cell adhesion and migration thanks to the microscopic tools and dielectric spectroscopy, a strategy of addition of microcarriers to maintain an average number of cells per microcarriers (around 7) thanks to the daily cell counting in stirred tank bioreactors has been considered. Moreover, as the concentration in microcarriers and the mode of agitation were crucial for cell viability, fed-batch bioreactors were performed in the next chapter.

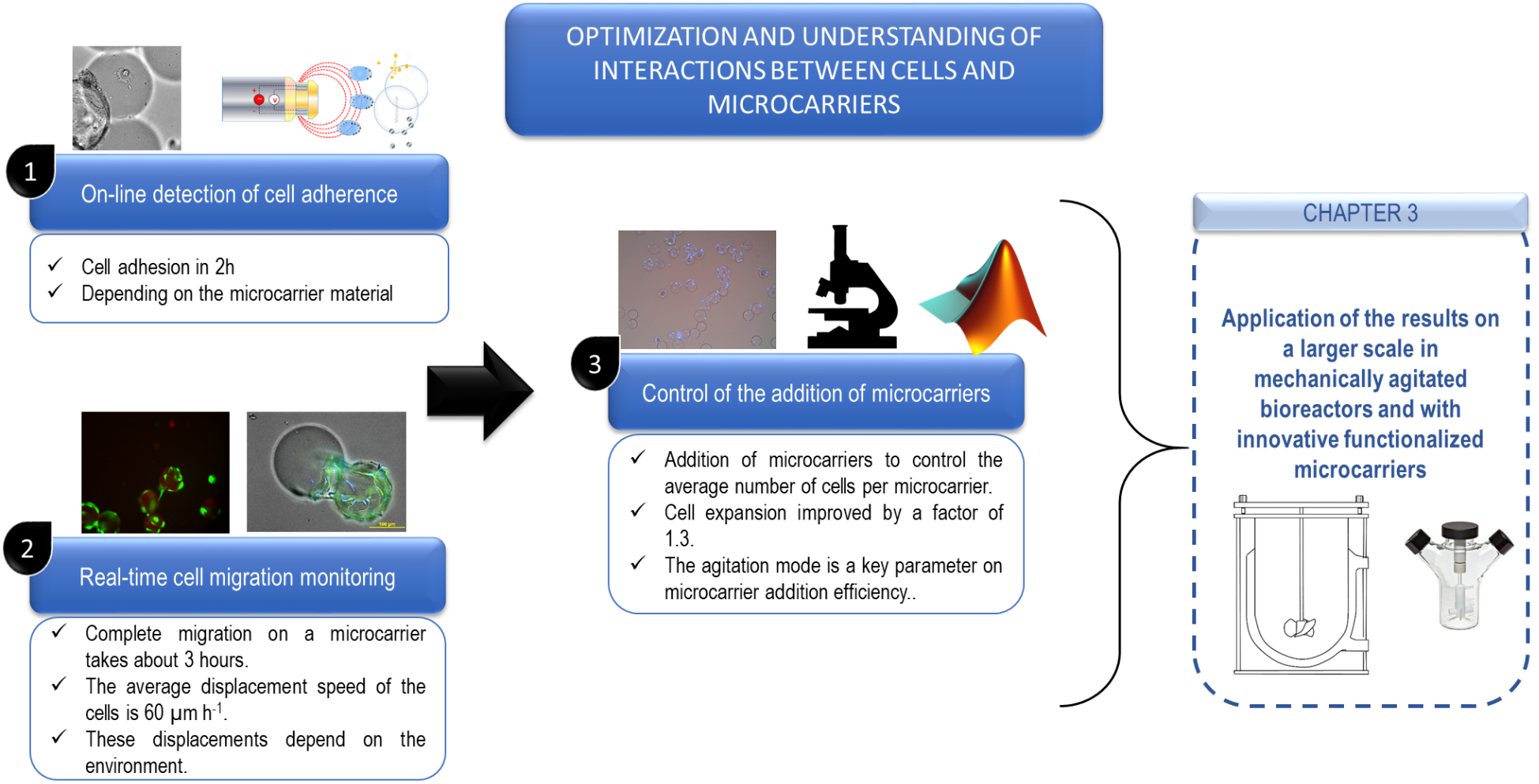

Figure 2.21 – Synthesis of the results of the chapter 2.

Bibliography

[1] D. L. Troyer and M. L. Weiss. Concise review: Wharton's jelly-derived cells are a primitive stromal cell population. *Stem Cells*, 26(3):591–599, 2008.

[2] C. F. Opel, J. Li, and A. Amanullah. Quantitative modeling of viable cell density, cell size, intracellular conductivity, and membrane capacitance in batch and fed-batch cho processes using dielectric spectroscopy. *Biotechnology Progress*, 26(4):1187–1199, 2010.

[3] E. Petiot, A. El-Wajgali, G. Esteban, C. Gény, H. Pinton, and A. Marc. Real-time monitoring of adherent vero cell density and apoptosis in bioreactor processes. *Cytotechnology*, 64(4):429–441, 2012.

[4] C. Justice, J. Leber, D. Freimark, P. P. Grace, M. Kraume, and P. Czermak. Online-and offline-monitoring of stem cell expansion on microcarrier. *Cytotechnology*, 63(4):325–335, 2011.

[5] T. Maskow, A. Röllich, I. Fetzer, J. Yao, and H. Harms. Observation of non-linear biomass–capacitance correlations: reasons and implications for bioprocess control. *Biosensors and Bioelectronics*, 24(1):123–128, 2008.

[6] C. Huang, A. Chen, L. Wang, M. Guo, and J. Yu. Electrokinetic measurements of dielectric properties of membrane for apoptotic hl-60 cells on chip-based device. *Biomedical Microdevices*, 9(3):335–343, 2007.

[7] S. Arora, S. Saha, S. Roy, M. Das, S. S. Jana, and M. Ta. Role of nonmuscle myosin ii in migration of wharton's jelly-derived mesenchymal stem cells. *Stem Cells and Development*, 24(17):2065–2077, 2015.

[8] C. Götherström, O. Ringdén, M. Westgren, C. Tammik, and K. Le Blanc. Immunomodulatory effects of human foetal liver-derived mesenchymal stem cells. *Bone Marrow Transpl*, 32(3):265–272, August 2003.

[9] D. L. Troyer and M. L. Weiss. Concise Review: Wharton's Jelly-Derived Cells Are a Primitive Stromal Cell Population. *Stem Cells*, 26(3):591–599, 2008.

[10] F. Petry, J. R. Smith, J. Leber, D. Salzig, P. Czermak, and M. L. Weiss. Manufacturing of human umbilical cord mesenchymal stromal cells on microcarriers in a dynamic system for clinical use. *Stem Cells Int*, 2016, 2016.

[11] M. Bernardo, L. Ball, A. Cometa, H. Roelofs, M. Zecca, M. Avanzini, A. Bertaina, L. Vinti, A. Lankester, R. Maccario, et al. Co-infusion of ex vivo-expanded, parental mscs prevents life-threatening acute gvhd, but does not reduce the risk of graft failure in pediatric patients undergoing allogeneic umbilical cord blood transplantation. *Bone Marrow Transpl*, 46(2):200, 2011.

[12] K. Le Blanc, F. Frassoni, L. Ball, F. Locatelli, H. Roelofs, I. Lewis, E. Lanino, B. Sundberg, M. E. Bernardo, M. Remberger, et al. Mesenchymal stem cells for treatment of steroid-resistant, severe, acute graft-versus-host disease: a phase ii study. *Lancet*, 371(9624):1579–1586, 2008.

[13] L. M. Ball, M. E. Bernardo, H. Roelofs, M. J. van Tol, B. Contoli, J. J. Zwaginga, M. A. Avanzini, A. Conforti, A. Bertaina, G. Giorgiani, et al. Multiple infusions of mesenchymal stromal cells induce sustained remission in children with steroid-refractory, grade iii–iv acute graft-versus-host disease. *Brit J Haematol*, 163(4):501–509, 2013.

[14] F. F. dos Santos, P. Z. Andrade, C. L. da Silva, and J. M. Cabral. Bioreactor design for clinical-grade expansion of stem cells. *Biotechnol J*, 8(6):644–654, 2013.

[15] A. S. Simaria, S. Hassan, H. Varadaraju, J. Rowley, K. Warren, P. Vanek, and S. S. Farid. Allogeneic cell therapy bioprocess economics and optimization: Single-use cell expansion technologies. *Biotechnol Bioeng*, 111(1):69–83, 2014.

[16] S. Frauenschuh, E. Reichmann, Y. Ibold, P. M. Goetz, M. Sittinger, and J. Ringe. A microcarrier-based cultivation system for expansion of primary mesenchymal stem cells. *Biotechnol Progr*, 23(1):187–193, 2007.

[17] G. Eibes, F. dos Santos, P. Z. Andrade, J. S. Boura, M. M. Abecasis, C. L. da Silva, and J. M. Cabral. Maximizing the ex vivo expansion of human mesenchymal stem cells using a microcarrier-based stirred culture system. *J Biotechnol*, 146(4):194–197, 2010.

[18] C. J. Hewitt, K. Lee, A. W. Nienow, R. J. Thomas, M. Smith, and C. R. Thomas. Expansion of human mesenchymal stem cells on microcarriers. *Biotechnol Lett*, 33(11):2325, November 2011.

[19] Q. A. Rafiq, K. M. Brosnan, K. Coopman, A. W. Nienow, and C. J. Hewitt. Culture of human mesenchymal stem cells on microcarriers in a 5 l stirred-tank bioreactor. *Biotechnol Lett*, 35(8):1233–1245, 2013.

[20] C. Loubière, I. Chevalot, N. De Isla, C. Sion, L. Reppel, E. Guedon, and E. Olmos. Impact of the type of microcarrier and agitation modes on the expansion performances of mesenchymal stem cells derived from umbilical cord. *Biotechnol Progr*, 35:e2887, 2019.

[21] B. Li, X. Wang, Y. Wang, W. Gou, X. Yuan, J. Peng, Q. Guo, and S. Lu. Past, present, and future of microcarrier-based tissue engineering. *J Orthop Transl*, 3(2):51–57, 2015.

[22] R. S. Cherry and E. T. Papoutsakis. Physical mechanisms of cell damage in microcarrier cell culture bioreactors. *Biotechnol Bioeng*, 32(8):1001–1014, 1988.

[23] R. Cherry and E. Papoutsakis. Growth and death rates of bovine embryonic kidney cells in turbulent microcarrier bioreactors. *Bioprocess Eng*, 4(2):81–89, 1989.

[24] M. S. Croughan, J.-F. Hamel, and D. I. Wang. Hydrodynamic effects on animal cells grown in microcarrier cultures. *Biotechnol Bioeng*, 67(6):841–852, 2000.

[25] Y. J. Li, N. N. Batra, L. You, S. C. Meier, I. A. Coe, C. E. Yellowley, and C. R. Jacobs. Oscillatory fluid flow affects human marrow stromal cell proliferation and differentiation. *J Orthop Res*, 22(6):1283–1289, 2004.

[26] M. R. Kreke, W. R. Huckle, and A. S. Goldstein. Fluid flow stimulates expression of osteopontin and bone sialoprotein by bone marrow stromal cells in a temporally dependent manner. *Bone*, 36(6):1047–1055, 2005.

[27] S. Scaglione, D. Wendt, S. Miggino, A. Papadimitropoulos, M. Fato, R. Quarto, and I. Martin. Effects of fluid flow and calcium phosphate coating on human bone marrow stromal cells cultured in a defined 2d model system. *J Biomed Mater Res A*, 86(2):411–419, 2008.

[28] T. M. Maul, D. W. Chew, A. Nieponice, and D. A. Vorp. Mechanical stimuli differentially control stem cell behavior: morphology, proliferation, and differentiation. *Biolech Model Mechanobiol*, 10(6):939–953, 2011.

[29] J. Hupfeld, I. H. Gorr, C. Schwald, N. Beaucamp, K. Wiechmann, K. Kuentzer, R. Huss, B. Rieger, M. Neubauer, and H. Wegmeyer. Modulation of mesenchymal stromal cell characteristics by microcarrier culture in bioreactors. *Biotechnol Bioeng*, 111(11):2290–2302, 2014.

[30] A. Mizukami, A. Fernandes-Platzgummer, J. G. Carmelo, K. Swiech, D. T. Covas, J. M. Cabral, and C. L. da Silva. Stirred tank bioreactor culture combined with serum-/xenogeneic-free culture medium enables an efficient expansion of umbilical cord-derived mesenchymal stem/stromal cells. *Biotechnol J*, 11(8):1048–1059, 2016.

[31] C. Ferrari, F. Balandras, E. Guedon, E. Olmos, I. Chevalot, and A. Marc. Limiting cell aggregation during mesenchymal stem cell expansion on microcarriers. *Biotechnol Progr*, 28(3):780–787, 2012.

[32] Q. A. Rafiq, S. Ruck, M. P. Hanga, T. R. J. Heathman, K. Coopman, A. W. Nienow, D. J. Williams, and C. J. Hewitt. Qualitative and quantitative demonstration of bead-to-bead transfer with bone marrow-derived human mesenchymal stem cells on microcarriers: Utilising the phenomenon to improve culture performance. *Biochem Eng J*, 135:11–21, July 2018.

[33] T. Lawson, D. E. Kehoe, A. C. Schnitzler, P. J. Rapiejko, K. A. Der, K. Philbrick, S. Punreddy, S. Rigby, R. Smith, Q. Feng, et al. Process development for expansion of human mesenchymal stromal cells in a 50 l single-use stirred tank bioreactor. *Biochem Eng J*, 120:49–62, 2017.

[34] L. Reppel. *Potentialité des cellules stromales de la gelée de Wharton en ingénierie du cartillage*. PhD thesis, Université de Lorraine, October 2014.

[35] S. Laner-Plamberger, T. Lener, D. Schmid, D. A. Streif, T. Salzer, M. Öller, C. Hauser-Kronberger, T. Fischer, V. R. Jacobs, K. Schallmoser, et al. Mechanical fibrinogen-depletion supports heparin-free mesenchymal stem cell propagation in human platelet lysate. *J Transl Med*, 13(1):354, 2015.

[36] E. Olmos, K. Loubiere, C. Martin, G. Delaplace, and A. Marc. Critical agitation for microcarrier suspension in orbital shaken bioreactors: Experimental study and dimensional analysis. *Chem Eng Sci*, 122:545–554, 2015.

[37] C. J. Hewitt, K. Lee, A. W. Nienow, R. J. Thomas, M. Smith, and C. R. Thomas. Expansion of human mesenchymal stem cells on microcarriers. *Biotechnol Lett*, 33(11):2325, 2011.

[38] J. Büchs, U. Maier, C. Milbradt, and B. Zoels. Power consumption in shaking flasks on rotary shaking machines: I. power consumption measurement in unbaffled flasks at low liquid viscosity. *Biotechnol Bioeng*, 68(6):589–593, 2000.

[39] U. Nekanti, L. Mohanty, P. Venugopal, S. Balasubramanian, S. Totey, and M. Ta. Optimization and scale-up of wharton's jelly-derived mesenchymal stem cells for clinical applications. *Stem Cell Res*, 5(3):244–254, 2010.

[40] J. M. Santos, S. P. Camões, E. Filipe, M. Cipriano, R. N. Barcia, M. Filipe, M. Teixeira, S. Simões, M. Gaspar, D. Mosqueira, et al. Three-dimensional spheroid cell culture of umbilical cord tissue-derived mesenchymal stromal cells leads to enhanced paracrine induction of wound healing. *Stem Cell Res Ther*, 6(1):90, 2015.

[41] M. António, A. Fernandes-Platzgummer, C. L. da Silva, and J. M. Cabral. Scalable microcarrier-based manufacturing of mesenchymal stem/stromal cells. *J Biotechnol*, 236:88–109, 2016.

[42] T. J. Bartosh, J. H. Ylöstalo, A. Mohammadipoor, N. Bazhanov, K. Coble, K. Claypool, R. H. Lee, H. Choi, and D. J. Prockop. Aggregation of human mesenchymal stromal cells (mscs) into 3d spheroids enhances their antiinflammatory properties. *P Natl Acad Sci-Biol*, 107(31):13724–13729, 2010.

[43] S. Sart, A.-C. Tsai, Y. Li, and T. Ma. Three-dimensional aggregates of mesenchymal stem cells: cellular mechanisms, biological properties, and applications. *Tissue Eng Part B-Re*, 20(5):365–380, 2013.

[44] Y. Yamakita, G. Totsukawa, S. Yamashiro, D. Fry, X. Zhang, S. K. Hanks, and F. Matsumura. Dissociation of fak/p130cas/c-src complex during mitosis: role of mitosis-specific serine phosphorylation of fak. *J Cell Biol*, 144(2):315–324, 1999.

[45] M. S. Croughan, J.-F. P. Hamel, and D. I. Wang. Effects of microcarrier concentration in animal cell culture. *Biotechnol Bioeng*, 32(8):975–982, 1988.

[46] J. Razungles, V. Cavaillès, S. Jalaguier, and C. Teyssier. L'effet warburg-de la théorie du cancer aux applications thérapeutiques en cancérologie. *M S-Med Sci*, 29(11):1026–1033, 2013.

[47] R. Cherry and E. Papoutsakis. Hydrodynamic effects on cells in agitated tissue culture reactors. *Bioprocess Eng*, 1(1):29–41, 1986.

[48] A. Nienow and R. Conti. Particle abrasion at high solids concentration in stirred vessels. *Chem Eng Sci*, 33(8):1077–1086, 1978.

[49] C. P. Peter, Y. Suzuki, and J. Büchs. Hydromechanical stress in shake flasks: correlation for the maximum local energy dissipation rate. *Biotechnol Bioeng*, 93(6):1164–1176, 2006.

Chapter 3

New knowledge and characterization of innovative microcarriers for the expansion of mesenchymal stem cells

Contents

Introduction

The objective of the INTERREG 'Improve-Stem' project is to innovate in the field of mesenchymal stem cell expansion processes by the development of new techniques improving their larger-scale expansion. Microcarriers with optimized surface properties for controlling the adhesion of stem cells, and a bioreactor specifically designed for their use in cell culture and with operating conditions adjusted for stem cell culture on microcarriers, are among the developed axes. Cell expansion will be monitored to ensure their quality, homogeneity and purity. This project is carried-out in the frame of a multidisciplinary consortium gathering keys skills in material science, bioprocess engineering and cell biology. The consortium organisation and key actions of this European project are presented in the figure 3.1.

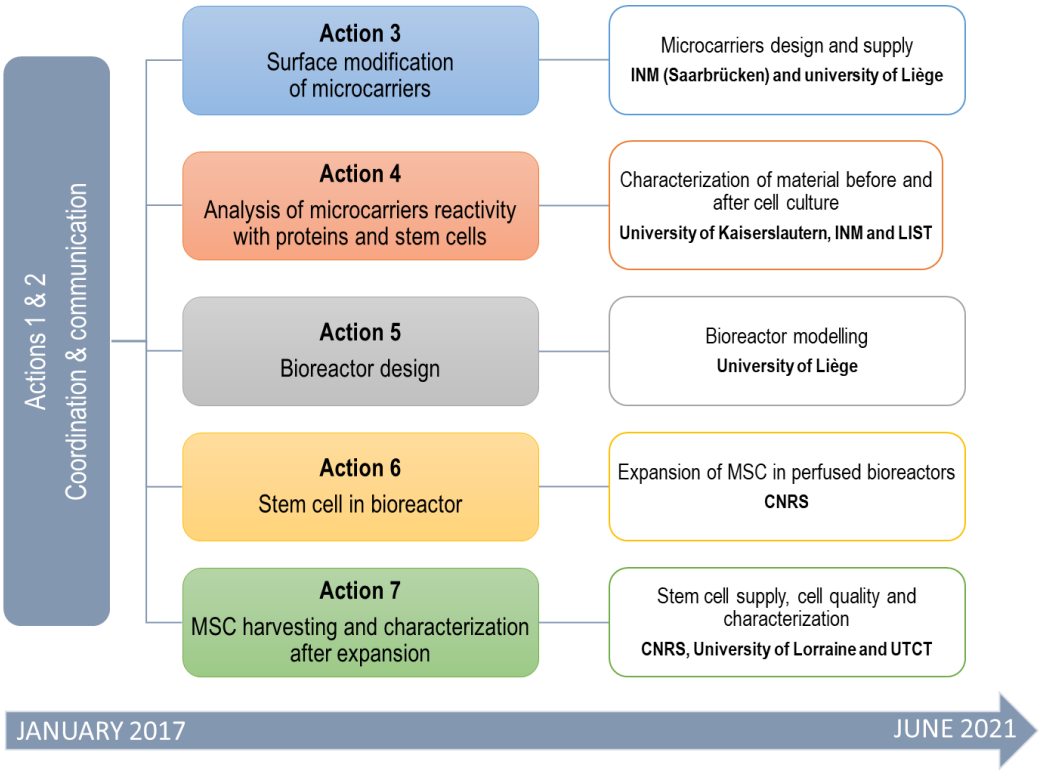

Figure 3.1 – Consortium organization and key actions in the frame of the INTERREG 'IMPROVE STEM' project.

More specifically, the performance of the microcarriers for MSC culture realized by the different scientific teams of the INTERREG project specialized in material sciences are presented in this chapter. As presented in the figure 3.2, the first part of this chapter is to study the different characteristics of the innovative microcarriers in terms of cell adherence and cell detachment. The second part of this chapter presents the expansion of WJ-MSC on the innovative microcarriers in fed-batch bioreactors. Thus, the aim of this chapter is to optimize the WJ-MSC expansion in stirred tank bioreactors by determining the most adaptive set of operating conditions and microcarrier chemistry by integrating the strategy developed in the previous chapter.

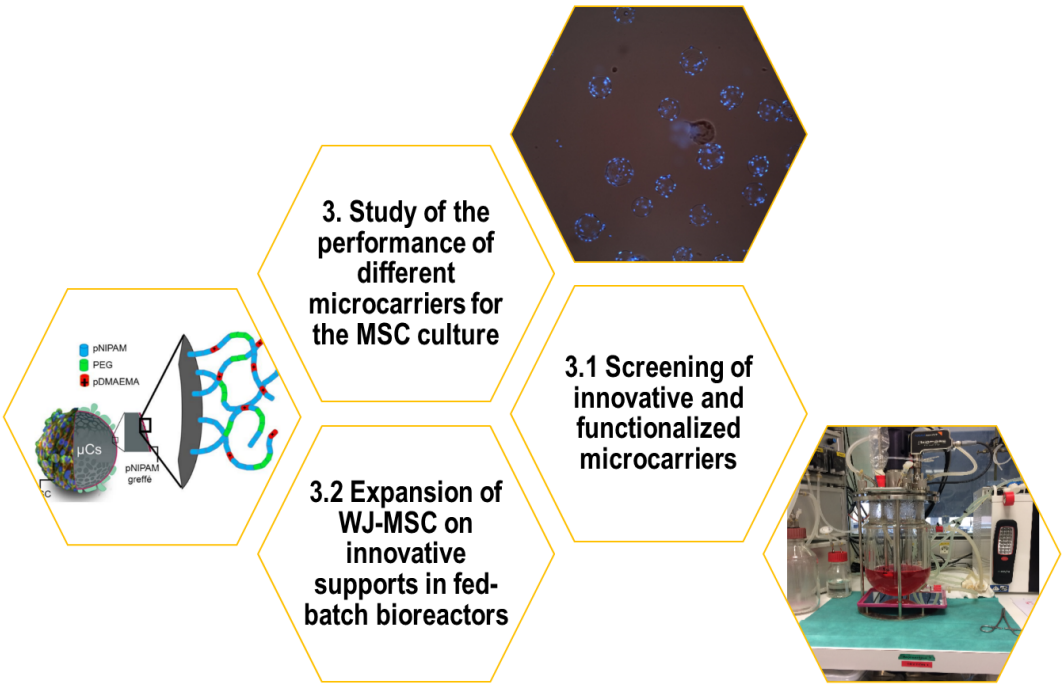

Figure 3.2 – Presentation of the different sections of chapter 3 dedicated to the characterization of microcarriers in dynamic cultures.

3.1 Screening of innovative and functionalized microcarriers performance for small scale cultures of MSCs

As part of the INTERREG project, collaborations have been set up between teams specialized in materials science and teams specialized in cell culture and biology. Thus, one task of the project was to develop innovative surfaces dedicated to stem cell growth. According to the literature and previous PhD studies performed in the laboratory [1, 2], one of the main bottlenecks in stem cell culture process is cell detachment step from microcarriers. As previously developed in the bibliography, many protocols of detachment are available in literature and provide different efficiency rates. Based on previous laboratory results, significant limitations however remained in the use of Cytodex-1 due to the difficulty of cell detachment yields. Thus, teams of University of Liège and of Leibniz Institute for New Material (INM - Saarbrücken) developed smart surfaces to enhance either cell adhesion or cell detachment.

From the list of commercial available microcarriers, all the materials including animal components were excluded. Based on the experience of the group of Nancy, polystyrene based microcarriers (called PlasticPlus) and Cytodex-1 microcarriers appeared to be the better choice of microcarriers to be modified for further studies. The first step of the microcarrier surface improvement was based on a surface activation, either by an organic chemical grafting with pNIPAM (University of Liège), or by a plasma activation (INM). Then, the functionalization could be carried-out, by grafting a zwitterionic polymer layer or adhesive ligands respectively.

Material and Methods

Preparation of pNIPAM microcarriers by University of Liège

Commercial Cytodex-1 microcarriers were activated by grafting a bromide group (2-bromo-2-methyl propionyl bromide - BMBP) on alcool group of dextran in the presence of triethylamine. XPS measurements permitted to check the good activation of the Cytodex-1. Then a layer of NIPAM was grafted on the activated microcarriers. This NIPAM polymerization was carried-out in presence of copper bromide as a catalyst and of the bipyridine, as a ligand. Finally, cytotoxicity and proliferation assays on functionalized Cytodex-1 were carried-out during fibroblast L929 culture.

Preparation of functionalized microcarriers by INM

The first activation of commercial microcarriers is based on a plasma activation. This plasma activation method has the advantage of being considered as universal. PlasticPlus and Cytodex-1 microcarriers were inserted into an oxygen plasma chamber and exposed to plasma for two minutes, in order to oxidize molecular species of the surface, becoming hydrophilic and reactive. Then, the surfaces were functionalized in an aqueous solution of triethoxyaminopropylsilane (APTES). The amine groups were thus removed from the microcarriers surface to favor stem cell adhesion.

Preparation of screening in microwell-plates

In order to evaluate cytotoxicity, attachment and detachment efficiencies of functionalized microcarriers, cultures were carried-out with WJ-MSC using 6 well-plates ultra-low attachment (Corning CLS3471). Functionalized microcarriers were prepared according to the instructions of the teams who provided the beads. They were loaded in the wells at a concentration of 2.35 g L^{-1} and 25 g L^{-1} for Cytodex-1 and PlasticPlus microcarriers respectively, rinsed with cell culture medium, and incubated at 37°C and 5 % CO_2 in cell culture medium. After seeding cells at a cell density of 15,000 cells cm^{-2}, 6-well plates were agitated after one hour without agitation in the incubator. Then, after 24 h, cell adherence was evaluated by DAPI staining and microscopic observation. The percentage of initial adherence was calculated thanks to the cell counting Matlab program used in the previous chapter. After two days of culture, the cell detachment was tested and evaluated.

Cell detachment

The protocol of cell detachment was based on the protocol developed by Nienow *et al.* [3]. The cell culture medium was withdrawn, the microcarriers and cells were rinsed with PBS. Then 2.5 mL of TrypLE was added in each well and incubated 5 minutes and agitated at 70 rpm. To stop the action of TrypLE, cell culture medium containing HPL was added (2.5 mL) before to filter the cells and microcarriers suspension through stainer (70 µm). Detached cells were then counted with an automatic cell counter (ViCell Beckman). In order to evaluate cell detachment efficiency, microcarriers were stained with DAPI, before and after cell detachment, cells were counted by using

the algorithm developed in the previous part. The percentage of detachment was then calculated comparing the total number of cells before and after cell detachment.

Scanning Electron Microscopy

This part of analysis was carried-out by INM team. Samples were prepared as follow. First, they were fixed (in glutaraldehyde for example), then dehydrated by successive baths in ethanol with increasing concentration. After the dehydration step, samples were dried and coated by gold or platinum, and finally visualized by SEM.

Confocal imaging

This analysis was also performed by INM team. During the culture, 200 µL of samples were taken and fixed with 4 % (v/v) paraformaldehyde (PFA) at room temperature. After three washing steps with PBS, samples were permeabilized using 500 µL of 0.5 % Triton x-100 buffer for 10 minutes. Then the buffer was removed, and 500 µL of blocking solution (0.1 % Triton x-100, 5 % BSA in PBS) was added for 20 minutes, followed by addition of staining solution. The 200 µL actin staining was prepared by mixing 1:1000 anti-vinculin (Merck) in blocking buffer. Samples were incubated for 1 hour at room temperature, and after PBS washing, the secondary antibody (goat anti-mouse Alexa 647) was added for one hour. After several washing steps, DAPI (1:1000) was added for 5 minutes. Finally, samples were either visualized or stored at 4°C until use.

3.1.1 Evaluation of cell attachment and detachment efficiencies of the innovative microcarriers

First, cell adhesion was evaluated for each functionalized microcarrier and compared to commercial Cytodex-1 or commercial PlasticPlus microcarriers as controls. The best cell attachment was obtained for the candidates without plasma treatment and with APTES Cytodex-1 (w/o-pl + APTES Cytodex-1) and with plasma treatment and with APTES Cytodex-1 (w-pl + APTES Cytodex-1) ; these microcarriers seemed to allow an improvement in cell attachment (+30 %) in comparison with the commercial Cytodex-1 (Figure 3.3 A).

According to the figure 3.4 A, the DAPI staining highlighted that almost all the microcarriers were well covered by cells. It was also noticed that some debris of microcarriers were present when Cytodex-1 grafted with silane were used and could have a negative impact on cell viability. A choice of a high initial cell density was made in order to have a representative cell population on the microcarriers after three days of culture, in order to properly assess cell detachment performance.

Concerning the PlasticPlus based microcarriers, the surface modifications seemed, in both cases, to improve the percentage of initial attachment, becoming equivalent to the percentage of initial cell attachment on commercial Cytodex-1 (60 %) (Figure 3.3 B). However, standard deviation of percentage values measured of cell attachment were high for (w-pl + APTES) and (w-pl + Si)-PlasticPlus. It was certainly due to the cell counting method and the nature of the microcarriers

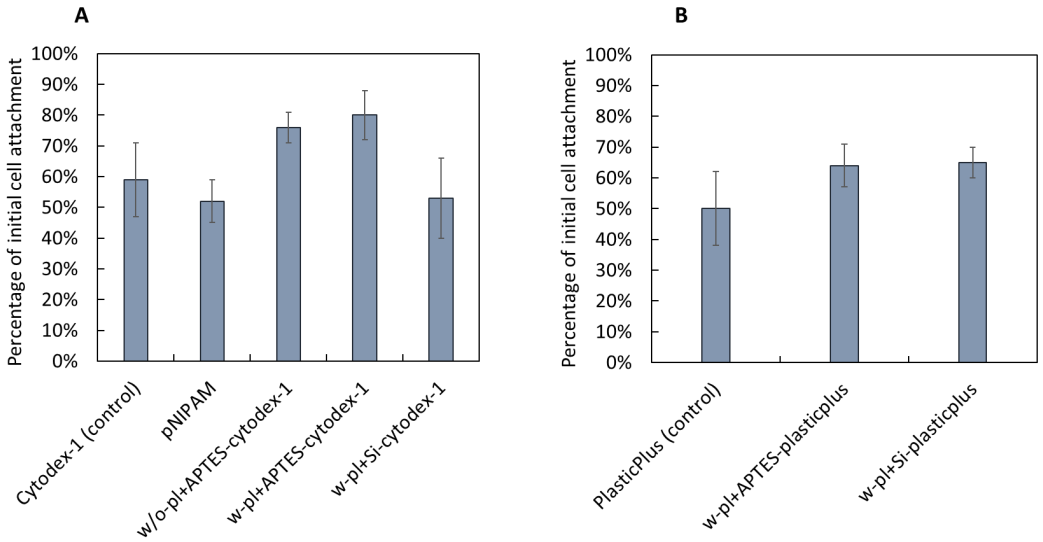

Figure 3.3 – Evaluation of initial cell attachment yield on innovative microcarriers cultivated in well-plates. (A) Percentage of initial cell attachment on Cytodex-1 modified microcarriers. (B) Percentage of initial cell attachment on PlasticPlus modified microcarriers after one day of culture. Term of w/o-pl+APTES signifies that microcarriers were treated without plasma treatment then grafted with APTES. Term of w-pl+APTES signifies that microcarriers were treated with a plasma treatment then grafted with APTES.

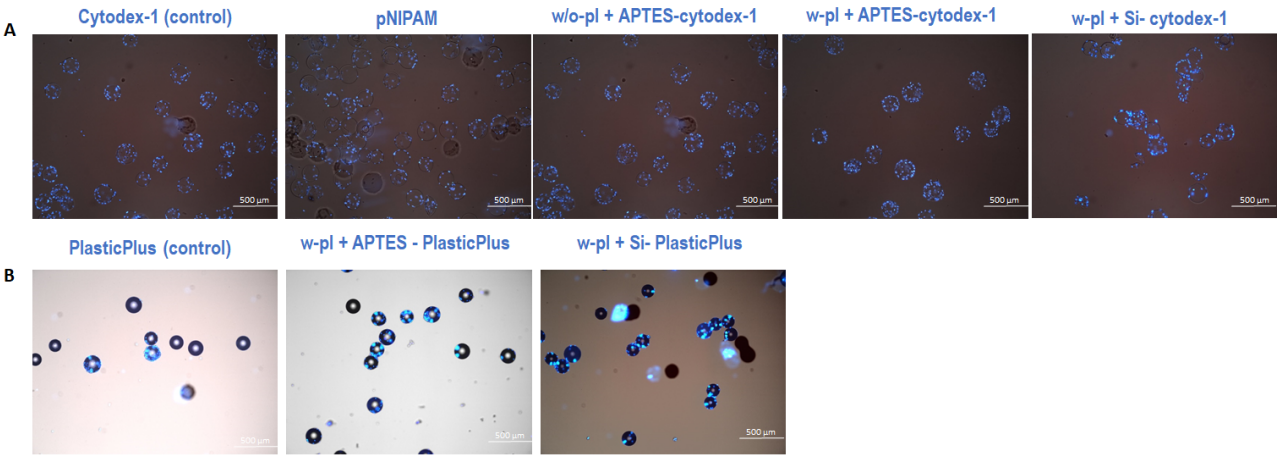

Figure 3.4 – DAPI staining of cells attached on home-made microcarriers. (A) On Cytodex-1 modified microcarriers after one day of culture. (B) On PlasticPlus modified microcarriers. Term of w/o-pl+APTES signifies that microcarriers were treated without plasma treatment then grafted with APTES. Term of w-pl+APTES signifies that microcarriers were treated with a plasma treatment then grafted with APTES.

which were not transparent. Moreover, DAPI staining underlined the improvement of cell adhesion confered by the chemical modification of the microcarriers. Indeed, only few empty particles could be observed on the pictures (Figure 3.4 B).

After the evaluation of cell attachment on the modified microcarriers, the cell detachment was also quantified. After one more day of culture under agitation, cells were detached according to the protocol described in material and methods section. Only the pNIPAM carriers were detached according to a shift of temperature, from 37°C to 20°C. The supernatant was removed, then cells were washed with PBS, and cold medium was directly added into the six well plates. The plate was agitated at 20°C during 1h30. After cell detachment, pictures were taken with DAPI stain-

ing in order to calculate the efficiency of cell detachment ; the viability after cell detachment was also determined. The addition of APTES or silane on Cytodex-1 did not seem to improve the cell detachment, but rather improve cell attachment. However after tryspination, a good cell viability of 90 % approximately was observed, excepted for Cytodex-1 grafted with silane (60 %), and pNIPAM-Cytodex-1 (25 %) (Figure 3.5 A). In addition for pNIPAM-Cytodex-1, it seemed that the effect of temperature alone did not permit to detach cells efficiently and had a negative impact on cell viability (Figure 3.5 A).

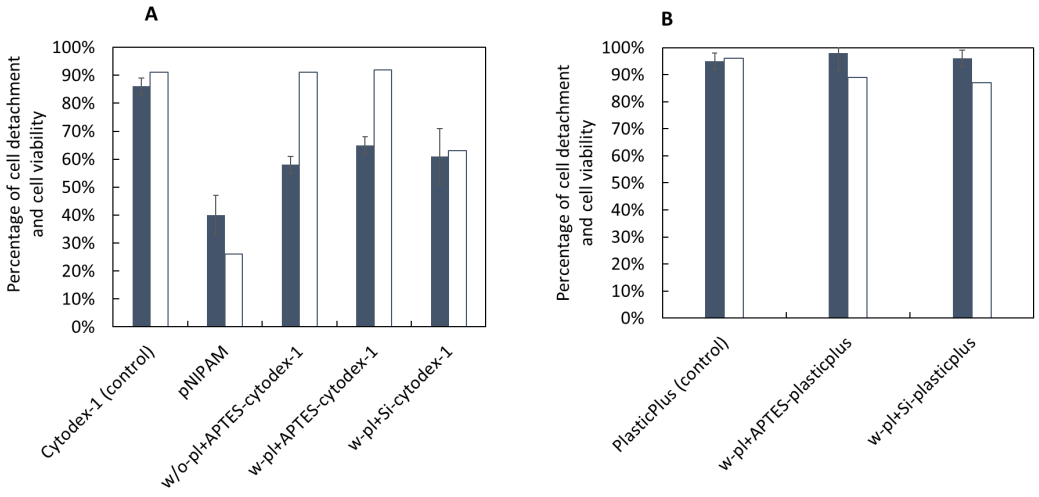

Figure 3.5 – Evaluation of cell detachment (black bars) and cell viability (white bars) on home-made microcarriers for MSC expansion cultivated in well-plates. (A) Percentage of cell detachment on Cytodex-1 modified microcarriers. (B) Percentage of cell detachment on PlasticPlus modified microcarriers after two days of culture. Term of w/o-pl+APTES signifies that microcarriers were treated without plasma treatment then grafted with APTES. Term of w-pl+APTES signifies that microcarriers were treated with a plasma treatment then grafted with APTES.

DAPI staining (Figure 3.6 A) showed that cells remained attached on the modified microcarriers despite the step of detachment, suggesting that surfaces modifications that favored cell adhesion, did not completely solve the difficulties concerning cell detachment. However, the pNIPAM microcarriers could still be further developed, despite the low viability rate post detachment. The action of an enzyme coupled to the decrease of temperature may indeed have a positive impact on cell detachment and cell viability.

The microcarriers allowing the best cell detachment efficiency were made of PlasticPlus microcarrier basis (treated polystyrene based microcarrier) (Figure 3.5 B). For all these three conditions, the best detachment yield and post-detachment viability were obtained, as verified by DAPI staining (Figure 3.6 B) showing that all PlasticPlus based microcarriers were deprived of cells.

In conclusion, after analysis of these different results, the choice was made to quantity the efficiency of the following microcarriers in bioreactors: pNIPAM-cytodex-1, w-pl + APTES cytodex-1 (with APTES treatment), and (w-pl + Si)-PlasticPlus (with silane addition) microcarriers. However, before that, cell behavior on commercial microcarriers had to be studied first.

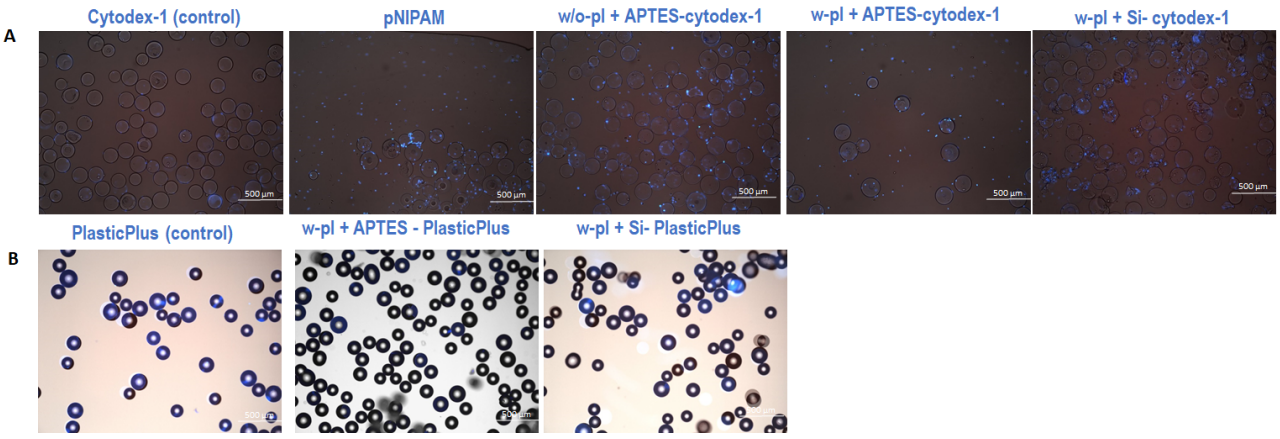

Figure 3.6 – DAPI staining of cells after the detachment step (A) on modified Cytodex-1, (B) on modified PlasticPlus microcarriers. Term of w/o-pl+APTES signifies that microcarriers were treated without plasma treatment then grafted with APTES. Term of w-pl+APTES signifies that microcarriers were treated with a plasma treatment then grafted with APTES.

3.1.2 Imaging of microbeads recovered by WJ-MSCs

In this part, correlative scanning electron microscopy (SEM) and fluorescent microscopy were carried-out by the INM laboratory. Images obtained are only qualitative but they give a good overview of the cell behavior adhered on the different microcarriers. Microscopy experiments were carried-out only with Cytodex-1, pNIPAM and PlasticPlus + fibronectin microcarriers. Ac-

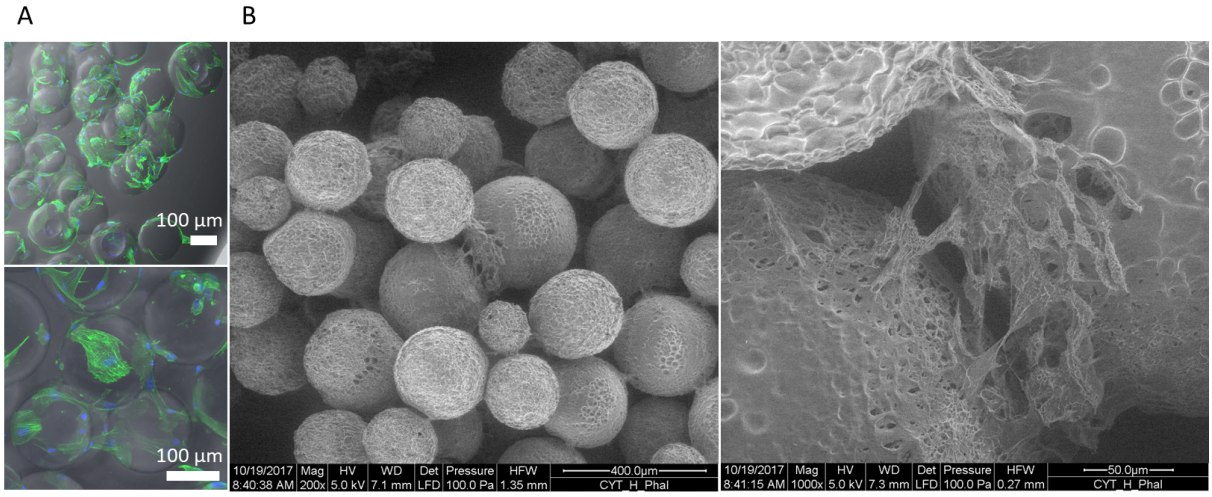

Figure 3.7 – Images of Cytodex-1 microcarriers with WJ-MSCs. (A) Confocal imaging with actin fibers stained in green and cell nuclei stained in blue by DAPI. (B) SEM imaging at magnifications of 200x (left) and 1000x (right).

cording to the figure 3.7 A it appeared that cells were able to densely colonize the Cytodex-1 microcarriers. No single particles without cells were detected. Moreover, cells formed good attachments observed in their size, with presence of actin cytoskeletal fibers. In addition, SEM images (Figure 3.7 B) showed a dense population of cells making bridges between the microcarriers.

According to the figure 3.8, and similarly to Cytodex-1, pNIPAM microcarriers were densely covered by MSC. Only a few empty single particles were observed. Cells seemed also to form strong attachment links, as demonstrated by the presence of actin cytoskeletal fibers. Such attachment

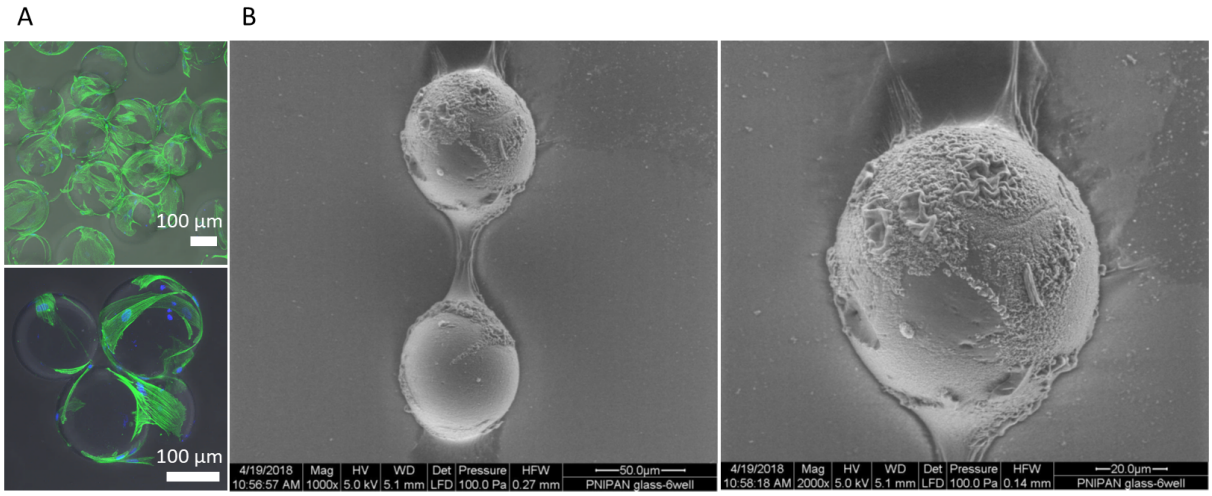

Figure 3.8 – Images of pNIPAM microcarriers with WJ-MSCs. (A) Confocal imaging with actin fibers stained in green and cell nuclei stained in blue by DAPI. (B) SEM imaging at magnifications of 1000x (left) and 2000x (right).

in terms of cell size and stress fibers would appear even stronger when compared to Cytodex-1 microcarriers. SEM images were difficult to obtain due to the shrinkage of the microcarriers during the dehydration protocol, resulting in the deformation of cells morphology.

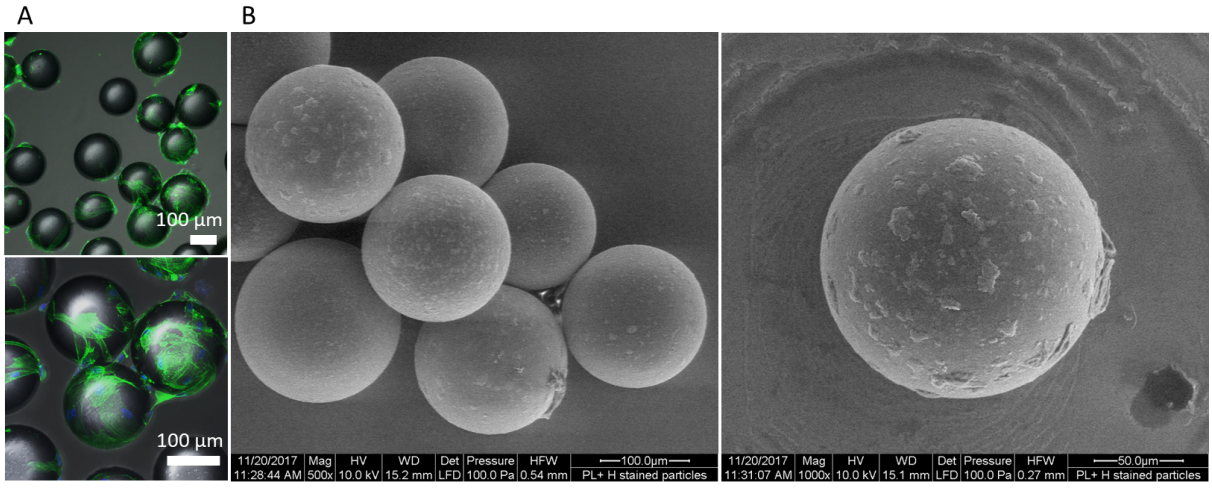

Figure 3.9 – Images of PlasticPlus microcarriers with WJ-MSCs. (A) Confocal imaging with actin fibers stained in green and cell nuclei stained in blue by DAPI. (B) SEM imaging at magnifications of 500x (left) and 1000x (right).

Cells adhered on raw PlasticPlus microcarriers were also imaged by confocal microscopy and SEM. It appeared that the area occupied by cells were restricted to few particles, some others were empty, and, on the others, cells formed bridges (Figure 3.9 A and B). It was also possible to detect some cells nuclei without cell body, meaning a cell death occurred.

According to the figure 3.10 A, cells spread widely over PlasticPlus microcarriers coated with fibronectin with formation of rich actin stress fiber. However, cells were rarely found on single microcarriers, as they were mostly bridging over multiple microcarriers, as shown on SEM images (Figure 3.10 B). Therefore, it can be concluded that the coating of PlasticPlus microcarriers with fibronectin qualitatively improved cell adhesion and cell spreading. Finally, images permitted to

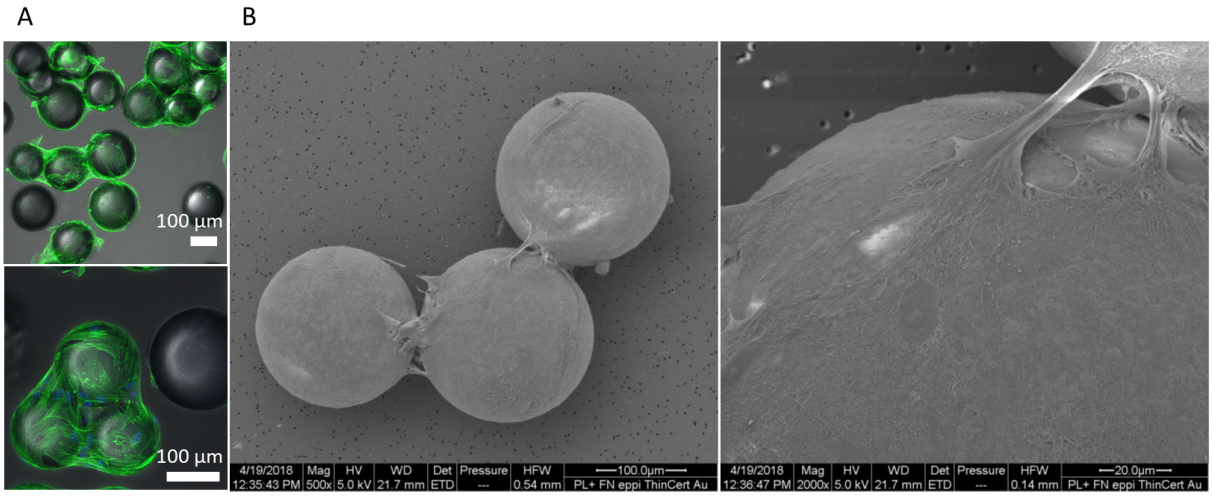

Figure 3.10 – Images of PlasticPlus microcarriers coated with fibronectin and with WJ-MSCs. (A) Confocal imaging with actin fibers stained in green and cell nuclei stained in blue by DAPI. (B) SEM imaging at magnifications of 500x (left) and 2000x (right).

have an overview of cell behavior on different microcarriers. Organization of actin fibers, formation of bridges between several microcarriers and cell spreading are valuable information permitting to choose the best candidate among all the microcarriers. Thus, it appeared that cells attachment and cell behavior were apparently more efficient on modified microcarriers such as pNIPAM microcarriers and PlasticPlus microcarriers coated with fibronectin compared to Cytodex-1 and PlasticPlus without coating, respectively.

In the rest of the study, expansion of WJ-MSCs in stirred tank bioreactors will be carried-out on Cytodex-1 and PlasticPlus coated with fibronectin as commercial references, and on pNIPAM and PlasticPlus grafted with silane as home-made references. This part will be the subject of a publication, which will be submitted to Journal of Biotechnology.

3.2 Expansion of Wharton's jelly mesenchymal stem cells cultivated on innovative microcarriers in fed-batch bioreactors

Expansion of Wharton's jelly mesenchymal stem cells cultivated on innovative microcarriers in fed-batch bioreactors

C. Sion, M.K. Wlodarczyk-Biegun, D. Ghannoum, R. Vandeberg, D. Doblas-Jimenez, S. Ramesh, F. Gallo, T. Kraus, C. Grandfils, N. De Isla, E. Guedon, I. Chevalot, D. Toye, E. Olmos

Abstract

In the last decades, mesenchymal stem cells (MSCs) have been studied as promising tool for cell-based therapies. Wharton jelly mesenchymal stem cells (WJ-MSCs) represent an attractive source of MSCs because of the lack of ethical concerns and non-invasive collection procedures. Clinical therapies require generally billion or trillion cells dose delivered repeatedly and frequently. It is therefore crucial to develop scalable and efficient method of WJ-MSCs production to meet the demand while maintaining the inner characteristics of the cells defined by the international society of cell therapy (ISCT). The aim of this study was to characterize functionalized home-made and commercial microcarriers for specific culture of WJ-MSCs. In this work, WJ-MSCs cultures in spinner vessels (batch mode) and in stirred tank bioreactors (fed-batch mode) were run in order to compare the impact on cell expansion of four different types of microcarriers: Cytodex-1 and PlasticPlus (commercial) and pNIPAM coating grafted on Cytodex-1 and PlasticPlus with silane (home-made). The specificity of the fed-batch mode proposed in the study is the addition of fresh microcarriers extended to different type of microcarriers, home-made and commercial. Finally, a detailed analysis of cell performance (including cell shape, size and distribution) was conducted, to understand the link between the material and cell behaviour in agitated cell cultures.

Key words: *Umbilical mesenchymal stem cells* / *Microcarriers* / *Stirred tank bioreactors* / *Fed-batch modes* / *Microscopy* / *Marker expression.*

Introduction

In recent years, improvement in cell therapy permitted to explore potential of mesenchymal stem cells as promising candidates for cell therapy. Wharton jelly mesenchymal stem cells (WJ-MSC) are not embryonic stem cells nor non-adult stem cells but they exhibit properties of both types, and thus could provide a useful source for therapeutic clinical trials [4]. Moreover, WJ-MSC are mostly promising by the abundance of the cell source and the lack of ethical concerns [5]. Planar multilayer flasks are currently most often applied for the commercial production of WJ-MSC [6]. However, these systems of cell culture present numerous drawbacks as there are time-consuming, present high risks of contamination due to handling multiple flasks and also various difficulties in controlling the parameters of cultures. Bioreactors systems appear more adapted thanks to their ease to scale-up, the possible monitoring and the limitation of nutrient concentration gradients. Different types of bioreactors systems exist: (i) non instrumented as spinner vessels [7, 8, 9, 10]

or Erlenmeyer's flasks [11, 12], (ii) instrumented bioreactors from small scale (15 mL up to 0.25 L) to benchtop scale (1.5 up to 2.4 L). In MSC cultures, to the knowledge of the authors, the maximal scale reached was 50 L [13]. MSC cultures, and in particular WJ-MSC cultures require specific surfaces of growth such as microcarriers that have already been established as the most reliable technical mean from a scale-up point of view. Moreover, growth surface can be easily extended by addition of fresh microcarriers [9, 14, 15]. Microcarriers can differ in size (90-380 µm), core material (polystyrene, dextran, and gelatine), and coating. It is therefore important to choose the most appropriate microcarrier for a given cell source, among the numerous existing microcarriers. Modification through incorporation of chemical groups is also often applied on the microcarriers to improve adherence, growth or detachment. The most common modification is based on the addition of amino-groups (-NH_2) to improve cell adhesion, as it is the case for commercially Cytodex-1 & 2 and for Hillex II [16]. It has been shown that addition of (-NH_2) groups promotes MSCs proliferation, spreading and also osteogenic state. An enhanced chondrogenesis and a lowered MSCs spreading have been observed with surfaces with a high concentration in carboxyl groups (-COOH) [17]. Additionally, they enhance cell adhesion by increasing hydrophobicity of the surface. Different methods of modification can be used such as ultra-violet (UV) treatment or a combination of UV and ozone plasma treatment [16]. Other modifications are based on specific coating with extracellular matrix proteins, but a higher cost may be expected. Finally, beyond surface modifications, stiffness also affects the cell growth and differentiation. It has been shown that increased matrix stiffness (i.e. 34 kPa) promotes spindle-like shape, and osteogenic state by activating RhoA/Rock signalling [18]. On the other hand, soft matrix (i.e. 1 kPa) encouraged chondrogenic, adipogenic or neuronal differentiation [19]. Cell adhesion and detachment are major critical steps that may influence final quantity and quality of culture on microcarriers. In recent years a high number of commercial microcarriers were already implemented in spinner vessels, as for example Cultispher-G [20], Plastic Plus [8], and Plastic [21] with Bone Marrow Mesenchymal Stem Cells (BM-MSC) or WJ-MSC. In addition, some of the microcarriers such as, Plastic P-102L [22], Cultipsher-G [23], and Cytodex-1 [24], have already been used in stirred tank bioreactors. In most of these studies, the culture time was around 6 or 8 days, and the culture ended due to the limitation of the surface of growth, because cells on microcarriers reached confluence. As the cells are the final product of the process, cell detachment and quality approval of the detached cells were also important bottlenecks of the upstream process. According to Jossen *et al.* [25], these unsolved bottlenecks could be a reason why MSC cultures are still limited to 150-200 L per batch. Nowadays, cell detachment is mainly performed using proteolytic enzymes and requires filtration steps after detachment. The use of proteolytic enzymes may also negatively impact cell quality. Therefore, microcarriers that permit cell detachment by applying shift of temperature or pH, were developed. Their functionalization was performed by grafting chemical layers that were sensitive to physicochemical changes in the cell environment. Some authors described a new bio-degradable microcarrier used for BM-MSC culture made of polycaprolactone and coated with ECM proteins [26]. Microcarriers modified with a specific layer made of poly N-isopropylacrylamide (pNIPAM), which is a repeated chain of hydrophilic amide and hydrophobic

isopropyl groups, were also reported. The layer is thermoresponsive: at the temperature above 32°C, the pNIPAM layer takes a globule form, suitable for cell adhesion, at the temperature below 32°C, the layer takes a swelled shape which cause cell detachment [27]. This thermo-sensible polymer layer was conjugated with a cell adhesive motif and used for chondrocyte culture surface in the work of Kim *et al.* in 2002 that described the ability of this substrate to a reversible swell around 32°C, inducing chondrocytes detachment [28]. Yang *et al.* (2010) reported a successful coating of Cytodex-3 microcarriers with pNIPAM allowing human bone marrow mesenchymal stem cells to adhere, grow and spread in spinner flasks in the same way as on non-grafted microcarriers [29]. In addition of the ease of detachment by the shift of temperature, authors also demonstrated a reduction of apoptosis and cell death using this strategy instead of proteolytic enzymes. Till now, this approach of grafting sensitive polymer layer has been applied to other type of microcarriers such as dextran, glass, polystyrene, for example [30]. However, cytotoxicity and functionality test controls must be performed to ensure that no changes in cell quality were induced due to the physiochemical stimuli used for detachment. It is known that microcarriers can regulate MSCs proliferation and differentiation through the modulation of cell morphology and cell organization [18]. However, complementary works are still necessary to address the full characterization of microcarriers and their impact on MSCs in microcarrier-fed cultures. Therefore the aim of the present work was firstly to compare WJ-MSC culture performance in terms of expansion and cell detachment efficiency, on different types of commercial and homemade microcarriers in stirred tank bioreactors with addition of microcarriers during the culture. The second objective was to analyze the cellular shape and to quantify the formation of cell-microcarriers clusters in function of the studied microcarriers in stirred tank bioreactors. Lastly, the influence of the microcarrier type was evaluated on the cell behavior (including cell shape, size and cluster formation) and on the biological characteristics of WJ-MSC cultivated in stirred tank bioreactors.

Material and Methods

Cell extraction and primary cell culture of WJ-MSC

Umbilical cord stem cells were extracted from fresh umbilical cords of just born babies at the 'Unité de Thérapie Cellulaire et banque de Tissus (UTCT)' (CHU Nancy). Umbilical cords were treated during 24 h following the birth. The method of extraction was non-enzymatic using cells spontaneous migration on the 175 cm^2 plastic culture flask [31]. The cell culture medium was alpha-minimum essential medium (α-MEM medium) (Lonza BE12-169F), supplemented with 5 % of Human Platelet Lysate (HPL) (Cook Regentec PL-NH-500), 4 mM glutamine (Sigma G7513), and 1 % antibiotics (Antibiotic antimycotic solution, Sigma A5955). The medium was changed twice a week. After two weeks, cord pieces were removed, and the remaining adherent cells were trypsinized and seeded in new 75 cm^2 T-flasks at a density of 1000 cells cm^{-2}. After one supplementary passage, WJ-MSC were pooled and cryopreserved at a concentration of 2 x10^6 cells mL^{-1}, in fetal bovine serum and 10 % of dimethyl sulfoxyde (DMSO) for cell banking and kept in liquid nitrogen. Thereafter, cells were thawed and seeded at a concentration of 1000 cells cm^{-2} in T-75

cm^2 and cultivated for a week before their use in dynamic conditions. All the cells were used at the same passage (passage 4) in the stirred tank bioreactors for all the conditions tested.

Microcarriers preparation

Different microcarriers were used during this study, commercial microcarriers and home-made microcarriers. They are listed in Table 3.1.

Table 3.1 – Characterisation of the microcarriers used during the study

Name	Abbreviation	Surface	Core material	Density (g mL^{-1})	Manufacturer
Cytodex-1	Cy-1	Hydrophilic DEAE exchanger	Crosslinking dextran	1.03	GE Healthcare
Cytodex-1 - pNIPAM	Cy-p	Hydrophilic DEAE exchanger	pNIPAM	1.02	Present study
Plastic Plus	P+ - FN	Polystyrene	Fibronectin	1.02	Solohill
Plastic Plus - Silane	P+ - Si	Polystyrene	Silane	1.02	Present study

Cy-1 microcarriers (GE Healthcare) were preliminary hydrated at a concentration of 20 g L^{-1} in phosphate buffer saline (dPBS, Sigma D8537), autoclaved and then rinsed with cell culture medium. Whereas, PlasticPlus (Solohill Pall) were hydrated in ultrapure water at 100 g L^{-1}, autoclaved, rinsed with sterile ultrapure water, and coated with fibronectin at 16 µg mL^{-1}.

Cy-p microcarriers preparation: Grafting of N-isopropylacrylamide (NIPAM) onto activated microcarriers was conducted in accordance with the relevant literature [32], as follows. The synthesis of pNIPAM-microcarriers was carried-out by a two-step reaction. All glassware was siliconed prior to synthesis. Cy-1 microcarriers (1 g) were dried at 80 °C before activation. Dried microcarriers were then transferred to stirring reactor containing 40 mL of the dried activating solvent (i.e. DMSO, MeCN, MeCN-PC, THF or Cyclohexane) and triethylamine (2.67 mmol) and equilibrated for 1 hour. The initiator, 2-bromopropionyl bromide (2.175 mmol) was added dropwise to the microcarriers suspensions (Cy-1 + Br) and stirred at room temperature for 1 hour. Then, washings were performed: once with activation solvent, three times with methanol and once with diethylether. Cy-1 + Br were finally dried under air flow. After the activation step, Cyt-Br (0.2 g) were transferred and equilibrate for 1 hour in a stirring reactor containing a mixture of MeOH and Water (2:1 v/v) previously purged with nitrogen-vacuum cycling prior to polymerization. Then, NIPAM (40 mmol), CuBr (0.14 mmol) and HMTETA (0.18 mmol) were added to the reactor and the mixture was purged with nitrogen for 30 min. ATRP reaction on Cyt-Br was allowed to continue for 24 hours. Finally, resulting Cy-p microcarriers were washed with EDTA (50 mmol) for 24 hours, three times with methanol and once with diethylether. Cy-p microcarriers were finally dried under air flow.

P+-Si microcarriers preparation: One gram of Plastic Plus polystyrene microbeads was uniformly distributed on a glass dish forming a thin layer to avoid overlapping. The crystallizer was placed in an oven for an oxygen plasma treatment at 0.3 mbar for 1.5 minutes. Microbeads were then rapidly transferred to a glass beaker with 80 mL of milli-Q water and 3-(Triethoxysilyl)propio nitrile 0.5 mM (Sigma-Aldrich). The mixture was stirred for 24 hours in an orbital shaker at low speed to minimize the number of collisions between microbeads. After stirring, the supernatant was removed with a syringe and microbeads were washed twice with milli-Q water.

All the microcarriers, before use with cells, were incubated in cell culture medium for one hour at a temperature of 37°C and 5 % CO_2.

WJ-MSC inoculation on microcarriers in Spinner vessels and in stirred tank bioreactors

In this study, different types of microcarriers were investigated, mainly composed of dextran or polystyrene. They will be refereed as 'Cytodex-1 types', regrouping, Cy-1 and Cy-p microcarriers. The others as P+-FN and the P+-Si will be refereed as 'PlasticPlus types' microcarriers. According to manufacture indications, 0.3 g and 3 g of Cytodex-1 types and PlasticPlus types microcarriers were prepared in cell culture medium and let one hour at 37°C and 5 % CO_2 in the incubator. The cultivated WJ-MSC were trypsinized and seeded on the microcarriers with a cell density of 9000 cells cm^{-2}, in a final volume of 200 mL in spinner vessels (SV). After one hour in static condition, cultures were agitated at 40 rpm using magnetic stirring in spinner vessels (SV). Overnight cultures were transferred into stirred tank bioreactor (STR) (Tryton, Pierre Guerin) with the same amount of empty microcarriers (0.3 g for Cytodex-1 types and 3 g for PlasticPlus types microcarriers). The volume of the stirred tank bioreactor (STR) was completed to 500 mL. The cells attached on the initial microcarriers and the new empty microcarriers settled for one hour, then an intermittent agitation at 70 rpm was applied, then stopped for one more hour. Finally, a continuous agitation at 70 rpm was set.

Cell expansion in pH and [O_2] controlled stirred tank bioreactor

Based on the previous studies [24, 23, 22], pH was adjusted to 7.4 and dissolved oxygen concentration to 20 % of air saturation, to provide optimal culture conditions. The pH adjustment was performed by addition of base (NaOH 0.1 M) or by CO_2 injection in the headspace of the bioreactor. Dissolved oxygen concentration was maintained by headspace flushing of nitrogen (N_2) and oxygen (O_2). Agitation rate was adjusted to 70 rpm in order to reach the just-suspended state, with an axial impeller HTPG. The temperature was controlled to 37°C using a hot water jacket. Cultures were daily visually monitored under a microscope for cell counting, and to characterize cell viability, and spreading. Based on these observations, additions of fresh microcarriers were controlled in order to maintain the cell number per microcarrier around 6 or 7. Microcarriers were added suspended in 200 mL of cell culture medium. After microcarrier and cell culture medium addition, the agitation was stopped for one hour in order to favour cell migration. Then, agitation was re active for 10 minutes and stopped for one more hour. Finally, a continuous agitation at an agitation rate of 70 rpm was set-up.

Fluorescent staining of WJ-MSC on microcarriers

The number of cells in the stirred tank bioreactors was quantitatively determined with DAPI staining. Every day, three samples of 500 µL were taken from the bioreactor. The supernatant was discarded and 500 µL of DAPI (1 µg/mL) (Sigma 10236276001) prepared in methanol was added to the cells on microcarriers. After fifteen minutes of incubation protected from the light, samples were

washed with PBS and observed by epi-fluorescence microscopy. Six different microscopic fields were chosen per sample and for each field two pictures were taken: one with the bright filter and the other with the fluorescent filter. The viability was determined using a Live/Dead staining (Calcein AM/ Ethidium Homodimer, Life Sciences, ThermoFisher). The supernatant was discarded and the samples were incubated with 3 µM of calcein AM and 3 µM of ethidium homodimer-1 for thirty minutes in the dark at 37 °C and 5 % CO_2. Samples were then visualized on a Leica LEITZ DMR epi-fluorescence microscope. The automatic counting method described by Loubière *et al.* [33] was used to determine cell distribution on microcarriers, the average number of cells per microcarrier and the total cell number. The maximal growth rate (μ_{max}) was estimated from the slope and the best-fitting line of the logarithm of cell number versus time during the exponential phase.

WJ-MSC immunostaining

Samples taken at different moments of culture were fixed with 4 % (v/v) PFA at room temperature (RT), and rinsed 2-3 times in PBS for 5-10 min (to remove PFA). Washed samples were permeabilized with 500 µL of 0.5 % Triton X-100 for 10 minutes. After removal of Triton X-100, 500 µL of blocking solution (0.1 % Triton X-100, 5 % BSA in PBS) were added for at least 20 minutes. Next, the blocking solution was removed, and the samples were incubated in actin staining solution at RT for 1 hour or at 4°C overnight. The staining solution was composed of Phalloidin-Alexa 488 (1:200 dilution) in PBST (Triton X-100 0.1 % (v/v) and BSA 5 % (w/v) in PBS). After 2 washes with PBST and 1 wash with PBS, samples were incubated in DAPI (1:1000 dilution in PBS) for 5 minutes, and washed 3 times in PBS again. Such prepared samples were imaged directly or stored at 4°C until use.

For imaging, a Nikon Ti-Ecllipse (Nikon Instruments Europe B.V., Germany) was used, equipped with a Sola SE 365 II (Lumencor Inc., Beaverton, USA) solid state illumination device and an Andor Clara CCD camera for detection. Images captures at 4x magnification (in tailing mode, to include 100-300 particles) were used to estimate the clustering of the particles, *i.e.* number of particles visualized as a part of clusters of different sizes. Z-stack images captured at 20 x magnification (7-10 particles visualized per timepoint) were used to : (1) observe the shape of the cell, (2) calculate average area of the cell (calculated as a summed area of the cell bodies visible on the particle divided by the number of visible nuclei. Only cells fully visible on the particle were used for calculations), (3) calculate the average area of the particle occupied by the cells. Image analyses were performed with ImageJ software.

WJ-MSC metabolite analysis

Analysis of glucose, lactate and lactate dehydrogenase (LDH) concentrations in the medium were performed using the Gallery multiparametric analyzer (Thermo Fisher Scientific). Specific metabolite consumption/production rates (q_{Met}) were calculated for every exponential phase interval with the following equation 3.1:

$$q_{\mathrm{M}et} = \Delta_{\mathrm{M}et} / (\Delta_t \cdot \overline{\mathrm{X}}_v) \tag{3.1}$$

where Δ_{Met} is the variation of nutrient/metabolite quantities (in mol) during the time interval (Δ_t) and $\overline{X_v}$ is the average viable cell number over that period. The lactate yield based on the consumption of glucose was calculated during the exponential phase, with the following equation 3.2

$$Y_{Lac/Glu} = q_{lac}/q_{glu} \tag{3.2}$$

Where q_{lac} is the specific rate of lactate produced by cells (pmol cell^{-1} day^{-1}) and q_{glu}, the specific rate of glucose consumed by cells (pmol cell^{-1} day^{-1}) during the exponential phase.

Release of LDH, which is involved in the production of lactate in the cell culture medium is usually linked to cell damages (e.g. disrupted membranes) and thus cell death. As a control sample, two samples of 5 million of cells were subjected to three cycles of freezing at -80 °C and thawing at 37 °C, which ensured lysis of all cells. The LDH release was then measured by absorbance using the Gallery multiparametric analyser and the kit of dectection LDH (SCE) (Reference 981781). The lysis of 5 million of cells produced an average of 876 units of LDH.

WJ-MSC detachment

After 7 days of culture in spinner vessels (SV), the ability of detachment of microcarriers was evaluated. Before cell detachment, samples were taken and the total number of cells was evaluated by microscopic counting, as presented before. The protocol used for the cell detachment was based on the one described in the work of Nienow *et al.,* [3]. Microcarriers were let settled, then the supernatant was removed. Microcarriers and cells were washed with 100 mL of PBS. Then, TrypLE was added (25 mL) and agitated at 200 rpm for 7 min at 37 °C and 5 % CO_2. After that, cell culture medium (50 mL) was added and the solution was filtered through a 70-µm filter. Cell suspension was then centrifuged and counted by an automated cell counter (Vi-Cell).

In the case of pNIPAM microcarriers, after that cells and microcarriers settled, the cell culture medium was removed. Microcarriers and cells were washed with cold PBS. Then, Accutase was used for cell detachment at 20 °C, and for 20 min, at 40 rpm. Then, cell culture medium (50 mL) was added and the solution was filtered through a 70-µm filter. Cell suspension was then centrifuged and counted by Vi-Cell.

Then the efficiency of detachment was evaluated thanks to the ratio of detached cells (Vi-Cell counting) over the total number of cells calculated before cell detachment.

WJ-MSC characterization

At the end of the culture, cells were detached and expanded in flasks to characterize their differentiation capabilities. Cells were placed in 24-well plates and specific differentiation media (StemPro Differentiation kit, Gibco, LifeTechnologies) were added following manufacturer's instructions. The medium was changed every three days during 40 days culture. At the end of the differentiation period, cells were rinsed three times with PBS, fixed with 4 % (v/v) PFA at room temperature. Adipocytes were stained with 1 % (w/v) Oil Red O. Osteoblasts were incubated with Alizarin Red S. Finally, chondrocytes were stained with Alcian Blue. After staining, differentiated

cells were rinsed with distilled water and observed by light microscopy.

Flow cytometry analysis

MSCs were propagated for three passages in T75 cm^2 flask before expansion in bioreactors. Cells derived from these two culture methods were analyzed for their expression of typical mesenchymal and lineage-specific surface markers. Approximately 100,000 MSCs were re-suspended in 100 µl Phosphate Buffer Saline (PBS). First, MSCs were stained with a viability dye, livedead (Thermofisher) or Zombie Green (Ozyme) then blocked with Bovine serum albumin (0.5 % in PBS). Secondly, MSCs were incubated with antibodies or corresponding isotypes for 1 hour at room temperature. Antibodies and isotypes with their references and clones are listed in the table of supplementary data (Table 3.4). After incubation, MSCs were washed with PBS, centrifuged at 300 g for 5 min then re-suspended in 250 µl PBS or in 250 µl of 1 % paraformaldehyde (PFA) until the analysis is performed. Finally, MSCs were analyzed in a FACS flow cytometry (Beckman Coulter Gallios Cytometry). To compensate potential spectral fluorochrome overlap, compensation beads were used before each analyze. This analyze was performed on living MSCs, dead cells, cell debris and cell doublets were excluded by using forward scatter (FS) and side scatter (SS) gate. Gallios for Kaluza analysis version 2.1 was the software used in this analyze. For CD105-PE, CD146-BV421, CD157-APC, CD200-PE, CD140b PerCpCy5.5 and CD71-APC, ΔX-Med was calculated and corresponds to the difference between the median value of fluorescence of positive cells before and after expansion in bioreactor and ΔE was calculated and defines the difference between the % of marker expression before and after expansion in bioreactor. For HLA-DR-FITC, CD166-PE, CD44-FITC, CD90-FITC, CD73-PE, CD34-PE, CD45-FITC and CD106-PE, only ΔE was calculated.

3.2.1 Cell growth, cell kinetics and efficiency of bead-to-bead transfer for each type of microcarrier

Quantification of cell growth in batch mode

Without addition of fresh microcarriers in the spinner vessels (SV), the duration of the culture was around 7 days for each microcarrier tested and the percentage of attachment was determined for all the microcarriers. After one hour without agitation, the total number of adhered cells was calculated and results are presented in the Table 3.2.

Table 3.2 – Characterisation of the microcarriers used during the study.

Microcarriers	Initial adherence (%)	Specific maximal growth rate (μ_{max}) (day^{-1})	Detachment efficiency (%)
Cy-1	49 ± 23	0.16 ± 0.01	78 ± 7
Cy-p	60 ± 3	0.13 ± 0.04	1 ± 0.1
P+-FN	39 ± 16	0.18 ± 0.13	88 ± 14
P+-Si	21 ± 19	0.09 ± 0.12	100

As it could be observed, a high variability of adherence was obtained in all conditions tested, except for pNIPAM microcarriers. Moreover, a better adherence was obtained (60 %) for Cy-p microcarriers. The addition of fibronectin on PlasticPlus type microcarriers seemed to enhance the

cell adhesion (40 % of cell adhesion), but it remained inferior to the one obtained for Cytodex-1 type microcarriers. The commercial PlasticPlus microcarriers, without coating, have been previously tested, and poor cell attachment was obtained (data not shown). The percentage of initial adherence is a critical point of the process, because cell growth kinetics is linked to the initial number of cells per microcarriers. Indeed, it has been demonstrated in a previous work the importance of an optimal number of cells per microcarriers [12].

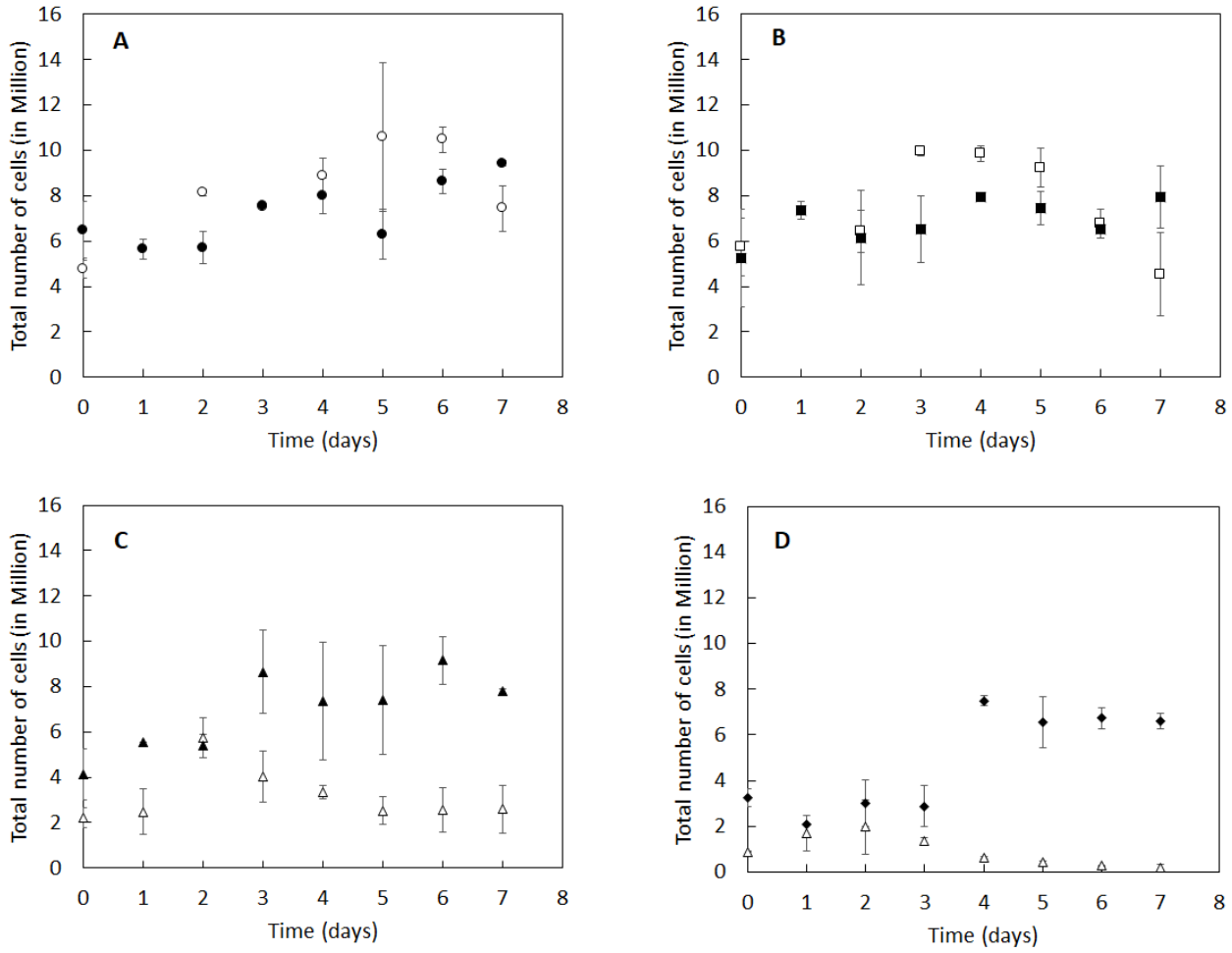

Figure 3.11 – Cell expansion in spinner vessel (SV) using various microcarriers. (A) on Cy-1 microcarriers, (B) onCy-p microcarriers, (C) on P+-FN microcarriers, (D) on P+-Si microcarriers. Two different spinner vessels (full and empty marks) were carried-out. Each day, two different counting were realized for each sample and values are presented as mean value ± standard deviation ($n = 2$).

As shown on the figure 3.11, Cy-1 and Cy-p microcarriers allowed to obtain a maximal number of cells of 10 million, in a reproducible manner. After 6 days of culture, a decrease in the growth rate was noticed in association with a decrease of the total cell number. This decrease of the total cell number could be explained by the appearance of important aggregates leading to a loss of accuracy of the cell counting method. In comparison, P+-FN allowed to obtain about 10 million of cells, but high variabilities were obtained between the two cultures performed in the same conditions. Finally, the home-made microcarriers (P+-Si) only allowed a maximal number of 8 and 4 million, with high variabilities between the two cultures.

Additionally, maximal values of specific growth rates were 0.18 day^{-1} and 0.16 day^{-1}, obtained

with P+-FN and the commercial microcarriers Cy-1, respectively. However, the specific growth rate obtained with Cy-p microcarriers was close to these maximal values (0.13 day^{-1}). In conclusion, it seems that Cytodex-1 type microcarriers and P+-FN microcarriers are the most suitable for WJ-MSCs expansion in agitated modes of culture. Petry *et al.* [8] cultivated UC-MSC on PlasticPlus microcarriers in spinner flasks and obtained a mean maximal growth rate μ_{max} of 0.1 day^{-1}. In the study of Mizukami *et al.* [23], a specific growth rate of 0.9 day^{-1} was obtained by cultivating UC-MSC on CultiSpherS. Finally, in Tozetti *et al.* [22] work, UC- MSC were cultivated on PlasticP102L, in spinner flasks, and obtained a mean μ_{max} of 0.54 day^{-1}. The impact of the nature of the microcarrier on the WJ-MSC expansion is thus particularly pronounced on the maximal specific growth rate. Moreover, the initial cell adhesion yield had a significant impact on latency.

The detachment efficiency was also determined in order to identify which microcarrier would be the most suitable for WJ-MSC production. As it could be seen on the table 3.2, the highest percentage of cell detachment (100 %) was obtained for P+-Si, with all the cells detached, probably due to lower adherence force of cells on these carriers. The second best percentage of cell detachment was obtained for P+-FN (88 %). On the Cytodex-1 type microcarriers, the highest percentage of detachment was obtained for Cy-1 microcarrier, with a detachment efficiency of 78 %. Despite the presence of a specific temperature sensitive layer, cell detachment was poor (1 %) with Cy-p microcarriers, the only shift of temperature was not enough to allow the cell detachment.

In SV, after 6 days of culture, aggregates began to form and resulted in a growth arrest, as figured by the white arrows on the graph (Figure 3.12) whereas critical minimal glucose concentration (1 mM) and/or critical maximal lactate concentration (35 mM) were not reached.

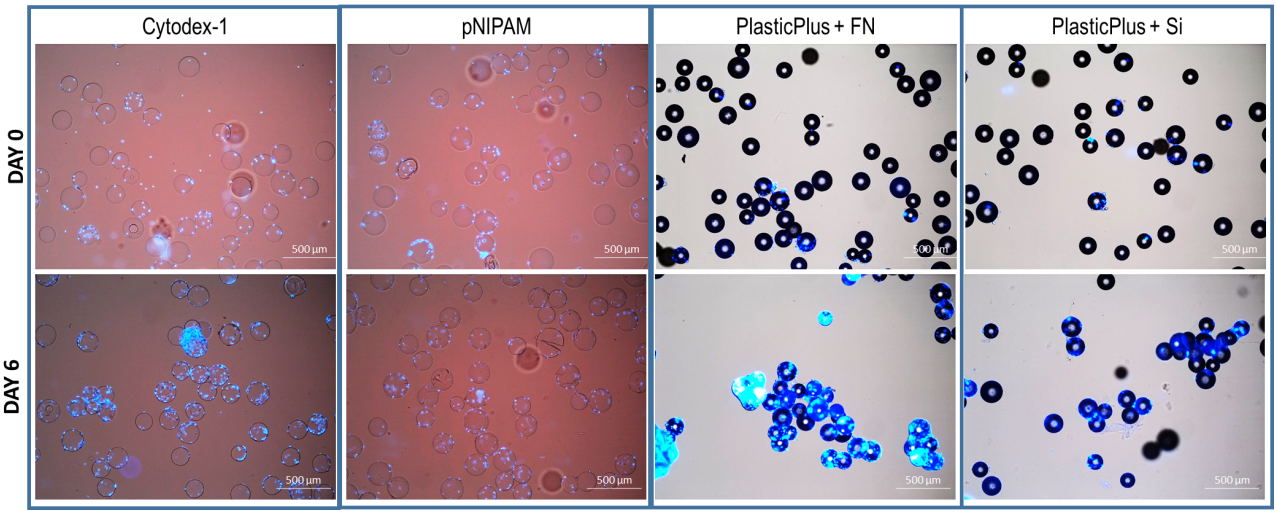

Figure 3.12 – Examples of DAPI staining of MSC cultivated in spinner flasks, depending on the microcarrier types at Day 0 and Day 6 of culture.

Kinetics of substrates consumption and metabolite production were compared depending on the type of microcarriers. After 7 days and in supposed normoxic conditions, yields of lactate on glucose (mol/mol) were calculated during exponential phase of each culture. The theoretical maximal yield of lactate on glucose was 2 mol/mol, meaning that most of glucose was oxidized by cells through the glycolysis pathway, which is less efficient than the oxidative phosphorylation for the energy production. According to the figure 3.13 A, the lactate on glucose yield was the highest for

cells cultivated on PlasticPlus type microcarriers, with a value of 2. For cells cultivated on Cytodex-1 type microcarriers, the yield of lactate on glucose tend to 1, meaning a more efficient energetic metabolism. In the figure 3.13 B, the specific glucose consumption and lactate production are presented. An average specific rate of 20 pmol cell^{-1} day^{-1} of glucose was determined, whatever the type of microcarrier used. The specific lactate production rate reached a value of 60 pmol cell^{-1} day^{-1} in the case of cell culture with PlasticPlus types microcarriers, whereas with Cytodex-1 type microcarriers, the specific production rates of lactate were around 20 pmol cell^{-1} day^{-1}. According to Schop *et al.* [34], at low growth rates (< 0.24 d^{-1}) cells consumed more efficiently glucose for energy production. In this study, in SV, WJ-MSC consumed glucose at an average specific rate of 20 pmol cell^{-1} day^{-1} (Figure 3.13B) while in Mizukami study [23], WJ-MSC in SV consumed glucose only at 8.6 pmol cell^{-1} day^{-1}.

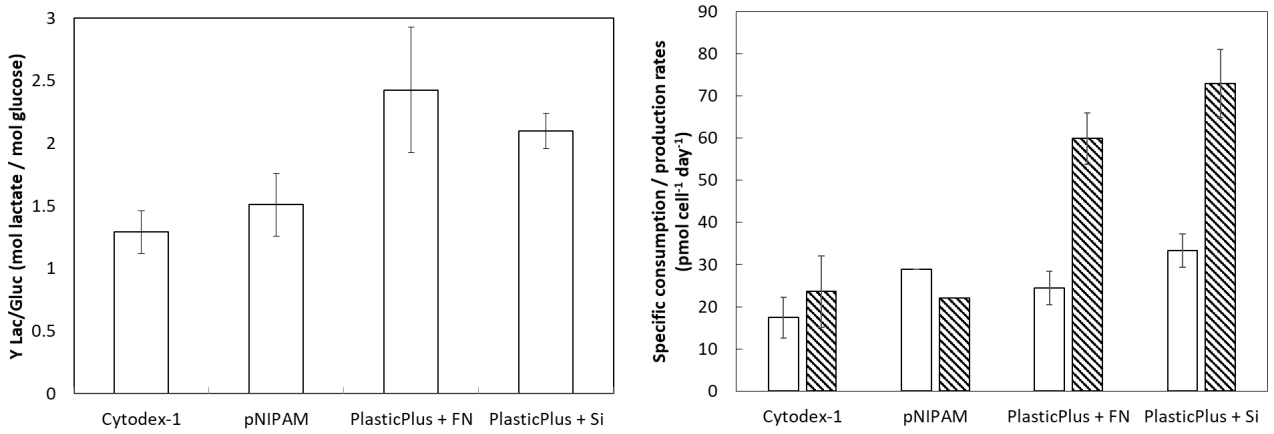

Figure 3.13 – Kinetics of metabolites consumption and production as a function of the type of microcarrier used during cell expansion. (A) Yield of lactate on glucose profiles in SV. (B) Specific consumption and production rates of glucose and lactate in SV. The values of specific glucose consumption in SV are represented by plain white bars. The values of specific lactate production in SV are represented by hatched white and black bars. Values are presented as mean value ± standard deviation ($n = 2$).

In conclusion, as observed on figures 3.11 and 3.12, a limitation of growth surface could be a cause of growth delay or even of growth arrest, as already observed in a previous work [12]. In this study, a high cell adhesion of WJ-MSCs was obtained with Cy-p microcarriers, as well as an efficient expansion but difficulties remained for cell detachment. In order to scale-up the cultures, stirred tank bioreactors were used, and the addition of fresh surfaces was carried-out for each type of microcarriers.

Evaluation of cell growth and bead-to-bead transfer in fed-batch mode for each type of microcarriers

In a previous study, it has been shown that added microcarriers could be colonized by cells and finally allowed a higher expansion factor [12]. In this work, it was first verified that this result could be reproduced using chemically modified microcarriers and transpose in stirred tank bioreactor. In order to limit the appearance of cell aggregates and to increase the duration of cell expansion, fresh microcarriers were thus added at specific times of cultures in STR to keep the average number

of cells per microcarrier constant.

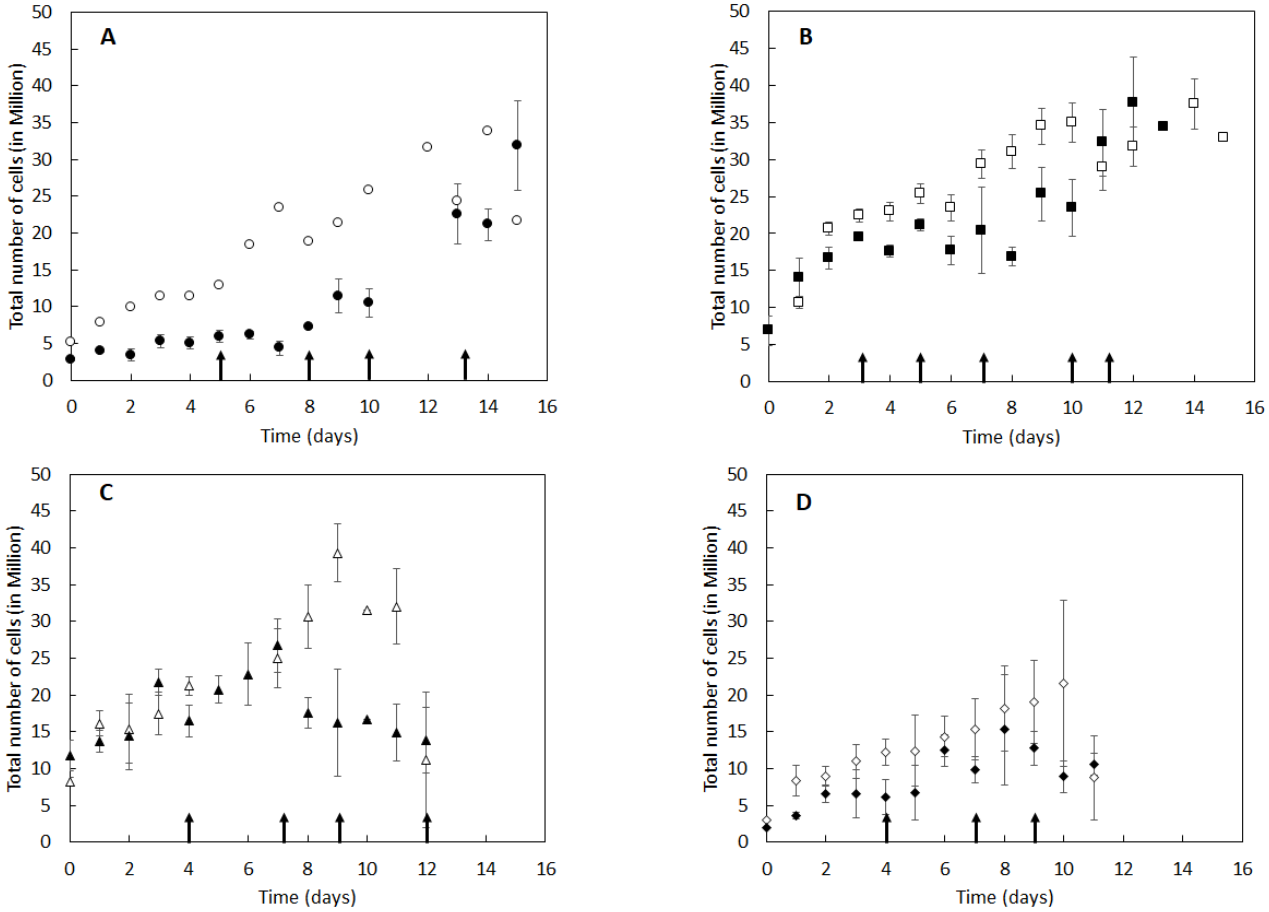

Figure 3.14 – Cell expansion in stirred tank bioreactors depending on the type of microcarrier used. (A) On Cy-1 microcarriers, (B) on Cy-p microcarriers, (C) on P+-FN microcarriers, (D) on P+-Si microcarriers. Two different WJ MSC sources (full and empty marks) were used. Black arrows represent the addition time of microcarriers. Values are presented as mean value ± standard deviation ($n = 3$).

Cell growth kinetics for each type of studied microcarrier are reported in figure 3.14. Cultures with Cy-1 permitted to obtain a maximal number of cells of 35 million, in 14 days with an initial seeding number of 5 or 7 million adhered cells at Day 0 (Figure 3.14 A). These results highlighted the variability of the initial cell adherence on Cy-1. As it could be observed, with a low cell adhesion factor (under 7 cells per microcarrier), a latency phase occurred for a week, then, the cell growth began with a better expansion factor with the addition of microcarriers thanks to the bead-to-bead transfer. Cells grown on Cy-p microcarriers reached a maximal number of 37 million, in 12 days, with 10 to 15 million of initial adhered cells on microcarriers (Figure 3.14 B). The variability between both cultures was less significant than with commercial Cy-1, where a high variability was observed, certainly due to initial variability of adherence at the beginning of the culture. One culture with P+-FN allowed to reach a maximal number of cells of 40 million, in 9 days (Figure 3.14 C). For the second culture, the maximal cell number was only 26 million, in 7 days, then dropped after 8 to 10 days of culture, despite the addition of microcarriers. Finally, the production of MSCs on P+-Si microcarriers was only of 21 million of cells after 10 days of culture, then the total number of cells dropped rapidly (Figure 3.14 D).

Moreover, concerning the process itself, numerous parameters should be determined and optimized, as for example, initial microcarrier loading density and cell seeding density, medium feeding and medium composition, substrate-coating material, stirring protocol, bioreactor shape and design, aeration protocol, initial culture volume, and initial pH among others [35]. For each expansion, specific growth rates and expansion factor were compared and presented in the Table 3.3.

Table 3.3 – Influence of microcarriers types on specific growth rates and expansion factors of MSC cultivated in STR in fed-batch mode.

Microcarrier	Specific growth rate (μ_{max}) (day^{-1})	Expansion factor
Cy-1	0.11	6 ± 2
Cy-p	0.07 ± 0.02	3 ± 1
P+-FN	0.12 ± 0.01	3 ± 0.4
P+-Si	0.13 ± 0.03	3 ± 1

Values of μ_{max} obtained for P+-FN and P+-Si could be considered as similar (0.12 day^{-1} and 0.13 day^{-1} respectively) and were equivalent to the one calculated with MSC cultivated on Cy-1 (0.11 day^{-1}). In comparison, μ_{max} established when cells are cultivated on Cy-p was significantly lower (0.07 day^{-1}). Compared to the literature data, the specific rate measured in the this study were slower. For example, in the study of Mizukami *et al.* [23], UC-MSC were cultivated in STR on CultiSpherS for 7 days, and a μ_{max} value of 1.1 day^{-1} was found. In the study of Tozetti *et al.* [22], UC-MSC were cultivated on PlasticP102L and had a μ_{max} value of 0.46 day^{-1}, in a serum containing medium.

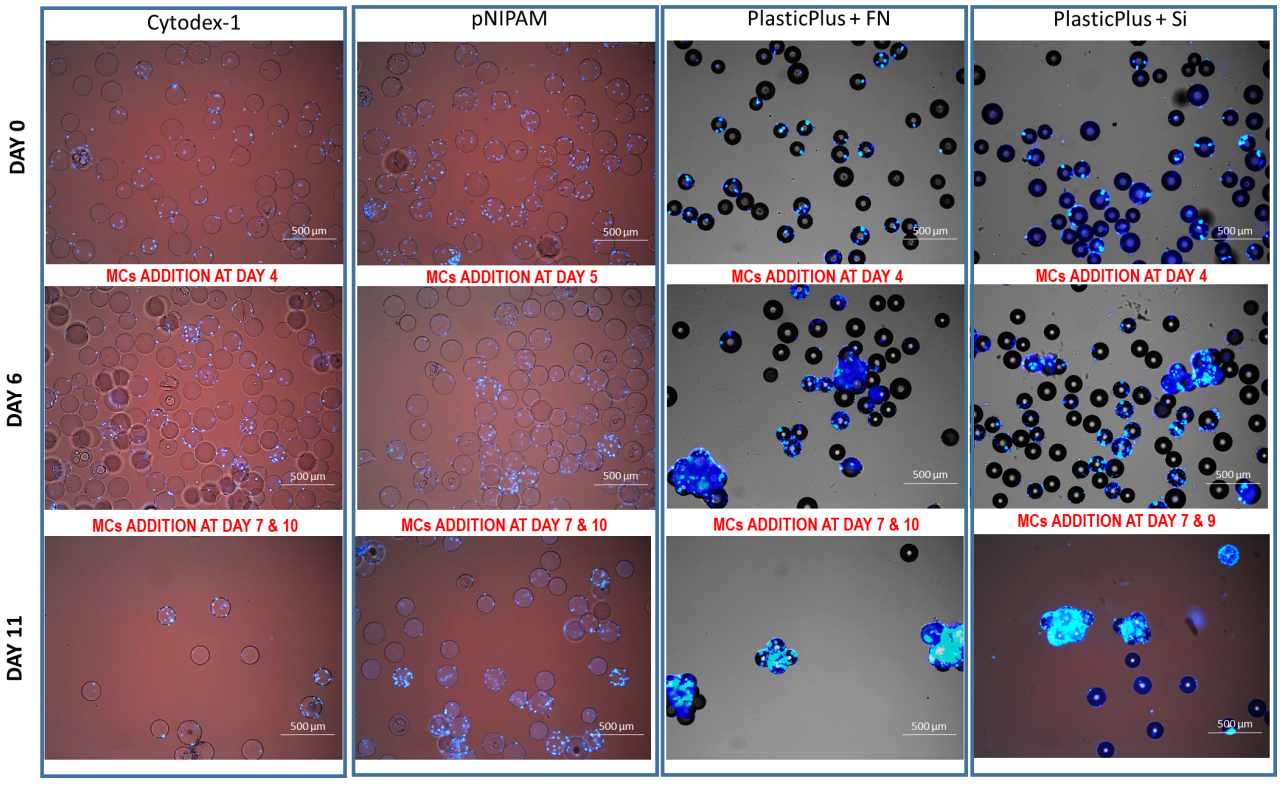

Figure 3.15 – Representative pictures of DAPI staining of MSCs cultivated in stirred tank bioreactors for different types of microcarriers at Day 0, Day 6 and Day 11 culture.

Nevertheless, thanks to the addition of fresh microcarriers correlated with addition of fresh

cell culture medium, conditions of cell aggregates appearance were avoided for Cy-1 and Cy-p, as shown in the figure 3.15. However, it was found that addition of PlasticPlus type microcarriers did not permit to avoid formation of cell aggregates, indicating that the addition of fresh surfaces seemed to be not sufficient to prevent the apparition of clusters and cell aggregates as it could be seen on the figure 3.15. After 6 days of culture, first clusters and cell aggregates appeared in the STR. It could be hypothesized that a longer time for cell migration would be necessary in case of cell expansion with PlasticPlus type microcarriers.

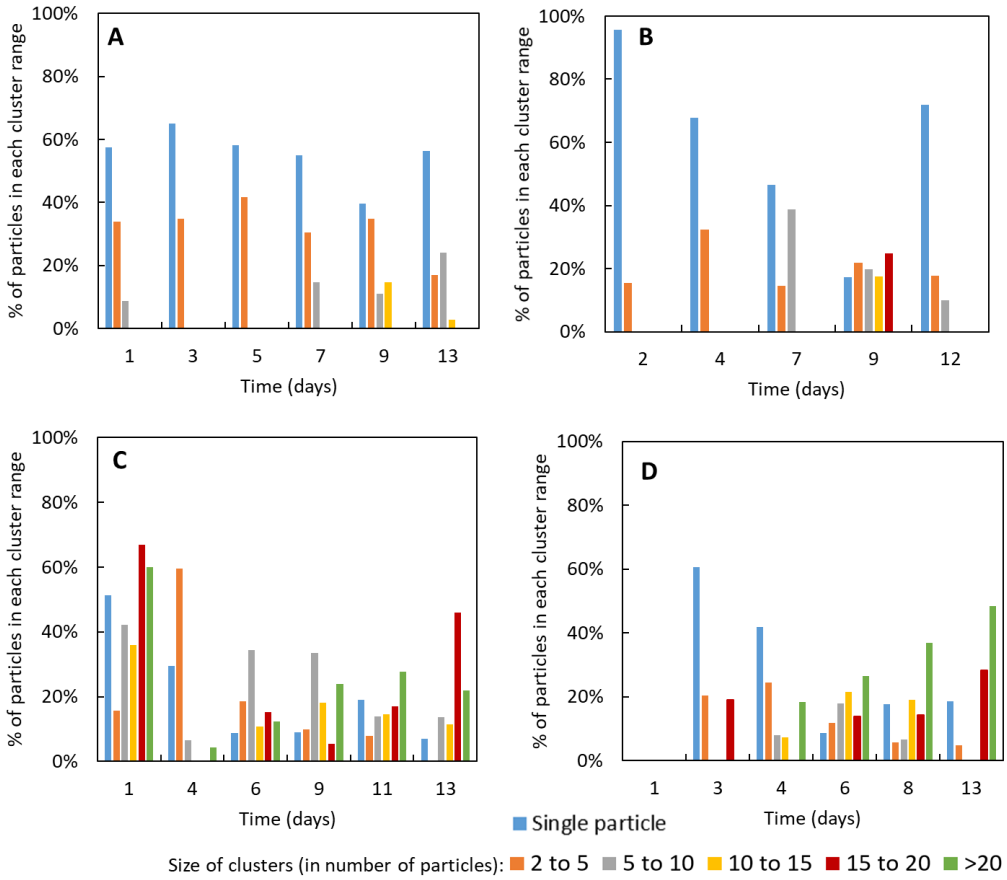

Figure 3.16 – Percentage of occurrence of microcarrier cluster depending of their size. Cultures carried-out with (A) Cy-1, (B) Cy-p, (C) P+-FN and (D) P+-Si microcarriers.

A detailed analysis of these cluster formation was carried-out and revealed that the clusters for PlasticPlus microcarriers derivatives appeared very early during the culture, before day 6 (Figure 3.16). Cultures with PlasticPlus type microcarriers seemed to lead to a high number of clusters and of different sizes (Figures 3.16 C and 3.16 D). At day 1 and from day 6, large number of clusters were formed and trapped an important number of particles, occupied or not by cells. On the contrary, with Cytodex-1 type microcarriers, when they occurred, the size of the clusters were generally composed of two particles (up to day 9), and were the main representative cluster in the culture. At day 9, clusters composed with a higher number of particles were observed but, after addition of fresh microcarriers, they were no longer visible on day 13 (Figures 3.16 A and 3.16 B). In the literature, the presence of these cell aggregates was often discussed. In fact, cell distribution heterogeneities could favour cell death by limiting nutrients and gases flux. In addition, aggrega-

tion can modify the cell properties, since it has been shown that micropellets or larger aggregates enhanced the chondrogenic differentiation [36]. Apparent aggregation can also be responsible for the induction of specific osteogenic lineage differentiation as shown by Brammer *et al.* [37].

In conclusion, the addition of microcarriers, in some cases, prevented the formation of those aggregates and led to a better specific growth rate and a better cell factor expansion as observed for Cy-1 and Cy-p microcarriers. Finally, it has been shown that the home-made microcarrier pNIPAM was a good candidate for WJ-MSCs expansion, thanks to a good yield of cell adhesion and the possibility of bead-to-bead transfer.

Effects of microcarrier type on specific consumption / production rates of MSCs cultivated in stirred tank bioreactors.

The effect of microcarrier types on metabolites kinetics of cell cultures were first evaluated. After 13 days of culture in STR, yields of lactate on glucose (mol/mol) were compared between different microcarriers in hypoxia conditions (Figure 3.17 A). It seemed that cells grown on Cy-1 or P+-FN microcarriers had both the lowest yield (0.7 mol lactate / mol glucose). Petry *et al.* [8] showed a significant decrease in the yield of lactate on glucose in the case of a switch from the static mode of culture to the dynamic one. The authors explained this decrease by a better oxygen transfer in spinner vessels, contributing to the change of the cellular metabolism from the glycolytic pathway to the oxidative phosphorylation. In the present study, all the cultures performed in STR promoted yields of lactate on glucose lower than 2 whatever the type of microcarrier used (Figure 3.17 A), and were significantly lower than those obtained in SV for these same microcarriers (Figure 3.13 A).

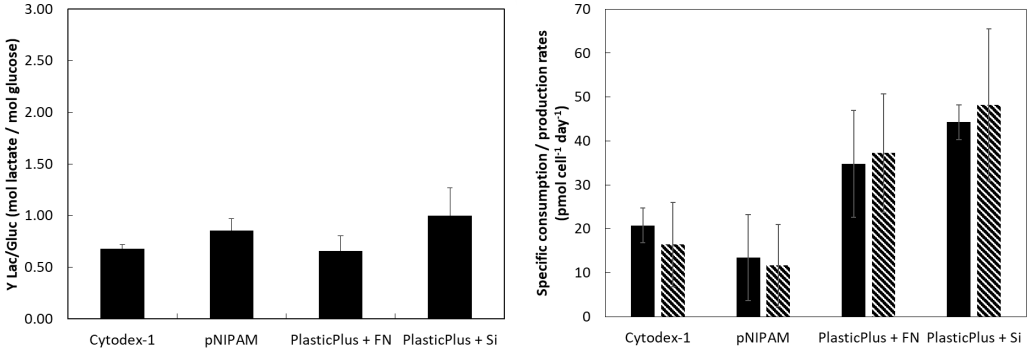

Figure 3.17 – Effect of microcarrier types on kinetics of metabolites consumption and production during cell expansion. (A) Yield of lactate on glucose profiles in hypoxia (STR). (B) Specific consumption and production rates of glucose and lactate in hypoxia (STR). The values of specific glucose consumption in stirred tank bioreactor are represented in plain black bars. The values of specific lactate production in stirred tank bioreactor are represented in hatched white and black bars. Values are presented as mean value ± standard deviation ($n = 2$).

In parallel, specific glucose consumption rates were calculated (Figure 3.17 B). When cells were grown on Cytodex-1 types microcarriers (Cy-1 & Cy-p), specific glucose consumption rates were around 20 pmol cell^{-1} day^{-1}, regardless the system of culture (SV or STR). When cells were grown on PlasticPlus types microcarriers (P+-FN & P+-Si), specific glucose consumption rates were sensibly higher and around 30-40 pmol cell^{-1} day^{-1} in STR. Specific production of lactate was higher

in SV than in STR, regardless the type of microcarrier used for cell expansion (Figures 3.13 B and 3.17 B). In SV and with PlasticPlus type microcarriers, yield of lactate on glucose was thus 2 or 3 times higher than in STR (Figure 3.13 A). In the case of cell expansion on Cytodex-1 type microcarriers, in STR, cells produced an average of 20 pmol cell^{-1} day^{-1} while in the case of cell expansion on PlasticPlus type microcarriers, in STR, cells produced an average of 40 – 50 pmol cell^{-1} day^{-1}. Whereas cultivated under feeding medium and microcarriers conditions, these results are close to those reported by Mizukami *et al.* (2016). In their study, cells were grown on CultispherS, consumed an average of 68 pmol cell^{-1} day^{-1} of glucose, and produced 52 pmol cell^{-1} day^{-1}, when cultivated in hypoxic conditions in stirred tank bioreactors. Specific consumption and production rates increased during the first two days, corresponding to the initiation of the exponential growth phase, before to become constant.

Hypoxic conditions of culture mimic neonatal tissue and *in-vivo* conditions. In placenta and in umbilical cords, oxygen concentration rarely exceeds 5 % of pure O_2 [38, 39, 40]. Knowing this, WJ-MSC cultivated in normoxic condition could lead to cellular stress. It was demonstrated by Bétous *et al.*, Haque *et al.*, Fehrer *et al.*, & Estrada *et al.* [41, 42, 43, 44] that high O_2 concentrations could lead to early senescence, lower growth rate and DNA damages in MSCs.

In the present study, cells cultivated in STR were in hypoxic conditions (20 % of air saturation and a low oxygen solubility). In these conditions, it could be assumed that that consumed glucose could be used to produce energy either by oxidative phosphorylation, with a high production of ATP (36 + 2 per glucose), or through glycolysis only and with a less efficient production of ATP (only 2 per glucose). These results indicated that for all STR conditions, cells may have a respiratory metabolism (Figure 3.17 A) and that energy produced in this condition was dedicated to cell growth except in case of PlasticPlus type microcarriers. Indeed, cells consumed almost 2 times more glucose, but expansion factor and specific growth rate were equivalent to those found with Cy-1 microcarriers.

3.2.2 Effect of microcarrier types on cell mortality

The cell death in each STR was evaluated thanks to the measurement of LDH concentration which is directly related to the cell membrane damage. In the figure 3.18 A, it could be observed that the percentage of dead cells was below 20 % in each condition, except for P+-Si (25 %). The lowest percentage of dead cells was obtained in culture with pNIPAM microcarriers, and the highest with cells grown on PlasticPlus + Si microcarriers at day 11. According to figure 3.18 B, on representative live/dead pictures, a low ratio of dead cells could be detectable for pNIPAM and PlasticPlus + Si. It could be noticed that, in the case of Cytodex-1, dead cells could remain attached on the microcarriers while in PlasticPlus cultures, dead cells were observed only in the supernatant (figure 3.18 B).

According to the literature, the maximal concentrations of lactate and ammonium produced by cells were not critical for cell viability. Schop *et al.* (2009) indeed reported that, if concentration in lactate was higher than 35 mM, a growth inhibition could occur [45]. In addition, the authors advised to maintain a glucose concentration above 1 mM. As reported in figure 3.19 A, the maxi-

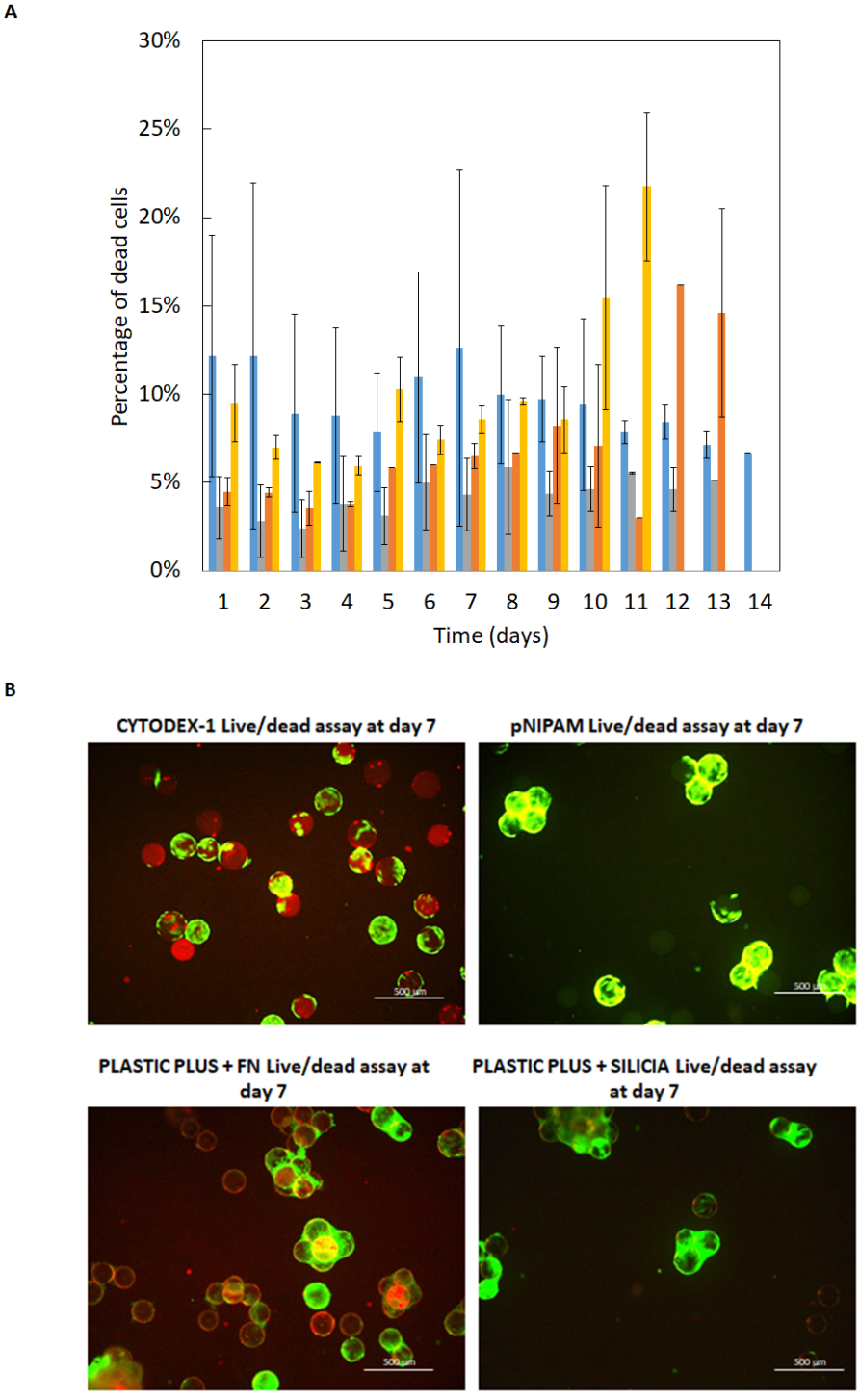

Figure 3.18 – Kinetics of cell death of MSCs cultivated in STR with different types of microcarriers. (A) Percentage of dead cells obtained by the measurement of LDH concentrations during culture with microcarriers Cy-1 (blue bars), Cy-p (grey bars), P+-FN (orange bars) and P+-Si (yellow bars). Values are presented as mean value ± standard deviation ($n = 2$). (B) Representative pictures of live/dead staining at day 7.

mal concentration of lactate in STR was around 15 mM, regardless the type of microcarriers used, which was thus not critical for cell expansion. However, concerning the maximal production of ammonium by cells, as reported in the figure 3.19 B, ammonium concentration values were higher than the maximal ones advised by literature (*i.e.* 2.5 mM) [45]. In fact, cultures carried-out with Cy-1, Cy-p, P+-FN and P+-Si respectively produced an average concentration of ammonium of

3, 2.5, 3.5 and 3 mM. However, it was shown in previous studies that sensitivity of cells towards lactate and ammonium are cell line specific and could widely vary [45]. It was also reported that cells cultivated at high lactate concentrations changed their morphology from fibroblast to more stretched cells [45]. In addition, cells cultivated at high ammonium concentrations could show cubic cell morphology [45]. However, daily staining and cell observations showed no significant changes in the cell morphology during our experiments (Figure 3.15 & 3.18).

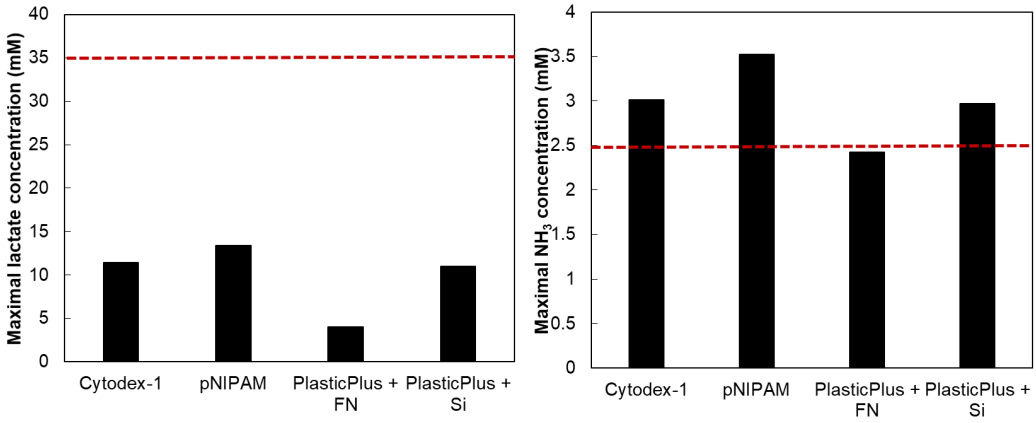

Figure 3.19 – Evaluation of maximal lactate and ammonium concentrations during WJ-MSC expansion in stirred tank bioreactor, using different microcarrier types. (A) Maximal lactate concentration (in mM). (B) Maximal ammonium concentration (in mM). Values are presented as mean value ± standard deviation (n = 2). The red dashed lines represent the maximal values supported by the cells according to Schop *et al.* [45].

3.2.3 Cell morphology and microcarrier colonization

To go further in the study of the impact of functionalized and home-made microcarriers impact on cell cultures, cell morphologies and microcarrier occupancies were compared for each microcarrier type.

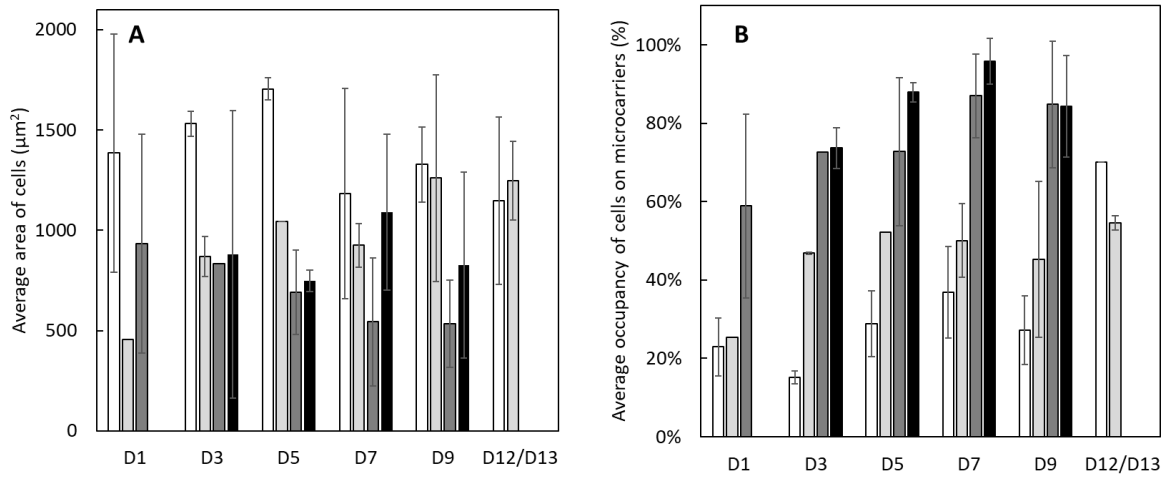

Figure 3.20 – Impact of the microcarrier type on cell size. (A) Average area of cells spread on microcarriers. (B) Average area of cell occupancy on microcarriers. Cy-1 (white bars), Cy-p (light grey), P+-FN (grey bars) and P+-Si (black bars) microcarriers

In the figure 3.20 A, the average size of cells measured at different time points is presented (calculations based on 70-90 cells approximately per time point). Even if the differences were reasonably significant the trend clearly showed that cells grown on Cy-1 microcarriers were bigger and occupied more space on microcarriers than cells grown on PlasticPlus type microcarriers. Generally, sizes of cells did not change during time culture. However, despite the addition of fresh microcarriers at different days of culture, the average of cell occupancy of PlasticPlus type microcarriers was above 70-80 % (Figure 3.20 B). This confluence could be the reason why the cells were smaller on PlasticPlus microcarriers, the cells may not have enough space to expand, forcing them to grow in multilayer and in 3 dimensions (3D). On the contrary, the average of cell occupancy of Cytodex-1 type microcarriers was around 50-60 % (Figure 3.20 B). Addition of fresh microcarriers in cultures with Cy-1 and Cy-p microcarriers were well colonized by cells and a cell confluence about 60 % could be maintained, which was not the case for the PlasticPlus microcarriers.

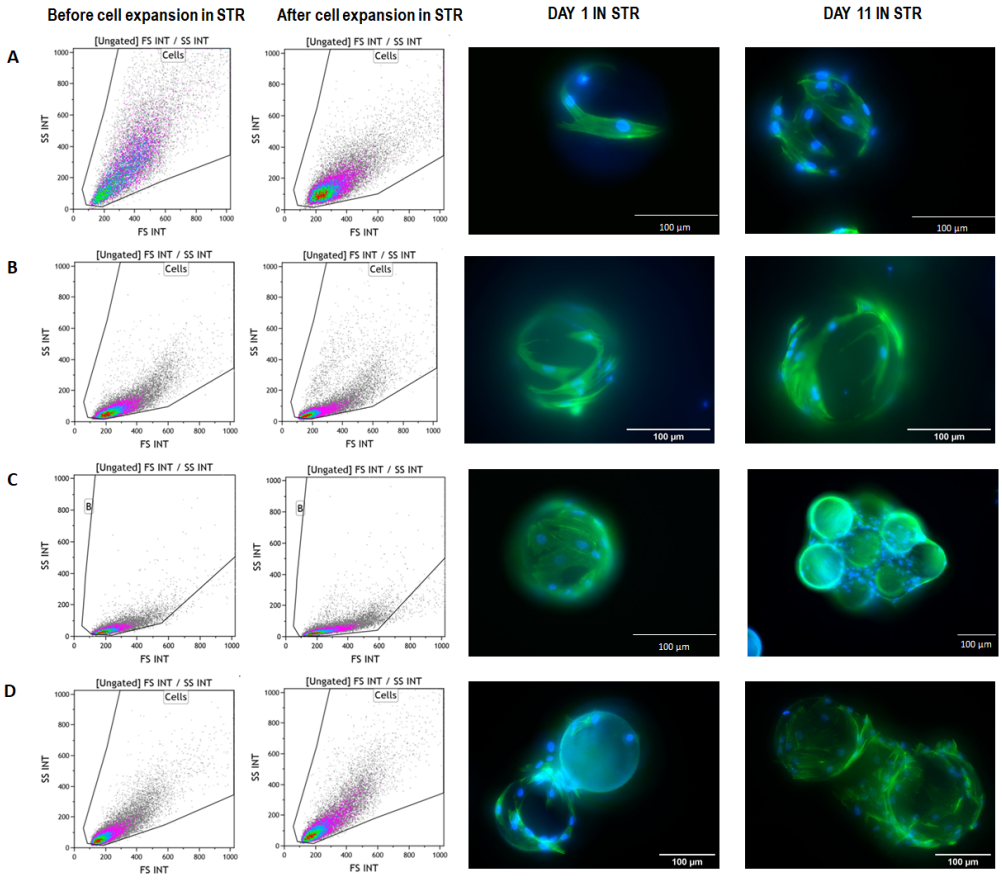

Figure 3.21 – Flow cytometry before and after cell culture in bioreactor. Forward scatter (FS) and side scatter (SS) were used to exclude dead cells, cell debris and cell doublets. Immunostaining of actin fibers (green) and cell nuclei stained in blue. (A) Cy-1, (B) Cy-p, (C) P+-FN, (D) P+-Si microcarriers.

Finally, flow cytometry analysis put into evidence possible morphological changes before and after cell culture in STR. Cells were analysed by flow cytometry after 14 days of culture in STR, and compared to the same cells grown on T-flasks. As presented in figure 3.21, flow cytometry highlighted that after an average of 14 days culture in STR, some groups of cells seemed to have a more grainy structure as showed by an increase of forward scatter (FC) and side scatter (SC) intensities. Moreover, thanks to immuno-staining carried-out during culture in STR, cells showed

a typical spindle-shape and covered the surface of carriers in Cy-1 and Cy-p microcarriers (Figure 3.21 A and 3.21 B), but seemed to be smaller and with a 'star shape' when they were cultivated on PlasticPlus type microcarriers (Figure 3.21 C and 3.21 D).

3.2.4 Cell characterization

Immunophenotypes of MSCs after cultivation in STR, ISCT markers

WJ-MSC immunophenotypes were characterized for operating conditions tested in this study. The figure 3.22 presents the percentage of expression obtained from MSC-specific cell surface markers. For each microcarrier studied, immunophenotypes were obtained before and after the culture in STR. Cells expressed negatively HLA-DR, CD45, CD106 and CD34, whereas positively expressed markers CD166, CD44, CD73, CD90 were expressed with Cytodex-1 microcarriers (Figure 3.22 A and 3.22 B), which met the ISCT criteria for these markers. Similar conclusions were obtained for the PlasticPlus type microcarriers (Figure 3.22 C and 3.22 D).

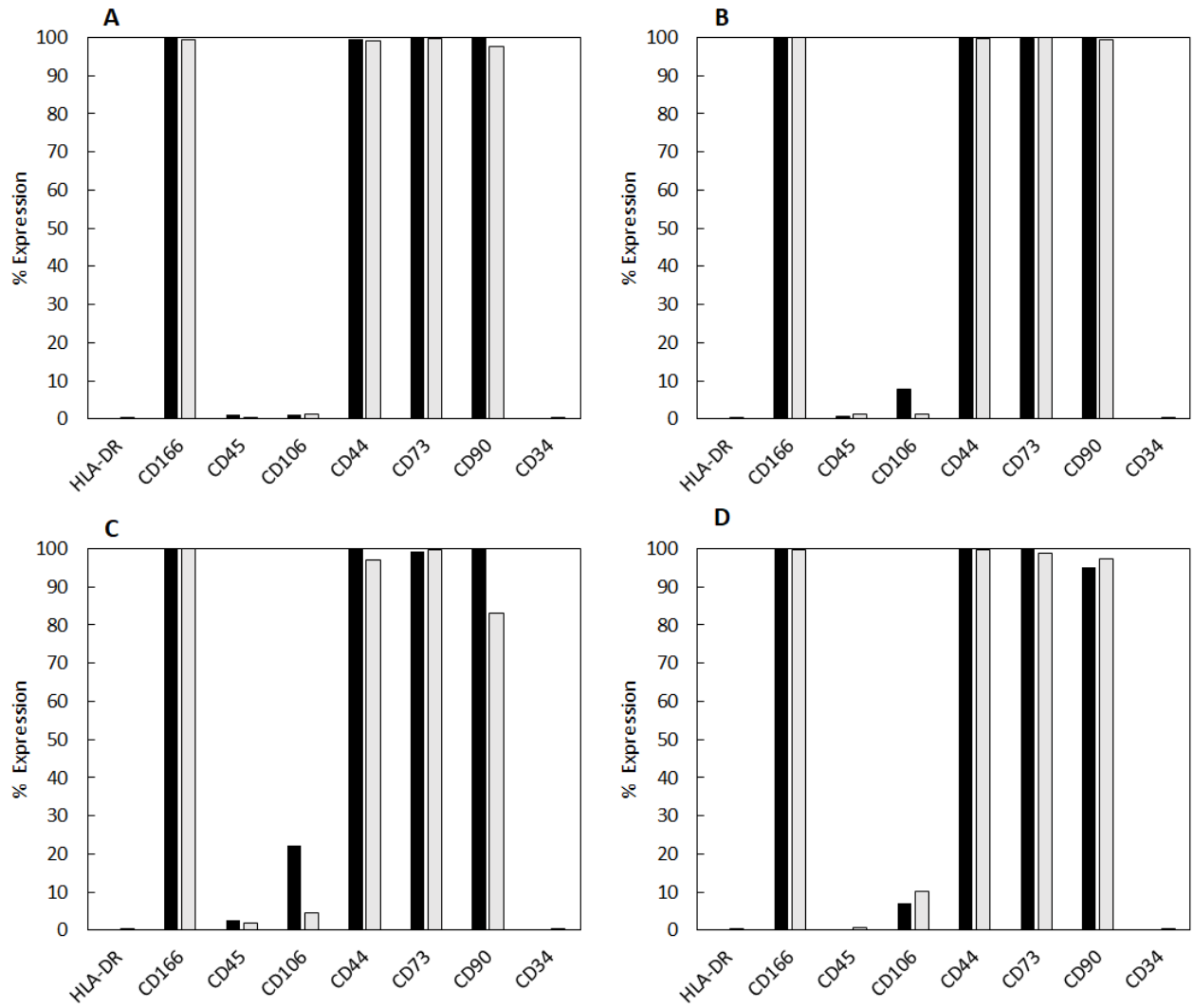

Figure 3.22 – Expression of markers by WJ-MSCs before and after cell culture. Black and light grey bars respectively indicate measurements before and at the end of cell culture in bioreactor. (A) Cy-1, (B) Cy-p, (C) P+-FN and (D) P+-Si microcarriers.

Thus, the cell detachment and the nature of the microcarrier did not seem to influence stemness of cells. However, further studies are required, in particular to determine whether or not physiochemical changes such as pH, temperature changes or concentration of dissolved oxygen could influence stemness of MSCs.

Immunophenotypes of MSCs after cultivation in STR, markers of functionalization

The MSC phenotype is being studied to be associated with the functionality of MSCs. So, in addition to ISCT markers analysis, alternative surface molecules were also analyzed. These markers were chosen based on bibliography studies that highlight their implication in many functions and processes such as, proliferation, migration, immune system regulation. The CD105 marker, also known as endoglin, is a typical marker of endothelial cells. It plays an essential role as co-receptor having a high affinity for transforming growth factor [46] and promotes the growth of blood vessels. According to the figure 3.23, it seemed that, after cell culture expansion in bioreactors, the expression of this marker was decreased slightly, whatever the type of microcarriers used. The CD146, also known as melanoma cell adhesion molecule (MCAM, MelCAM) or cell surface glycoprotein Muc18, is also a typical marker of endothelial cells. This marker is implicated in the migration, signal transduction and proliferation of MSCs [47]. It is over-expressed when cells are grown on Cy-1 (+20 %), but under-expressed when cultivated on Cy-p and P+-Si (-20 % and -2 %) respectively. The expression of CD157 marker is enhanced in bone marrow stromal cell lines derived from patients with rheumatoid arthritis [48]. This marker is a key player in regulating leukocyte adhesion and migration. In murine models, it is also an important marker regulating cell adhesion and cell migration [49]. This marker seemed to be over-expressed when cells were grown on Cy-1 (+24 %), but down-regulated with the other microcarriers. The marker CD200 is an immunoglobulin-like protein which is expressed by immune and vascular endothelial cells [50]. It is also a marker demonstrating the ability of stimulation of T-cell proliferation, and thus, of MSC potentiality [51]. It was over-expressed with cultures on Cy-1 (+26 %) and slightly over-expressed with P+-Si (+10 %), but decreased with Cy-p microcarriers (-46 %). The marker CD140b known as platelet-derived growth factor receptor beta (PDGFRβ) is sensible to growth factors and is over-expressed after culture with Cy-1 (+7.5 %), but reduced when cultivated with Cy-p (-11 %), and presented almost no difference before and after cell culture for P+-Si (+1.5 %). Finally, for the CD71 marker also called transferrin receptor, this gene encodes a cell surface receptor necessary for cellular iron uptake by the process of receptor-mediated endocytosis. Its expression seemed to be similar before and after cell culture in bioreactor.

Conclusion

The present study revealed, in a first point, the benefit of using a stirred tank bioreactors for WJ-MSCs expansion on microcarriers. Thanks to the addition of fresh microcarriers in association with cell culture medium, the expansion factor was improved by a factor 2. The additions of microcarriers at different times of the culture seemed to limit cell aggregates formation when Cytodex-1

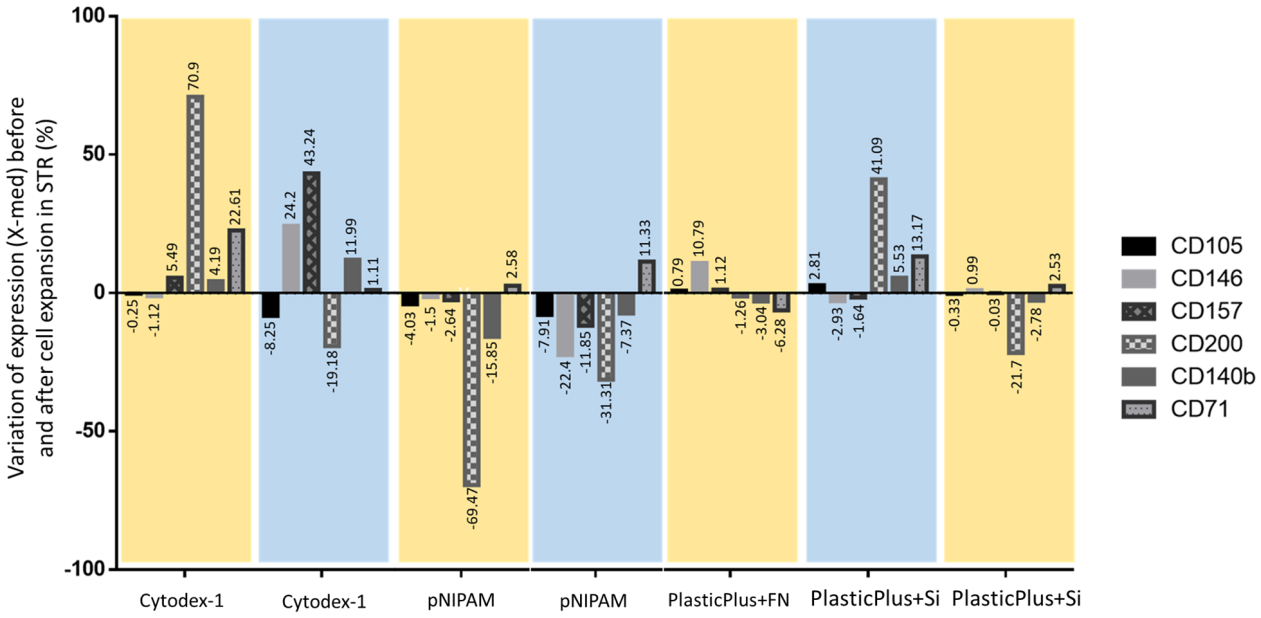

Figure 3.23 – Expression of functional markers before and after expansion on various microcarriers. Yellow and blue fields correspond to two different sources of WJ MSCs.

type microcarriers and derivatives were used, whereas such feeding strategy appeared less effective for the PlasticPlus type microcarriers. In addition, this study described the behaviour of cells according to the type of the microcarriers with which they are in contact. It seemed that addition of Cytodex-1 type microcarriers led to control the percentage of occupancy to 60 %, with well spread cells. On the contrary, the addition of PlasticPlus type microcarriers was not sufficient to prevent the formation of aggregates, and the average percentage of occupancy was above 70-80 %. Moreover, the size of the cells appears to have been impacted by the nature of the material on which they grew, as confirmed by cytometry and microscopy, showing larger cell size on Cytodex-1 type microcarriers than on PlasticPlus type microcarriers. After the biological characteristics described, this study analysed the possible modification of the expression of markers after cell expansion in STR. The markers described by the ISCT were still expressed after the expansion in STR, whatever the type of microcarrier used. Concerning the functionalized markers, some differences of expression were noticed after the expansion in STR, especially for the CD157, CD200 and CD71 markers.

Acknowledgment

The authors would like to thank the INTERREG 'Improve-stem' project for its financial support. They also acknowledge Fanny Gallo, Fabrice Blanchard (LRGP, Nancy), Dr. Jenny Brinkmann, Dr. Marcus Koch and Spoorti Ramesh (INM, Saarbrücken) for their technical contributions to this work.

Supplementary data

Table 3.4 – Lists of antibodies and isotypes with their references and clones.

Antibody	Supplier, reference	Clone
FITC Mouse IgG1 κ Isotype Control	Dako, X0927	DAK-GO1
PE Mouse IgG1 κ Isotype Control	Dako, X0928	DAK-GO1
CD90-FITC	Beckman Coulter, IM1839U	2G5 F15-42-1-5
CD34-PE	BD Pharmingen, 555822	581
CD45-FITC	Dako, F0861	T29/33
CD166-PE	Beckman Coulter, A22361	3A6
CD44-FITC	Beckman Coulter, IM1219U	J.173
CD105-PE	Beckman Coulter, B92442 A07414	TEA3/17.1.1 1G2
HLADR-FITC	Beckman Coulter, IM0463U	B8.12.2
CD73-PE	BD Pharmingen, 550257	AD2
CD200-PE	BD Pharmingen, 552475	MRC OX-104
CD106-PE	BD Pharmingen, 555647	51-10C9
BV421 Mouse IgG1, κ Isotype Control	BD Horizon, 562438	X40
CD146-BV421	BD Horizon, 564325	P1H12
APC Mouse IgG2a, κ Isotype Control	BD Pharmingen, 555576	G155-178
CD157-APC	ThermoFisher, 17-1579-42	SY/11B5
CD71-APC	BD Pharmingen, 551374	M-A712
PerCP-Cy5.5 Mouse IgG2a, κ Isotype Control	BD Pharmingen, 550927	G155-178
CD140b-PerCP-Cy5.5	BD Pharmingen, 562714	28D4

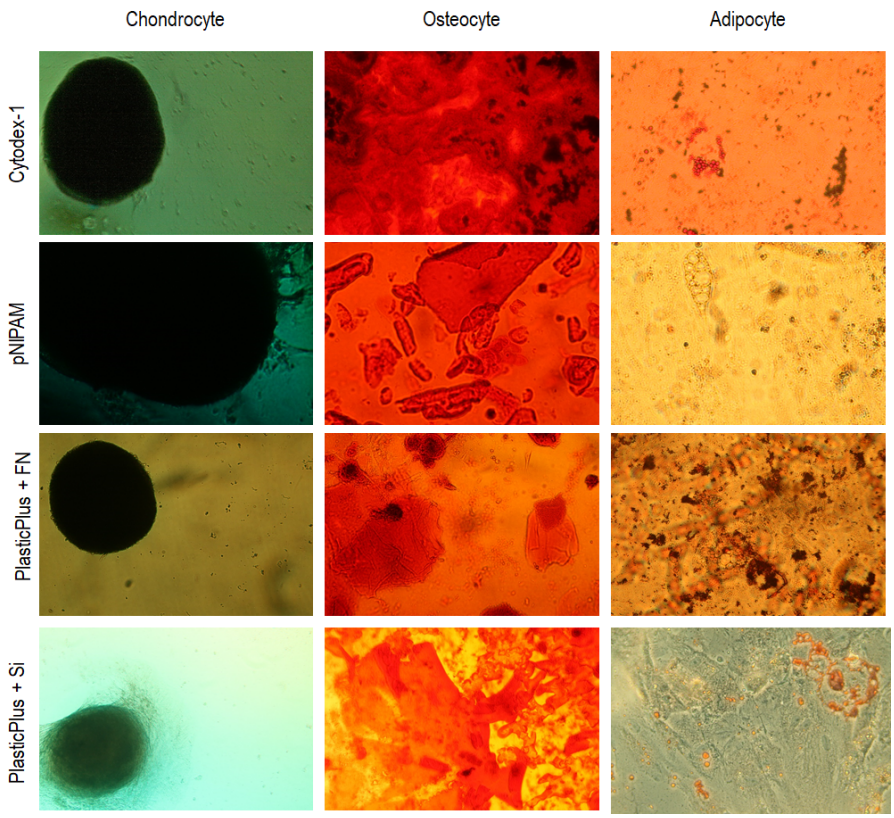

Figure 3.24 – Differentiation of WJ-MSCs in chondrocyte, osteocyte and adipocyte in function of the type of microcarrier used in culture in stirred tank bioreactor in fed-batch mode.

Conclusions of chapter 3

In this chapter a screening of innovative and functionalized microcarriers used to improve MSCs culture performance has been proposed. More particularly, the partnership with different european laboratories allowed to quantify efficiency of innovative microcarriers in terms of cell adhesion and cell detachment. Chemical grafting such as APTES, silane groups, or thermosensible layer (*i.e.* pNIPAM) were indeed compared during MSCs culture performed in static modes in 6-well plates. It has been shown that the functionalization by APTES graft (with or without plasma treatment) allowed to improve cell adherence (+ 30 %), but impacted the efficiency of cell detachment. The functionalization with silane had a negative impact on the microcarriers, with the presence of numerous debris, and therefore could negatively impact WJ-MSCs expansion and viability. Moreover, confocal and SEM pictures on Cytodex-1 and pNIPAM microcarriers demonstrated a wide cell spreading through a consistent organization of actin fibers on the microcarriers. The modified microcarriers with the pNIPAM sensitive layer permitted to obtain percentage of cell attachment (55 % of adhered cells) similar to Cytodex-1 microcarriers but did not permit to obtain an efficient cell detachment with only 40 % of detached cells and with a low viability. Further studies should be performed on the development of this sensitive layer in order to obtain better results. Concerning the PlasticPlus microcarriers, it has been shown that, to improve adhesion, the addition of fibronectin (+ 26 %), APTES (+ 20 %) or silane (+ 30 %) was beneficial.

After the screening in static modes, the most promising housemade microcarriers were compared with the commercial ones, in STR, with addition of microcarriers. Results showed that the best candidate for WJ-MSCs expansion in STR among the home-made microcarriers are pNIPAM microcarriers, with a cell expansion factor of 3, a specific growth rate about 0.07 day^{-1}. After the expansion in STR, cells kept their stem cells characteristics and were still able to differentiate into chondrocytes, adipocytes and osteocytes. Moreover, on these home-made pNIPAM microcarriers, cells were still able to migrate towards new microcarriers added. Microcarriers aggregation was reduced thanks to the addition of the fresh microcarriers, whereas it was not possible with the home-made PlasticPlus microcarriers (modified with silane). The choice for a commercial microcarrier should be Cytodex-1, with cell expansion factor of 6 and a specific cell growth rate of 0.11 day^{-1}.

Finally the flow cytometry showed the influence of the functionalization of microcarriers on cell spreading through the organization of the fiber actins. It seemed that 'softer' microcarriers (Cytodex-1 and pNIPAM- Cytodex-1 microcarriers) allowed to the cells to be more spread and elongated on the surfaces, while 'harder' surfaces, as polystyrene based microcarriers, allowed to the cells to be smaller and less elongated. The functionalization of the microcarriers also had an impact on the expression of markers of functionalization, thus over-expression of CD157, CD200 or CD140b markers were obtained with Cytodex-1 microcarriers while on pNIPAM Cytodex-1 microcarriers these markers were under-expressed.

Finally, as indicated in the figure 3.25, fed-batch bioreactors with addition of microcarriers allowed to improve the cell expansion factor by 3 compared to batch modes (in spinner vessels). Moreover, microcarriers aggregation were reduced with pNIPAM and Cytodex-1 microcarriers, but, some empty microcarriers were still noticed in stirred tank bioreactors. Functionalized microcarriers were effective for cell adhesion but improvements were still required concerning cell detachment. To further improve the performance of expansion process, the use of dissolvable microcarriers may bring valuable solutions to detachment issues ; this was the aim of the last chapter of this PhD thesis.

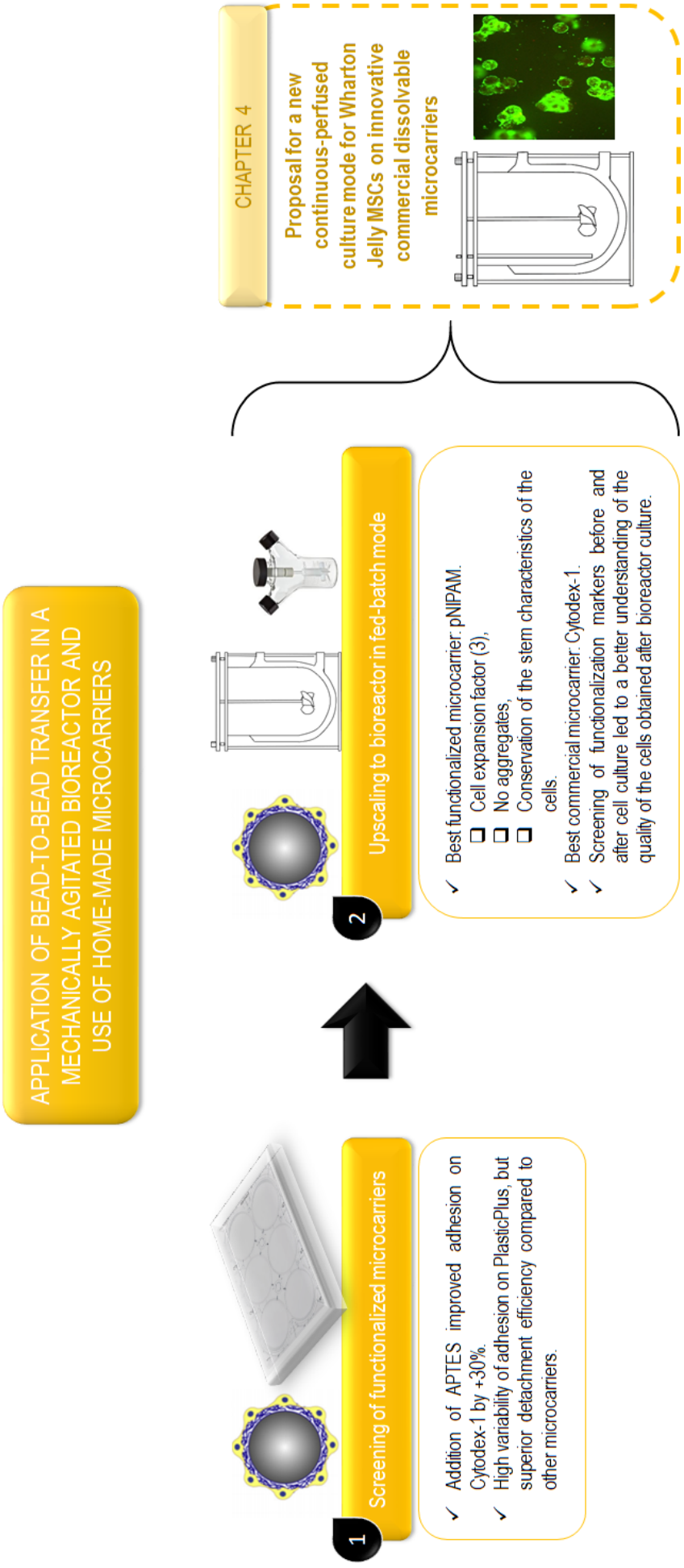

Figure 3.25 – Synthesis of the results of the chapter 3.

Bibliography

[1] C. Martin. *Etude des procédés d'amplification de cellules souches mésenchymateuses humaines*. PhD thesis, Université de Lorraine, 2016.

[2] C. Loubière. *Characterization and impact of the hydrodynamics on the performance of umbilical-cord derived stem cells culture in stirred tank bioreactors*. PhD thesis, Université de Lorraine, 2018.

[3] A. W. Nienow, C. J. Hewitt, T. R. Heathman, V. A. Glyn, G. N. Fonte, M. P. Hanga, K. Coopman, and Q. A. Rafiq. Agitation conditions for the culture and detachment of hMSCs from microcarriers in multiple bioreactor platforms. *Biochemical Engineering Journal*, 108:24–29, 2016.

[4] R. Carlin, D. Davis, M. Weiss, B. Schultz, and D. Troyer. Expression of early transcription factors oct-4, sox-2 and nanog by porcine umbilical cord (puc) matrix cells. *Reproductive Biology and Endocrinology*, 4(1):8, 2006.

[5] D. L. Troyer and M. L. Weiss. Concise review: Wharton's jelly-derived cells are a primitive stromal cell population. *Stem Cells*, 26(3):591–599, 2008.

[6] J. Rowley, E. Abraham, A. Campbell, H. Brandwein, and S. Oh. Meeting lot-size challenges of manufacturing adherent cells for therapy. *BioProcess Int*, 10(3):7, 2012.

[7] V. Jossen, R. Pörtner, S. C. Kaiser, M. Kraume, D. Eibl, and R. Eibl. Mass production of mesenchymal stem cells impact of bioreactor design and flow conditions on proliferation and differentiation. In *Cells and Biomaterials in Regenerative Medicine*, volume 2014. InTech, 2014.

[8] F. Petry, J. R. Smith, J. Leber, D. Salzig, P. Czermak, and M. L. Weiss. Manufacturing of human umbilical cord mesenchymal stromal cells on microcarriers in a dynamic system for clinical use. *Stem Cells International*, 2016, 2016.

[9] Q. A. Rafiq, S. Ruck, M. P. Hanga, T. R. Heathman, K. Coopman, A. W. Nienow, D. J. Williams, and C. J. Hewitt. Qualitative and quantitative demonstration of bead-to-bead transfer with bone marrow-derived human mesenchymal stem cells on microcarriers: Utilising the phenomenon to improve culture performance. *Biochemical Engineering Journal*, 135:11–21, 2018.

[10] D. Schop, R. van Dijkhuizen-Radersma, E. Borgart, F. Janssen, H. Rozemuller, H.-J. Prins, and J. D. de Bruijn. Expansion of human mesenchymal stromal cells on microcarriers: growth and metabolism. *Journal of Tissue Engineering and Regenerative Medicine*, 4(2):131–140, 2010.

[11] K. Siddiquee and M. Sha. Billion-cell hypoxic expansion of human mesenchymal stem cells in bioblu® 5c single-use vessels. *BioProcessing*, 14(2):1538–8786, 2015.

[12] C. Sion, C. Loubière, M. Wlodarczyk-Biegun, N. Davoudi, C. Müller-Renno, E. Guedon, I. Chevalot, and E. Olmos. Effects of microcarriers addition and mixing on WJ-MSC culture in bioreactors. *Biochemical Engineering Journal*, 157:107521, 2020.

[13] T. Lawson, D. E. Kehoe, A. C. Schnitzler, P. J. Rapiejko, K. A. Der, K. Philbrick, S. Punreddy, S. Rigby, R. Smith, Q. Feng, et al. Process development for expansion of human mesenchymal stromal cells in a 50 l single-use stirred tank bioreactor. *Biochemical Engineering Journal*, 120:49–62, 2017.

[14] C. Ferrari, F. Balandras, E. Guedon, E. Olmos, I. Chevalot, and A. Marc. Limiting cell aggregation during mesenchymal stem cell expansion on microcarriers. *Biotechnology Progress*, 28(3):780–787, 2012.

[15] J. Leber, J. Barekzai, M. Blumenstock, B. Pospisil, D. Salzig, and P. Czermak. Microcarrier choice and bead-to-bead transfer for human mesenchymal stem cells in serum-containing and chemically defined media. *Process Biochemistry*, 59:255–265, 2017.

[16] S. Derakhti, S. H. Safiabadi-Tali, G. Amoabediny, and M. Sheikhpour. Attachment and detachment strategies in microcarrier-based cell culture technology: A comprehensive review. *Materials Science and Engineering: C*, page 109782, 2019.

[17] J. Curran, R. Chen, and J. Hunt. Controlling the phenotype and function of mesenchymal stem cells in vitro by adhesion to silane-modified clean glass surfaces. *Biomaterials*, 26(34):7057–7067, December 2005.

[18] S. Sart, S. N. Agathos, and Y. Li. Engineering stem cell fate with biochemical and biomechanical properties of microcarriers. *Biotechnology Progress*, 29(6):1354–1366, November 2013.

[19] A. J. Engler, S. Sen, H. L. Sweeney, and D. E. Discher. Matrix Elasticity Directs Stem Cell Lineage Specification. *Cell*, 126(4):677–689, August 2006.

[20] G. Zhao, F. Liu, S. Lan, P. Li, L. Wang, J. Kou, X. Qi, R. Fan, D. Hao, C. Wu, et al. Large-scale expansion of whartons jelly-derived mesenchymal stem cells on gelatin microbeads, with retention of self-renewal and multipotency characteristics and the capacity for enhancing skin wound healing. *Stem Cell Research & Therapy*, 6(1):38, 2015.

[21] A. M. de Soure, A. Fernandes-Platzgummer, F. Moreira, C. Lilaia, S.-H. Liu, C.-P. Ku, Y.-F. Huang, W. Milligan, J. M. Cabral, and C. L. da Silva. Integrated culture platform based on

a human platelet lysate supplement for the isolation and scalable manufacturing of umbilical cord matrix-derived mesenchymal stem/stromal cells. *Journal of Tissue Engineering and Regenerative Medicine*, 11(5):1630–1640, 2017.

[22] P. A. Tozetti, S. R. Caruso, A. Mizukami, T. R. Fernandes, F. B. da Silva, F. Traina, D. T. Covas, M. D. Orellana, and K. Swiech. Expansion strategies for human mesenchymal stromal cells culture under xeno-free conditions. *Biotechnology Progress*, 33(5):1358–1367, 2017.

[23] A. Mizukami, A. Fernandes-Platzgummer, J. G. Carmelo, K. Swiech, D. T. Covas, J. M. Cabral, and C. L. da Silva. Stirred tank bioreactor culture combined with serum-/xenogeneic-free culture medium enables an efficient expansion of umbilical cord-derived mesenchymal stem/stromal cells. *Biotechnology Journal*, 11(8):1048–1059, 2016.

[24] J. Hupfeld, I. H. Gorr, C. Schwald, N. Beaucamp, K. Wiechmann, K. Kuentzer, R. Huss, B. Rieger, M. Neubauer, and H. Wegmeyer. Modulation of mesenchymal stromal cell characteristics by microcarrier culture in bioreactors. *Biotechnology and Bioengineering*, 111(11):2290–2302, 2014.

[25] V. Jossen, C. van den Bos, R. Eibl, and D. Eibl. Manufacturing human mesenchymal stem cells at clinical scale: process and regulatory challenges. *Applied Microbiology and Biotechnology*, 102(9):3981–3994, 2018.

[26] A. Shekaran, A. Lam, E. Sim, L. Jialing, L. Jian, J. T. P. Wen, J. K. Y. Chan, M. Choolani, S. Reuveny, W. Birch, and S. Oh. Biodegradable ECM-coated PCL microcarriers support scalable human early MSC expansion and in vivo bone formation. *Cytotherapy*, 18(10):1332–1344, October 2016.

[27] A. Tamura, J. Kobayashi, M. Yamato, and T. Okano. Thermally responsive microcarriers with optimal poly (n-isopropylacrylamide) grafted density for facilitating cell adhesion/detachment in suspension culture. *Acta Biomaterialia*, 8(11):3904–3913, 2012.

[28] M. Kim, J. Jeong, and T. Park. Swelling Induced Detachment of Chondrocytes Using RGD-Modified Poly(N-isopropylacrylamide) Hydrogel Beads. *Biotechnology Progress*, 18(3):495–500, June 2002.

[29] H. S. Yang, O. Jeon, S. H. Bhang, S.-H. Lee, and B.-S. Kim. Suspension Culture of Mammalian Cells Using Thermosensitive Microcarrier that Allows Cell Detachment without Proteolytic Enzyme Treatment. *Cell Transplantation*, 19(9):1123–1132, September 2010.

[30] H. Tavassoli, S. N. Alhosseini, A. Tay, P. P. Chan, S. K. Weng Oh, and M. E. Warkiani. Large-scale production of stem cells utilizing microcarriers: A biomaterials engineering perspective from academic research to commercialized products. *Biomaterials*, 181:333–346, October 2018.

[31] L. Reppel. *Potentialité des cellules stromales de la gelée de Wharton en ingénierie du cartillage*. PhD thesis, Université de Lorraine, 2014.

[32] D. J. Kim, J.-y. Heo, K. S. Kim, and I. S. Choi. Formation of thermoresponsive poly (n-isopropylacrylamide)/dextran particles by atom transfer radical polymerization. *Macromolecular Rapid Communications*, 24(8):517–521, 2003.

[33] C. Loubière, C. Sion, N. De Isla, L. Reppel, E. Guedon, I. Chevalot, and E. Olmos. Impact of the type of microcarrier and agitation modes on the expansion performances of mesenchymal stem cells derived from umbilical cord. *Biotechnology Progress*, page e2887, 2019.

[34] D. Schop, F. Janssen, E. Borgart, J. D. de Bruijn, and R. van Dijkhuizen-Radersma. Expansion of mesenchymal stem cells using a microcarrier-based cultivation system: growth and metabolism. *Journal of Tissue Engineering and Regenerative Medicine*, 2(2-3):126–135, 2008.

[35] S. Jung, K. M. Panchalingam, R. D. Wuerth, L. Rosenberg, and L. A. Behie. Large-scale production of human mesenchymal stem cells for clinical applications. *Biotechnology and Applied Biochemistry*, 59(2):106–120, 2012.

[36] T. J. Bartosh, J. H. Ylostalo, A. Mohammadipoor, N. Bazhanov, K. Coble, K. Claypool, R. H. Lee, H. Choi, and D. J. Prockop. Aggregation of human mesenchymal stromal cells (MSCs) into 3D spheroids enhances their antiinflammatory properties. *Proceedings of the National Academy of Sciences*, 107(31):13724–13729, August 2010.

[37] K. S. Brammer, C. Choi, C. J. Frandsen, S. Oh, and S. Jin. Hydrophobic nanopillars initiate mesenchymal stem cell aggregation and osteo-differentiation. *Acta Biomaterialia*, 7(2):683–690, February 2011.

[38] B. Fischer and B. Bavister. Oxygen tension in the oviduct and uterus of rhesus monkeys, hamsters and rabbits. *Reproduction*, 99(2):673–679, 1993.

[39] T. Ma, W. L. Grayson, M. Fröhlich, and G. Vunjak-Novakovic. Hypoxia and stem cell-based engineering of mesenchymal tissues. *Biotechnology Progress*, 25(1):32–42, 2009.

[40] A. Lavrentieva, I. Majore, C. Kasper, and R. Hass. Effects of hypoxic culture conditions on umbilical cord-derived human mesenchymal stem cells. *Cell Communication and Signaling*, 8(1):18, 2010.

[41] R. Bétous, M.-L. Renoud, C. Hoede, I. Gonzalez, N. Jones, M. Longy, L. Sensebé, C. Cazaux, and J.-S. Hoffmann. Human adipose-derived stem cells expanded under ambient oxygen concentration accumulate oxidative dna lesions and experience procarcinogenic dna replication stress. *Stem Cells Translational Medicine*, 6(1):68–76, 2017.

[42] N. Haque, M. T. Rahman, A. Kasim, N. Hayaty, and A. M. Alabsi. Hypoxic culture conditions as a solution for mesenchymal stem cell based regenerative therapy. *The Scientific World Journal*, 2013, 2013.

[43] C. Fehrer, R. Brunauer, G. Laschober, H. Unterluggauer, S. Reitinger, F. Kloss, C. Gülly, R. Gaßner, and G. Lepperdinger. Reduced oxygen tension attenuates differentiation capacity of human mesenchymal stem cells and prolongs their lifespan. *Aging Cell*, 6(6):745–757, 2007.

[44] J. Estrada, C. Albo, A. Benguria, A. Dopazo, P. Lopez-Romero, L. Carrera-Quintanar, E. Roche, E. Clemente, J. Enriquez, A. Bernad, et al. Culture of human mesenchymal stem cells at low oxygen tension improves growth and genetic stability by activating glycolysis. *Cell Death & Differentiation*, 19(5):743–755, 2012.

[45] D. Schop, F. W. Janssen, L. D. van Rijn, H. Fernandes, R. M. Bloem, J. D. de Bruijn, and R. van Dijkhuizen-Radersma. Growth, metabolism, and growth inhibitors of mesenchymal stem cells. *Tissue Engineering Part A*, 15(8):1877–1886, 2009.

[46] N. P. Barbara, J. L. Wrana, and M. Letarte. Endoglin is an accessory protein that interacts with the signaling receptor complex of multiple members of the transforming growth factor-β superfamily. *Journal of Biological Chemistry*, 274(2):584–594, 1999.

[47] S. Stopp, M. Bornhäuser, F. Ugarte, M. Wobus, M. Kuhn, S. Brenner, and S. Thieme. Expression of the melanoma cell adhesion molecule in human mesenchymal stromal cells regulates proliferation, differentiation, and maintenance of hematopoietic stem and progenitor cells. *Haematologica*, 98(4):505–513, 2013.

[48] E. Ortolan, P. Vacca, A. Capobianco, E. Armando, F. Crivellin, A. Horenstein, and F. Malavasi. Cd157, the janus of cd38 but with a unique personality. *Cell Biochemistry and Function: Cellular biochemistry and its modulation by active agents or disease*, 20(4):309–322, 2002.

[49] E. Ortolan, S. Augeri, G. Fissolo, I. Musso, and A. Funaro. Cd157: From immunoregulatory protein to potential therapeutic target. *Immunology Letters*, 205:59–64, 2019.

[50] K. Minas and J. Liversidge. Is the cd200/cd200 receptor interaction more than just a myeloid cell inhibitory signal? *Critical Reviews™ in Immunology*, 26(3), 2006.

[51] M. Najar, G. Raicevic, F. Jebbawi, C. De Bruyn, N. Meuleman, D. Bron, M. Toungouz, and L. Lagneaux. Characterization and functionality of the cd200–cd200r system during mesenchymal stromal cell interactions with t-lymphocytes. *Immunology Letters*, 146(1-2):50–56, 2012.

Chapter 4

An innovative perfused mode of culture of WJ-MSCs with empty microcarrier removal and on-line monitoring of cell concentration

Contents

Introduction

The development of bioprocesses able of producing large numbers of hMSCs in a robust and safe manner is crucial for therapeutic applications. Scalable expansion of hWJ-MSCs on Cytodex-1 or other types of microcarriers usually found in cell cultures, involved specific cell detachment using trypsin. However, trypsin or other cell detachment enzymes may provoke harmful effects on cell viability and cell detachment yield can be low (see Chapter 3). Besides, a filtration step is required because carriers remained in the cell culture medium. In this study, the efficiency of novel xeno-free dissolvable microcarriers for the culture and detachment of hWJ-MSCs was first evaluated in stirred tank bioreactors.

Then, in a second time and in order to improve cell expansion factor, a new continuous perfused mode of culture was proposed by implementing a settling tube inside the bioreactor and in order to improve cell expansion factor. The diameter of the tube was preliminary calculated to fulfill two process constraints. The first one is to maintain microcarriers colonized by cells in the bioreactor despite the continuous flow rate applied to ensure MSCs physiological requirements (definition of the continuous perfused mode). Moreover, it has been demonstrated in the Chapter 2 that cells were able to migrate towards fresh microcarriers added, but were not able to adhered any more on used microcarriers. Thus, during perfused cultures with additions of microcarriers, an increase in concentration of empty microcarriers may be expected in the STR, which could then lead to cell damage because of particle collisions, as shown in Erlenmeyer's flasks [1]. The strategy applied to this continuous perfused mode was thus to remove empty microcarriers (useless for cell expansion while potentially responsible of harmful bead-bead collisions), while maintaining microcarriers covered by cells inside the STR. These two requirements impose a precise determination of the draft tube design and perfusion rate. Lastly, aiming at proposing a on-line method of cell counting, the use of an on-line dielectric probe will be investigated to show whether measurements can be related to cell growth and adherence. Finally, a cost-analysis of the developed mode of culture is proposed and compared with standard modes of cultures of MSCs in STRs (batch or fed-batch). The global scope of Chapter 4 is synthesized on Figure 4.1.

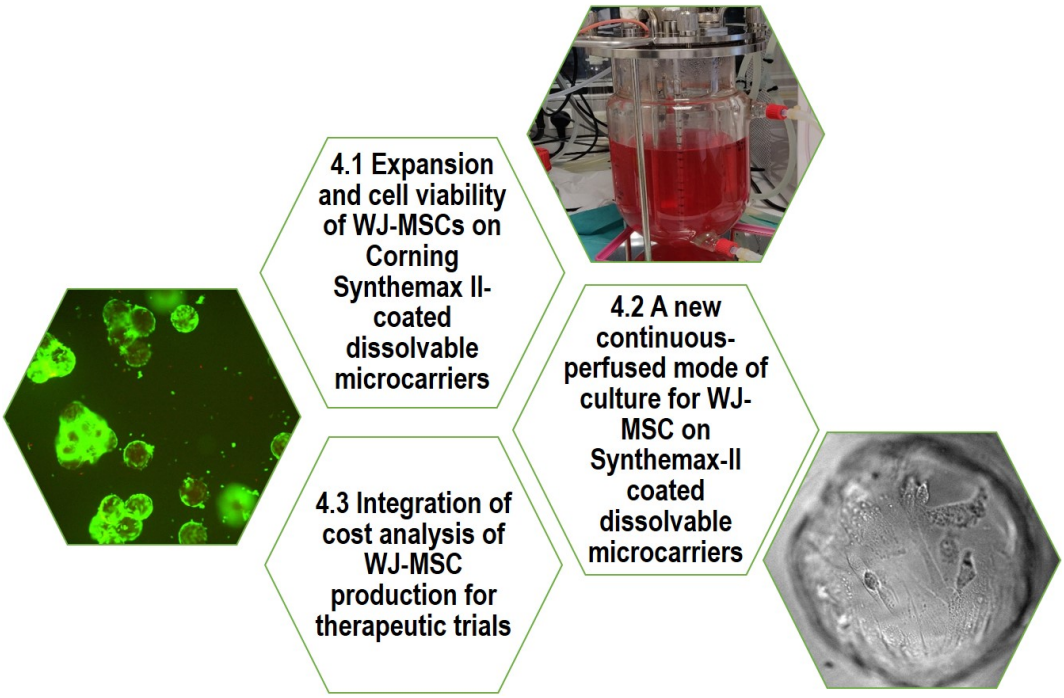

Figure 4.1 – Presentation of the different sections of chapter 4 to study the expansion and cell viability of WJ-MSCs on dissolvable microcarriers in batch and perfused mode.

4.1 Expansion and cell viability of WJ-MSCs on dissolvable microcarriers.

Material and Methods

Microcarrier preparation protocol

Corning Synthemax II-coated dissolvable microcarriers (Corning Cat No. 4983) were preliminary hydrated at a concentration of 6.7 g L^{-1} in sterile water with a gently swirling to ensure a homogeneous hydration while minimizing aggressive mixing and air incorporation. Once mixed, microcarriers were hydrated 10 minutes and subsequently rinsed with cell culture medium. Corning Synthemax-II coated dissolvable microcarriers are named as dissolvable microcarriers in the rest of the study.

WJ-MSC expansion on dissolvable microcarriers in 6-well plates

In order to evaluate cytotoxicity, attachment and detachment efficiencies of dissolvable microcarriers, cultures were carried-out with WJ-MSCs P4 using 6 well plates ultra-low attachment (Corning CLS3471) and compared with Cytodex-1 and PlasticPlus commercial microcarriers. They were loaded at a concentration of 2 g L^{-1} for dissolvable microcarriers , 2.35 g L^{-1} for Cytodex-1 and 25 g L^{-1} for PlasticPlus microcarriers, rinsed with cell culture medium and incubated at 37°C and 5 % of CO_2 in cell culture medium. After seeding cells at a cell density of 7,800 cells cm^{-2}, 6-well plates were agitated at 70 rpm after one hour without agitation in the incubator.

WJ-MSC expansion on microcarriers in spinner vessels, in batch mode

In siliconized spinner vessels, 2 g L^{-1} of dissolvable microcarriers and 2.35 g L^{-1} of Cytodex-1 were incubated with 100 mL of cell culture medium for one hour and, during this equilibration step, WJ-MSCs were tryspined. T-75 cm^2 flasks containing the cells were washed with 10 mL of dPBS, then cells were incubated with 2.5 mL of TrypLE™ Express Enzyme (1X) (Thermo Fisher Scientific Cat No. 12604013) for 3 minutes, then the action of the enzyme was inhibited with 10 mL of cell culture medium. Following cell dissociation, cells were centrifuged at 130 x *g* for 5 minutes. 1 mL of the cell suspension was collected in order to calculate the total number of cells and viability. Cells were seeded at a density of 4 000 cells cm^{-2}, and the final volume of the spinner vessel was 200 mL. The cell culture medium used was alpha-minimum essential medium (α MEM medium) (Lonza BE12-169F), supplemented with 5 % of Human Platelet Lysate (HPL) (Cook Regentec PL-NH-500), 4 mM glutamine (Sigma G7513), 1 % antibiotics (Antibiotic antimycotic solution, Sigma A5955), and a glucose final concentration of 3 g L^{-1}. For the attachment phase protocol, an intermittent agitation was applied: the first hour of culture was performed without agitation, then a 40-rpm agitation was applied. The culture was performed for 7 days in batch mode at this agitation rate.

Cell detachment from dissolvable microcarriers

Cells were harvested from the dissolvable microcarriers after 5 or 7 days of expansion. A harvest solution was prepared to fully dissolve the microcarriers and release the cells. It was recommended to use 250 mL of harvest solution per gram of dry microcarriers. The harvest solution is composed of 100 U/mL pectinase (MilliporeSigma Cat. No. P2611), 10 mM EDTA (Sigma), 1X TrypLE Express Enzyme (1X) (Thermo Fisher Scientific Cat No. 12604013). The harvest solution was filter-sterilized and pre-warm at 37°C prior to use. First, cell culture medium was removed, microcarriers were washed with dPBS. To dissolve the microcarriers 1 mL per well or 67 mL per spinner vessel of harvest solution was used, flasks were incubated for 10-15 min under agitation. Once a single cell suspension was observed, the cells were centrifuged, filtered and counted with the Vi-CELL XR Cell Viability Analyzer Counter.

Results

First, the efficiency of WJ-MSCs expansion on dissolvable microcarriers was assessed in low binding six well plates and compared with Cytodex-1 and PlasticPlus microcarriers performance. As presented in the figure 4.2, glucose consumption and lactate production were compared for the three cultures using these microcarriers. The consumption rate of glucose was the highest for Cytodex-1 (0.2 g/L/day), but WJ-MSCs consumed more glucose on dissolvable microcarriers (0.13 g/L/day) than on PlasticPlus microcarriers (0.1 g/L/day).

As presented by figure 4.3, the cell adherence on the dissolvable microcarriers was effective and the cell viability was also clearly maintained. After 5 days of culture, the efficiency of cell detachment was determined. As it could be observed on the figure 4.3, the microcarriers were efficiently dissolved and most of the cells detached from microcarriers.

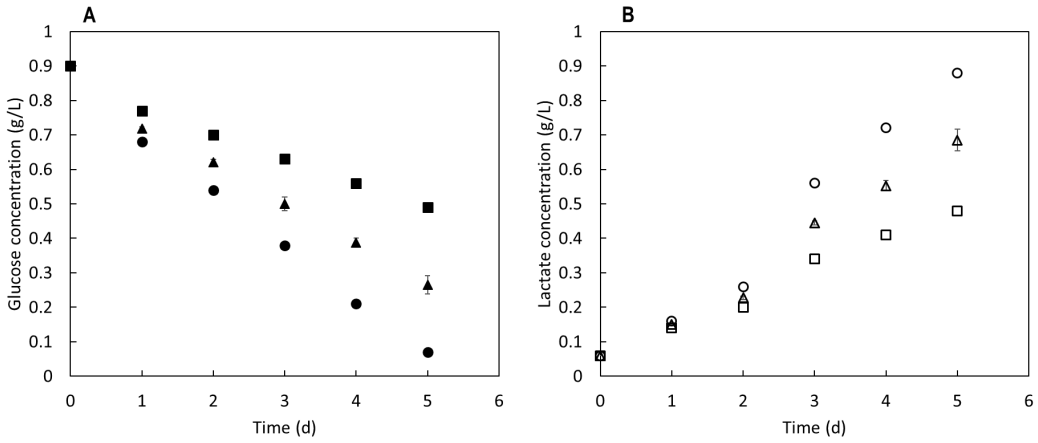

Figure 4.2 – Metabolite kinetics of WJ-MSCs using two types of microcarriers. (A) Glucose consumption during cultures using (•)-Cytodex-1, (▲)-dissolvable microcarriers and (■)-PlasticPlus microcarriers. (B) Lactate production during cultures using (∘)-Cytodex-1, (△)-dissolvable microcarriers and (□)-PlasticPlus microcarriers.

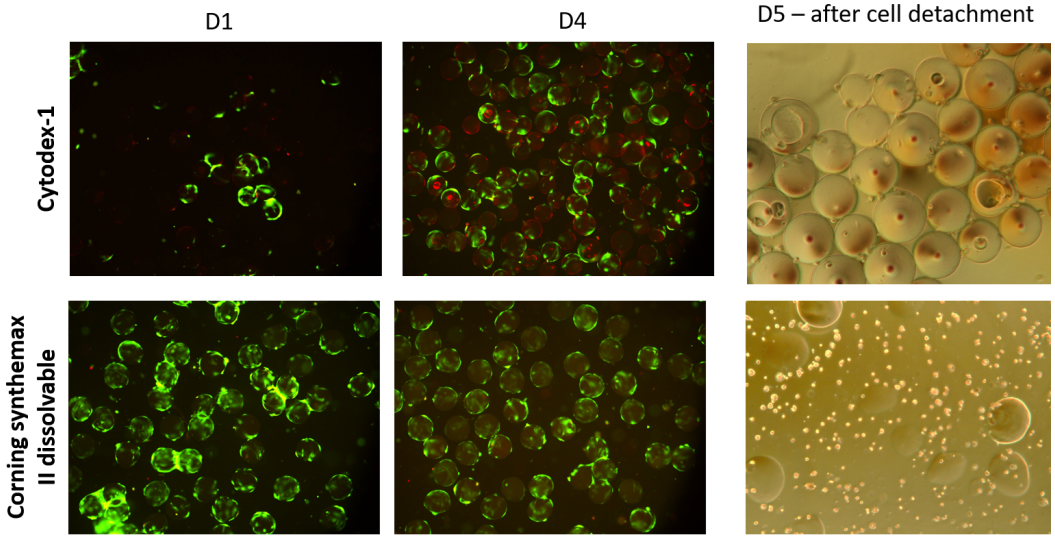

Figure 4.3 – Live/dead images of WJ-MSCs cultivated on Cytodex-1 or dissolvable microcarriers after one and four days of culture, and after cell detachment.

Secondly, cultures were carried-out in spinner vessels (SV) and compared to Cytodex-1 as a commercial reference (Figure 4.4). During the first days of culture, the total number of cells between cultures on dissolvable and Cytodex-1 microcarriers were similar. Then, from day 4, the cultures performed with dissolvable microcarriers permitted to obtain a good cell factor expansion (5). The maximal number of cells obtained in the SV were 40 and 50 millions approximately, in 5 and 7 days respectively, whereas the maximal number of cells obtained with Cytodex-1 was only about 10 million in 5 days (Figure 4.4). Thus, the expansion in dynamic cultures of WJ-MSCs on dissolvable microcarriers permitted to obtain a cell factor of expansion of 5±1 and with Cytodex-1 of 1.2. In these experimental conditions, a good cell viability was noticed as indicated by microscopic observations and the fluorescent staining. In literature, using these types of microcarriers, a 7-fold expansion factor was obtained in spinner vessels after 7 days of culture [2] with UC-MSCs, and a 4-fold expansion factor was obtained also in spinner vessels with induced pluripotent stem

cells (iPS) [3].

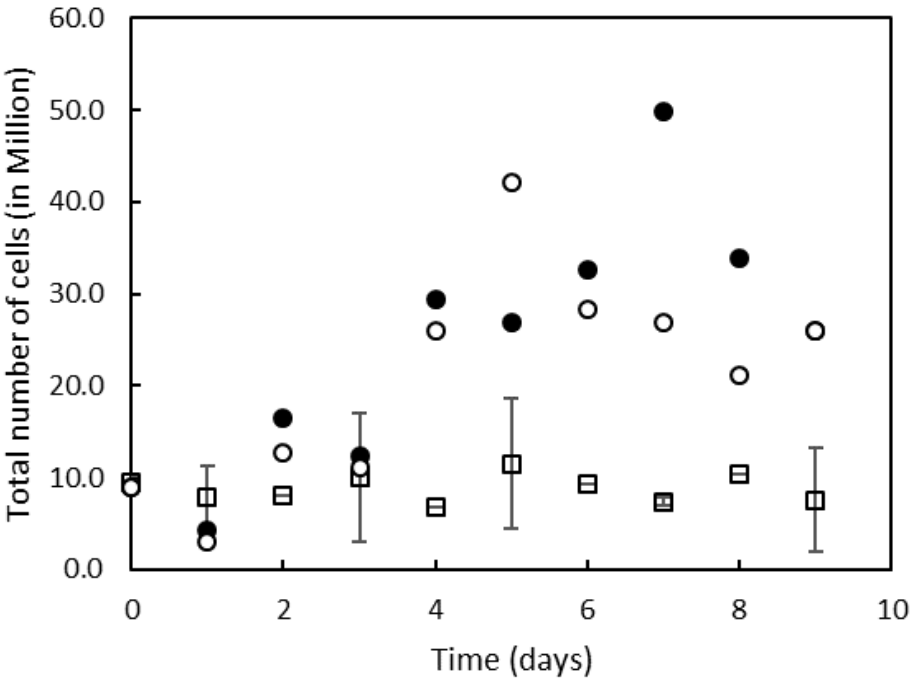

Figure 4.4 – Comparison of cell growth kinetics between WJ-MSCs grown on (□) Cytodex-1 or duplicate (○)-and (•) on dissolvable microcarriers in spinner vessels (n = 2).

Moreover, Dapi (Figure 4.5 A) and Live/dead (Figure 4.5 B) staining permitted to show the appearance of aggregates in day 7. Dissolvable microcarriers did not seem to be damage by the mechanical agitation despite they are composed of polygalaturonic polymers with a soft structure.

After these preliminary results, dynamics cultures in stirred tank bioreactor were performed. A comparison of the different expansion rates according to different culture modes was realized and a publication describing the main results will be submitted to Biotechnology and Bioengineering.

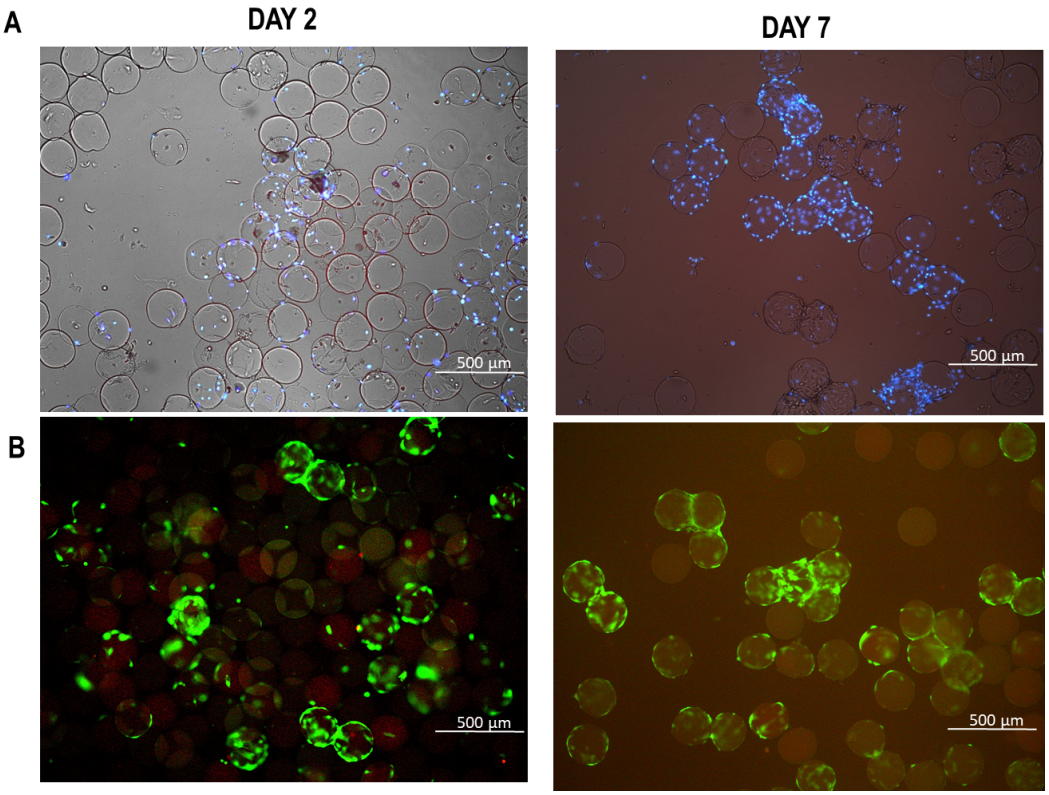

Figure 4.5 – Pictures of fluorescent staining of WJ-MSCs cultivated on Corning dissolvable microcarriers coated with Synthemax-II in spinner vessels. (A) Dapi staining at Day 2 and 7. (B) Live/dead staining at Day 2 and Day 7.

4.2 A new perfused culture mode for mesenchymal stem cell expansion in a stirred and on-line monitored bioreactor

A new perfused culture mode for mesenchymal stem cell expansion in a stirred and on-line monitored bioreactor

C. Sion, D. Ghannoum, F. Gallo, E. Guedon, I. Chevalot, E. Olmos

Abstract

Mesenchymal stem cells (MSCs) are expected to become powerful biologics for cell therapies and tissue engineering thanks to their inner characteristics. Wharton jelly mesenchymal stem cells (WJ-MSCs) represent, in particular, an attractive source of MSCs regarding a non-invasive procedure of extraction, the absence of ethical concerns for their use and a good proliferation rate. In order to meet the demand for treating patients at clinical scales, development of bio-processes at high scales for the generation of a significant number of WJ-MSCs is required. Since a clinical dose requires a minimum of 10^6 cells per kilogram of patients, it is therefore crucial to develop a scalable method of production of WJ-MSCs with maintained inner characteristics. Scalable expansion of WJ-MSCs on Cytodex-1 or other types of microcarriers usually found in cell culture, involved specific cell detachment using trypsin. Trypsin or other cell detachment enzymes could have harmful effects on cells and their viability. Therefore, the aim of this study is to analyze the efficiency of a xeno-free dissolvable microcarriers for MSC culture and detachment. In this work, performance of different modes of culture, batch, fed-batch and continuous-perfused mode respectively, were compared using these xeno-free dissolvable microcarriers. The batch and fed-batch modes resulted in expansion factors of 4 and 40, respectively. The continuous-perfused mode strategy consisted in the implementation of a settling tube inside the bioreactor. The diameter of the tube was calculated to precisely maintain microcarriers colonized by cells in the bioreactor whereas empty microcarriers were removed (useless for cell expansion while responsible of harmful bead-bead collisions) and using a continuous flow rate based on MSCs physiological requirements. Using this strategy a maximal number of 800 million of cells was obtained in 1.5 L bioreactor in 10 days. Lastly, on-line monitoring of permittivity was implemented in the stirred tank bioreactor and indicated that measurements could be related to cell growth and probably adherence.

Introduction

Mesenchymal stem cells (MSCs) are of great interest in clinical trials because they have been shown to treat many diseases, such as cardiac, immune, neurodegenerative and orthopaedic diseases [4]. The reasons why MSCs are promising candidates for cell therapy are numerous, thanks to their ease of isolation and expansion *in vitro*, paracrine effects, as well as their immunomodulatory properties. MSCs can be isolated from a large variety of tissue or organs such the bone marrow [5], adipose tissue [5], muscles [6] and peripheral bloods [7] or perinatal tissues [8, 9]. In recent years, Wharton Jelly Mesenchymal Stem Cells (WJ-MSCs) have been studied more and

more because of the absence of ethical problems regarding their use, their youthful character, faster doubling population than adult MSCs, and the lack of some immune suppression properties present in the adult MSCs [10]. However, the only isolation from tissues or organs does not provide sufficient quantities of cells to meet clinical doses and therapeutic uses; *in vitro* expansion is thus necessary. In particular, development of cultures in stirred tank bioreactors (STR) is compatible with clinical-scale GMP MSCs expansion and overcomes limitations of 2D culture in flasks [11].

As MSCs are adherent-dependent cells, adhesion surfaces are required to expand them in STR. The most widely used technique is the use of microcarriers, small particles of 100 - 300 µm, that can be synthesized from different materials such as plastics (polystyrene, polyethylene, polyester, polypropylene), glass, acrylamide, silica, cellulose, dextran, collagen, glycosaminoglycan, and designed to be either non-porous (*e.g.* plastic microcarriers), microporous (*e.g.* dextran based microcarriers) or macroporous (*e.g.* gelatin type microcarriers). Apart from the core material that defines the matrix of each microcarriers, some functionalized surfaces are added in order to improve either cell adhesion, growth or detachment. After the cell expansion, a step of detachment is required to harvest the cells. Proteolytic enzymes are often used, as for example trypsin, to harvest the cells. But detachment yields can dramatically drop if non-optimized conditions are applied. Employment of proteolytic enzymes for detachment can also lead to damages of the cell membrane proteins and to a decrease of cell viability [12]. This leads to a decrease of grafting efficiency in transplantation [13], and to overcome these difficulties, environmentally sensitive microcarriers have been developed such as temperature-sensitive microcarriers, pH-sensitive microcarriers and finally field-sensitive microcarriers (photo-, electro-, magnetic- and ultrasound field-sensitive) [13]. Dissolvable microcarriers could provide a promising solution for cell harvesting. They are indeed made of cross-linked polysaccharide polymers, dissolvable under the action of an enzymatic mix [2].

Thanks to classical on-line monitoring in STR culture, temperature can be set at 37°C, pH between 7.2 and 7.4, and generally, in MSCs cultures, hypoxia condition is preferred and the value of dissolved oxygen (DO) was set at 20 % of air saturation. Agitation must be precisely defined to effectively homogenize the liquid-solid suspension, to allow good oxygen transfer, while limiting mechanical hydrodynamic stresses. The possibility of on-line monitoring and the agitation systems make it possible to obtain homogeneous cultures with reduced culture handling and costs. MSC cultures on microcarriers were mostly performed in batch mode in bioreactors with volumes from one up to ten liters. As for example, Hupfeld *et al.* (2014) developed cultures in STR with Cytodex-1 to expand umbilical cord derived MSCs (UC-MSC) [14]. In 2016, Mizukami *et al.* expanded UC-MSCs on CultisphereS in 0.8 L STR in xenogenic-free cell culture medium [15]. Finally, in 2017, Tozetti *et al.* cultivated UC-MSCs on PlasticP102-L in 0.8 L STR in serum-based cell culture medium [16]. Moreover, MSCs viability and cell growth may also be monitored with dielectric spectroscopy probes as demonstrated by Justice *et al.* (2011) [17]. Other authors as Lawson *et al.* (2016) or Dos Santos *et al.* (2014) applied a fed-batch mode in STR for the expansion of bone marrow and umbilical cord derived MSCs, respectively [18, 19]. Feeding strategies were

proposed in order to provide nutrients supply and to limit concentration of metabolic products to non-inhibitory levels. In this study, the fed-batch method used by Lawson *et al.* [18] was implemented with the microcarrier feed strategy developed in Chapter 2. Strategies of human Wharton Jelly's MSCs expansion process in 1.5 L bioreactor were also investigated with dissolvable microcarriers. First, a controlled addition of microcarriers was implemented. Liquid volume of the culture was progressively increased from 500 mL to 1.5 L (fed-batch mode) and cell expansion was achieved without so-called 'passage'. However, as fed-batch mode does not permit to eliminate the toxic metabolites that accumulate during the cell culture, but only slows it down, perfusion mode was also studied for the expansion of MSCs. In 2013, Mizukami *et al.* indeed developed a fixed-bed bioreactor for UC-MSCs with an expansion factor of 7. Moreover, Dos Santos *et al.* (2014) also proposed a continuous perfused bioreactor with BM-MSCs cultivated on Plastic P102L microcarriers, with an expansion factor of 18.5. Finally, Cunha *et al.* (2015) used a system of cell retention based on a tangential flow filtration system, with only one addition of microcarriers at day 6, and obtained a 14.6 expansion factor [20]. However, in classic cell retention devices used during cultures with microcarriers, no sorting between the empty and colonized microcarriers were carried out. As observed in fed-batch bioreactors (see Chapter 3, Figure 3.15), some empty microcarriers were indeed observed. These useless microcarriers will never be re-colonized and thus only favour cell damages, as demonstrated in the Chapter 2. Thus the strategy of this study is to propose an innovative system of production removing 'on-line' these microcarriers, useless for cell expansion while responsible of harmful bead-bead collisions, as shown by Sion *et al.* [1]. Therefore, the second strategy consisted in a new continuous perfused mode of culture by implementing a settling tube placed inside the bioreactor, to solve this issue. The diameter of the tube was calculated to precisely maintain microcarriers colonized by cells in the bioreactor whereas empty microcarriers were removed , using a continuous flow rate based on MSCs physiological requirements. Lastly, on-line dielectric probe indicated that measurements could be related to cell growth and thus be used to monitor cell concentration.

The different modes of production used for the WJ-MSCs expansion on dissolvable microcarriers are presented in the Figure 4.6.

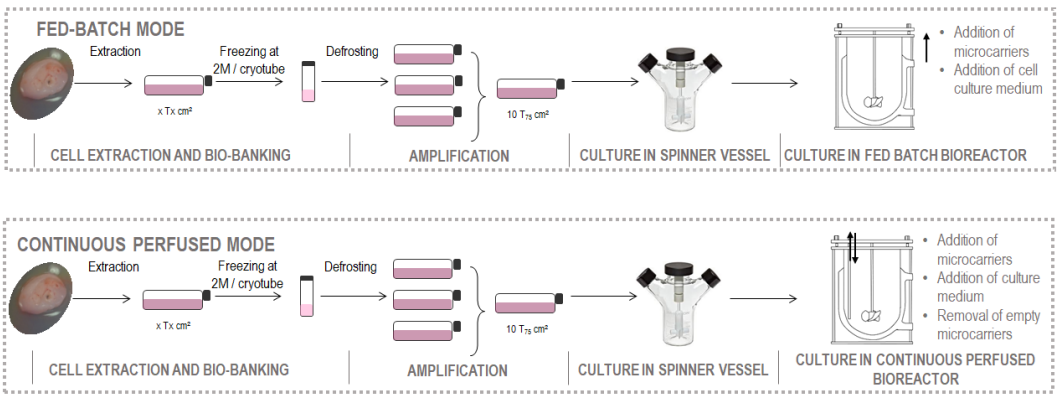

Figure 4.6 – Diagram illustrating the two modes of production of WJ-MSCs on dissolvable microcarriers.

Material and Methods

Cell extraction and primary cell culture of WJ-MSC

Umbilical cord stem cells were extracted from fresh umbilical cords of just born babies (Centre Hospitalier Universitaire Nancy, France). Umbilical cords were treated during the 24 h following the birth. The method of extraction was non-enzymatic using cells spontaneous migration on 175 cm^2 plastic culture flasks [21]. The cell culture medium was alpha-minimum essential medium (α MEM medium) (Lonza BE12-169F), supplemented with 5 % of Human Platelet Lysate (HPL) (Cook Regentec PL-NH-500), 4 mM glutamine (Sigma G7513), 1 % antibiotics (Antibiotic antimycotic solution, Sigma A5955), and 2 IU/mL heparin (Sigma H3149). The medium was changed twice a week. After ten days, the remaining adherent cells were trypsinized and seeded in new 175 cm^2 T-flasks at a density of 1000 cells cm^{-2}. After one supplementary passage, WJ-MSC were pooled and cryopreserved at a concentration of 2×10^6 cells mL^{-1}, in fetal bovine serum and 10 % of dimethyl sulfoxyde (DMSO) for cell banking and kept in liquid nitrogen. Thereafter, cells were thawed and seeded at a concentration of 1000 cells cm^{-2} in T-75 cm^2 flasks and cultivated for a week before their use in dynamic conditions.

Microcarrier preparation protocol

Corning Synthemax II-coated dissolvable microcarriers (Corning Cat No. 4983) were preliminary hydrated at a concentration of 6.7 g L^{-1} in sterile water with a gently swirling to ensure a homogeneous hydration while minimizing aggressive mixing and air incorporation. Once mixed, microcarriers were hydrated 10 minutes and subsequently rinsed with cell culture medium.

WJ-MSC expansion on microcarriers in stirred tank bioreactors, in fed-batch mode

For larger scale expansion, the cultures were carried-out in stirred tank bioreactor (Tryton, Pierre Guerin). First, 0.2 g of dissolvable microcarriers were added in siliconized spinner vessel with cell culture medium. The WJ-MSCs were trypsinized and seeded onto the microcarriers at a cell density of 9000 cells cm^{-2}, in a final volume of 200 mL in spinner vessels (SV). After one hour in static conditions, cultures were agitated at 40 rpm using magnetic stirring in spinner vessels (SV). After culture overnight, the suspension was transferred into a stirred tank bioreactor (STR) (Tryton, Pierre Guerin) with the same amount of empty microcarriers (0.2 g for Corning Synthemax II-coated dissolvable microcarriers). Volume of liquid was completed to 500 mL with cell culture medium. The cells attached on the initial microcarriers and the new empty microcarriers settled for one hour, then an intermittent agitation at 70 rpm was applied, then stopped for one more hour. Finally, a continuous agitation at 70 rpm was set.

pH was adjusted to 7.4 and dissolved oxygen concentration to 20 % of air saturation. The pH control was performed by addition of base (NaOH 0.1 M) or by CO_2 injection in the headspace of the bioreactor. Dissolved oxygen concentration was maintained by headspace flushing of nitrogen and oxygen. Agitation rate was adjusted to 70 rpm in order to reach the just-suspended state, with an axial impeller HTPG. The temperature was controlled to 37°C using a hot water jacket. Cultures

were daily visually monitored under a microscope for counting, and for viability. From day 4, and each two days, 20 mL of fresh microcarriers at a concentration of 6.7 g L^{-1} was added with 200 mL of cell culture medium into the stirred tank bioreactor. After each microcarrier and cell culture medium addition, the agitation was stopped for one hour in order to favour cell migration. Then, an intermittent agitation at 70 rpm was applied for 10 minutes and stopped for one more hour. Finally, continuous agitation was settled at 70 rpm.

WJ-MSC expansion on microcarriers in stirred tank bioreactors in continuous-perfused mode

After 7 days of culture in fed-batch mode, a continuous withdrawal of the culture supernatant was started while the fresh medium was continuously supplied with the same flow rate of 0.48 vol d^{-1}, *i.e.* 0.37 mL min^{-1}, approximately one liquid volume replacement each two days. In order to avoid cells washout, the bioreactor was fitted with a perfusion system based on the settling principle. It is a 4.5 mm diameter tube with an inner 1 mm diameter sampling PTFE hose.

• **Settling tube design**

Sizing of the tube was based on the terminal velocity difference between empty and loaded microcarriers. Thus, it was necessary to determine the terminal velocity of empty microcarriers and as well as microcarrier aggregates. Then, according to these values, the settling tube diameter was determined in order to pump only used cell culture medium and empty microcarriers.

First, after image analyzing, a mean diameter of cell aggregates was determined in function of the time of culture (data not shown), and a sedimentation velocity was calculated.

The terminal falling velocity u_t can be determined by the following correlations, Re_t=f(Ar) with Re_t the terminal Reynolds number and Ar the Archimedes number, respectively defined by equations Eq. 4.1 and Eq. 4.2.

$$Re_t = \rho_L \cdot u_t \cdot d_p / \mu_L \tag{4.1}$$

$$Ar = \rho_L \cdot (\rho_p - \rho_L) \cdot g \cdot d_p^3 / \mu_L^2 \tag{4.2}$$

with ρ_L the density of liquid (993 kg m^{-3}) and ρ_p, the density of microcarriers (1030 kg m^{-3}) at 37°C, d_p the microcarrier diameter or aggregate diameter, g the gravity and μ_L (μ_L = 0.7 mPa s) the viscosity of the liquid. Regarding the low volume fraction of microcarriers, it was supposed that the settling velocity of microcarrier dispersion was similar to single particle's one.

The calculation of the terminal falling velocity of microcarrier aggregates was based on an aggregation of two microcarriers and with a mean diameter of 420 µm. The Archimedes number obtained was Ar = 62 and for empty microcarriers with a mean diameter of 200 µm, the Archimedes number obtained was Ar = 6.7. For a small particle moving slowly in a viscous fluid the inertia forces are low and therefore the viscous forces are preponderant (Stokes regime). In the Stokes regime, an analytical relationship exists between Archimedes and Reynolds numbers (Eq. 4.3).

$$Re_t = Ar/18 \tag{4.3}$$

Finally, the terminal falling velocity u_t could be calculated by the equation Eq. 4.4:

$$u_t = g \cdot d_p^2 \cdot (\rho_p - \rho_L)/(18\mu_L) \tag{4.4}$$

For microcarrier aggregates, a theoretical terminal falling velocity $u_{t,agg}$ of 5.8 mm s^{-1} was found and, for empty microcarriers, a theoretical terminal falling velocity $u_{t,empty}$ of 1.3 mm s^{-1} was calculated. Thus, it is theoretically easily possible to discriminate by the terminal falling velocity u_t the empty microcarriers from the aggregates. Experimentally, the rate of sedimentation of empty microcarriers was also determined and $u_{t,empty}$ was 3 mm s^{-1}. By choosing a tube of diameter of 4.5 mm and with a PTFE sampling hose of 1 mm of inner diameter, with a flow rate of 0.48 vol day^{-1} (0.37 mL min^{-1}), the withdrawal of empty microcarriers should be possible while maintaining the cell aggregates inside the STR.

• **Analysis of fluid flow in the settling tube**

In the cylindrical tube the assumption of a laminar regime with a parabolic profile was made. Thus, in these conditions, the maximal velocity of the fluid u_{max} is:

$$u_{max} = 2 \cdot \langle u \rangle \tag{4.5}$$

with $\langle u \rangle$, and the diameter D (m) can then be calculated, as :

$$D = 2 \cdot \sqrt{\frac{2Q}{\pi u_{max}}} \tag{4.6}$$

with Q the flow rate (m^3 s^{-1}). The settling condition applied on u_{max} is:

$$u_{t,empty} < u_{max} < u_{t,agg} \tag{4.7}$$

Finally, once D and Q were set, the laminar regime hypothesis is verified by first determining the mean velocity.

$$\langle u \rangle = \frac{4Q}{\pi D^2} \tag{4.8}$$

with $Q = 6.2 \cdot 10^{-9}$ m^3 s^{-1}, and $D = 4.5$ mm, the value of $\langle u \rangle$ obtained was $4.3 \cdot 10^{-4}$ m s^{-1}, and u_{max} was calculated as $8.6 \cdot 10^{-4}$ m s^{-1}, inferior to the value of the falling velocity of aggregates ($u_{t,agg}$ = $5.8 \cdot 10^{-3}$ m s^{-1}), but close to the falling velocity of empty microcarriers ($u_t = 1.3 \cdot 10^{-3}$ m s^{-1}).

Calculation of a Reynolds number was possible thanks to Eq. (4.9):

$$Re = \frac{\rho \langle u \rangle D}{\mu} \tag{4.9}$$

The calculated Reynolds number was 1.38, which is inferior to 2100, confirming the laminar regime inside the settling tube. The efficiency of the settling tube was verified experimentally: less than 2 % of microcarrier aggregates were counted in the withdrawal liquid.

WJ-MSC growth analysis

Three homogeneous samples of 1 mL were daily taken and settled in three Eppendorf tubes. The supernatants were discarded and 1 mL of the harvest solution was added in each Eppendorf tubes, incubated for 10 minutes under agitation. After the total dissolution of the microcarriers, the solution was filtered through a 40-µm filter, and then cells were counted using Vi-CELL XR Cell Viability Analyzer Counter (Beckman Counter), based on a Trypan Blue Dye Exclusion method. This harvest solution was previously prepared in order to fully dissolve the microcarriers and release the attached cells. 250 mL of harvest solution was composed of 6.6 mL of pectinase (MilliporeSigma Cat. No.P2611), 5 mL of EDTA 0.5 M (Sigma), and 238.4 mL of TrypLE™ Express Enzyme (1X) (Thermo Fisher Scientific Cat No. 12604013).

A fluorescent staining of the cells was performed for quantification of cell distribution on microcarriers. Every days, 500 µL of homogeneous sample was withdrawn from the STR. The supernatant was discarded and 0.5 mL solution of DAPI (1 µg/mL) (Sigma 10236276001) prepared in methanol was added to the cells on microcarriers. After fifteen minutes of incubation protected from the light, samples were washed with PBS and observed by epi-fluorescence microscopy. Six different areas were randomly chosen per sample and for each area two pictures were taken: one with the bright field and the other with the fluorescent field [1].

The viability was determined using a Live/Dead staining (Calcein AM/ Ethidium Homodimer, Life Sciences, ThermoFisher). The supernatant was discarded and the samples were incubated with 3 µM of calcein AM and 3 µM of ethidium homodimer-1 for thirty minutes in the dark at 37 °C and 5 % CO_2. Samples were then visualized with a Leica LEITZ DMR epi-fluorescence microscope.

WJ-MSC metabolite analysis

Analysis of glucose, lactate and lactate dehydrogenase (LDH) concentrations in the culture medium were performed using the Gallery multiparametric analyzer (Thermo Fisher Scientific).

Specific metabolite consumption/production rates (q_{Met} in pmol cell^{-1} day^{-1}) were averaged over the exponential phase of growth following equation 4.10:

$$q_{\mathrm{M}et} = \frac{\Delta_{\mathrm{M}et}}{\Delta_t \cdot \overline{\mathrm{X}}_v} \tag{4.10}$$

where $\Delta_{\mathrm{M}et}$ is the variation of nutrient/metabolite quantity during the time interval (Δ_t) and $\overline{\mathrm{X}_v}$ is the average viable cell number for that period. For the stirred tank bioreactors realized in continuous-perfused mode, the specific metabolite consumption/production rates (q_S and q_P) were calculated on short intervals taking into account the intake and withdrawal of the medium with a perfusion rate $D = Q/V$ and the supply concentration of substrate S_0.

$$q_{\mathrm{S}} = \frac{1}{\mathrm{X}} \cdot \left[\mathrm{D} \cdot (\mathrm{S}_0 - \mathrm{S}) - \frac{\mathrm{dS}}{\mathrm{d}t} \right] \tag{4.11}$$

with X, the concentration of cells (cell L^{-1}), D the perfusion rate (day^{-1}), S the concentration in glucose (g L^{-1}) and S_0 (g L^{-1}) the concentration in glucose of the fresh medium added. The specific

metabolite consumption (q_S) is expressed in pmol cell^{-1} day^{-1}.

$$q_P = \frac{1}{X} \cdot \left[D \cdot P + \frac{dP}{dt} \right] \tag{4.12}$$

with X, the concentration of cells (cell L^{-1}), D the perfusion rate (day^{-1}) and P the concentration in lactate. The specific lactate production (q_P) is expressed in pmol cell^{-1} day^{-1}.

The yield of lactate on glucose was calculated during the exponential phase, with the following equation 4.13

$$Y_{Lac/Glu} = q_{lac} / q_{glu} \tag{4.13}$$

Where q_{lac} is the specific rate of lactate produced by cells (mol cell^{-1} day^{-1}) and q_{glu}, the specific rate of glucose consumed by cells (mol cell^{-1} day^{-1}) during the exponential phase.

Release of LDH, an enzyme involved in the production of lactate in the cell culture medium is usually linked to cell damages (e.g. disrupted membranes) and thus cell death. As a control sample, two samples of 5 million of cells were subjected to three cycles of freezing at -80 °C and thawing at 37 °C, which ensured lysis of all cells. The LDH release was then measured by absorbance using the Gallery multiparametric analyser and the kit of dectection LDH (SCE) (Reference 981781). As reference, the lysis of 5 million of cells produced an average of 876 units.

Flow cytometry analysis

The protocol used for the flow cytometry analysis is the same that the one used in the chapter 3 (Section 3.2 Expansion of Wharton's jelly mesenchymal stem cells cultivated on innovative microcarriers in fed batch bioreactors) in the material and methods part.

Results

4.2.1 Dynamic expansion of WJ-MSCs on dissolvable microcarriers

For scale-up purpose, the cultures of WJ-MSCs performed in stirred tank bioreactors were considered with an addition of fresh microcarriers from Day 4 and each two days, in order to avoid a stop of growth due to a limitation of cell adhesion surfaces.

As shown by cell growth curves obtained in fed-batch mode (Figure 4.7), a latency occurred during the first two days of culture, then, from day 3, the exponential phase began. The maximal number of cells (215 and 220 million of cells) were obtained at Day 12 or Day 13 respectively. Then, the total number of cells decreased. The cell expansion factor obtained was about 43±3, with a maximal growth rate of 0.3 day^{-1}. In Rodriguez *et al.* study [3], expansion of iPSC on dissolvable microcarriers led to expansion factor of 6.7, using a vertical-wheel single-use bioreactor. It seems that after addition of microcarriers in stirred tank bioreactor, as proposed in the present study, WJ-MSCs were able to migrate towards new particles thanks to the bead-to-bead transfer, and permitted to produce a higher amount of viable cells. Indeed, percentage of cell colonization on microcarriers was high and only a few empty microcarriers were visible (Figure 4.8). Scaling-up

cultures from spinner vessels to stirred tank bioreactor was thus possible and increased the yield of cell production.

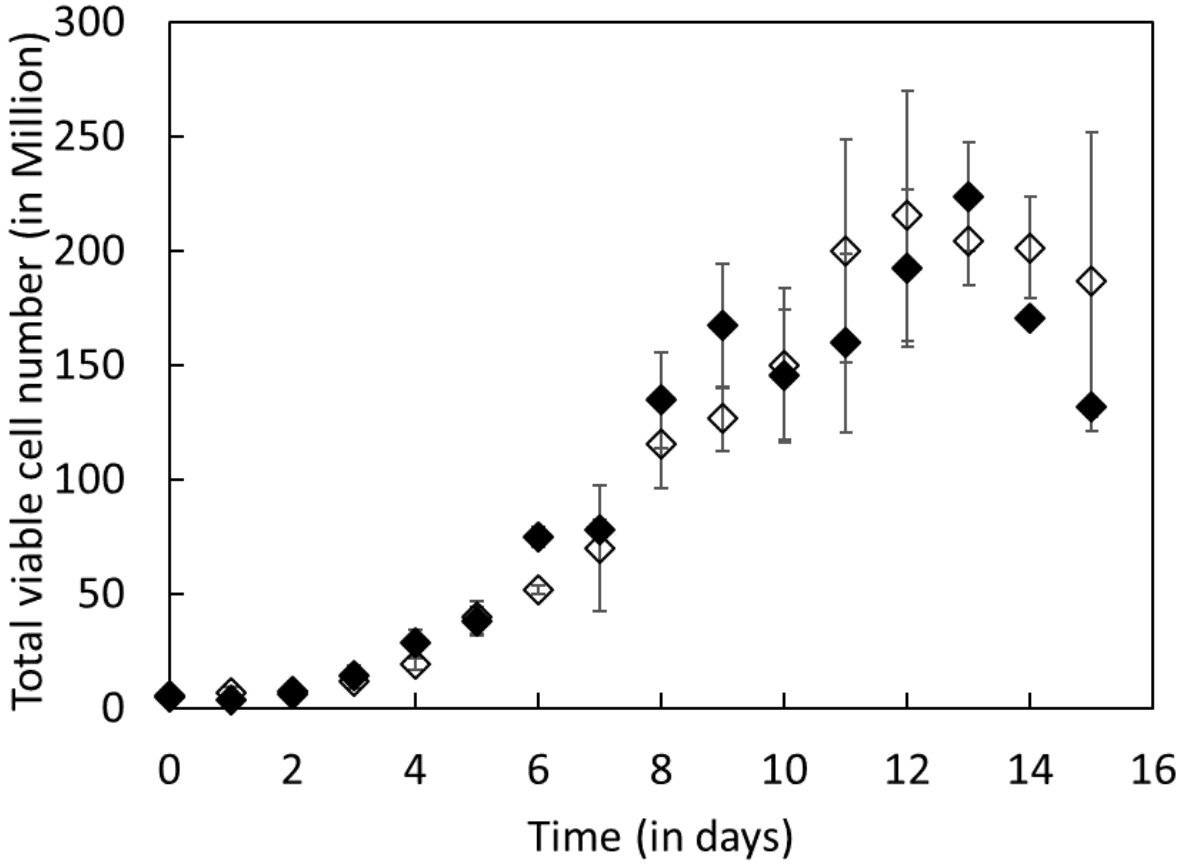

Figure 4.7 – Cell growth kinetics of WJ-MSCs cultivated on dissolvable microcarriers in fed-batch mode (STR ; n = 2).

As in SV cultures, cells were monitored everyday and fluorescent staining were carried-out and showed that the culture conditions in STR did not impact the cell morphology and the cell adhesion. As presented in the figure 4.8, microcarrier aggregates also appeared in day 7, and increased in size, as observed at day 11. Thus indicating that the addition of fresh microcarriers favored aggregate size increase. However, as shown on the live/dead image at day 11 (Figure 4.8), some microcarriers were occupied by dead cells, and as demonstrated in the chapter 2, they were no longer usable by cells. It can be thus interesting to remove those empty microcarriers, no longer usable by cells, in order to limit the increase in concentration of microcarriers while addition of fresh microcarriers, usable by cells, was carried-out.

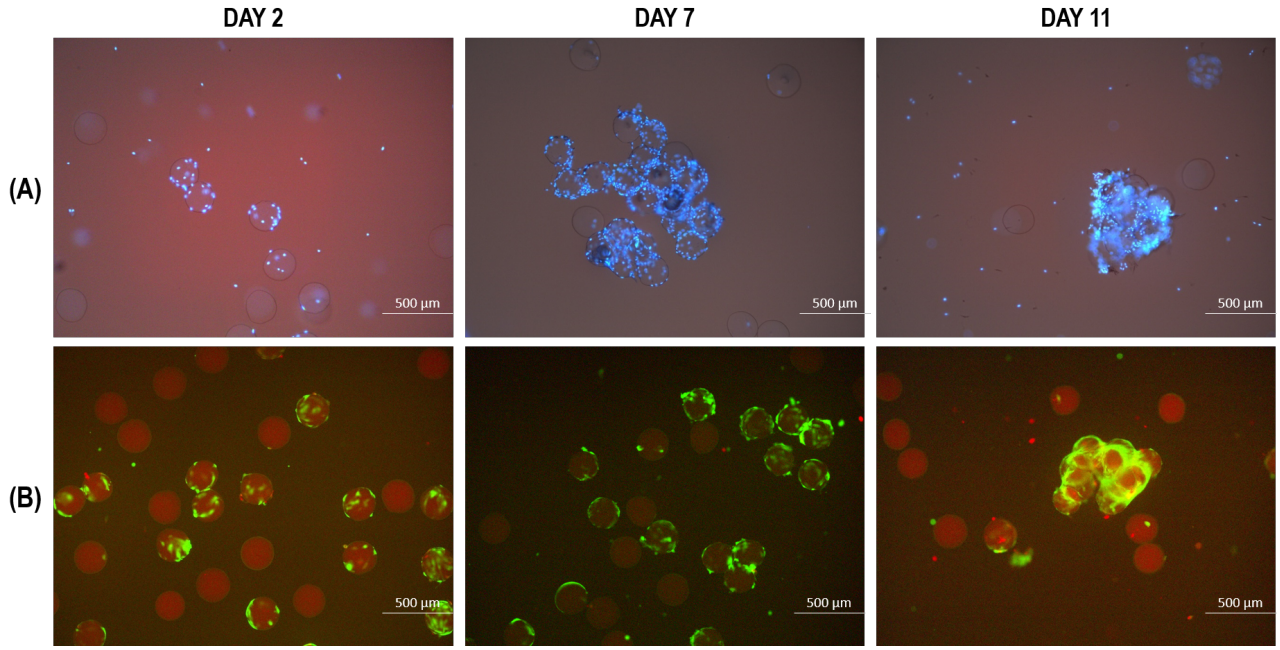

Figure 4.8 – Pictures of fluorescent staining of WJ-MSCs cultivated on dissolvable microcarriers in fed-batch STR. (A) Dapi staining at Days 2, 7 and 11. (B) Live/dead staining at Days 2, 7 and 11.

4.2.2 A new continuous-perfused mode of culture for WJ-MSCs on dissolvable microcarriers

Cell growth in the continuous-perfused stirred tank bioreactor

As soon as the first aggregates appeared (day 7 of culture), the perfusion were switched on. According to the figure 4.9, the maximal specific growth rate was higher during the perfusion mode than during the fed-batch mode (day 1 to 6) with a doubling population time of 1.5 day whereas in fed-batch mode this doubling population time was about 3 days (Figure 4.7 and Figure 4.9). The maximal number of cells was obtained at Day 9 and Day 10, with about 600 million and 800 million cells respectively. The expansion factor obtained thanks to the continuous-perfused mode was 60±17, whereas it was only of 5±1 in SV, and 43±3 in fed-batch mode. In comparison, in the study of Dos Santos *et al.* [19], a 18.5-fold expansion factor was obtained in perfused mode. On the other hand, in Cunha *et al.* study [20], a 14.5 fold expansion factor was obtained by using a tangential flow filtration system to maintain both cells and microcarriers in the stirred tank bioreactor.

Live/dead images and Dapi staining permitted to qualitatively observe a good cell viability but also the formation of aggregates (Figure 4.10). Moreover, no empty microcarriers were observed on these representative pictures.

Metabolic kinetics in continuous-perfused mode

Concerning the metabolic kinetics, yields of lactate on glucose were calculated and compared between batch, fed-batch and continuous-perfused modes. Yields of lactate on glucose values provide a good overview of the metabolic pathway used to produce energy for cells. In the expansion

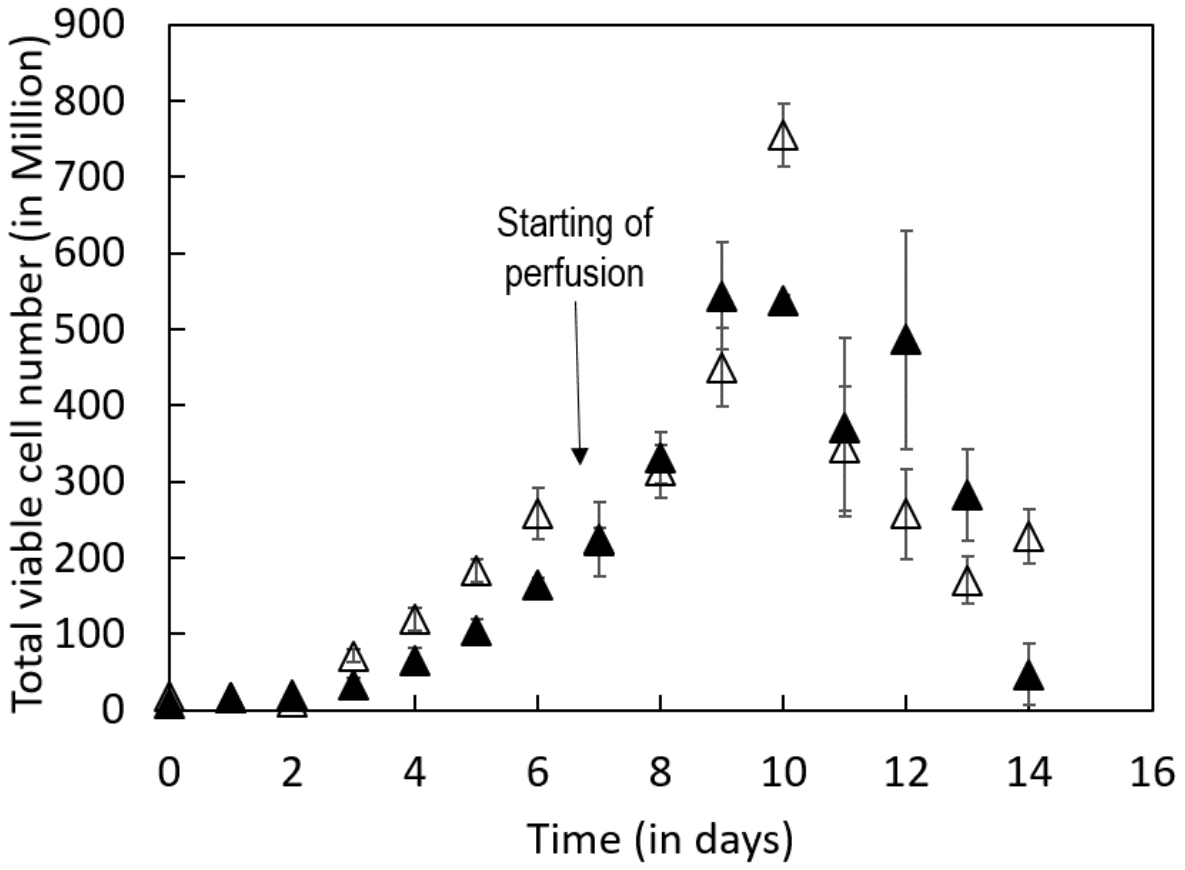

Figure 4.9 – Cell growth kinetics of WJ-MSCs grown on dissolvable microcarriers in continuous-perfused STR (n = 2).

of WJ-MSCs on dissolvable microcarriers, yields of lactate on glucose were lower than 1, as presented in the figure 4.11 A. Thus, with a yield of lactate on glucose (g/g) equal or higher than 1, glycolysis is mainly used by cells to produce energy, while with a yield of lactate on glucose (g/g) lower than 1 glycolysis and the tricarboxilic acid (TCA) cycle and the mitochondrial respiratory chain are used by cells. It was thus demonstrated that WJ-MSCs cultivated in batch, fed-batch or continuous-perfused mode had a similar efficient metabolic pathway to produce energy.

Specific glucose consumption and lactate production rates were also compared, depending on the culture mode of WJ-MSCs. According to the figure 4.11 B, it seemed that the WJ-MSCs consumed 6 times more glucose in SV (32 pmol cell^{-1} day^{-1}) than in stirred tank bioreactors (5 pmol cell^{-1} day^{-1}) (fed-batch and continuous-perfused modes). By comparing these values with literature data, it appeared that MSCs cultivated in continuous-perfused modes consumed 1.4 to 2.9 pmol cell^{-1} day^{-1} [20, 22]: a production of lactate of about 1 pmol cell^{-1} day^{-1} in Cunha *et al.* study [20], and about 3.2 pmol cell^{-1} day^{-1} in the study of Mizukami *et al.* study [22].

In addition to the analysis of the glucose consumption and lactate production, maximal rates of lactate and ammonium produced by cells were also calculated. According to figure 4.12 A and figure 4.12 B, it seemed that the perfusion mode permitted to limit the maximal concentration of

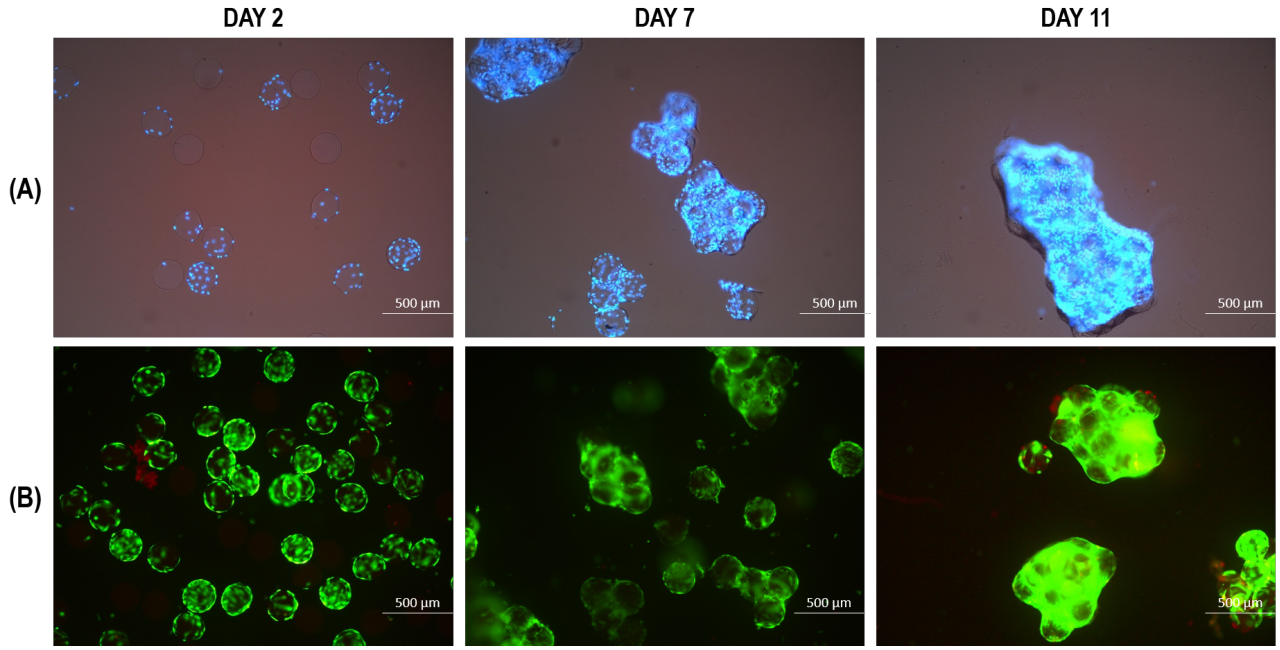

Figure 4.10 – Pictures of fluorescent staining of WJ-MSCs cultivated on dissolvable microcarriers in continuous-perfused STR. (A) Dapi staining at Days 2, 7 and 11. (B) Live/dead staining at Days 2, 7 and 11.

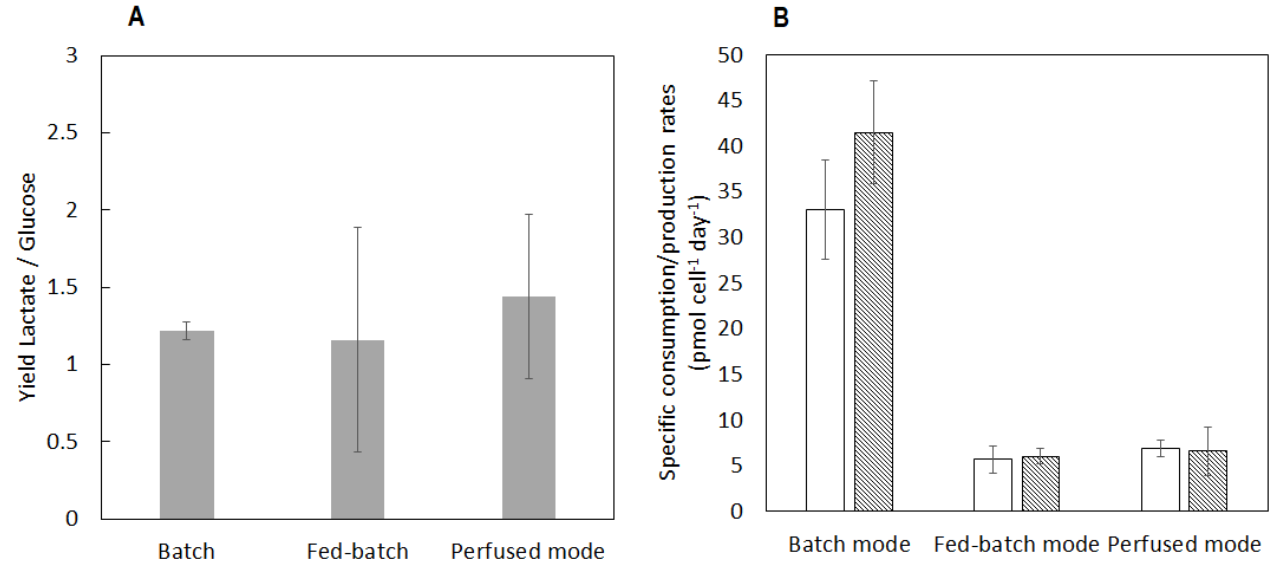

Figure 4.11 – Kinetic parameters of metabolites consumption and production of WJ-MSCs depending on the culture mode. (A) Yield of lactate on glucose profiles in function of the production mode. (B) Specific consumption and production rates of glucose and lactate. The values of specific glucose consumption in stirred tank bioreactor are represented in plain white bars. The values of specific lactate production in stirred tank bioreactor are represented in hatched white and black bars. Values are presented as mean value ± standard deviation (n = 2).

lactate (10 mM) and to decrease the maximal amount of NH_3 (2.5 mM, according to Schop *et al.* 2010 [23]), whereas in batch and fed-batch modes, values of the NH_3 were higher than the limit tolerated by cells. On figure 4.13, it appeared that the percentage of dead cells was under 20 % regardless of the cultivation method used, but in continuous-perfused mode this percentage of dead cells was under 5 % even at the beginning of the cell culture.

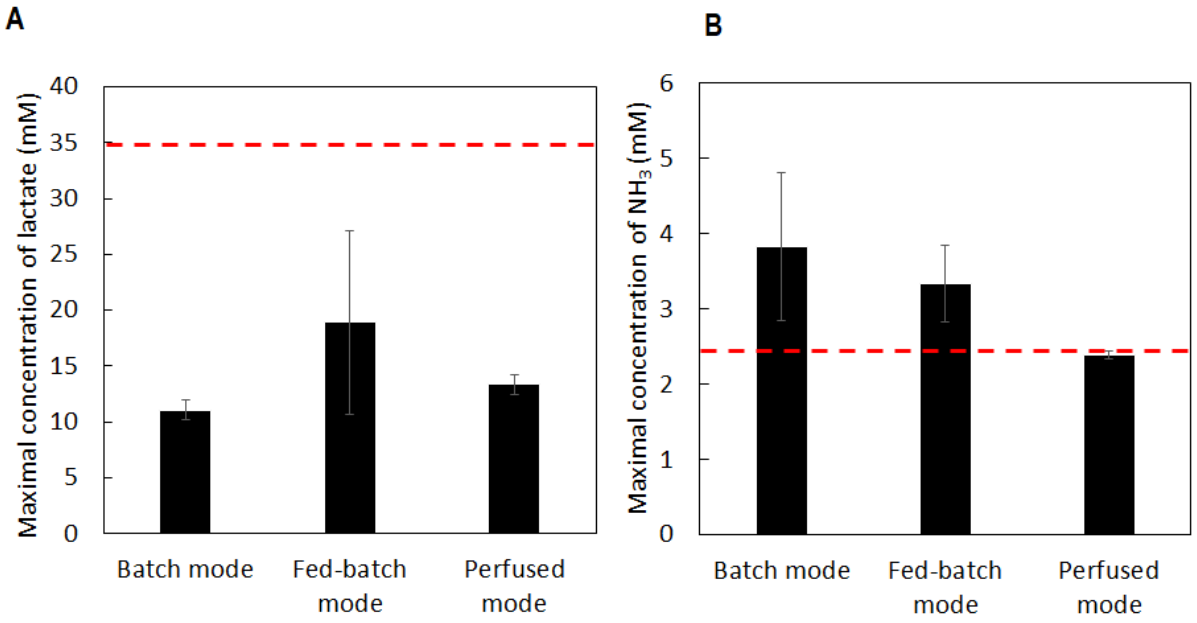

Figure 4.12 – Evaluation of critical metabolite parameters during WJ-MSC expansion in function of the mode of production. (A) Maximal lactate concentration (in mM) (B) Maximal ammonium concentration (in mM). Red hatched lines represent maximal concentration tolerated by cells according to the literature [23]. The batch mode is represented in white bars, the fed-batch mode is represented by black bars and the continuous-perfused mode is represented by grey bars. Values are presented as mean value ± standard deviation (n = 2).

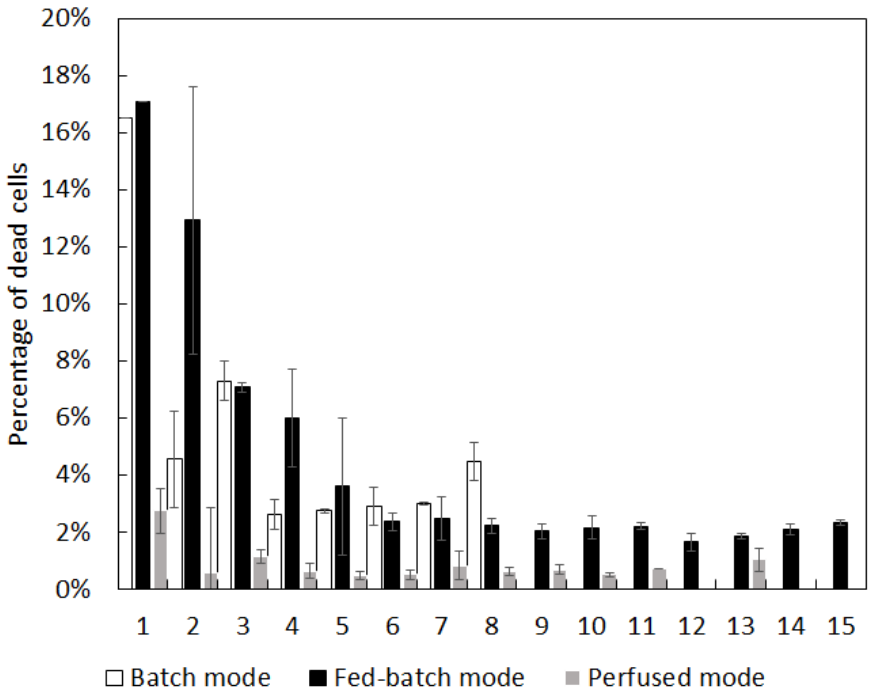

Figure 4.13 – Evaluation of percentage of dead cells during WJ-MSC expansion in function of the mode of production. Percentage of dead cells obtained by the measure of LDH. The batch mode is represented in white bars, the fed-batch mode is represented by black bars and the continuous-perfused mode is represented by grey bars. Values are presented as mean value ± standard deviation (n = 2).

4.2.3 Characterization of MSCs expanded in continuous-perfused mode

After the 14 days cultivation in continuous-perfused stirred tank bioreactor, expanded WJ-MSCs were characterized in terms of immunophenotypes and morphology.

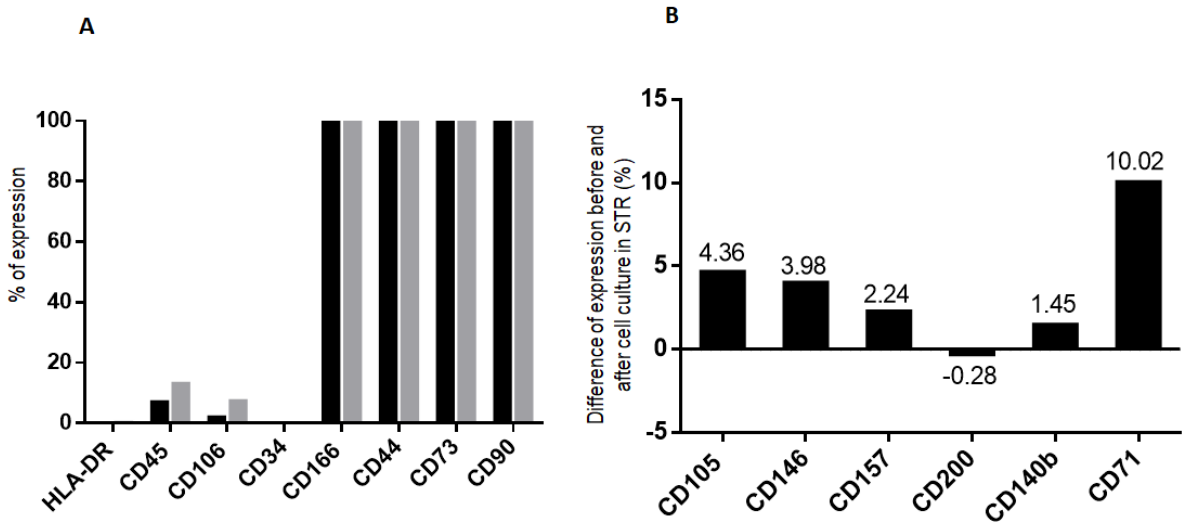

Figure 4.14 – Expression of markers by WJ-MSCs before and after cell culture. (A) ISCT markers with black and light grey bars respectively indicate measurements before and at the end of cell culture in bioreactor. (B) Expression of markers of functionalization.

The figure 4.14 A presents the percentage of expression obtained from MSC-specific cell surface markers. Immunophenotypes were obtained before and after cell culture in the continuous-perfused stirred tank bioreactor. Cells expressed negatively HLA-DR, CD34, CD45 and CD106 markers, whereas, they expressed positively CD166, CD44, CD73 and CD90 markers (Figure 4.14 A).

In the figure 4.14 B are presented the percentage of expression of markers of functionalization specific to the MSCs. These immunophenotypes were obtained before and after cell culture in perfused-continuous stirred tank bioreactor. Different markers were studied. The CD105 marker, also known as a typical marker of endothelial cells, plays an important role for growth of blood vessels and it is also a co-recepctor to transforming growth factors [24]. After the culture in perfused-continuous stirred tank bioreactor the expression of this CD105 marker was slightly over expressed (+5 %). The CD146 is also a typical marker of endothelial cells, and its expression was also over expressed after 14 days of culture in perfused-continuous bioreactor (+4 %). This marker is involved in the migration, signal transduction and proliferation of MSCs [25]. The CD157, slightly over-expressed (+2 %), has a key role in regulating leukocyte adhesion and migration [26]. However, the expression of the CD200 marker was not changed (-0.3 %). This marker is involved in the stimulation of T-cell proliferation and thus in the MSC potentiality [27]. The CD140b marker, also known as platelet-derived growth factor receptor beta is sensible to growth factors and it is over-expressed after the culture in perfused-continuous mode (+1.5 %). Finally, the last marker over-expressed (+10 %) after the cell expansion in continuous-perfused bioreactor was the CD71 marker, also called transferrin receptor, is involved in the process of endocytosis, a cellular process in which substances are brought into the cell.

Flow cytometry was also realized in order to observe if any morphological differences occurred

after the cell expansion on dissolvable microcarriers in perfused-continuous stirred tank bioreactor. First, after the cell expansion in flasks (Figure 4.15 A), the cell population is well homoge-

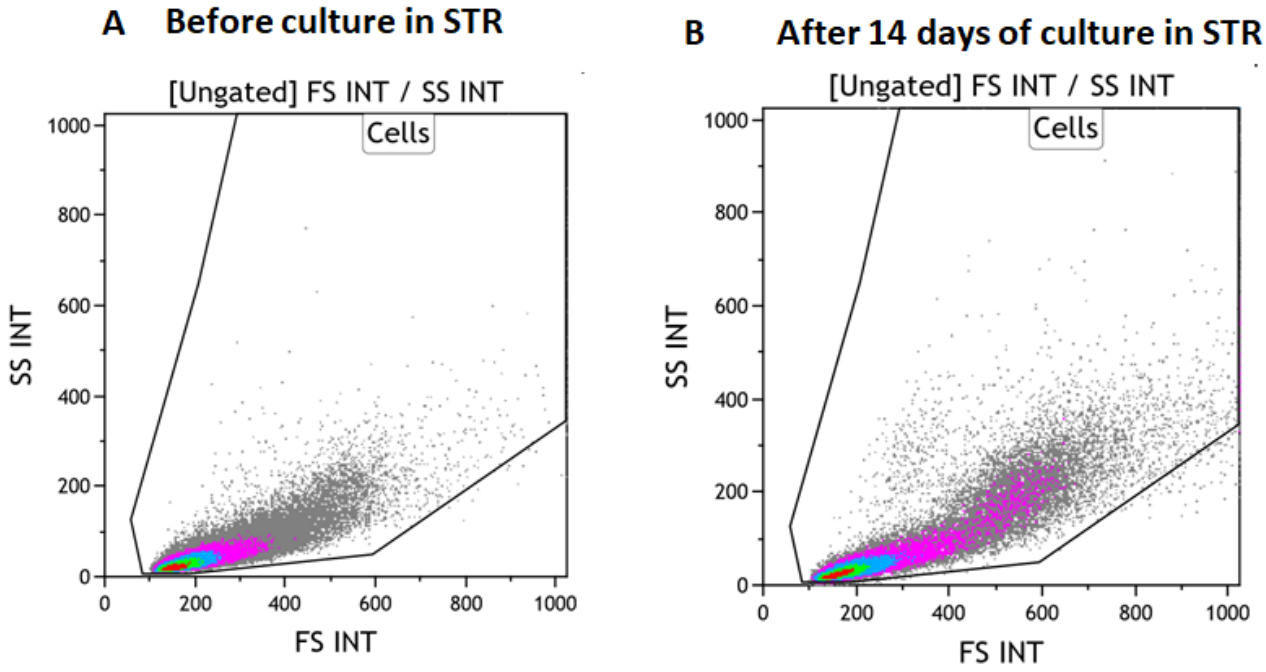

Figure 4.15 – Flow cytometry (A) before and (B) after cell culture in perfused-continuous stirred tank bioreactor. Forward scatter (FS) and side scatter (SS) were used to exclude dead cells, cell debris and cell doublets.

neous, with small and not very granular cells. After the expansion on dissolvable microcarriers in stirred tank bioreactors, the population of cells changed a little. One part of the cell population was indeed composed of larger cells and with a more granular composition than the initial cell population.

4.2.4 On-line monitoring of WJ-MSCs growth on dissolvable microcarriers

Figure 4.16 shows the growth curve of WJ-MSCs cultures during time and depending on the culture mode. As presented in the previous part, a good reproducibility of off-line of cell counting was observed. In fed-batch modes, the maximal number of cells was obtained at day 12 or 13, and was about 220 million. A similar permittivity kinetic evolution was noticed, with an increase in the permittivity to a maximal at day 12 and 11 with maximal values of permittivity around 18 pF cm^{-1} (Figure 4.16 A and B). In continuous-perfused systems, the maximal number of cells was obtained at day 10 and was about 500-600 million (Figure 4.16 C and D). A similar evolution of permittivity was also noticed with an increase of the permittivity to a maximal value of 30 pF cm^{-1} at day 10 (Figure 4.16 C) and at day 11 (Figure 4.16 D). Moreover, on the four graphs, it could be observed that at each addition of microcarriers (represented by the black arrows), a drop of permittivity occurred (Figure 4.16). There was no clear demonstration of any phenomenon explaining this drop was put into evidence. However, the arrests of agitation and microcarrier sedimentation were strongly suspected as well as cell morphology changes during the culture.

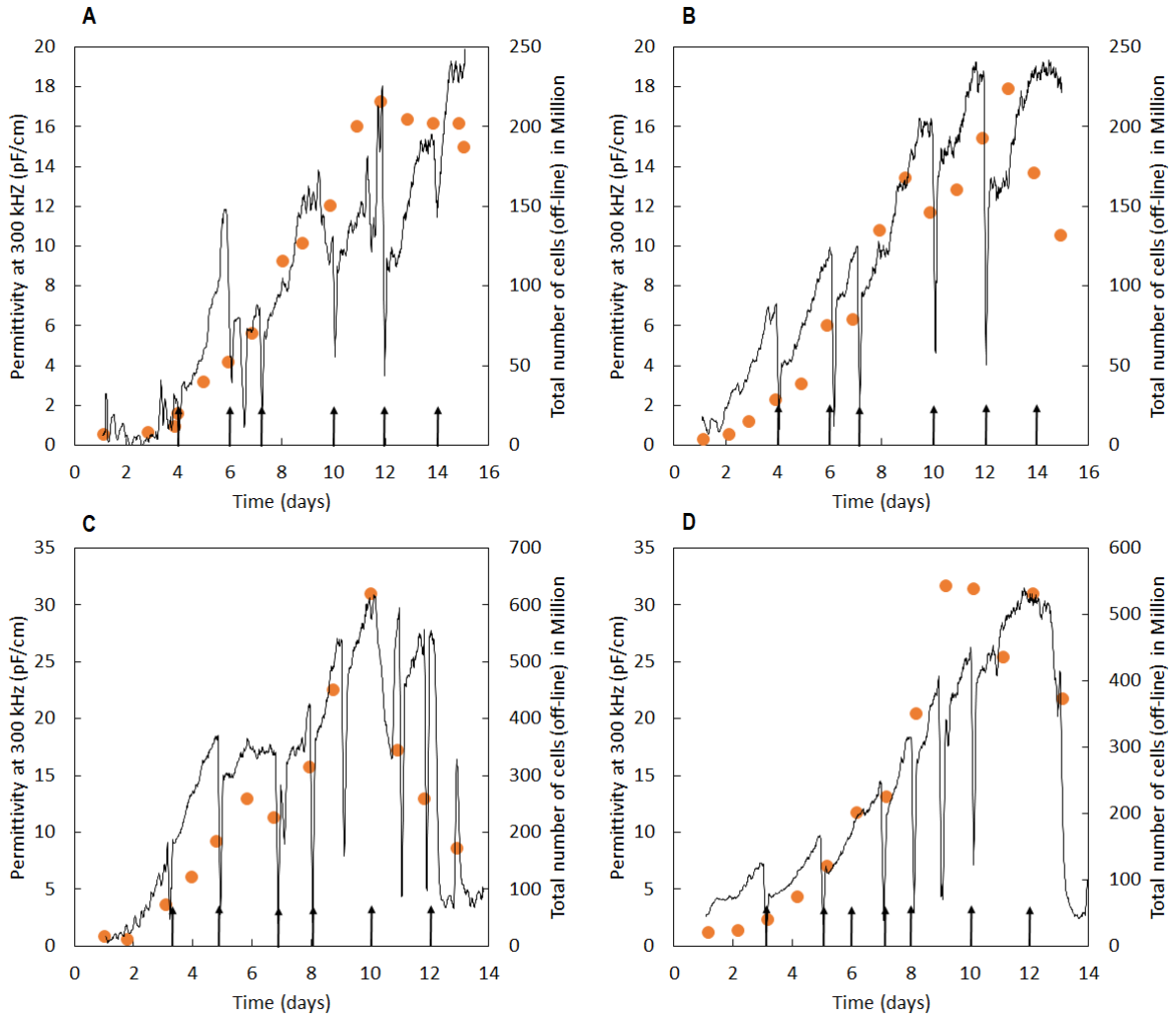

Figure 4.16 – Growth kinetics of WJ-MSCs cultures performed in (A) fed-batch modes or in (B) continuous-perfused modes. (•) off-line measurements of cell number and (continuous lines) on-line values of permittivity. Arrows indicate the additions of microcarriers during the culture.

Discussion

Major advances in the field of stem cell therapy require large-scale, low-cost production of high quality cells. Indeed, more and more clinical trials are carried-out and are promising for using mesenchymal stem cells, and required large amount of cells. The process developed in the present study permited to produce about 600 million of cells, corresponding to approximately one injection for 8 patients (70 kg) assuming 1x10^6 cells kg^{-1} is the regular dose. To produce the same amount of cells, 200 T-175 cm^2 flasks would have been necessary. Thus, dissolvable microcarriers seemed promising for large scale production of WJ-MSCs in stirred tank bioreactors and for clinical trials.

In this study, batch, fed-batch and a new continuous-perfused modes were compared for the expansion of WJ-MSCs. Previous studies found in literature also used a continuous mode to produce MSCs (bone-marrow or cord blood derived MSCs). In Dos Santos *et al.* (2014) study, a spin filter was used. However there was a risk of clogging [19]. In Cunha *et al.* (2015) study, the cell culture medium and cells were took off the stirred tank bioreactor without sorting [20]. Our study

proposed an innovative mean to sort empty microcarriers and microcarrier aggregates. It was indeed demonstrated that not only the used medium but also the empty microcarriers were removed by adapting the diameter of the settling tube and the withdrawal flow rate. Consequently, this allowed an expansion factor of 60, which is sensibly higher than in batch (5) or in fed-batch (43)

Concerning cell metabolism, it has been described in numerous studies that stem and progenitor cells proliferation were associated with glycolytic metabolism leading to an accumulation of lactate, whereas the preponderance of the oxydative phosphorylation was associated to stem cell differentiation [28]. The culture of umbilical cord derived mesenchymal stem cells in perfusion modes resulted in an efficient metabolism to produce energy by the oxydative phosphorylation, as demonstrated by appropriate yields of lactate on glucose [22]. Moreover, cells characterization carried-out after expansion in STR, indicated that mesenchymal stem cells preserved their stemness without early differentiation. In addition, specific cell consumption and cell lactate production rates were compared to values found in literature. It appears UC-MSC and BM-MSC cultivated in continuous-perfused mode consumed between 2.9 and 1.4 pmol cell^{-1} day^{-1} [22, 20]. In the present study, expanded cells consumed about 6 pmol cell^{-1} day^{-1}, a value slightly higher than the ones found in the literature.

The first study reporting the use of dielectric spectroscopy with MSCs cultures on microcarriers was realized by Justice *et al.* in 2011 [17]. Authors reported a linear correlation between permittivity data and cell concentration. In addition, they were able to monitor the impact of aeration on hMSC-TERT. As soon as the aeration stops, the cells became necrotic, their morphology changed and this was detected by the dielectric spectroscopy. One other major point of this study was the on-line monitoring of the WJ-MSCs growth thanks to dielectric spectroscopy with an excellent accuracy. However, this method was less accurate when aggregates occurred. Indeed, with regular additions of microcarriers, in the continuous-perfusion mode of STR, the concentration of microcarriers increased, and some large aggregates sticked to the glass wall of the vessel, disturbing the signal of the dielectric probe.

Conclusion

In conclusion the results showed the expansion of more than 250 million of cells in fed-batch on 12 days, with maintained stemness characteristics (differentiation potential) and without any detachment steps. However this addition of microcarriers led to the presence of some empty microcarriers, not used by cells. An innovative process consisting in the implementation of a settling tube permitted to develop a continuous-perfused mode of cell expansion. This new process allowed to produce larger amounts of cells for clinical applications considering the use of 1x10^6 cells kg^{-1} as the therapeutic dose. More than 600 million cells have been produced using this system in 11 days, maintaining the differentiation potential and the immunophenotypes of the cells. The implementation of a settling tube, permitting a continuous medium perfusion and the withdrawal of empty microcarriers increased the cell expansion factor to a value of 60. To limit aggregation size increase, it would be interesting to increase agitation rates in order to maintain cell aggregates to

a more controlled size. As comparison, the production of the same amount in 2D systems of cells (*i.e.*: T-flasks) would have required more than 150 T-175 cm^2 flasks. Moreover continuous feed in medium and microcarriers could be a valuable strategy to avoid cell passages, well known to be deleterious for cells. Thus, through this means, this continuous and integrated process could be advantageous.

Acknowledgment

The authors would like to thank the Interreg project 'IMPROVE-STEM' for its financial support. They also acknowledge Fabrice Blanchard (LRGP, Nancy), Jennifer L Weber (Corning) and Constanza Curotto (Corning) for their technical contribution to this work.

Following this study, further work was carried out to investigate the cost of producing Wharton's jelly cells on a therapeutic scale.

4.3 Integration of cost analysis of WJ-MSCs production for therapeutic trials

In order to evaluate the operating cost of WJ-MSC production for therapeutic trials, different simulations were carried-out. This analysis of cost was made for culture of WJ-MSCs on dissolvable microcarriers in batch (spinner vessels), in fed-batch and continuous-perfused (STR) modes. Assumptions were made in order to model the different costs and some others were based on experimental results. The production cost simulator allowed the modeling of the operating cost of production of Wharton Jelly mesenchymal stem cells for therapeutic purposes and by taking into account material (reagents, consumables) and labour for each unit operation.

4.3.1 Methodology

The consumption of materials (reagents and consumables) was first listed and the cost of each product was referenced (figure 16 in appendix). The required quantity and the duration of the operations were integrated in a simulation spreadsheet. Via cross-referenced between material prices and quantity used, a cost for each operation was calculated. The same methodology was taken applied with labour time: a cost per hour of engineer was crossed with the the time necessary to complete each operation. Each of the unit operations has thus been characterized by a material and labour costs. Example of those steps is presented in appendix.

Operating costs were compared on the assumption that the environmental costs were the same for each modes of culture (batch / fed-batch and continuous-perfused), as presented in the figure 4.6. Indeed, it was assumed that investment funds were already assumed and similar for the three modes of culture, with the need of a clean room with controlled atmosphere, incubators or stirred tank bioreactors equipments. Thus, each step of the process was detailed and costs were calculated, taking into account different hypothesis:

- The environment was the same between all the conditions (buildings, labs, ...).
- Stirred tank bioreactors were already bought and present at the laboratory, as the incubators or spinner vessels.
- Cost of sterilization, water, electricity or gas consumptions could be neglected.
- Only reagents and consumables were taken into account in this analysis.

4.3.2 Implementation of the spreadsheet for production cost simulation

According to the work of Margossian [29], after enzymatic digestion of one umbilical cord about 9.9×10^6 up to 23×10^6 adhered cells could be obtained. In this study, the minimal number of adhered cells was considered (9.9×10^6 cells per cord). After the cell extraction from the umbilical cord, a cell freezing step was performed. These two steps were part of the process qualified as 'Biobanking'. After the biobanking step, the WJ-MSC amplification was performed. The cells were

thawed and amplified in flasks for a week, up to 70 % confluence. Then, once the number of cells required was obtained, spinner vessels were used for cell amplification. This step was named as 'Agitated culture in spinner vessel'. Finally, after 12 h in spinner vessel, the culture was transferred into stirred tank bioreactor, for at least 15 days. This step was named as ' Agitated culture in stirred tank bioreactor', and the costs of the different modes of production (fed-batch and continuous-perfused mode) were calculated. All these different steps are reported in the figure 4.6 and, all the initial characteristics of the process were reported in the table 4.1.

Table 4.1 – Cost characteristics of each process unit

LABOR CHARACTERISTICS	
Operating labor salary cost	32 €/h
Supervision labor salary cost	50 €/h
PRODUCTION BATCH CHARACTERISTICS	
Tank size	2 L
Batch size (beginning of the culture)	0.5 L
Cell culture medium cost	141 €/L
CELL EXTRACTION YIELD	
1 umbilical cord	9×10^6 WJ-MSCs
P_0 seeding concentration	1×10^3 cells/cm^2
Number of cells per T-flask	7.5×10^4 cells
WJ-MSC CULTURE	
T-flask area	75 cm^2
Volume of medium per T-flask	10 mL
Seeding concentration	1×10^3 cells/cm^2
Number of cells per T-flask	7.5×10^4 cells
Cell concentration at 70 % of confluence	1.20×10^4 cells/cm^2
Number of cells in one T175 at 70 % confluence	9×10^5 cells
Passaging WJC: 1 T-Flask	3 T-Flasks
Cryotube concentration (WJC)	2×10^6 cells
Number of T-flasks done with one cryotube	3 T-flasks (T-75)
WJ-MSC PRE-CULTURE	
Microcarrier	DM-Corning
Microcarrier concentration in bioreactor	1.00 g/L
Microcarrier volume	20 mL
Microcarrier mass	0.13 g
Stock concentration	6.7 g/L
Initial cell seeding	8900 cells/cm^2
WJ-MSC CULTURE in STR	
Number of feed	5 times
Cell culture medium volume added	200 mL
Number of microcarrier feed	5 times
Volume of added microcarrier	20 mL

4.3.3 Comparison of costs of WJ-MSCs production depending on the mode of production

First, the total costs of the different modes of production of one dose of WJ-MSCs for clinical trials were compared. It has been established that one dose of WJ-MSCs for clinical trial required approximately 10^3 million of cells.

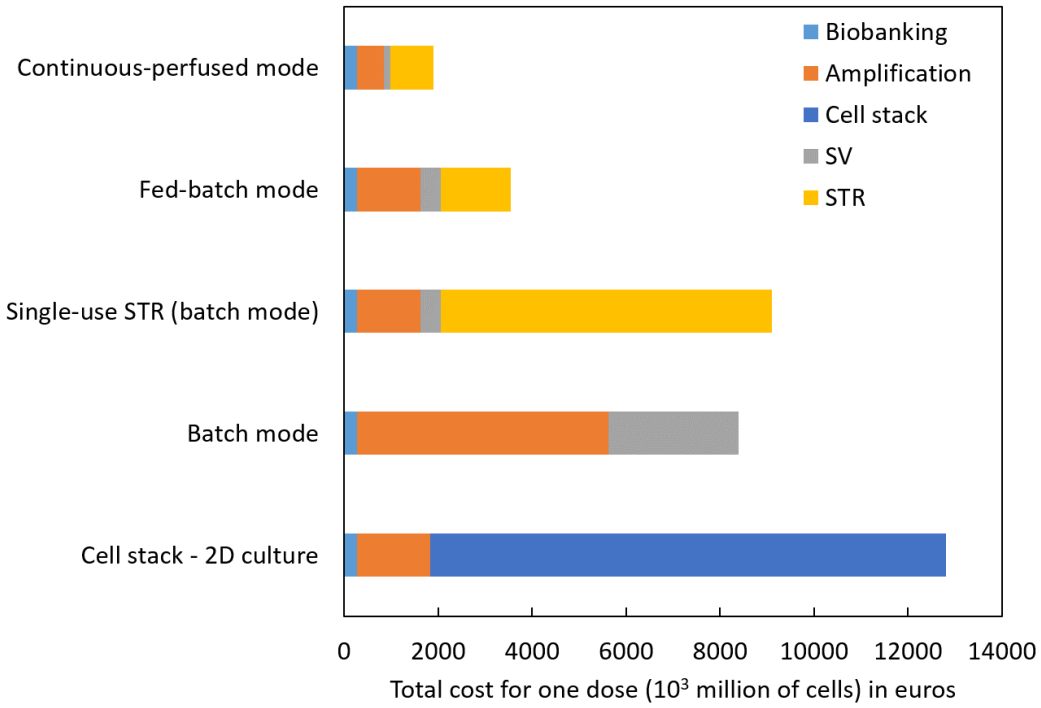

Figure 4.17 – Cost of production of WJ-MSCs for clinical trials in function of the mode of production: 2D-culture, single-use stirred tank bioreactor, batch, fed-batch and continuous-perfused modes.

According to the figure 4.17, the highest cost of production is in 2D cultures with cellstack chambers (12000 €/dose) ; the use of single-use stirred tank reactor was also expensive (9000 €/dose). Finally, the production cost for one dose of WJ-MSCs was 5 times more expensive in batch (8900 €/dose) and 2 times more expensive in fed-batch mode (3500 €/dose) than in continuous-perfused mode (1900 €/dose). Allocations of the cost seemed different between the three modes of production. Indeed, in batch mode, the contribution of cell amplification step in flasks was more important, as well as the culture in spinner vessel. This could be explained by the need of at least 12 spinner vessels to produce the amount of cells (10^3 million of cells). On the contrary, the contribution of the amplification step was less high for fed-batch and continuous-perfused modes in STR.

4.3.4 Cost allocation for the production of WJ-MSCs cells in a continuous-perfused bioreactor

The allocation of the production cost was determined for the WJ-MSCs in continuous-perfused mode. According to the figure 4.18 A, it appeared that the most expensive part of the process was the culture in STR, due to the high reagent consumption. The second most expensive source of the process concerned the amplification of WJ-MSCs in flasks, due to high use of consumables and high labor work. Referring to the figure 4.18 B, the main part of the total cost of the process was due to reagents as the cell culture medium or the microcarriers (62 %), then the labor costs (21 %) and finally the consumables (18 %).

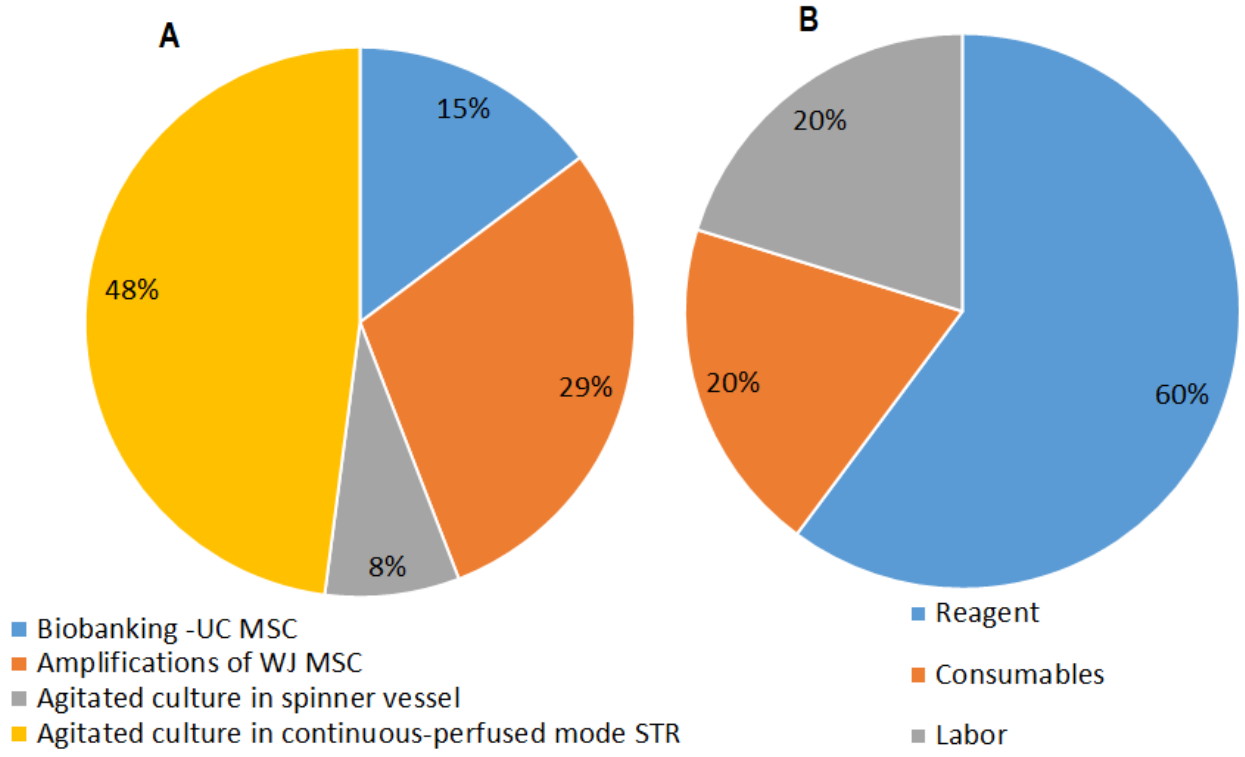

Figure 4.18 – Allocation of the costs of WJ-MSC production for clinical trials in continuous-perfused STR. (A) Allocation in function of the process step. (B) Distribution of costs associated with reagents, consumables or working time.

For each step of the process, an evaluation of the cost distribution was carried-out, as shown on the Figure 4.19. It appeared that for the biobanking, the principal source of cost was the labor cost, due to multiple handling, medium renewal and cell passaging (Figure 4.19 A). During the amplification step of the process, the main source of cost was the use of consumables as T-Flasks, pipettes, as it was the case for the culture in spinner vessels. Finally, in stirred tank bioreactor, costs of perfused cell culture medium and of the feed in microcarriers represented about 88 % of the total operating costs.

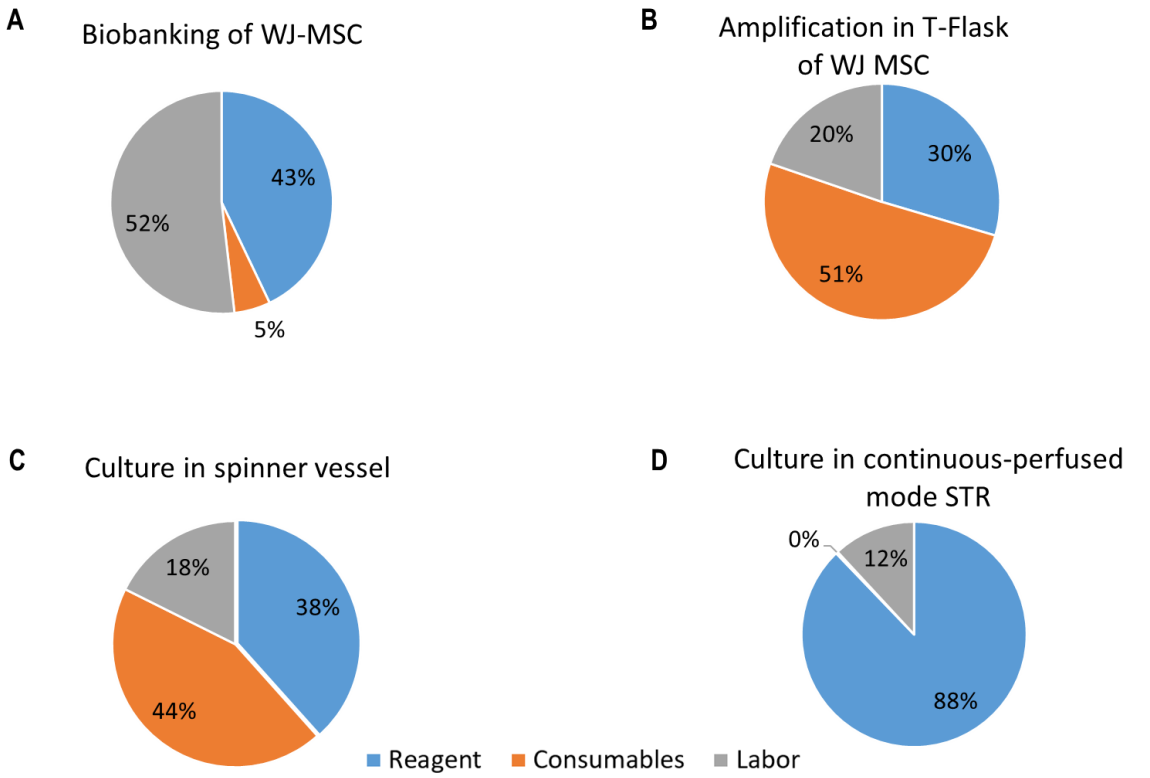

Figure 4.19 – Distribution of costs associated with reagents, consumables or working time for WJ-MSC production for clinical trials in continuous-perfused STR. (A) Allocation of costs in the biobanking, (B) in the amplification in 2D, (C) in the culture in spinner vessel and (D) in the culture in STR.

Conclusion

This economic evaluation was carried-out using an academic laboratory as a reference. The actual time spent for each operation was taken into account, whereas in a start-up or company system, these costs would have to be re-evaluated taking into account the environment, the monthly salaries charged and the depreciation of machines. Experimental and economic evaluation of different production modes are interesting for a commercial exploitation of WJ-MSCs for clinical-based therapies. These results pointed out the economic advantages to choose a continuous-perfused mode for the production of WJ-MSCs in stirred tank bioreactor with dissolvable microcarriers. Indeed, in a batch mode, the operating costs were 5-time more expensive, and in fed-batch mode 2-time more expensive than in perfused-continuous mode. These conclusions should be taken with caution as economical analysis results strongly depend on the performance of cell expansion. Maximal specific growth rates and efficiency of detachment are indeed specific to the umbilical cords, and clearly determine costs of production.

Conclusions of chapter 4

In this chapter the performance of commercial dissolvable microcarriers for UC-MSCs culture was studied (Figure 4.20). Thanks to their ease of detachment, a simplified downstream processing and a high yield of MSCs recovery was shown. Dissolvable microcarriers efficacy was first studied in culture with WJ-MSCs at small scale, in 6-well plates and without agitation. It has been shown that good cell adherence and cell viability could be obtained. The metabolism kinetics were close to the one obtained with the commercial Cytodex-1, used as a control. Moreover, the rapid dissolution of the microcarriers allowed a 100 % of cell recovery.

After the expansion in well-plates, a scale-up of the cultures was carried-out. Thus, WJ-MSCs were cultivated in spinner vessels of 200 mL of working volume with the novel microcarriers. A 9 days culture permitted to obtain a maximal number of cells of 50 millions whereas, in the same culture conditions, the use of Cytodex-1 permitted to have only 10 million of cells. However, as demonstrated in the previous chapter, limits of batch mode rose from nutrient depletion and limitation of the growth capabilities available for the cells. As soon as microcarrier confluence was reached, the cell growth rate was indeed slowed down. Fed-batch modes with addition of microcarriers coupled with cell culture medium were thus carried-out and allowed a maximal number of cell production of 250 million. But, even with the addition of fresh microcarriers and adapted strategies of adherence, it appeared that some of them remained unoccupied and could contribute to cell damage. In order to further add microcarriers (*i.e.*: cell adherence surface), but with the necessity to overcome a too high concentration of empty microcarriers, an innovative continuous-perfused mode was set-up. A settling tube allowed to segregate empty microcarriers and aggregates of cells on microcarriers, on the basis of their specific relative settling velocities. Thanks to this system, with the removal of cell culture medium, empty microcarriers were also removed from the bioreactor, while aggregates and cells were retained inside. Moreover, the continuous flow rate ensured MSCs physiological requirements. With this innovative continuous-perfused bioreactor, a maximal number of cells of 600 millions was produced, in 11 days, which is an increase of the productivity of a 1.5 factor. In addition, during the cultures in stirred tank bioreactors (fed-batch and continuous perfused modes), a on-line monitoring of cells was proposed using the dielectric spectroscopy. It appeared that the permittivity was a very good indicator of the cell growth inside the bioreactor.

Finally, the last part of this chapter presented the possible cost of WJ-MSCs for clinical trials, in different modes of production. In order to produce one dose of 10^3 million of cells, different strategies of production were evaluated. 2D culture in cellstacks appeared to be the most expensive mode of production. Production in single-use stirred tank bioreactors or batch modes seemed equivalent in terms of production costs. In this study, it appeared that the less expensive mode of production of the cells was the continuous-perfused mode (5 times less expensive).

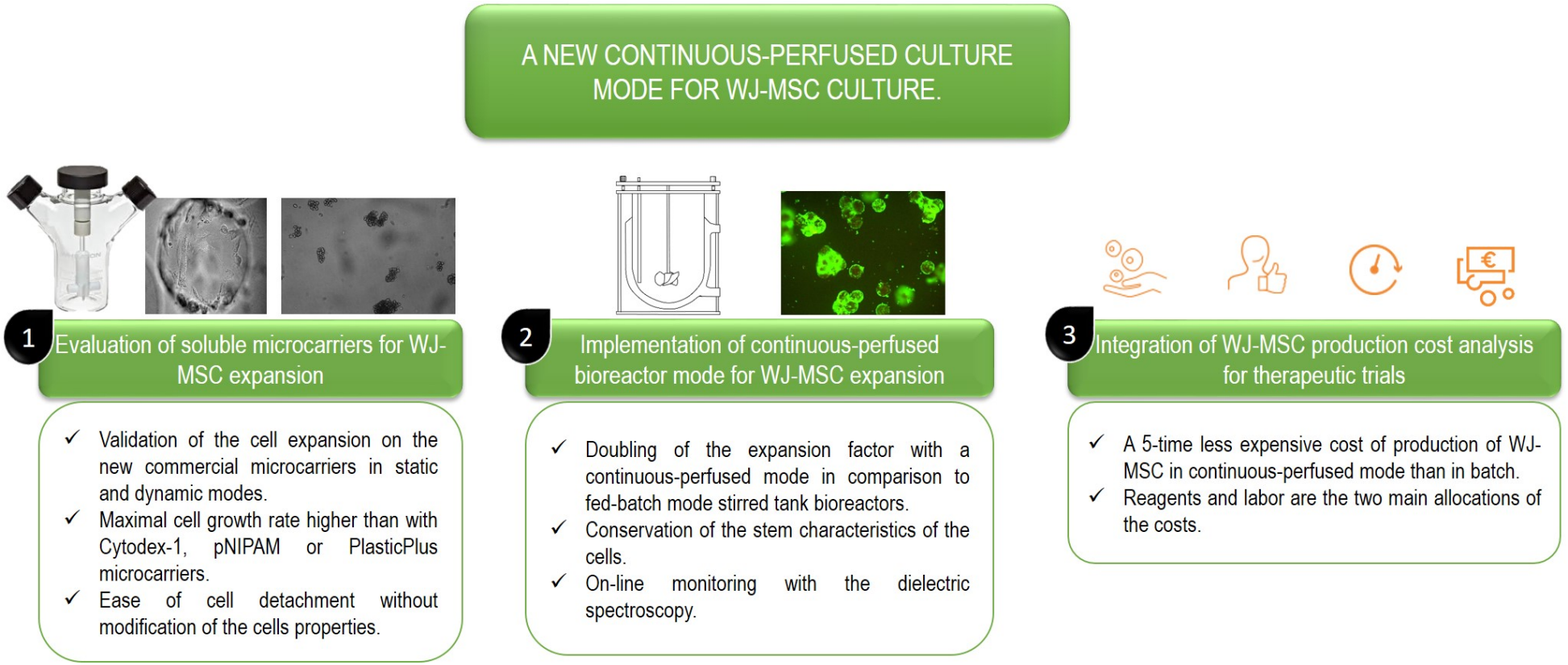

Figure 4.20 – Synthesis of the results of the chapter 4.

Bibliography

[1] C. Sion, C. Loubière, M. Wlodarczyk-Biegun, N. Davoudi, C. Müller-Renno, E. Guedon, I. Chevalot, and E. Olmos. Effects of microcarriers addition and mixing on wj-msc culture in bioreactors. *Biochemical Engineering Journal*, 157:107521, 2020.

[2] J. J. Scibek and P. Dolley-Sonneville. Expansion of human mesenchymal stem cells on corning® synthemax ii-coated corning dissolvable microcarriers in a serum-free cell culture medium. Application Note, 2018.

[3] A. L. Rodrigues, C. A. Rodrigues, A. R. Gomes, S. F. Vieira, S. M. Badenes, M. M. Diogo, and J. M. Cabral. Dissolvable microcarriers allow scalable expansion and harvesting of human induced pluripotent stem cells under xeno-free conditions. *Biotechnology Journal*, 14(4):1800461, 2019.

[4] G. Brooke, M. Cook, C. Blair, R. Han, C. Heazlewood, B. Jones, M. Kambouris, K. Kollar, S. McTaggart, R. Pelekanos, et al. Therapeutic applications of mesenchymal stromal cells. In *Seminars in Cell & Developmental Biology*, volume 18, pages 846–858. Elsevier, 2007.

[5] D. A. De Ugarte, K. Morizono, A. Elbarbary, Z. Alfonso, P. A. Zuk, M. Zhu, J. L. Dragoo, P. Ashjian, B. Thomas, P. Benhaim, et al. Comparison of multi-lineage cells from human adipose tissue and bone marrow. *Cells Tissues Organs*, 174(3):101–109, 2003.

[6] W. Jackson, A. Aragon, F. Djouad, Y. Song, S. Koehler, L. Nesti, and R. Tuan. Mesenchymal progenitor cells derived from traumatized human muscle. *Journal of Tissue Engineering and Regenerative Medicine*, 3(2):129–138, 2009.

[7] P.-P. Chong, L. Selvaratnam, A. A. Abbas, and T. Kamarul. Human peripheral blood derived mesenchymal stem cells demonstrate similar characteristics and chondrogenic differentiation potential to bone marrow derived mesenchymal stem cells. *Journal of Orthopaedic Research*, 30(4):634–642, 2012.

[8] G. Brooke, T. Rossetti, R. Pelekanos, N. Ilic, P. Murray, S. Hancock, V. Antonenas, G. Huang, D. Gottlieb, K. Bradstock, et al. Manufacturing of human placenta-derived mesenchymal stem cells for clinical trials. *British Journal of Haematology*, 144(4):571–579, 2009.

[9] S. Knudtzon. In vitro growth of granulocytic colonies from circulating cells in human cord blood. *Blood*, 43(3):357–361, 1974.

[10] D. L. Troyer and M. L. Weiss. Concise Review: Wharton's Jelly-Derived Cells Are a Primitive Stromal Cell Population. *Stem Cells*, 26(3):591–599, 2008.

[11] F. d. Santos, P. Z. Andrade, M. M. Abecasis, J. M. Gimble, L. G. Chase, A. M. Campbell, S. Boucher, M. C. Vemuri, C. L. d. Silva, and J. M. Cabral. Toward a clinical-grade expansion of mesenchymal stem cells from human sources: a microcarrier-based culture system under xeno-free conditions. *Tissue Engineering Part C: Methods*, 17(12):1201–1210, 2011.

[12] T. W. Gilbert, T. L. Sellaro, and S. F. Badylak. Decellularization of tissues and organs. *Biomaterials*, 27(19):3675–3683, 2006.

[13] H. Tavassoli, S. N. Alhosseini, A. Tay, P. P. Chan, S. K. W. Oh, and M. E. Warkiani. Large-scale production of stem cells utilizing microcarriers: a biomaterials engineering perspective from academic research to commercialized products. *Biomaterials*, 181:333–346, 2018.

[14] J. Hupfeld, I. H. Gorr, C. Schwald, N. Beaucamp, K. Wiechmann, K. Kuentzer, R. Huss, B. Rieger, M. Neubauer, and H. Wegmeyer. Modulation of mesenchymal stromal cell characteristics by microcarrier culture in bioreactors. *Biotechnology and Bioengineering*, 111(11):2290–2302, 2014.

[15] A. Mizukami, A. Fernandes-Platzgummer, J. G. Carmelo, K. Swiech, D. T. Covas, J. M. Cabral, and C. L. da Silva. Stirred tank bioreactor culture combined with serum-/xenogeneic-free culture medium enables an efficient expansion of umbilical cord-derived mesenchymal stem/stromal cells. *Biotechnology Journal*, 11(8):1048–1059, 2016.

[16] P. A. Tozetti, S. R. Caruso, A. Mizukami, T. R. Fernandes, F. B. da Silva, F. Traina, D. T. Covas, M. D. Orellana, and K. Swiech. Expansion strategies for human mesenchymal stromal cells culture under xeno-free conditions. *Biotechnology Progress*, 33(5):1358–1367, 2017.

[17] C. Justice, J. Leber, D. Freimark, P. P. Grace, M. Kraume, and P. Czermak. Online-and offline-monitoring of stem cell expansion on microcarrier. *Cytotechnology*, 63(4):325–335, 2011.

[18] T. Lawson, D. E. Kehoe, A. C. Schnitzler, P. J. Rapiejko, K. A. Der, K. Philbrick, S. Punreddy, S. Rigby, R. Smith, Q. Feng, et al. Process development for expansion of human mesenchymal stromal cells in a 50 l single-use stirred tank bioreactor. *Biochemical Engineering Journal*, 120:49–62, 2017.

[19] F. dos Santos, A. Campbell, A. Fernandes-Platzgummer, P. Z. Andrade, J. M. Gimble, Y. Wen, S. Boucher, M. C. Vemuri, C. L. da Silva, and J. M. Cabral. A xenogeneic-free bioreactor system for the clinical-scale expansion of human mesenchymal stem/stromal cells. *Biotechnology and Bioengineering*, 111(6):1116–1127, 2014.

[20] B. Cunha, T. Aguiar, M. M. Silva, R. J. Silva, M. F. Sousa, E. Pineda, C. Peixoto, M. J. Carrondo, M. Serra, and P. M. Alves. Exploring continuous and integrated strategies for the up-and downstream processing of human mesenchymal stem cells. *Journal of Biotechnology*, 213:97–108, 2015.

[21] L. Reppel. *Potentialité des cellules stromales de la gelée de Wharton en ingénierie du cartillage*. PhD thesis, Université de Lorraine, 2014.

[22] A. Mizukami, M. D. Orellana, S. R. Caruso, K. de Lima Prata, D. T. Covas, and K. Swiech. Efficient expansion of mesenchymal stromal cells in a disposable fixed bed culture system. *Biotechnology Progress*, 29(2):568–572, 2013.

[23] D. Schop, R. van Dijkhuizen-Radersma, E. Borgart, F. Janssen, H. Rozemuller, H.-J. Prins, and J. D. de Bruijn. Expansion of human mesenchymal stromal cells on microcarriers: growth and metabolism. *Journal of Tissue Engineering and Regenerative Medicine*, 4(2):131–140, 2010.

[24] N. P. Barbara, J. L. Wrana, and M. Letarte. Endoglin is an accessory protein that interacts with the signaling receptor complex of multiple members of the transforming growth factor-β superfamily. *Journal of Biological Chemistry*, 274(2):584–594, 1999.

[25] S. Stopp, M. Bornhäuser, F. Ugarte, M. Wobus, M. Kuhn, S. Brenner, and S. Thieme. Expression of the melanoma cell adhesion molecule in human mesenchymal stromal cells regulates proliferation, differentiation, and maintenance of hematopoietic stem and progenitor cells. *Haematologica*, 98(4):505–513, 2013.

[26] E. Ortolan, S. Augeri, G. Fissolo, I. Musso, and A. Funaro. Cd157: From immunoregulatory protein to potential therapeutic target. *Immunology Letters*, 205:59–64, 2019.

[27] M. Najar, G. Raicevic, F. Jebbawi, C. De Bruyn, N. Meuleman, D. Bron, M. Toungouz, and L. Lagneaux. Characterization and functionality of the cd200–cd200r system during mesenchymal stromal cell interactions with t-lymphocytes. *Immunology Letters*, 146(1-2):50–56, 2012.

[28] S. Sart, S. N. Agathos, and Y. Li. Process engineering of stem cell metabolism for large scale expansion and differentiation in bioreactors. *Biochemical Engineering Journal*, 84:74–82, 2014.

[29] T. Margossian. *Caractérisation des cellules souches mésenchymateuses du sang placentaire et de la gelée de Wharton*. PhD thesis, 2013.

Conclusion and perspectives

The aim of the present work of thesis was to promote the use of hMSCs in cell therapy by producing sufficient quantities of cells with preserved quality (differentiation capability, stem phenotype, immunosuppressive properties) while minimizing production costs. As it was detailed in the manuscript, an explosion of MSCs is occurring, requiring new expansion strategies. This thesis work focused on culture scales till 2 L, but promising trends were highlighted and thus, suggestions for improvement have been made (Figure 4.21).

To reach these goals this study first focused on the choice or the functionalization of the microcarrier (cell adherence, cell detachment), and, in a second time, on the mode of culture. Different parameters have to be considered and optimized, (i) the possible feed in microcarriers, but also (ii) the concentration in microcarriers in the stirred tank bioreactor. A good balance between sufficient surface area of growth for cells *versus* the increase of risks of collision was found.

Concluding results

Improvement of WJ-MSCs culture on microcarriers

First, the interactions between cells and microcarriers were studied. It was possible to demonstrate the ability of WJ-MSC to spontaneously migrate towards fresh microcarriers. Thanks to stained and unstained microcarriers it was possible to visualize the cell migration. Moreover with the time-lapse observations, the kinetics of migration were also determined. Thus, at least two hours were required for a complete migration from one microcarrier to another. Finally, at small scale of cultures the addition of fresh microcarriers permitted to improve the cell expansion with a 1.5 factor. However, it has been noticed that with a too high microcarrier concentration, a significant cell mortality occurred, and this cell mortality was also non negligible in orbital systems of culture, such as Erlenmeyer's flasks. Thus, the process had to be established in mechanical stirred systems such as spinner vessels. With a mechanical agitation the mortality of cells was indeed reduced and seemed more suitable for WJ-MSC culture and, the bead-to-bead transfer was also efficient for expansion improvement. In that respect, new protocols of fresh microcarriers addition coupled with adapted increase of cell culture volume were transferred in stirred tank bioreactors.

Use of functionalized microcarriers for expansion of WJ-MSCs in bioreactor

Thanks to the partnership established during the INTERREG project, performance of different functionalized microcarriers were determined for WJ-MSC expansion in stirred tank bioreactors. By using the developed methods of bead-to-bead transfer, the cell expansion was improved by a factor 3 in comparison to the cultures carried-out in spinner vessel, in batch mode. Poorer results were obtained for PlasticPlus types microcarriers as it seemed that the bead-to-bead transfer was not efficient for this type of microcarriers. From the morphological analysis performed on these microcarriers, it was indeed shown that, cells could still grew beyond 80 % of confluence, while exhibiting small diameter and low spreading. On the other hand, higher expansions were obtained with the Cytodex-1 types microcarriers (Cytodex-1 and pNIPAM Cytodex-1), in terms of total cell number, 'bead-to-bead transfer' and cell morphology, while the cell detachment was still inefficient. Finally, after the WJ-MSC production, a verification of the preservation of their characteristics was required. Flow cytometry and analyses of expressed markers were carried-out and showed a preservation of the inner characteristics of the cells. In conclusion, in fed-batch modes, in stirred tank bioreactors, even if the quantities of produced cells were still not sufficient for therapeutic purpose, the preservation of the stemness was clearly demonstrated. A commercial enzymatically dissolvable microcarrier was also evaluated as its ease of detachment made it a good candidate for the WJ-MSC production and harvest. High yields of cells recovery were obtained, and in addition good cell expansion performance was obtained in spinner vessels with these dissolvable microcarriers in comparison with Cytodex-1 microcarriers.

Innovative mode of MSC culture

In the last part of this thesis work commercial dissolvable microcarriers were used. These microcarriers efficiencies were compared in function of the different modes of cultures used, such as in batch, fed-batch and continuous-perfused modes. The continuous perfused mode relied on the design and use of a innovative system to maintain the cells and occupied microcarriers inside the tank. Thus, a settling tube was used to discriminate empty microcarriers from microcarriers aggregates. By calculating a specific flow rate it was indeed possible to withdraw used cell culture medium and empty microcarriers while cell aggregates were retained inside the bioreactor. New cell culture medium and fresh microcarriers were also brought in the stirred tank bioreactor. Thanks to this system, a cell expansion factor of 60, and about 800 million of cells were produced in 12 days. In addition, the on-line monitoring by capacitance probe appeared to be conclusive to monitor the cell growth. Thanks to the continuous-perfused mode of culture and the dissolvable microcarrier, a large quantity of cells was obtained with preserved characteristics. Finally, Operating costs estimation pointed-out the advantages of using such mode for larger-scale expansion of MSCs.

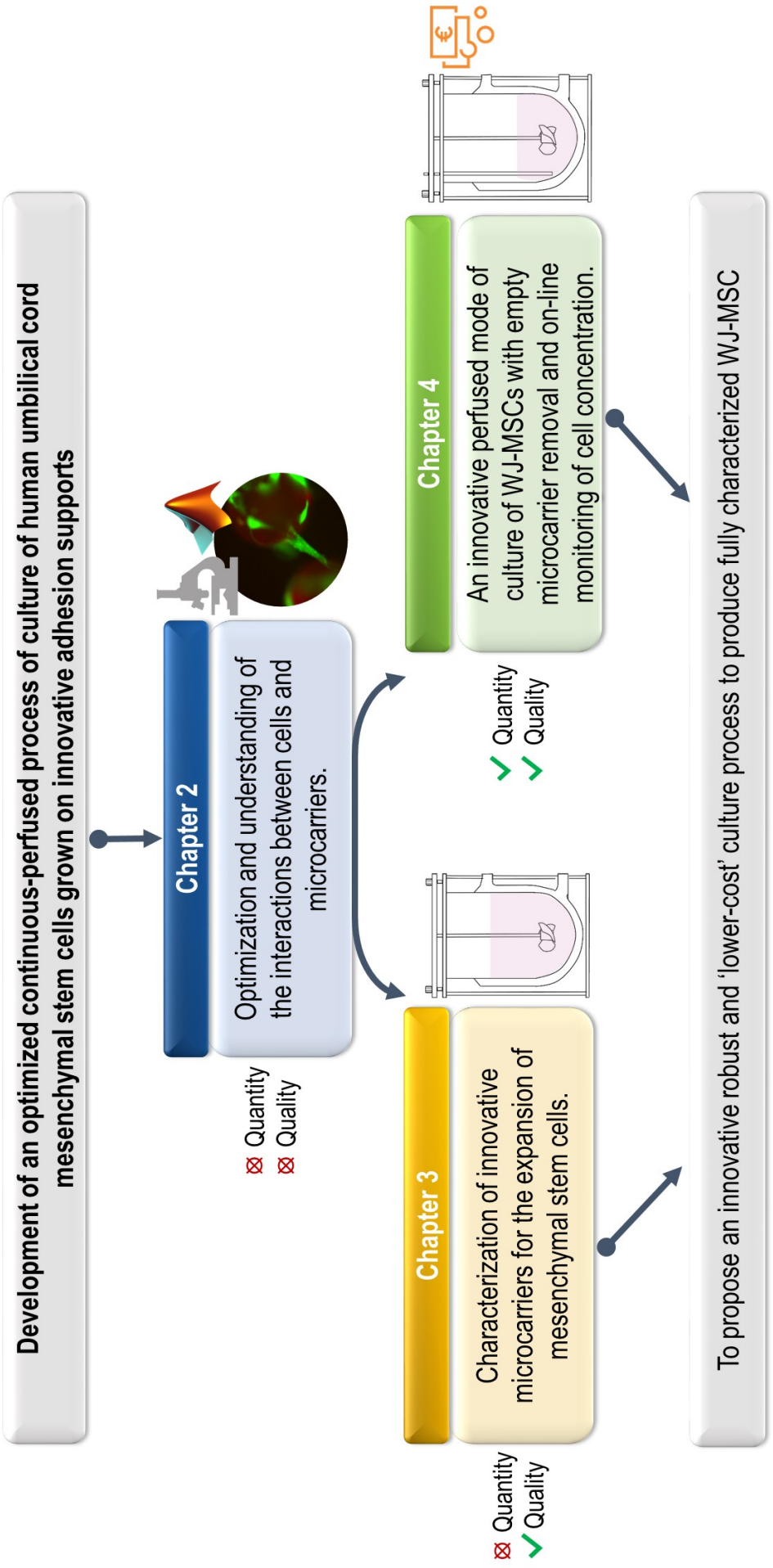

Figure 4.21 – Objectives and achievements of the thesis work.

Perspective of works

The present work proposes an innovative mode of production of WJ-MSCs but more investigations are still necessary to intensify WJ-MSCs culture on microcarriers, and to be able to use these cells in clinical therapies. Some short and medium term perspectives are here proposed to further improve the expansion process.

- *Microcarriers functionalization*
  As it was shown in one of the part of this thesis work, the impact of the nature of the material used for cell expansion was not negligible. A more in-depth study of the forces of attachment on the various surfaces used in cell culture would be an asset to better develop the expansion of the WJ-MSC. A thesis work is in progress on the modelling of different mechanisms of cellular adhesion to improve the knowledge of these phenomena. Moreover, cell detachment is also another main problematic in the investigation of the intensification of WJ-MSCs culture on microcarriers. As the cells are used for clinical therapies, an efficient and non deleterious detachment is required. The modification of microcarrier surfaces, such as with addition of sensible layers to the cell environment (temperature, pH, ...) or the synthesis of enzymatically soluble microcarriers are promising cues for the intensification of the WJ-MSCs culture on microcarriers.

- *Cell culture medium composition*
  Composition of the cell culture medium is essential for the efficiency and the safety of the *ex vivo* culture of MSCs. Ideally, media have to maintain the phenotype, the genetic stability, and the functions of the cells during the culture. In the present work, the cell culture medium was composed of a basal medium (α-MEM) and was completed with human platelet lysate (HPL - Cook Regentec), in order to bring to the cells all the growth factors required. However, in order to produce cells for use in human therapy, very strict rules have to be respected, such as a clinical grade certification for the HPL. Thus, a chemically defined cell culture medium should be in the mid-term preferred.

- *Direct MSCs extraction from UCs*
  In order to meet the demand of GMP processes, a new design of bioreactor could be considered, and required to be totally closed and automated. Some preliminary experiments demonstrated the possible migration of MSCs from the umbilical cord towards microcarriers. A new system allowing *in situ* WJ-MSCs extraction and their culture on microcarriers could be envisaged to limit the risk of human errors.

- *Perfusion system design and agitation conditions*
  In the present work, a new perfused-continuous mode of WJ-MSCs production demonstrated that a 1.5 higher cell expansion factor was obtained in comparison with fed-batch modes. Numerous culture parameters seemed important to control and optimize in order to obtain a efficient perfused-continuous bioreactor, such as, the microcarrier concentration, the rate of agitation, the diameter of the settling tube, the flow rate of perfusion. A

decrease of the agitation rate could favor cell migration, but will also promote an increase of aggregates sizes, whereas, an increase of the agitation rate could be a solution for the aggregates dissolution. Moreover, in a problematic of intensification of process, the scale-up of this system of perfusion has to be considered. According to a previous thesis work dedicated to VERO cells culture (Dr. Amal El Wajgali), scale-up laws were determined thanks to a dimensional study, and allowed to consider the limits of scale-up. For bioreactor volumes lower than 100 L, no technical issues should arise from the use of this system.

- *On-line monitoring of cell growth*
  Thanks to dielectric probe, a linear correlation was found between the permittivity and the cell viable concentration. However, during the additions of microcarriers, and with the stops of agitation, the signal appeared disturbed, in particularly, when microcarriers formed aggregates due to a high quantity of cells. Usually, in these systems of cell monitoring, cells were considered as perfect spheres, with a constant diameter and a constant cytoplasmic content. It would be interesting to develop new models, better adapted to the morphological characteristics of adherent cells, and in particularly, to mesenchymal stem cells. Moreover, Raman on-line monitring could also a promising tool for the better understanding and the intensification of the expansion process of WJ-MSCs in stirred tank bioreactors.

All these different considerations could be interesting elements for a intensification of the WJ-MSCs culture on microcarriers in stirred tank bioreactors, and could be the subject of further studies in the framework of the INTERREG project. In addition, other scientific proposals could be considered as long term perspectives.

- *Stemness markers*
  A large variety of MSCs source exists but no consensus has been found about the definition of these cells yet [1]. In 2006, the International Society of Cell Therapy (ISCT) described a set of minimal criteria to characterize MSCs [2]. However, it seems that these commonly described markers are not distinctive and not sufficient for defining a cellular composition or biological functions of MSCs [3]. Now, efforts are made towards obtaining consensus on MSCs definition, that it would be indeed, a useful development. Thus, numerous comparisons across studies could be used and facilitate the use of MSCs in clinical, by correlating MSCs surface protein markers expression with their *in vitro* and *in vivo* bioactivity [3]. Moreover, no markers for senescence or proliferation states have been described yet. Relating the expression of specific markers to a specific bioactivity of the cells could be a great help for the use in therapy.

- *Stress markers*
  Among the expressed markers or the secreted proteins, it certainly exists some of them characterizing the cell stress. Indeed, when cultured on microcarriers, the cells are subjected to hydromechanical stresses. Works have been carried-out in order to optimize the impeller design for MSCs culture on microcarriers in stirred tank bioreactor, such as the PhD work of

Dr. Céline Loubière [4]. It could also be interesting to study markers expressed by cells as function of hydromechanical stresses.

- *Downstream process of the production of MSCs*
  The downstream process has not been developed in this thesis work but still remains a key milestone of the production of MSCs for a clinical use. The transfer to the cell culture medium to a cryopreserved state should be carried-out in a really short time [5]. After cell detachment, cells are separated from the microcarriers by size exclusion. In small scale cultures, sterile sieves can be used, but in larger culture it will be not suitable [6]. A solution from Thermo Scientific does exist and its called the Harvestainer BioProcess Container (BPC). After the detachment and separation steps, washing steps are required before the cryopreservation. Majority of MSC-based products are cryopreserved in order to be stored and transported. Challenges are important in evaluating the potential functionality of MSC directly after thawing before their infusion in patients [7]. Despite a non-destructive storage, it has been shown that under 1 % of injected cells were able to engraft to the injured study, leading to think that the paracrine effect of MSCs is important and non negligible [8]. Thus, secreted factors of MSCs can be a reliable alternative to their injections.

- *MSCs for the tissue engineering*
  As presented in the literature, MSCs can also be used in tissue engineering. It requires the conception of functionalized scaffolds. Creation of reconstructed organs can be lead by the lack of organs available for transplantation. MSCs seemed to be good candidates for the recellularization of the scaffolds to produce reconstructed organs thanks to their ease to proliferate [9]. Promising work has recently shown the feasibility to recreate organs for the reconstruction of heart, lung, liver and kidney [9]. Many work remains to do about the scaffold, the recellularization and the vascularization of these new bioorgans. Moreover, tissue engineering can also have applications in food products. Cultured stem cells derived from muscles seemed to emerge in publications. Some developed methods of production of stem cells were used for production of derived myoblasts in order to develop cultured meat [10]. For synthetic meat production several stem cells are of interest, notably myoblasts or satellite cells, firstly described in 1961 by Mauro [11]. However, limits were described and concerned the lack of well known techniques to isolate them. Moreover, still some ethical and societal concerns exist about tissue engineering.

Bibliography

[1] A. Keating. Mesenchymal stromal cells: new directions. *Cell Stem Cell*, 10(6):709–716, 2012.

[2] M. Dominici, K. Le Blanc, I. Mueller, I. Slaper-Cortenbach, F. Marini, D. Krause, R. Deans, A. Keating, D. Prockop, and E. Horwitz. Minimal criteria for defining multipotent mesenchymal stromal cells. the international society for cellular therapy position statement. *Cytotherapy*, 8(4):315–317, 2006.

[3] M. Mendicino, A. M. Bailey, K. Wonnacott, R. K. Puri, and S. R. Bauer. MSC-based product characterization for clinical trials: an fda perspective. *Cell Stem Cell*, 14(2):141–145, 2014.

[4] C. Loubière. *Characterization and impact of the hydrodynamics on the performance of umbilical-cord derived stem cells culture in stirred tank bioreactors*. PhD thesis, Université de Lorraine, 2018.

[5] E. Abraham, S. Gupta, S. Jung, and E. McAfee. Bioreactor for scale-up: process control. In *Mesenchymal Stromal Cells*, pages 139–178. Elsevier, 2017.

[6] V. Jossen, C. van den Bos, R. Eibl, and D. Eibl. Manufacturing human mesenchymal stem cells at clinical scale: process and regulatory challenges. *Applied Microbiology and Biotechnology*, 102(9):3981–3994, 2018.

[7] J. Galipeau. The mesenchymal stromal cells dilemma—does a negative phase iii trial of random donor mesenchymal stromal cells in steroid-resistant graft-versus-host disease represent a death knell or a bump in the road? *Cytotherapy*, 15(1):2–8, 2013.

[8] F. J. Vizoso, N. Eiro, S. Cid, J. Schneider, and R. Perez-Fernandez. Mesenchymal stem cell secretome: toward cell-free therapeutic strategies in regenerative medicine. *International Journal of Molecular Sciences*, 18(9):1852, 2017.

[9] J.-F. Stoltz, N. De Isla, Y. Li, D. Bensoussan, L. Zhang, C. Huselstein, Y. Chen, V. Decot, J. Magdalou, N. Li, et al. Stem cells and regenerative medicine: myth or reality of the 21th century. *Stem Cells International*, 2015, 2015.

[10] S. Verbruggen, D. Luining, A. van Essen, and M. J. Post. Bovine myoblast cell production in a microcarriers-based system. *Cytotechnology*, 70(2):503–512, 2018.

[11] M. J. Post. Cultured meat from stem cells: Challenges and prospects. *Meat Science*, 92(3):297–301, 2012.

Chapter 5

Résumé du travail de thèse

Contents

Cette thèse s'inscrit dans le cadre d'un projet européen INTERREG associant plusieurs laboratoires multidisciplinaires de la Grande Région transfrontalière. L'objectif principal de cette thèse est de développer un procédé d'expansion en culture continue perfusée de cellules souches humaines de cordon ombilical (CSMh). Ces cellules présentent un très haut potentiel en thérapie cellulaire et/ou ingénierie tissulaire mais la réussite de ces thérapies repose sur une expansion quantitativement et qualitativement efficace. Leur quantité, et donc leur production ainsi que leurs propriétés phénotypiques seront des indicateurs cruciaux pour répondre aux besoins des essais cliniques.

Le but de cette thèse est ainsi de proposer un procédé d'expansion de cellules souches humaines extraites de cordons ombilicaux, adhérées sur des surfaces innovantes. De plus la mise en place du procédé en mode perfusé sera réalisée en cherchant à maximiser le ratio qualité-quantité sur le coût de production, afin de généraliser ce type de productions le plus largement possible. Néanmoins, les milieux de culture spécifiques à ces cellules présentant des coûts importants, une réflexion devra donc être menée conjointement pour réduire les consommations de substrats, grâce à l'optimisation de l'alimentation (compositions, débits, moments d'ajout), ou grâce à la proposition de stratégies innovantes, telles que le transfert des cellules de microporteur à microporteur, observable lors de la mise à disposition de nouvelles surfaces d'adhérence dans une culture des CSMh sur microporteurs déjà établie. Or, le détachement des CSMh des microporteurs après leur expansion, demeure un pré-requis obligatoire dans le cadre d'une utilisation thérapeutique. Ainsi, après l'étude des performances d'expansion cellulaire sur des microporteurs commerciaux, des microporteurs expérimentaux présentant des surfaces innovantes, développées pour faciliter notamment le détachement des cellules ont été évalués. L'impact de la formulation des matériaux sur la croissance, l'adhérence et le détachement cellulaire ont été étudiés au cours de ce travail de thèse. Pour aider à la compréhension des mécanismes sous-jacents à la phase d'adhérence des cellules et ainsi améliorer celle-ci, mais afin aussi de disposer d'un indicateur "en-ligne" de la croissance cellulaire, l'utilisation de mesures spectroscopiques en ligne permettant de détecter l'adhérence, a également été évaluée. Sur la base de ces travaux, un nouveau mode de production de CSM-GW est proposé répondant aux exigences (quantité et qualité) pour leur utilisation en thérapie cellulaire.

5.1 Etat de l'art

5.1.1 Caractéristiques et propriétés des cellules souches

Intérêt thérapeutique des cellules souches

Le terme de cellules souches est apparu à partir de la fin du XIX^{ème} siècle, directement traduit de l'anglais « stem cells ». Il existe plusieurs types de cellules souches : les cellules souches embryonnaires, les cellules souches pluripotentes induites, et les cellules souches multipotentes. Les cellules souches multipotentes sont les plus utilisées en thérapie cellulaire et, au sein de leur catégorie, les cellules souches mésenchymateuses ont été pour la première fois décrites par Caplan

et al. [1]. Les cellules souches embryonnaires et pluripotentes sont à l'origine de tous les types de cellules de l'organisme tandis que les cellules souches mésenchymateuses (CSM) ne se différencient qu'en des cellules cartilagineuses (chondrocytes), osseuses (ostéoblastes), graisseuses (adipocytes) ou des fibres musculaires (myocytes) [2, 3].

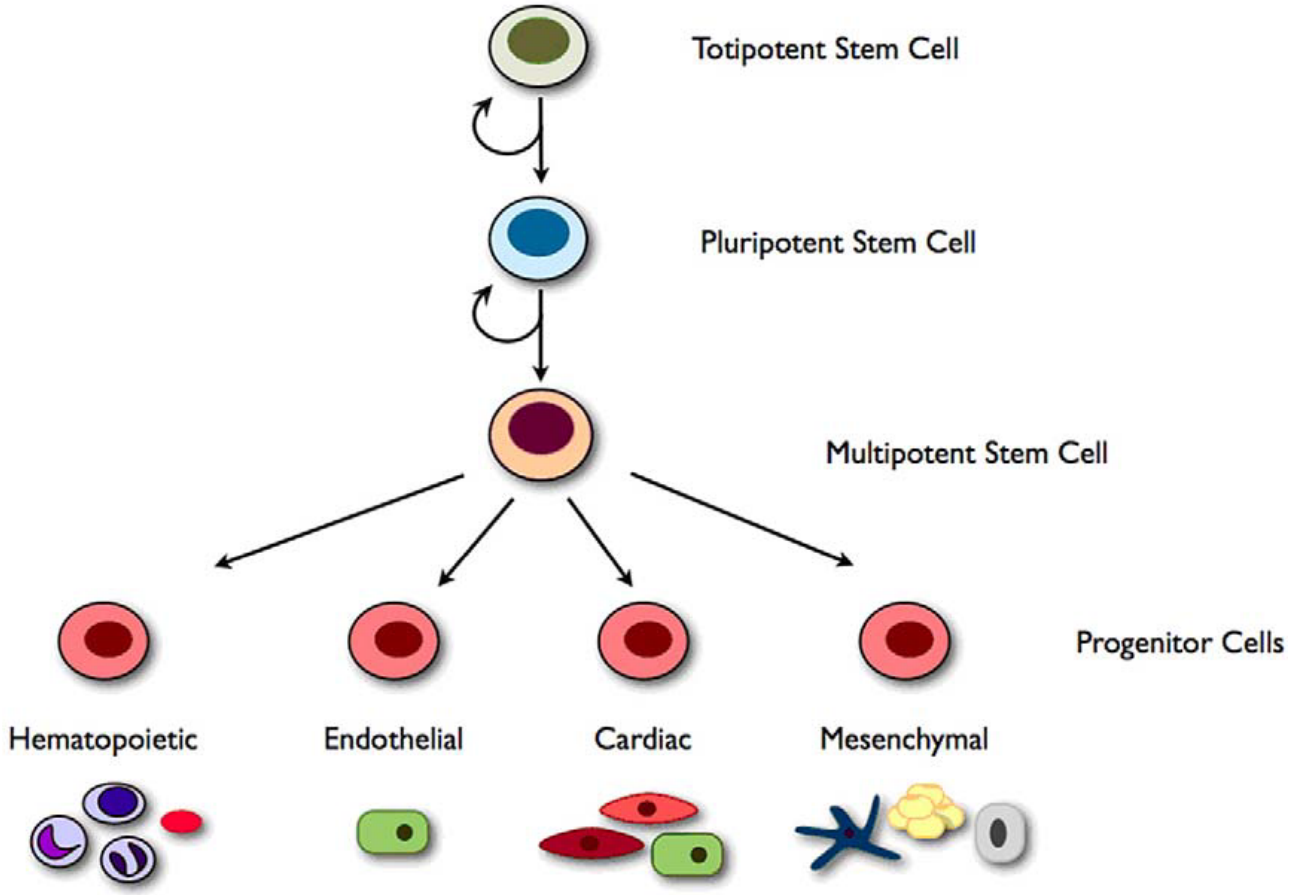

FIGURE 5.1 – Schéma représentant la classification des cellules souches [4].

L'intérêt porté aux CSM a grandi au cours du temps du fait de leur grand potentiel d'utilisation en thérapie cellulaire et ingénierie tissulaire. Grâce à un effet d'immuno-modulation et par un effet trophique, les CSM sont utilisées dans des études précliniques sur animaux, notamment pour le traitement de maladies neurodégénératives, de cancers, de maladies cardio-vasculaires, etc. [5] (Figure 5.2).

En mai 2016, soixante-sept essais cliniques utilisant des cellules souches mésenchymateuses en greffe allogénique étaient en cours [6], alors qu'en 2018, ce sont plus de deux cent trente-cinq essais cliniques qui ont été menés. De plus, comme le montrent différents travaux [7], le caractère immature des CSM permet leur injection chez les patients sans traitement d'immunosuppresseurs. Elles ne stimulent aucune alloréactivité, et échappent à la lyse des cellules T cytotoxiques et des cellules tueuses naturelles (NK-cells).

Les cellules souches mésenchymateuses de la gelée de Wharton (CSM-GW)

Les cellules souches mésenchymateuses sont présentes au sein du tissu adipeux, de la moelle osseuse, des tissus de soutien des organes, et ont été découvertes dans le cordon ombilical dans

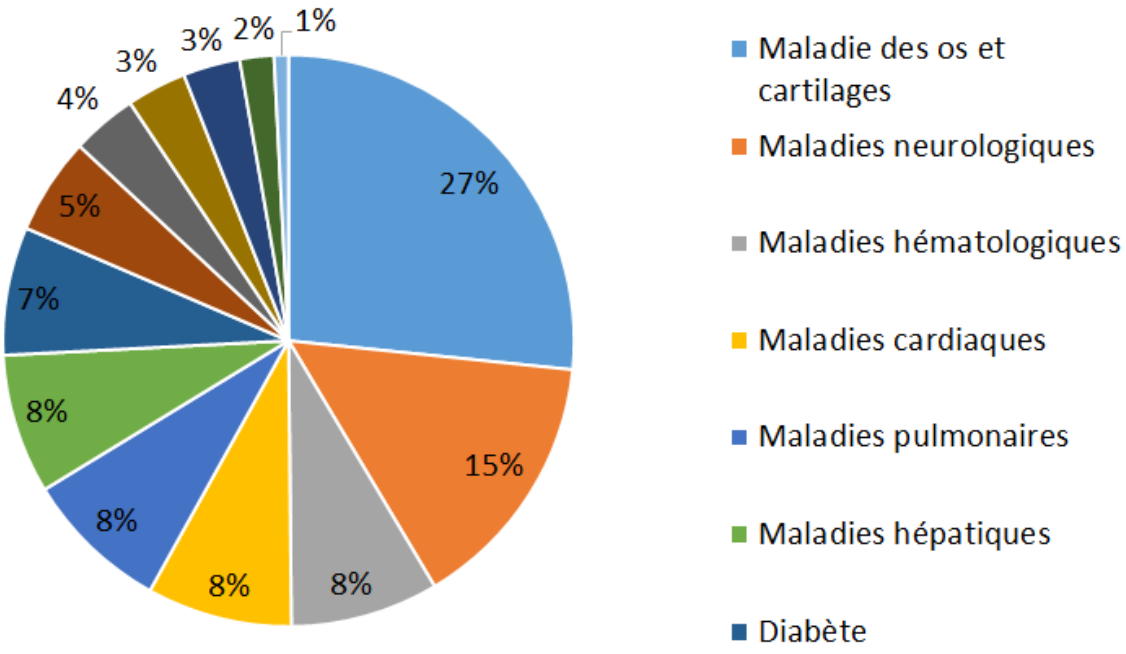

FIGURE 5.2 – Pourcentage de répartition des essais cliniques impliquant des CSM. Etude sur 620 cas du site clinicaltrial.gov, consulté en février 2020.

les années 1990. Ces cellules ont d'abord été décrites comme ayant un profil de cellules fibroblastiques [8], mais ce n'est que plus tard que les critères d'appartenance au groupe des cellules souches mésenchymateuses définis par l'International Society for Cellular Therapy (ISCT) ont été publiés [9]. Les cellules souches mésenchymateuses de cordon ombilical sont très intéressantes car elles sont notamment plus abondantes que les cellules souches de la moelle osseuse. De plus, elles présentent des performances de prolifération prometteuses. De telles caractéristiques reflètent la nature relativement primitive de ces cellules par rapport à leurs homologues adultes [10]. Un autre élément important de ces cellules de la gelée de Wharton, démontré par Lu *et al.* (2006) [11] est leur capacité à sécréter des cytokines, mais aussi d'autres facteurs tels que les GM-CSF (Granulocyte Macrophage Colony Stimulating Forming) et les G-CSF (Granulocyte Colony Stimulating Factor) qui permettent la multiplication des globules blancs. Ceci est très intéressant d'un point de vue thérapeutique, notamment lors d'un traitement de chimiothérapie, après une greffe de moelle osseuse ou encore au cours d'un traitement contre le VIH (Virus de l'Immunodeficience Humaine).

5.1.2 Procédés d'amplification pour des utilisations cliniques

Culture statique

Les CSM extraites de la gelée de Wharton (CSM-GW) sont des cellules adhérant au plastique. Ainsi, leur culture *in vitro* se réalise la plupart du temps dans des flacons de culture adaptés à la culture de cellules adhérentes. Tout comme les CSM extraites de la moelle osseuse, les CSM-GW possèdent des capacités d'auto-renouvellement. Elles sont ainsi capables de proliférer jusqu'à atteindre 100 % de la confluence puis, une fois la totalité de la surface des boites de culture colonisée, les cellules,

par un effet appelé « inhibition de contact », cessent de proliférer. La particularité des CSM-GW est leur capacité, au-delà de la confluence, à former des agrégats qui se détachent de manière spontanée des supports de culture. Ce procédé d'expansion est donc limité car il nécessite de réaliser un « passage » des cellules afin de multiplier leur nombre, c'est à dire un détachement enzymatique des cellules de leur surface d'adhésion, suivi par un ensemencement de ces mêmes cellules sur des surfaces plus grandes. Ces passages provoquent un vieillissement prématuré des cellules, et augmentent le risque de contamination par l'intervention du manipulateur [12]. C'est pourquoi des techniques de culture en mode agité ont été développées, afin d'améliorer le rendement d'expansion des CSMh.

Culture en mode agité

Afin de maximiser les surfaces d'adhérence disponibles pour les cellules, les procédés de culture de lignées continues adhérentes industrielles utilisent depuis de nombreuses années des microporteurs [13] en bioréacteur agité. Les microporteurs sont des particules de diamètre compris entre 100 et 300 µm, et qui peuvent être constituées de différents matériaux. L'agitation (culture en mode agité) doit être soigneusement définie afin d'homogénéiser efficacement la suspension liquide-solide, permettre des transferts de matière suffisants (oxygène, nutriments, produits) tout en limitant les contraintes hydromécaniques. A noter également que de nombreuses études sont menées pour optimiser le matériau utilisé en vue de favoriser conjointement l'adhérence, la croissance et le détachement cellulaire, tout en limitant l'altération de la qualité des CSM [14]. En dépit des contraintes hydromécaniques accrues en comparaison des cultures statiques, ces procédés sont très performants pour accroître l'expansion, jusqu'à un facteur 20 pour des CSMh extraites de la moelle osseuse [15]. Plusieurs types de bioréacteur sont décrits dans la littérature tels que des spinners, des cuves agitées et aérées, des systèmes à lit fluidisé, etc ...(Figure 5.3).

Migration cellulaire, un phénomène à contrôler pour la montée en échelle des procédés

Un des verrous technologiques connus lors de l'expansion de cellules adhérentes est la limitation en surface d'adhérence observée suite à l'expansion cellulaire. Comme le montre la figure 5.3, il existe différents systèmes de production des cellules souches mésenchymateuses; cependant, certains, comme les systèmes statiques, sont limités en surface disponible pour les cellules une fois la confluence atteinte. Ce n'est pas le cas des bioréacteurs agités utilisant les microporteurs, qui par principe, offre déjà des ratio surface/volume plus élevés, et qui permettent en plus, l'ajout de nouvelles surfaces à coloniser. En effet, plusieurs études ont montré la capacité des cellules souches à migrer vers de nouvelles surfaces sans l'intervention d'enzymes de détachement [17, 18, 19]. Ce phénomène de migration inter-particulaire (ou « bead-to-bead transfer »), permet de prolonger la culture de CSM en évitant la formation d'agrégats. Il est donc clair que cette capacité de migration devra être intégrée dans la conception du système de culture continue et perfusée.

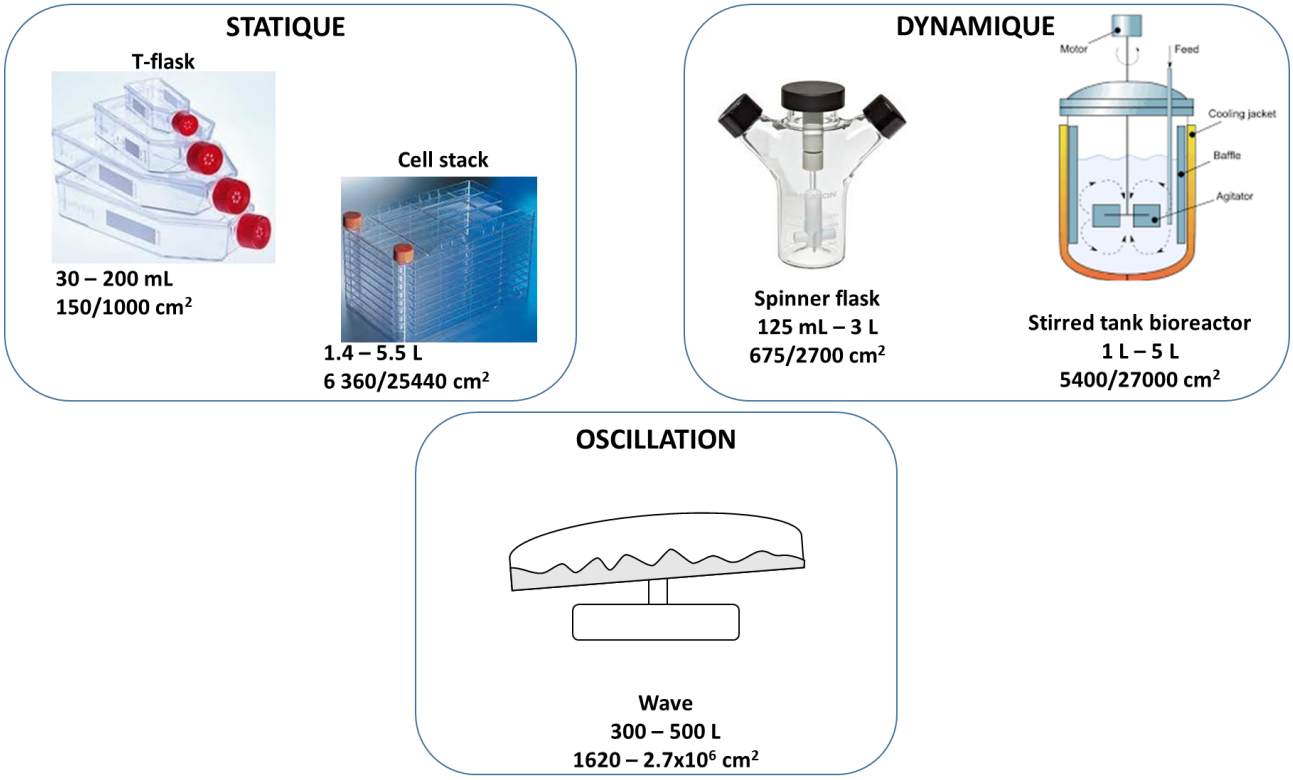

FIGURE 5.3 – Les différents procédés de culture des CSM (Schnitzler, A. C. *et al.* [16]).

5.1.3 Les méthodes de suivi en-ligne et la maîtrise de la qualité cellulaire

Comme indiqué précédemment, les CSM présentent un fort potentiel thérapeutique, sous réserve que leur propriétés et fonctionnalités restent opérationnelles, notamment qu'elles respectent les critères de l'ISCT [20]. Cela consiste en :

1. Pouvoir adhérer sur des surfaces plastiques dans des conditions standards de culture.

2. Répondre de manière positive aux marqueurs de surface CD105, CD73, CD90 et négative pour les marqueurs CD45, CD34, CD14 ou CD11b, CD79a, CD19, et pour les marqueurs HLA.

3. Avoir la capacité de se différencier in vitro en ostéoblastes, chondrocytes et adipocytes.

Au cours des procédés d'expansion, notamment en bioréacteur, il est important de mettre en place des méthodes de contrôle en temps réel afin d'avoir la possibilité de maîtriser au mieux la qualité cellulaire. Parmi les paramètres suivis, certains le sont classiquement, tels que la température, le pH ou l'oxygène dissous. En plus de ces derniers, le suivi des métabolites et des substrats a été développé au cours de ces dernières années par utilisation de la spectroscopie RAMAN ou NIR [21]. Par ailleurs, le suivi de la concentration cellulaire par spectroscopie diélectrique peut présenter, dans notre cas, des potentialités intéressantes, puisque cette méthode permet d'estimer en temps réel, la concentration des cellules vivantes au cours d'une culture. En effet, par cette technique, les cellules sont soumises à différentes fréquences (500 – 1000 kHz), et si elles possèdent une membrane plasmique intacte, les cellules se polarisent, phénomène détecté par la sonde. Du

fait de cette polarisation, il est également possible de déceler un changement de forme des cellules ainsi que leur viabilité. Ce procédé a été mis en place en bioréacteur perfusé pour suivre l'expansion et la viabilité de cellules adhérées sur microporteurs [22]. La spectroscopie diélectrique a aussi été utilisée en culture de cellules souches pour mesurer la concentration cellulaire au cours du temps. Cette technique en ligne est très intéressante car elle permet de suivre le nombre de cellules au cours du temps sans procéder à un détachement des cellules de leurs porteurs [23]. Certains auteurs ont également modélisé la concentration cellulaire viable, la taille des cellules, la conductivité intracellulaire ainsi que la capacitance membranaire grâce à la spectroscopie diélectrique [24]. Cette technologie permet donc au final d'accéder à des informations complémentaires sur l'état physiologique des cellules en cours de culture. L'utilisation de la sonde diélectrique dans ce travail de thèse trouve son originalité dans son utilisation pour détecter les premiers instants d'adhérence et l'étalement progressif des cellules sur leurs microporteurs. Ainsi, en plus de suivre la concentration des cellules et leur viabilité, nous évaluerons également plus précisément la cinétique du phénomène d'adhésion des cellules sur leur support.

5.2 Interactions cellules - supports

5.2.1 Détection de la phase d'adhésion cellulaire au cours de la culture par l'utilisation de la spectroscopie diélectrique

Comme cela a été développé précédemment dans l'état de l'art, les cellules vivantes peuvent être assimilées à des petits condensateurs capables de se charger ou de se décharger. Ce mouvement de charges est détectable par spectroscopie diélectrique. Nous avons alors cherché à mesurer le moment d'adhésion des cellules sur leurs supports en utilisant la spectroscopie diélectrique (Hamilton).

Le diamètre prédictif des cellules sur leurs porteurs peut être calculé grâce aux valeurs de permittivité et de fréquences critiques obtenues au cours de l'expérience. Des modèles faisant intervenir les résultats expérimentaux donnent ainsi des résultats intéressants (Figure 5.4 a).

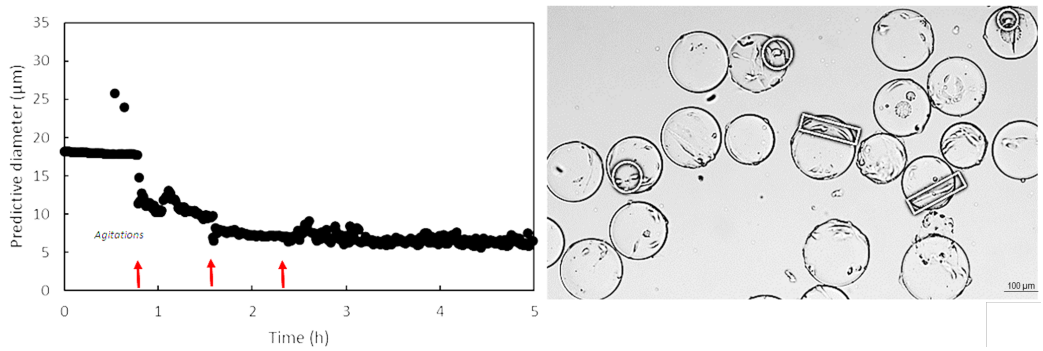

FIGURE 5.4 – (a) Evolution du diamètre prédit au cours du temps. (b) Photos des cellules étalées et encore circulaires adhérées sur les microporteurs après six heures de culture.

Nos résultats montrent que le diamètre cellulaire prédit est divisé par trois, passant de 15 µm à 5 µm, après deux heures de culture. Cette diminution est très vraisemblablement à relier à un

changement de forme des cellules. En effet, tandis qu'en suspension les CSM présentent une morphologie sphérique, celles-ci s'étalent et adhèrent dès qu'une surface compatible est rencontrée. Des photos prises ont montré que ces deux morphologies (circulaire et étalée) pouvaient effectivement être observées sur un microporteur après six heures de culture (Figure 5.4 b). En conclusion, il semble possible de détecter un changement de forme des cellules lors de leur adhésion sur le microporteur par cette technique de spectroscopie diélectrique. Cette méthode sera par la suite implémentée sur un bioréacteur, et permettra un suivi en ligne des cultures au cours du temps des cellules vivantes.

5.2.2 La migration cellulaire permet un maintien des cultures pendant quelques jours et améliore le facteur d'expansion

La capacité des cellules à migrer vers de nouveaux supports, sans détachement préalable, a été évaluée au cours de ce travail de thèse. Les cultures ont été dans un premier temps réalisées dans des fioles d'Erlenmeyer. Après quatre jours de culture, de nouveaux microporteurs « frais » sont ajoutés dans le milieu. Tous les deux jours, les échantillons prélevés sont photographiés afin d'évaluer le nombre de cellules par microporteur, leur viabilité ainsi que le nombre total de cellules. Les résultats sont présentés dans la figure 5.5.

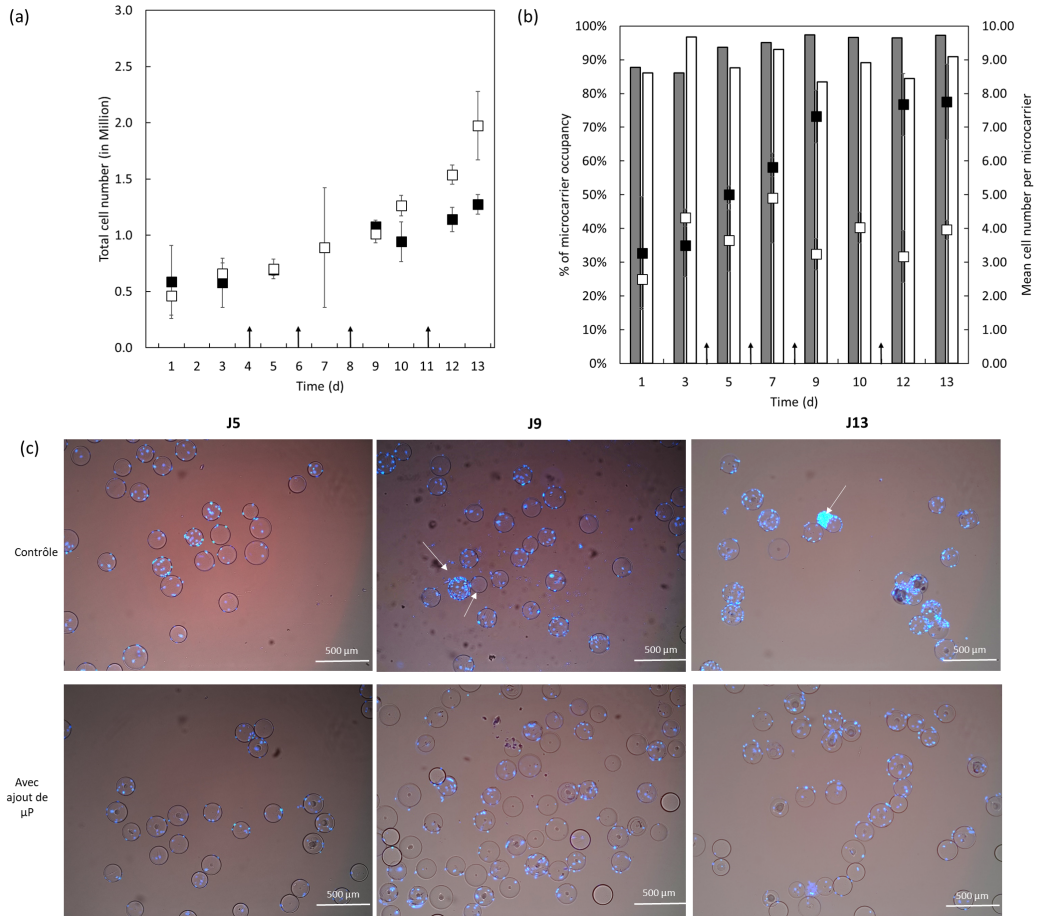

FIGURE 5.5 – (a) Evolution du nombre total de cellules au cours du temps. (b) Evolution de la colonisation des microporteurs et étude du nombre de cellules par microporteur au cours du temps. (c) Photos prises suite au marquage DAPI des noyaux cellulaires après 5, 9 et 13 jours de culture.

Lors de l'ajout de microporteurs, l'expansion cellulaire est augmentée d'un facteur supérieur à deux, après huit jours de culture. Le suivi de la colonisation des microporteurs (Figure 5.5 a) montre ainsi une baisse de la colonisation des porteurs et une stabilisation du nombre de cellules par microporteur autour de six à huit. En analysant les photos réalisées, on peut observer que les cellules sont capables de migrer vers les nouvelles surfaces mises à leur disposition (Figure 5.5 c). Au contraire, s'il n'y a pas d'ajout de microporteurs après une dizaine de jours de culture, les cellules forment des agrégats sur leurs porteurs et se détachent. Ce phénomène n'est pas observé si des microporteurs sont ajoutés en cours de culture. Cette expérience a été reproduite une seconde fois et ces résultats ont été validés. Ainsi, grâce à la démonstration de ce phénomène de migration des cellules, une stratégie d'optimisation a été mise en place. Après l'analyse des photos réalisée automatiquement par un script Matlab, le moment de l'ajout ainsi que la quantité de microporteurs à apporter à la culture ont pu être déterminés. Ces ajouts de porteurs, réalisés de manière séquentielle, ont permis de maintenir un nombre maîtrisé et optimal de cellules sur les microporteurs, favorisant ainsi l'expansion des CSMh au cours du procédé.

Par ailleurs, grâce à l'interprétation de certaines données spécifiques enregistrées par le spectroscope, notamment la fréquence critique, des informations sont disponibles sur l'état physiologique, le biovolume et le rayon des cellules. Les étapes d'adhésion peuvent être détectées et analysées. Ainsi, environ 2 heures seraient nécessaires pour que les premières étapes d'adhésion soient établies (interactions électrostatiques et de Van der Waals). Cependant, des études supplémentaires seront nécessaires, avec différents matériaux de surface des microporteurs par exemple, pour affiner ces résultats préliminaires. Par la suite, la spectroscopie diélectrique sera mise en œuvre dans des bioréacteurs pour suivre en ligne la croissance des cellules et les états et modifications de la physiologie cellulaire.

En ce qui concerne l'état physiologique des CSM-GW, les mécanismes de migration de ces cellules ont été décrits dans la littérature. On sait déjà que les CSM-GW sont capables de se déplacer vers les sites de blessure grâce à leurs propriétés de migration. Cette capacité des CSM-GW à être mobile a été visualisée pour la première fois par microscopie en temps réel dans cette étude. Il a été possible de calculer un temps moyen pour une migration complète d'un microporteur à un autre. Ainsi, environ 3 heures seraient nécessaires pour une migration cellulaire complète, avec une vitesse moyenne de déplacement de 60 $\mu m\ h^{-1}$. Ce processus de migration prend du temps et semble dépendre de différents facteurs, comme la présence de cellules sur le microporteur ciblé ou le contact cellule-cellule, par exemple. Des études supplémentaires seront nécessaires pour mieux étudier ce phénomène. En outre ces expériences ont été réalisées en mode statique, ce qui n'est probablement pas représentatif de ce qui pourrait se passer dans des cultures dynamiques.

Ainsi, ce potentiel de migration optimisé pourrait être utilisé afin d'améliorer l'expansion cellulaire et d'éviter la limitation de la surface cellulaire dans les cultures dynamiques. À petite échelle, l'ajout de quantités bien déterminées de microporteurs à un moment précis des cultures semble améliorer l'expansion cellulaire d'un facteur 1,3 dans les fioles d'Erlenmeyer. Cependant, cet ajout de microporteurs a eu un impact sur les cultures puisqu'une augmentation de la mort cellulaire a été observée ainsi qu'une altération de la composition des supports. Avec une augmentation

de la concentration et une agitation non adaptée, les collisions et les frictions des microporteurs semblent générer un stress sur les cellules, provoquant une mort prématurée. Un système d'agitation mécanique plus adapté à la culture de CSM-GW sur microporteurs a été proposé. En outre, les bases d'une stratégie de culture en mode fed-batch ont également été établies pour la culture de CSM-GW dans des bioréacteurs à cuve agitée. Les principaux résultats obtenus ont été résumé dans la figure 5.6.

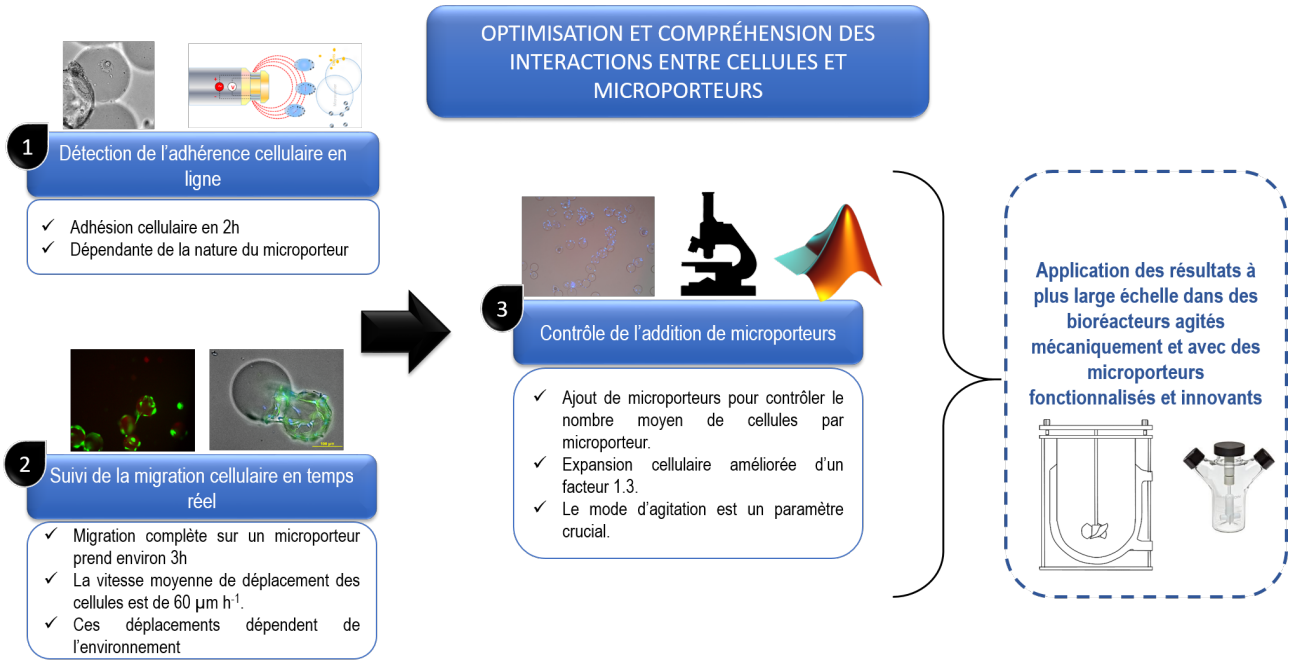

FIGURE 5.6 – Schéma récapitulatif des résultats obtenus dans le chapitre 2.

5.3 Développement de bioréacteurs en mode fed-batch pour la production de CSM-GW sur microporteurs innovants

Dans le cadre du projet INTERREG, des collaborations ont été mises en place entre des équipes spécialisées en matériaux et des équipes spécialisées en culture et biologie cellulaires. Ainsi, une des tâches du projet était de développer des surfaces innovantes pour la croissance des cellules souches. Selon la littérature et les études précédentes, en particulier dans les deux dernières thèses réalisées au laboratoire sur ce sujet [14, 25], l'une des principales limitations dans la culture de cellules souches est la phase de détachement. Comme indiqué précédemment dans la bibliographie, de nombreux protocoles de détachement étaient disponibles dans la littérature et offraient différents taux d'efficacité. Sur la base des résultats précédents du laboratoire, de grandes difficultés subsistaient dans l'utilisation du microporteur Cytodex-1 en raison de la difficulté de détachement des cellules. C'est pourquoi, des équipes de l'université de Liège et de l'Institut Leibniz (INM - Saarbrucken) ont modifié la surface de microporteurs commerciaux, surfaces dites 'smart', pour améliorer l'adhésion et le détachement des cellules.

Dans la liste des microporteurs disponibles dans le commerce, tous ceux intégrant des com-

posants d'origine animale, ont été exclus. Sur la base de l'expérience du LRGP, les microporteurs à base de polystyrène (appelés PlasticPlus) et les microporteurs Cytodex-1 sont apparus comme les meilleurs choix de microporteurs à modifier. La première étape de modification de la surface des microporteurs est basée sur une activation de surface, par un greffage chimique organique comme cela a été réalisé à l'Université de Liège, ou par une activation plasma comme cela a été réalisé à l'INM. Ensuite, la bio-fonctionnalisation peut être réalisée. A l'Université de Liège, cette fonctionnalisation a consisté en une polymérisation greffant une couche de polymère zwitterionique. L'équipe de l'INM a quant à elle greffé des ligands adhésifs.

5.3.1 Screening à petite échelle des propriétés d'adhésion et de détachement des microporteurs fonctionnalisés

Tout d'abord, l'adhésion cellulaire a été évaluée pour chaque microporteur fonctionnalisé et comparée à un microporteur commercial témoin, Cytodex-1 ou PlasticPlus. La meilleure adhérence cellulaire a été obtenue pour les candidats sans traitement plasma (w/o-pl + APTES Cytodex-1) et avec traitement plasma (w-pl + APTES Cytodex-1), l'ajout d'APTES a permis d'améliorer l'adhérence cellulaire (+30 %) par rapport au contrôle Cytodex-1 (Figure 5.7 A). Concernant les microporteurs de type PlasticPlus, une adhérence équivalente à celle du groupe contrôle Cytodex-1 (60 %) a été calculée. De plus, une plus grande sensibilité des résultats a été démontrée, certainement due à l'incertitude de comptage avec ces microporteurs, liée à leur opacité au microscope.

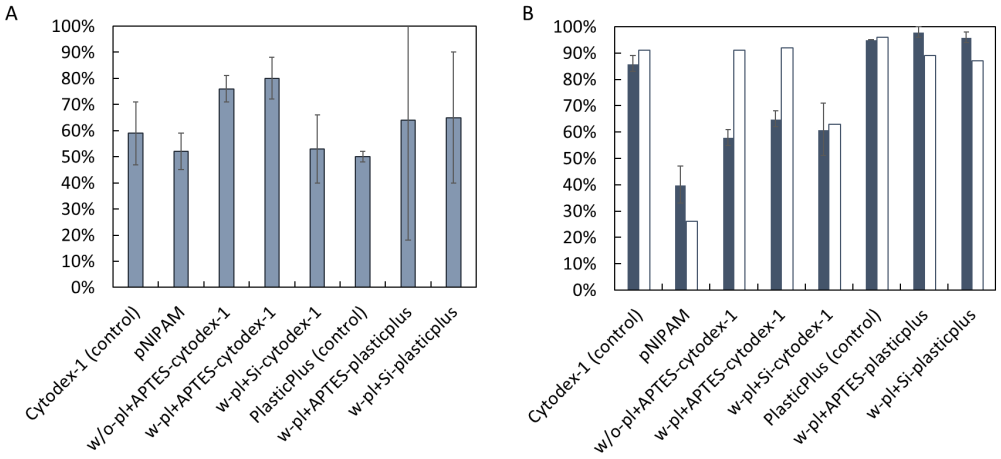

FIGURE 5.7 – Screening des propriétés d'adhésion et de détachement des CSM-GW des microporteurs fonctionnalisés (A) Pourcentage d'attachement en fonction de la chimie du matériau (B) Efficacité de détachement (barres noires) et viabilité cellulaire (barres blanches) post-détachement. Les termes w/o-pl et w-pl signifient sans traitement plasma et avec traitement plasma, respectivement.

L'ajout d'APTES ou de silane sur le Cytodex-1 n'a pas semblé améliorer le détachement des cellules, mais plutôt leur fixation. Cependant, la viabilité cellulaire après la trypsination est d'environ 90 %, sauf pour le Cytodex-1 greffé avec du silane (60 %), ce qui montre une bonne viabilité cellulaire (Figure 5.7 B). Pour le pNIPAM-Cytodex-1, il semble que l'effet de la température seule ne permette pas de détacher les cellules (Figure 5.7 B). Cependant, l'action d'une enzyme (comme par exemple l'Accutase), combinée à la température pourrait être plus efficace. Les microporteurs

permettant la meilleure efficacité de détachement des cellules sont les microporteurs PlasticPlus (à base de polystyrène traité) (Figure 5.7 B). Pour ces trois conditions, un meilleur rendement de détachement et une meilleure viabilité après détachement ont été obtenus.

Dans la suite de l'étude, l'expansion des CSM-GW dans les bioréacteurs à cuve agitée sera réalisée sur du Cytodex-1 et du PlasticPlus recouverts de fibronectine comme références commerciales, et sur du pNIPAM et du PlasticPlus greffés de silane.

5.3.2 Expansion des CSM-GW sur microporteurs innovants en bioréacteur fed-batch

Dans une étude précédente, il a été démontré que les microporteurs ajoutés pouvaient être colonisés par les cellules et permettaient un meilleur facteur d'expansion. Dans ce travail, il a été vérifié que, dans un système mécaniquement agité, les cellules sont toujours capables de migrer, de surcroît, avec des microporteurs "faits maison". Afin de limiter l'apparition d'agrégats cellulaires et d'augmenter la durée des cultures cellulaires, des microporteurs frais ont été ajoutés à des moments spécifiques des cultures en bioréacteur agité, pour maintenir à peu près constant le nombre moyen de cellules par microporteurs, autour de 6-7 cellules par microporteurs.

Dans la figure 5.8, les différentes croissances cellulaires en fonction du microporteur utilisé ont été représentées. Les cultures avec Cytodex-1 ont permis d'obtenir un nombre maximal de 35 millions de cellules, en 14 jours avec un nombre initial de 3 ou 5 millions de cellules adhérées (Figure 5.8 A). Deux lots cellulaires différents de cordon ont mis en évidence la variabilité de l'adhérence initiale des cellules sur le microporteur Cytodex-1. Comme il a pu être observé sur une des cultures, avec un faible facteur d'adhésion cellulaire (moins de 7 cellules par microporteur), une phase de latence s'est produite pendant une semaine, puis, avec l'ajout de microporteurs, la croissance cellulaire a débuté avec un meilleur facteur d'expansion (*i.e.* 7) grâce au "transfert inter-particulaire". Dans la figure 5.8 B, il est montré que les cellules cultivées sur des microporteurs pNIPAM ont atteint un nombre maximal d'environ 40 millions, en 12 jours, avec 7 millions de cellules initiales adhérées sur les microporteurs. Les deux lots réalisés semblaient relativement proches. Le lot de microporteurs pNIPAM produit par l'université de Liège semblait être reproductible en termes d'expansion de la culture cellulaire. Par rapport au Cytodex-1 commercial, pour lesquels une grande variabilité avait été détectée, certainement en raison de la variabilité initiale de l'adhérence au début de la culture. Dans la figure 5.8 C, il est montré qu'une culture avec les microporteurs PlasticPlus recouverts de fibronectine (PlasticPlus + FN) a permis d'obtenir au maximum environ 40 millions de cellules, en 9 jours. Alors que la deuxième culture a permis d'obtenir un nombre maximal de cellules de seulement 30 millions, en 7 jours. Le nombre total de cellules a chuté au $10^{ème}$ ou $8^{ème}$ jour de culture, même avec l'ajout de microporteurs. Dans la figure 5.8 D sont représentées les courbes d'expansion cellulaire avec PlasticPlus + Si et seulement une valeur de 22 millions de cellules environ a été obtenue après 10 jours de culture, puis le nombre total de cellules a chuté.

Une grande variabilité a été obtenue dans les résultats en raison de la variabilité des donneurs et de l'origine des cordons ombilicaux. En effet, pour chaque culture en bioréacteur effectuée,

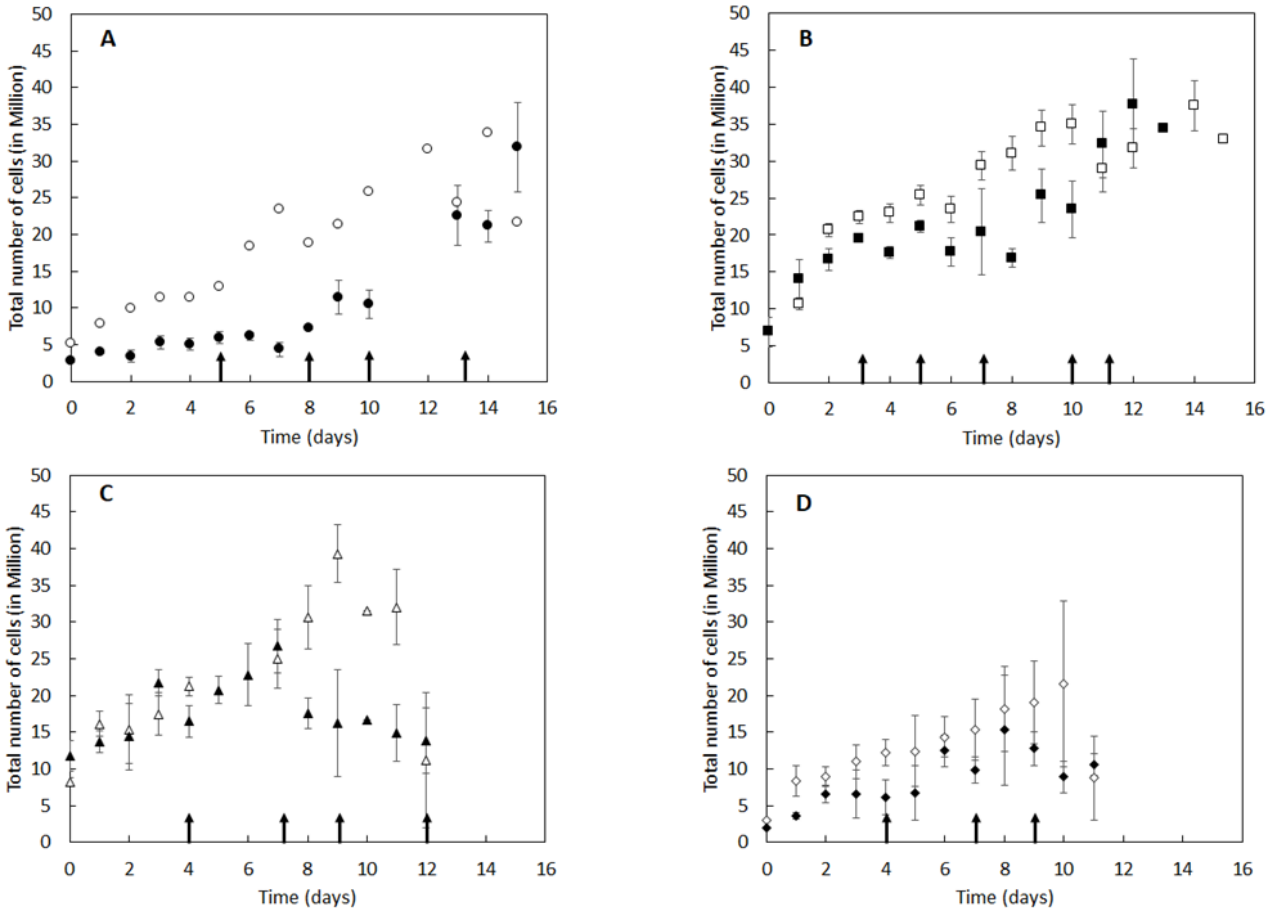

FIGURE 5.8 – Expansion cellulaire dans les bioréacteurs à cuve d'agitation en fonction du type de microporteur utilisé. (A) sur les microporteurs Cytodex-1, (B) sur les microporteurs pNIPAM, (C) sur les microporteurs PlasticPlus + FN, (D) sur les microporteurs PlasticPlus + silice. Les flèches noires représentent le moment d'addition des microporteurs. Les valeurs sont présentées sous forme de valeur moyenne ± écart type (n = 3). Les deux marques (pleines et vides) correspondent à deux prélèvements de cordon différents.

un lot différent de cellules a été utilisé. Même si le milieu de culture cellulaire, les passages et les densités d'ensemencement des cellules sont restés les mêmes, une grande variabilité a pu être constatée en fonction du donneur [26]. En outre, les conditions optimales de culture pouvaient être différentes pour chaque lignée cellulaire utilisée [27]. Par ailleurs, concernant le processus lui-même, plusieurs paramètres importants doivent être déterminés et optimisés, comme par exemple, la densité de chargement initiale des microporteurs et la densité d'ensemencement des cellules, l'alimentation et la composition du milieu, le matériau de revêtement du substrat, le protocole d'agitation, la forme et la configuration du bioréacteur, le protocole d'aération, le volume de culture initial et le pH initial [28].

Les principaux résulats de cette partie sont résumés dans la figure 5.9.

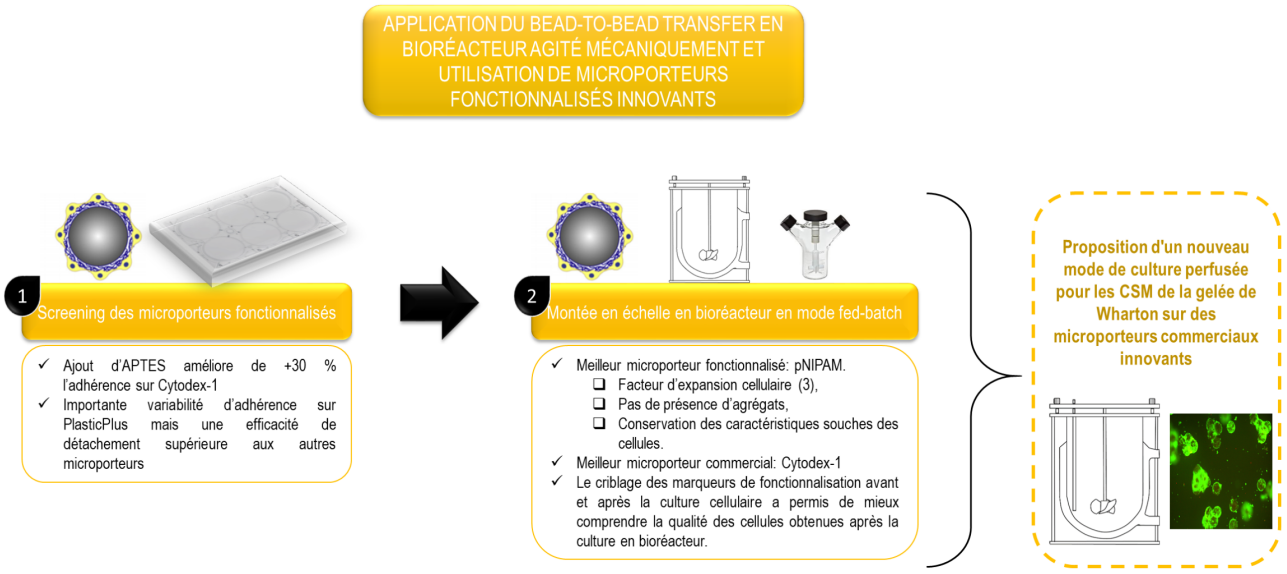

FIGURE 5.9 – Schéma récapitulatif des résultats obtenus dans le chapitre 3.

5.4 Proposition d'un mode opératoire innovant de bioréacteur pour la production de CSM-GW

Dans la dernière partie de la thèse (chapitre 4), un mode opératoire innovant a été proposé afin de produire une grande quantité de cellules souches tout en maîtrisant leur qualité. En effet, un nouveau mode de culture en perfusion continue, en utilisant un tube de décantation à l'intérieur du bioréacteur, et relié à une pompe de soutirage a été proposé afin d'améliorer l'expansion cellulaire. Le diamètre du tube a été calculé pour maintenir précisément les microporteurs colonisés par les cellules dans le bioréacteur alors que les microporteurs restés ou devenus vides ont été soutirés (inutiles pour l'expansion cellulaire et responsables de collisions potentiellement nuisibles), en utilisant un débit continu basé sur les exigences physiologiques des CSM. Enfin, la spectroscopie diélectrique en ligne a indiqué que les signaux spectraux pouvaient être reliés à la croissance et à l'adhérence des cellules. La particularité des microporteurs utilisés dans cette dernière partie est d'être soluble sous l'action de plusieurs enzymes, ce qui permet un détachement facilité des cellules. Enfin, une analyse du coût de fonctionnement de la production des CSM pour des traitements thérapeutiques a été réalisée.

5.4.1 Expansion des CSM-GW sur microporteurs solubles en bioréacteur perfusé

Dans un premier temps, les cultures ont été réalisées en mode fed-batch, comme décrit dans le chapitre précédent. Cependant, malgré l'ajout de microporteurs, nous avons noté la présence de microporteurs vides, non colonisés, et la formation d'agrégats de grande taille. Les facteurs d'expansion, la viabilité ainsi que les vitesses maximales de croissance étaient supérieures, surtout par rapport aux mêmes mesures réalisées avec les microporteurs évalués précédemment. De plus, ces microporteurs présentent l'avantage d'être solubles sous l'effet d'un mélange d'enzymes et

d'EDTA, permettant une libération rapide des cellules après culture (Figure 5.10).

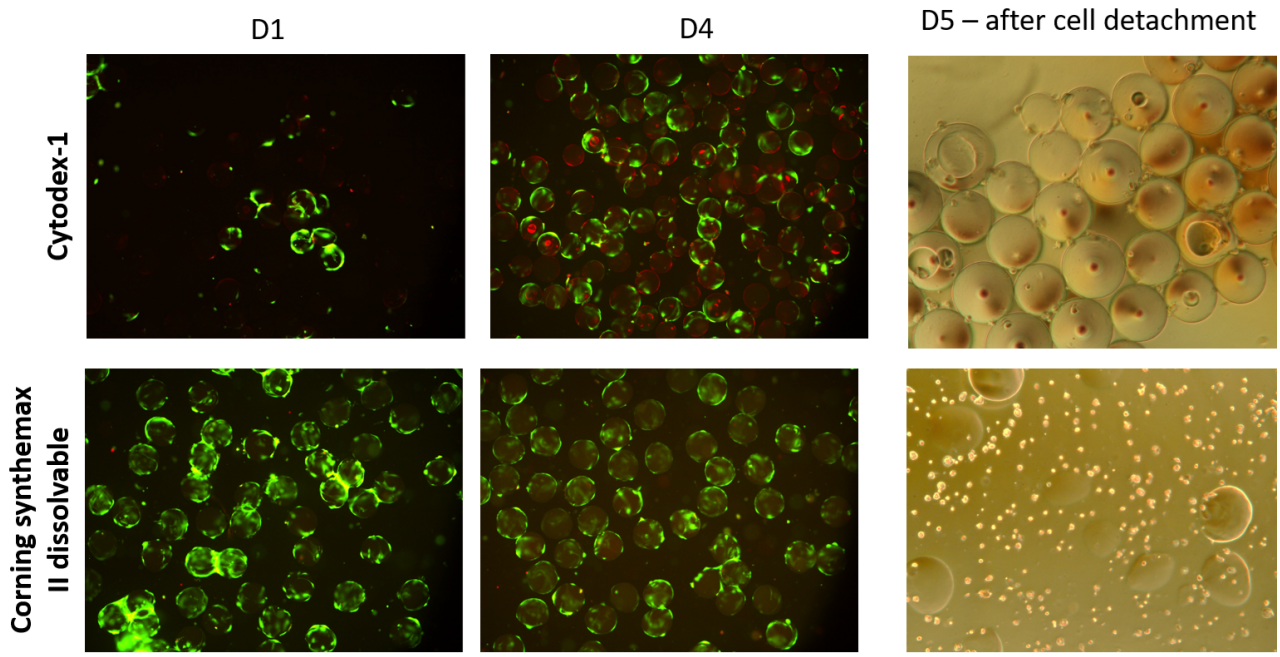

FIGURE 5.10 – Comparaison des microporteurs solubles Synthemax-II Corning et Cytodex-1, utilisés lors de cultures agitées de CSM-GW. Les cellules ont été observées par microscopie à fluorescence (D1-D4, coloration Live/dead et optique (D5).

A partir de cette observation, une nouvelle stratégie de conduite de bioréacteur a été mise en place, avec un maintien des microporteurs colonisés par les cellules dans le bioréacteur, tandis que le milieu usagé et les microporteurs vides ont été soutirés. Cette réalisation a été rendue possible grâce aux calculs de vitesses de sédimentation des deux systèmes particulaires. Les microporteurs impliqués dans les agrégats ont en effet une vitesse de sédimentation sensiblement plus grande que les microporteurs vides. En calculant la valeur du débit de soutirage, il est alors possible d'éliminer les microporteurs vides, grâce au dimensionnement du tube de décantation et à la sédimentation différenciées des microporteurs. Le montage est représenté dans la figure suivante (Figure 5.11).

Grâce à ce mode perfusé-continu, le facteur d'expansion cellulaire a pu être amélioré par rapport à la culture des CSM-GW réalisées en mode batch ou même fed-batch. Ainsi, un facteur d'expansion de 60 a été obtenu en continu-perfusé, alors que des facteurs de 43 et de 5 avaient été obtenus en mode fed-batch et batch respectivement. De plus, comme le montrent les photos de la figure 5.12, tous les microporteurs semblent colonisés dans la culture en mode perfusé. Des microporteurs vides ont bien été observés dans le milieu soutiré.

Un suivi en ligne de la croissance cellulaire a également été réalisé grâce à la spectroscopie diélectrique. Les résultats sont présentés sur le graphe de la figure 5.13. Il peut être noté que la permittivité et la croissance cellulaire semblent être corrélés linéairement. De plus, lors de l'ajout manuel de microporteurs nécessitant un arrêt d'agitation du réacteur, une diminution du signal de permittivité est observée de manière concomitante, probablement en raison de la sédimentation des microporteurs.

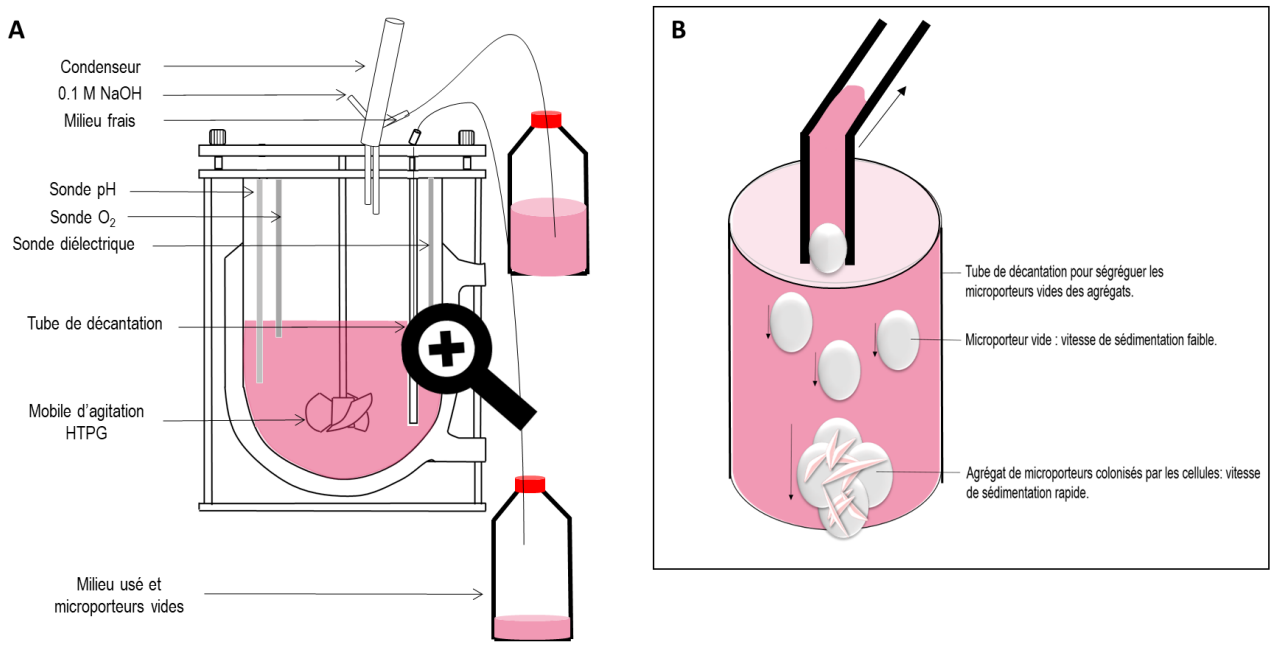

FIGURE 5.11 – (A)Schéma du montage du bioréacteur continu-perfusé. (B) Zoom sur le fonctionnement du tube de décantation.

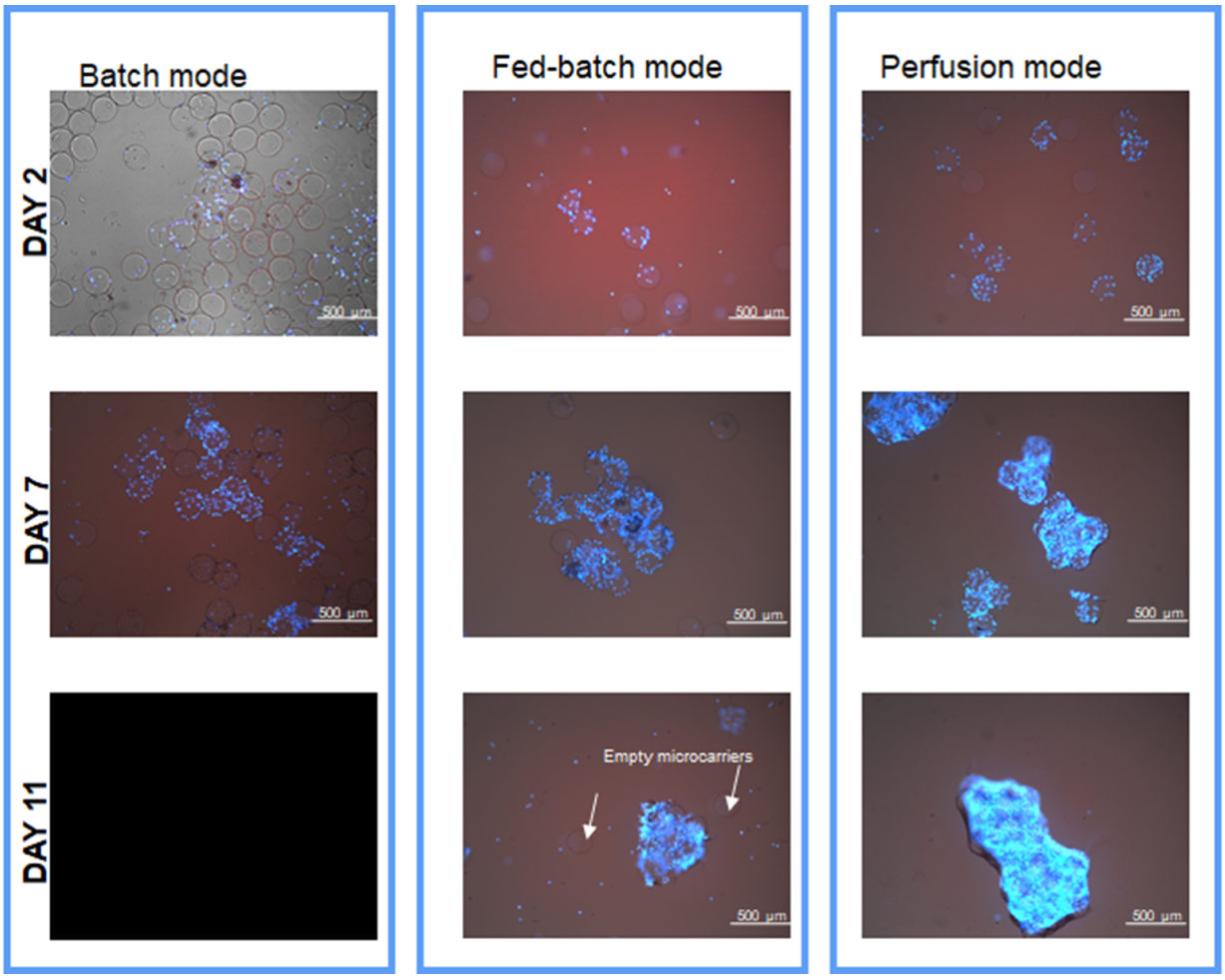

FIGURE 5.12 – Observations microscopiques avec marquage du noyau (DAPI) des CSM-GW sur les microporteurs solubles issus de procédés d'expansion en bioréacteur en mode batch, fed-batch et perfusé.

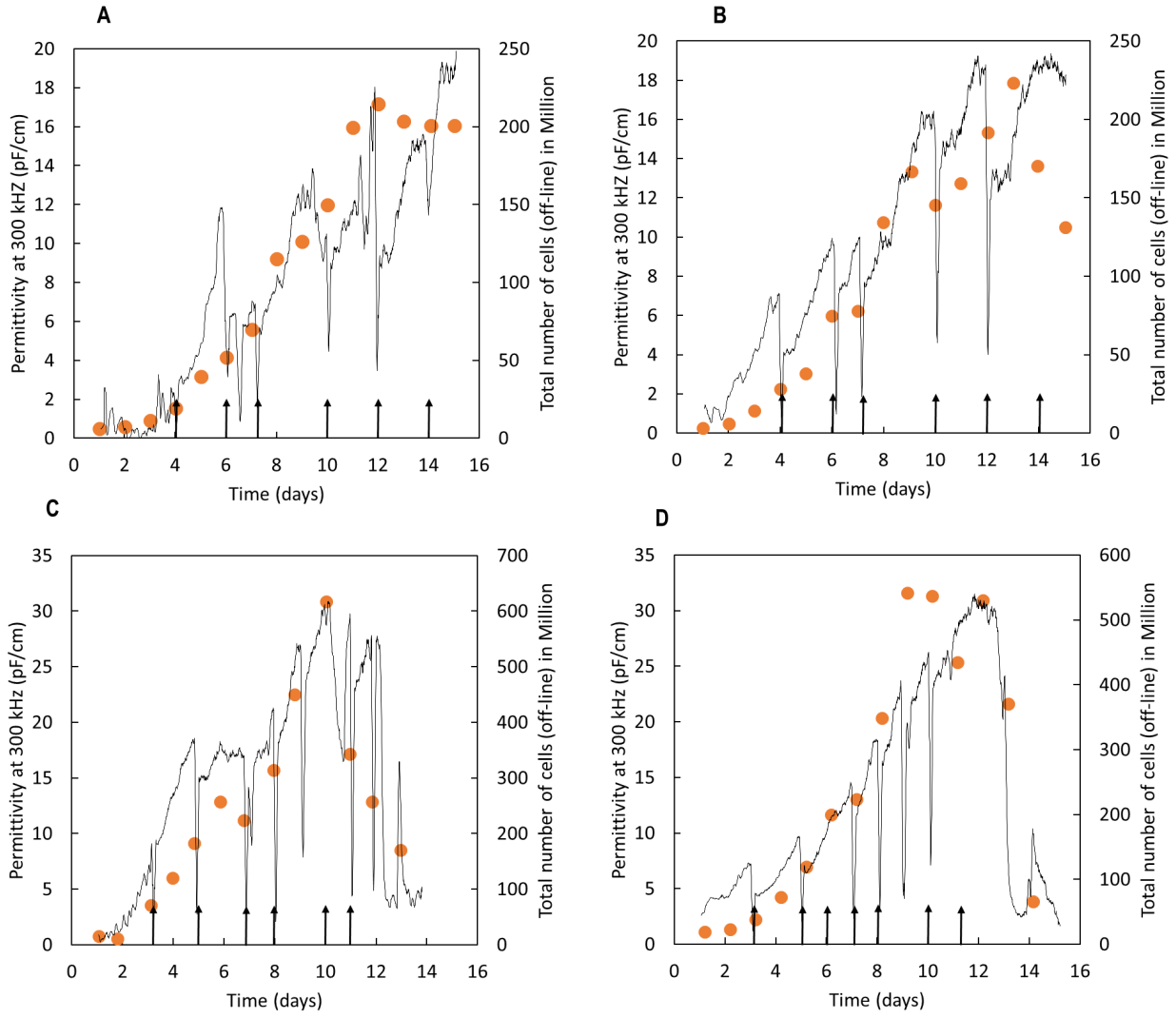

FIGURE 5.13 – Cinétique des cultures CSM-GW sur les microporteurs Corning effectuées en (A) mode fed-batch ou en (B) mode continu-perfusé. (•) mesures hors ligne et (lignes continues) valeurs en ligne. Les flèches indiquent les moments d'addition de microporteurs "frais".

5.4.2 Analyse du coût de production des CSM-GW en bioréacteur pour la thérapie cellulaire

Au cours de ce travail de thèse une étude des coûts a également été proposée. Les coûts opératoires de la production de CSM-GW ont été déterminés, en fonction du mode de production (batch, fed-batch et continu-perfusé). Ainsi, il a été montré que, pour une production en mode batch, dans des cuves de 250 mL de spinners simples, le coût de production des CSM était jusqu'à 4 fois supérieur que pour une production en bioréacteur. La méthode qui semble la moins coûteuse pour la production de CSM-GW serait le mode continu-perfusé. Ces résultats sont présentés dans la figure 5.14.

Puis une étude plus approfondie de l'origine des coûts a été réalisée. La première source de coût est la culture en bioréacteur, avec une forte consommation de réactifs. Il semblerait que la phase d'amplification en 2D soit coûteuse, due au temps de main d'œuvre et aux consommables utilisés.

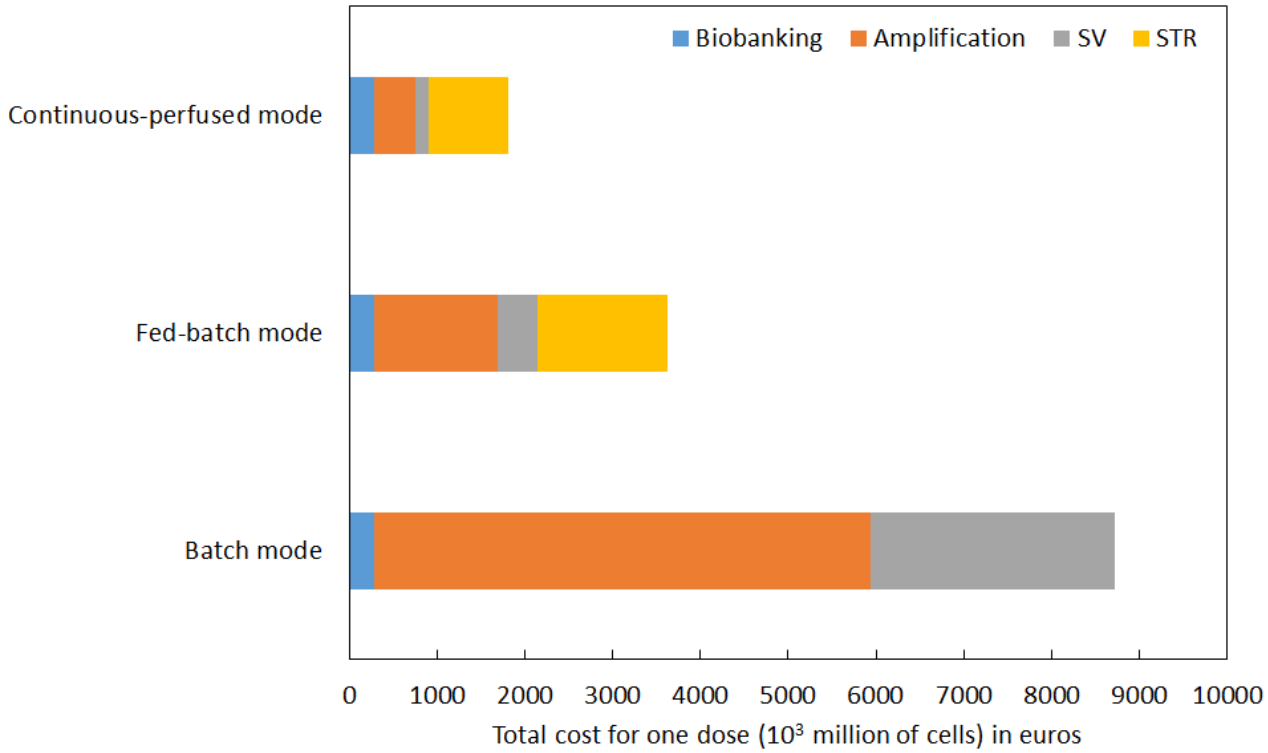

FIGURE 5.14 – Coût de production des CSM-GW pour les essais cliniques en fonction du mode de production : modes statique (Cell stack), batch (usage unique ou en spinner), fed-batch et continu - perfusé.

L'évaluation expérimentale et économique des différents modes de production est intéressante pour une exploitation commerciale des CSM-GW pour des thérapies cliniques. Les résultats montrent un intérêt pour le choix d'un mode de production en continu des WJ-MSC dans un bioréacteur à cuve agitée avec les microporteurs solubles. En effet, en mode batch, les coûts de production sont 5 fois plus élevés, et en mode fed-batch 2 fois plus élevés. Ces évaluations sont à prendre avec précaution car elles doivent prendre en compte la qualité des cellules. Par ailleurs, les taux de croissance spécifiques et l'efficacité du détachement sont directement dépendant de l'effet "lot" de différents cordons ombilicaux, des variations dans ces paramètres influenceront directement les coûts de production.

Les principaux résultats de cette partie sont résumés dans la figure 5.15.

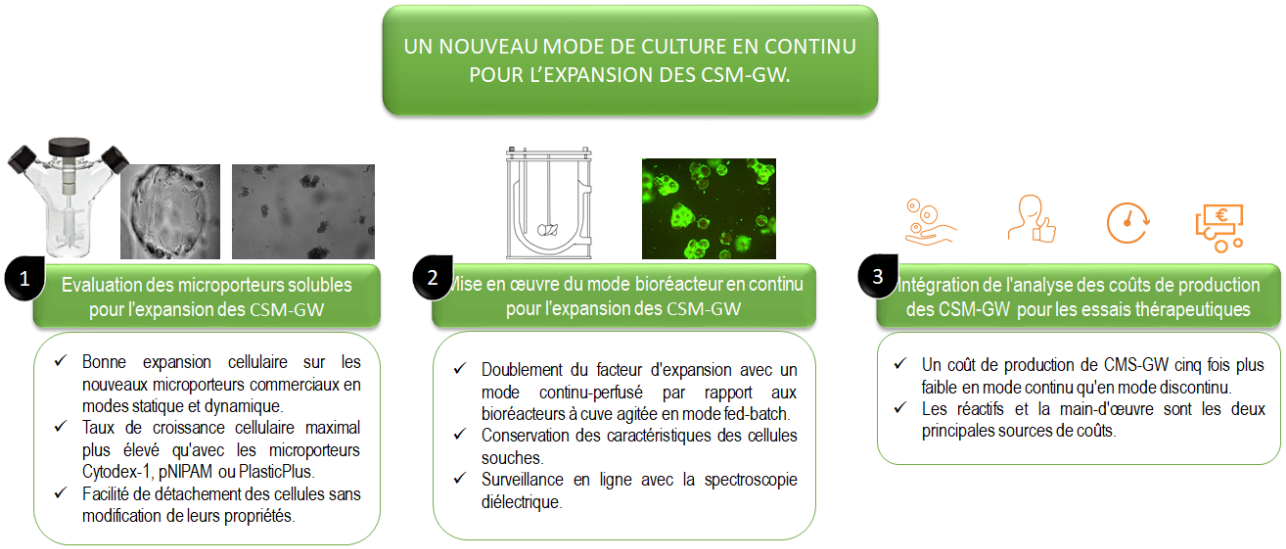

FIGURE 5.15 – Schéma récapitulatif des résultats obtenus dans le chapitre 4.

Conclusion et perspectives

Les différentes études réalisées ont permis de mieux appréhender le comportement des CSM de la gelée de Wharton en culture *in vitro*. Une première analyse a mis en évidence une migration possible d'un microporteur à un autre sans détachement préalable. Ces résultats ont été implémentés en bioréacteur afin de réaliser des cultures de CSM à plus grande échelle. L'ajout de microporteurs a été couplé avec un ajout progressif de milieu, afin de limiter le risque de collisions entre microporteurs à des plus fortes concentrations. De plus, les microporteurs réalisés dans le cadre de l'INTERREG ont montré une capacité intéressante pour l'expansion de CSM-GW en spinners et en bioréacteurs. Enfin dans une dernière partie, un microporteur commercial soluble a été évalué en bioréacteur en mode continu-perfusé. Il a été montré qu'un facteur d'expansion de 60 était obtenu grâce à ce nouveau système.

En termes de perspectives, afin de respecter au mieux les contraintes de culture GMP, il serait intéressant de réfléchir à un procédé totalement clos, de l'extraction cellulaire du cordon jusqu'à l'expansion en bioréacteur. De plus, l'utilisation de microporteurs solubles fonctionnalisés pourrait permettre un détachement in situ dans le bioréacteur, et limiter des étapes de tryspsination peu sûres et altérant potentiellement la qualité cellulaire. Des méthodes de purification du produit cellulaire sont également à réfléchir.

Il existe également encore d'autres inconnues dans les méthodes d'expansion de CSM-GW, comme par exemple la nature et l'impact des collisions entre microporteurs sur les cellules. Ces paramètres sont très importants à maîtriser pour optimiser au mieux les ajouts de microporteurs sans altérer la qualité cellulaire. Une meilleure connaissance des cinétiques métaboliques serait également un élément important à étudier afin de mieux ajuster les débits d'apport de milieu de culture dans le réacteur continu-perfusé et d'améliorer ainsi l'expansion cellulaire tout en réduisant ses coûts de fonctionnement.

Bibliographie

[1] A. I. Caplan. Mesenchymal stem cells. *Journal of Orthopaedic Research*, 9(5) :641–650, 1991.

[2] M. F. Pittenger, A. M. Mackay, S. C. Beck, R. K. Jaiswal, R. Douglas, J. D. Mosca, M. A. Moorman, D. W. Simonetti, S. Craig, and D. R. Marshak. Multilineage Potential of Adult Human Mesenchymal Stem Cells. *Science*, 284(5411) :143–147, April 1999.

[3] D. C. Colter, I. Sekiya, and D. J. Prockop. Identification of a subpopulation of rapidly self-renewing and multipotential adult stem cells in colonies of human marrow stromal cells. *Proceedings of the National Academy of Sciences*, 98(14) :7841–7845, July 2001.

[4] D. P. Sieveking and M. K. Ng. Cell therapies for therapeutic angiogenesis : back to the bench. *Vascular Medicine*, 14(2) :153–166, 2009.

[5] D. L. Troyer and M. L. Weiss. Concise Review : Wharton's Jelly-Derived Cells Are a Primitive Stromal Cell Population. *Stem Cells*, 26(3) :591–599, 2008.

[6] C. Elseberg, J. Leber, T. Weidner, and P. Czermak. The Challenge of Human Mesenchymal Stromal Cell Expansion : Current and Prospective Answers. In S. J. T. Gowder, editor, *New Insights into Cell Culture Technology*. InTech, May 2017.

[7] K. Le Blanc. Immunomodulatory effects of fetal and adult mesenchymal stem cells. *Cytotherapy*, 5(6) :485–489, December 2003.

[8] K. D. McElreavey, A. I. Irvine, K. T. Ennis, and W. I. McLean. Isolation, culture and characterisation of fibroblast-like cells derived from the Wharton's jelly portion of human umbilical cord. *Biochemical Society Transactions*, 19(1) :29S–29S, February 1991.

[9] H.-S. Wang, S.-C. Hung, S.-T. Peng, C.-C. Huang, H.-M. Wei, Y.-J. Guo, Y.-S. Fu, M.-C. Lai, and C.-C. Chen. Mesenchymal Stem Cells in the Wharton's Jelly of the Human Umbilical Cord. *Stem Cells*, 22(7) :1330–1337, 2004.

[10] R. J. Emnett, A. Kaul, A. Babic, V. Geiler, D. Regan, G. Gross, and S. Akel. Evaluation of Tissue Homogenization to Support the Generation of GMP-Compliant Mesenchymal Stromal Cells from the Umbilical Cord, *Stem Cells International*, (2016), 2016.

[11] L. L. Lu, Y. J. Liu, S. G. Yang, Q. J. Zhao, X. Wang, W. Gong, Z. B. Han, Z. S. Xu, Y. X. Lu, D. Liu, Z. Z. Chen, and Z. C. Han. Isolation and characterization of human umbilical cord mesenchymal stem cells with hematopoiesis-supportive function and other potentials. *Haematologica*, 91(8) :1017–1026, January 2006.

[12] L. Reppel. *Potentialité des cellules stromales de la gelée de Wharton en ingénierie du cartillage*. PhD thesis, Université de Lorraine, October 2014.

[13] A. L. V. Wezel. Growth of Cell-strains and Primary Cells on Micro-carriers in Homogeneous Culture. *Nature*, 216(5110) :64–65, October 1967.

[14] C. Martin. *Étude des procédés d'amplification de cellules souches mésenchymateuses humaines*. phdthesis, Université de Lorraine, December 2016.

[15] C. J. Hewitt, K. Lee, A. W. Nienow, R. J. Thomas, M. Smith, and C. R. Thomas. Expansion of human mesenchymal stem cells on microcarriers. *Biotechnology Letters*, 33(11) :2325, July 2011.

[16] A. C. Schnitzler, A. Verma, D. E. Kehoe, D. Jing, J. R. Murrell, K. A. Der, M. Aysola, P. J. Rapiejko, S. Punreddy, and M. S. Rook. Bioprocessing of human mesenchymal stem/stromal cells for therapeutic use : Current technologies and challenges. *Biochemical Engineering Journal*, 108 :3–13, April 2016.

[17] C. Ferrari, F. Balandras, E. Guedon, E. Olmos, I. Chevalot, and A. Marc. Limiting cell aggregation during mesenchymal stem cell expansion on microcarriers. *Biotechnology Progress*, 28(3) :780–787, 2012.

[18] M. Hervy, J. L. Weber, M. Pecheul, P. Dolley-Sonneville, D. Henry, Y. Zhou, and Z. Melkoumian. Long Term Expansion of Bone Marrow-Derived hMSCs on Novel Synthetic Microcarriers in Xeno-Free, Defined Conditions. *Plos One*, 9(3) :e92120, March 2014.

[19] Q. A. Rafiq, S. Ruck, M. P. Hanga, T. R. J. Heathman, K. Coopman, A. W. Nienow, D. J. Williams, and C. J. Hewitt. Qualitative and quantitative demonstration of bead-to-bead transfer with bone marrow-derived human mesenchymal stem cells on microcarriers : Utilising the phenomenon to improve culture performance. *Biochemical Engineering Journal*, 135 :11–21, July 2018.

[20] M. Dominici, K. L. Blanc, I. Mueller, I. Slaper-Cortenbach, F. C. Marini, D. S. Krause, R. J. Deans, A. Keating, D. J. Prockop, and E. M. Horwitz. Minimal criteria for defining multipotent mesenchymal stromal cells. The International Society for Cellular Therapy position statement. *Cytotherapy*, 8(4) :315–317, January 2006.

[21] F. Clementschitsch and K. Bayer. Improvement of bioprocess monitoring : development of novel concepts. *Microbial Cell Factories*, 5 :19, May 2006.

[22] A. El Wajgali, G. Esteban, F. Fournier, H. Pinton, and A. Marc. Impact of microcarrier coverage on using permittivity for on-line monitoring high adherent vero cell densities in perfusion bioreactors. *Biochemical Engineering Journal*, 70 :173–179, 2013.

[23] C. Justice, J. Leber, D. Freimark, P. P. Grace, M. Kraume, and P. Czermak. Online- and offline-monitoring of stem cell expansion on microcarrier. *Cytotechnology*, 63(4) :325–335, August 2011.

[24] C. F. Opel, J. Li, and A. Amanullah. Quantitative modeling of viable cell density, cell size, intracellular conductivity, and membrane capacitance in batch and fed-batch CHO processes using dielectric spectroscopy. *Biotechnology Progress*, 26(4) :1187–1199.

[25] C. Loubière. *Characterization and impact of the hydrodynamics on the performance of umbilical-cord derived stem cells culture in stirred tank bioreactors.* PhD thesis, Université de Lorraine, 2018.

[26] K. Y. Tan, S. Reuveny, and S. K. W. Oh. Recent advances in serum-free microcarrier expansion of mesenchymal stromal cells : parameters to be optimized. *Biochemical and Biophysical Research Communications*, 473(3) :769–773, 2016.

[27] K. Y. Tan, K. L. Teo, J. F. Lim, A. K. Chen, S. Reuveny, and S. K. Oh. Serum-free media formulations are cell line–specific and require optimization for microcarrier culture. *Cytotherapy*, 17(8) :1152–1165, 2015.

[28] S. Jung, K. M. Panchalingam, R. D. Wuerth, L. Rosenberg, and L. A. Behie. Large-scale production of human mesenchymal stem cells for clinical applications. *Biotechnology and Applied Biochemistry*, 59(2) :106–120, 2012.

Appendices

Methods of calculation of costs production of the WJ-MSCs culture

The appendices present the method of calculation of costs production of the WJ-MSCs culture expansion in batch, fed-batch and perfused-continuous modes.

1. List of the process unit characteristics and establishment of data bases (reagents and consumables).

HUMAN CHARACTERISTICS		
Operating labor salary cost	16	€/h
Supervision labor salary cost	25	€/h
PRODUCTION BATCH CHARACTERISTICS		
Cuve (L)	2	
Batch size of the begining	**500**	**mL**
CELL EXTRACTION YIELD		
1 umbilical cord → WJ cells	9.00E+06	cells
P0 seeding concentration	1.00E+03	cells/cm²
Number of cells per T-flask	**7.50E+04**	**cells**
WJ CELLS CULTURE		
T-flask area	75	cm²
Volume of medium per T-flask	10	mL
Seeding concentration	1.00E+03	cells/cm²
Number of cells per T-flask	**7.50E+04**	**cells**
Cell concentration at 70 % confluence	1.20E+04	cells/cm²
Number of cells in one T175 at 70 % confluence	**9.00E+05**	
Passaging WJC : 1 T-Falsks →	3	T-Flasks
Cryotube concentration (WJC)	2.00E+06	cells

Process Unit Characteristics | DB-Réactifs | DB-Consommables | Coû

Data base _ reagents

Réactifs	Fournisseur	Conditionnement		Prix	Prix unitaire (€/mL ou €/mg)	
α-MEM	Lonza	500	mL	10	0.02	
antibiotique antimycotique	Life technologie	100	mL	79.2	0.792	
Heparin	Sigma	250000	u	223	0.000892	prix/u
Glutamine	Sigma	250	g	167.5	0.00067	
LPH	Cook Regentec	500	mL	1195	2.39	
DMSO	Sigma	100	mL	213	2.13	
Cordon ombilical	UTCT	1	u	0	0	
PBS	Sigma	500	mL	14	0.028	
SVF	Thermo	50	mL	50.75	1.015	
TrypLE	Thermo	100	mL	21.51	0.2151	
EtOH	Sigma	5000	mL	47.5	0.0095	
Microporteurs (type DM)	Corning	1	g	117	117	
Microporteurs (type PlasticPlus)	Pall Solohill	100	g	273	2.73	
Microporteurs (types Cytodex-1)	GE	100	g	761.5	7.615	

FIGURE 16 – Analysis of the Excel file to calculate the costs of production of WJ-MSCs for clinical therapies. List of the process unit characterisitcs and establishment of data bases (reagents and consumables).

2. Calculation of balance sheets for materials, labour, consumables.

UO-04	WJ-MSC trypsination	4.0 T-flask	processed	Reagents (€)	Consumables (€)	Labor (€)	Labor (h)
	trypsination ; centrifigation ; counting	6.5 €	unit total costs	4.18	0.37	2.00	0.13
		26.2 €	total costs	16.71	1.49	8.00	0.50

Reagent / Consumable name	Quantity used	Unit cost (€)	Reagents (€)	Consumables (€)	Labor (€)	Labor (h)
PBS	40.00 mL	0.03	1.12			
TrypLE	20.00 mL	0.22	4.30			
WJC medium with LPH	80.00 mL	0.14	11.29			
Pipets	4.00	0.37		1.49		
Labor – trypsination ; centrifugation ; counting					8.00	0.50

UO-05	WJ-MSC freezing	10.0 cryotube	processed	Reagents (€)	Consumables (€)	Labor (€)	Labor (h)
	cryotube labelling ; freezing mix preparation ; cryotube filling	5.8 €	unit total costs	0.34	5.04	0.40	0.03
		57.8 €	total costs	3.40	50.40	4.00	0.25

Reagent / Consumable name	Quantity used (mL or mg)	Unit cost (€)	Reagents (€)	Consumables (€)	Labor (€)	Labor (h)
WJC medium	9.00 mL	0.14	1.27			
DMSO	1.00 mL	2.13	2.13			
Cryotube	10.0	5.04		50.4		
Labor - labelling ; mix preparation ; filling					4.00	0.25

3. Calculation of the total cost of a unit operation as the cell amplification.

				TOTAL (€)	Reagents (€)	Consumables (€)	Labor costs (€)
PO-02	Amplification P4 of WJC	Input	1 cryotube				
		Output	10 T-flasks	556	164.6	287.6	103.9
	AMPLIFICATION P3	Input	1 cryotube				
		Output	4 T-flasks	Costs (€)	22.6	12.4	42.7
UO-06	WJC thawing	1 cryotubes			5.6	10.2	8.0
	Number of flasks done with one cryotube	4 T-flasks					
UO-02	WJC medium renewal	4 T-flask			16.9	2.2	34.7
	Number of medium renewals	3					
	Total number of cells @70 % confluence	3.60E+06 cells					
	AMPLIFICATION P4	Input	4 T-flasks				
		Output	10 T-flasks	Costs (€)	142.0	275.1	61.2
UO-03	WJC passaging	4 T-flasks			16.7	32.4	7.2
	Number of flasks done with 4 T75	10 T-flasks					
UO-02	WJC medium renewal	10 T-flasks			125.3	242.8	54.0
	Number of medium renewals	3					
	Total number of cells @70 % confluence	9.00E+06 cells					

FIGURE 17 – Analysis of the Excel file to calculate the costs of production of WJ-MSCs for clinical therapies. Calculation of balance sheets for materials, labour and consumables. Calculation of the total cost of a unit operation as the cell amplification.

4. Total cost production

	Biobanking -Uc MSC	Amplifications of WJ MSC		Agitated culture in spinner vessel		Agitated culture in fed-batch mode STR	
Number of :							
Umbilical cord	1						
Cryotubes		1					
T-flasks			PO-02	24	24	PO-03	
Erlenmeyer					3	1	PO-04 3
			2.4		3	3.0E+00	
Equivalent number of cells		2.0E+06					6.0E+08
Costs € (TOTAL)	***280***		***1 335***		***449***		***1 483***
Reagent	120		395		172		1 151
Consumables	14.68		690		198		8
Equipment							
Labor	0.00		249		79		324

# of Million cells	600
Total cost (€)	3 547
€/Million cells	**5.9**
one dosis (in Million of cells)	1.00E+03
Cost of one dosis	***5 911***

FIGURE 18 – Analysis of the Excel file to calculate the costs of production of WJ-MSCs for clinical therapies. Total cost of production

List of communications and publications

Publications

• Sion C., Loubière C., Wlordarczyk-Biegun M.K., Davoudi N., Müller-Renno C., Guedon E., Chevalot I., Olmos E., **Effects of microcarriers addition and mixing on WJ-MSC culture in bioreactors**. Biochemical Engineering Journal. Accepted in January 2020.

• Loubière C., Chevalot I., De-Isla N., Sion C., Reppel L., Guedon E., Olmos E. **Impact of the type of microcarrier and agitation modes on the expansion performances of mesenchymal stem cells derived from umbilical cord**. Biochemical Engineering Journal. Accepted in February 2020.

Oral communications

• Sion C., Loubière C., Wlodarczyk-Biegun M., Davoudi N., Müller C., Guedon E. , Chevalot I., Olmos E. **Impact du mode d'agitation sur les performances de cultures de cellules souches humaines en bioréacteur**. Conference at the Société Française de Génie des Procédés (SFGP), Nantes, in October 2019.

• Sion C., Loubière C., Grandfils C, Sevrin C., Vandeberg R., Guedon E., Chevalot I., Olmos E. **Control of microcarrier feed time by quantitative determination of bead-to-bead transfer during hMSC cultures**. Conference at the European Society of Biochemical Engineering Science (ESBES), Lisbon, in September 2018.

Poster communications

• Sion C., Bailly S., Poncet S., Guedon E., Chevalot I., Olmos E., **Expansion of human mesenchymal stem cells on Corning® Synthemax II™ – coated dissolvable microcarriers in a serum-free cell culture medium**. Conference at the European Congress of Applied Biotechnology (ECAB), Florence, in September 2019.

• Sion C., Loubière C., Wlodarczyk-Biegun M., Davoudi N., Guedon E., Chevalot I., Olmos E., **Impact of bead collisions on hWJ-MSC culture performance**. Conference at the European Society Animal Cell Technology (ESACT), Copenhagen, in May 2019.

• Delafosse A., Sion C., Olmos E., Toye D. **Interreg Project developing new bioMaterials for PROliferation and in Vitro Expansion of STEM cells**. Conference at the European Society of Biochemical Engineering Science (ESBES), Lisbon, in September 2018.

Abstract

Mesenchymal stem cells (MSCs) show great interest in cellular therapies. Their various characteristics such as their immuno-modulatory properties, their ability to differentiate, and also the secretion of factors, are numerous and promising for new clinical treatments for diseases where few therapies are proposed or have few efficiencies. The doses to be injected for significant results must be repeated and generally contain high quantities of cells (10^6 cells kg^{-1} per patient approx). Large scale production methods must be implemented to meet the demand, and in the least costly way possible. In this PhD work, the main objective was to develop a scalable process adapted to these support-dependent cells. For this end, a first study allowed to understand part of the mechanisms of interaction of cells with their growth supports, the microcarriers. The adhesion time but also the cell migrations between microcarriers were characterized and evaluated. A strategy of fed-batch mode strategy with microcarriers addition at specific times in the culture was also proposed. Following this, the second part of the study of this work was to determine the efficiency on larger scale expansion process (1.5 L), using of innovative microcarriers developed by the partner teams of the 'ImprovesStem' European project. Several microcarriers candidates with chemically modified surface proved to be promising for the expansion of Wharton's jelly stem cells. Finally, in the last part of the thesis, an innovative process based on the removal of empty microcarriers, avoiding the risk of deleterious frictions between highly concentrated microcarriers was proposed. Moreover, an on-line monitoring of viable cell concentration was carried-out in the stirred tank bioreactor. Innovative commercial microcarriers, soluble under the action of enzymes, were used in this last part of the study. An improvement of the expansion factor (by a factor of 1.5) was obtained in this continuous-perfused mode of culture in the stirred bioreactor. In addition, these enzymatically-soluble commercial microcarriers allowed for an excellent detachment yield, essential to consider their use in cell therapy.

Résumé

Les cellules souches mésenchymateuses (CSM) ont un fort intérêt en utilisation clinique. Leurs différentes caractéristiques telles que leurs propriétés immuno-modulatrices, leur capacité à se différencier, et aussi la sécrétion de facteurs, sont nombreuses et prometteuses pour le traitement clinique de maladies où peu de thérapies sont proposées ou sont peu efficaces. Cependant, les doses à injecter pour des résultats cliniques significatifs doivent être répétées et contiennent généralement des quantités importantes de cellules (10^6 cellules kg^{-1} par patient). Ainsi, des méthodes de production à grande échelle doivent être mises en œuvre pour répondre à la demande, tout en minimisant les coûts de production. Dans ce travail de thèse, une première étude a permis de comprendre une partie des mécanismes d'interaction des cellules avec leurs supports de croissance, les microporteurs. Le temps d'adhérence et des migrations cellulaires entre microporteurs ont pu être mesurés et étudiés. Une stratégie d'ajout de microporteurs à des temps spécifiques de la culture a été proposée. Suite à cela, la deuxième partie d'étude de ces travaux a été de déterminer les performances d'expansion du procédé réalisé à plus grande échelle (1.5 L), en utilisant des microporteurs innovants développés par les équipes partenaires du projet européen, et présentant des chimies de surfaces variées. Plusieurs microporteurs candidats se sont révélés prometteurs pour l'expansion des cellules souches de la gelée de Wharton. Enfin, la dernière partie de la thèse a été consacrée au développement d'un procédé innovant reposant sur le soutirage de microporteurs vides, diminuant le risque de frictions délétères entre des microporteurs très concentrés, a été proposé. De plus, un contrôle en ligne de la concentration en cellules vivantes a été effectué dans le bioréacteur à cuve agitée. Des microporteurs commerciaux innovants, solubles sous l'action d'enzymes, ont été utilisés dans cette dernière partie. Une amélioration du facteur d'expansion (d'un facteur 1.5) a été obtenue par l'utilisation de ce mode continu et perfusé en bioréacteur. De plus, ces microporteurs, solubles sous l'action d'enzymes, ont permis un excellent rendement de détachement cellulaire, élément essentiel pour envisager l'utilisation des CSMs en thérapie cellulaire à un coût controlé.